The Author

Motivated by an interest in environmental topics, Friederike Neiske studied Geoecology (B.Sc.) at the University of Tübingen. She continued to explore soil-related processes during her Master's program in Geography at the University of Göttingen. She deepened this focus during her doctoral research at the Institute of Soil Science at the University of Hamburg, where she was part of an interdisciplinary research group investigating carbon dynamics in the Elbe Estuary. In her dissertation, she examined the biogeochemical drivers of carbon storage in estuarine marsh soils to better understand these systems in the context of climate change.

Verein zur Förderung der Bodenkunde Hamburg
c/o Institut für Bodenkunde - Universität Hamburg
https://www.geo.uni-hamburg.de/de/bodenkunde.html

Hamburger Bodenkundliche Arbeiten

2025

F. Neiske

Band 106

HBA

Friederike Neiske

Soil Organic Carbon Dynamics along Estuarine Gradients

Band 106
2025

ISSN: 0724-6382

Hamburger Bodenkundliche Arbeiten

Soil Organic Carbon Dynamics along Estuarine Gradients

DISSERTATION

with the aim of achieving a doctoral degree
at the Faculty of Mathematics, Informatics and Natural Sciences
Department of Earth System Sciences
at University of Hamburg

submitted by

Friederike Christine Maria Neiske

Hamburg, 2025

Accepted as Dissertation at the Department of Earth System Sciences

Date of Oral Defense:	20th March 2025
Supervision committee:	Prof. Dr. Annette Eschenbach Prof. Dr. Kai Jensen Prof. Dr. Jens Hartmann Dr. Joscha Becker
Reviewers:	Prof. Dr. Annette Eschenbach Prof. Dr. Kai Jensen
Members of the examination commission:	Prof. Dr. Annette Eschenbach Prof. Dr. Kai Jensen Prof. Dr. Lars Kutzbach Jun.-Prof. Dr. Philipp Porada Prof. Dr. Gerhard Schmiedl
Chair of the Subject Doctoral Committee Earth System Sciences:	Prof. Dr. Hermann Held
Dean of Faculty MIN:	Prof. Dr.-Ing. Norbert Ritter

Published as

Hamburger Bodenkundliche Arbeiten, Volume 106

ISSN: 0724-6382

Editor: Verein zur Förderung der Bodenkunde Hamburg
Allende-Platz 2, 20146 Hamburg
https://www.geo.uni-hamburg.de/bodenkunde/ueber-das-institut/hba.html

Editorship: Dr. Klaus Berger

Abstract

Estuarine tidal marshes are known for their substantial soil organic carbon (SOC) sequestration and storage capacities. To anticipate effects of climate change on SOC storage in estuarine marshes, a comprehensive understanding of its current biotic and abiotic controls is essential. Using the Elbe estuary in Northern Germany as a model system, this research assessed the role of estuarine environmental conditions on SOC storage and dynamics. The major focus was placed on the interactive effect of the estuarine salinity gradient, spatial variation in flooding frequency, local soil conditions, and biota on (I) litter decomposition, (II) SOC stocks and SOC stabilization mechanisms (aggregation, mineral-association), and (III) microbial SOC turnover and the potential SOC stability against mineralization.

To account for the large heterogeneity of estuarine marshes, three marsh types were selected along the salinity gradient (salt marsh, brackish marsh, and freshwater marsh), as well as three marsh zones characterized by different flooding regimes (pioneer zones = daily flooding, low marshes = monthly flooding, and high marshes = yearly flooding). Litter decomposition was evaluated using standardized litter (Tea Bag Index) and native litter from each marsh location. Associated prokaryotic communities were examined by 16S rRNA gene amplicon sequencing. Soil samples were analyzed for SOC stocks, SOC fractions (density fractionation to separate free particulate, occluded particulate, and mineral-associated organic matter), as well as the mineralizability of SOC pools (oxic incubation followed by a two-pool model quantifying the fast C pool, slow C pool, and mean residence times). Local environmental conditions (e.g. soil texture, pH, electric conductivity, redox, and plant biomass) were characterized to identify potential drivers of SOC dynamics along the estuarine gradients.

With increasing salinity, SOC contents decreased in the marshes of the Elbe Estuary. First, decreasing SOC contents aligned with a decline in aboveground biomass, as well as increasing litter decomposition rates due to reduced recalcitrance of the local vegetation. Second, the SOC associated with minerals decreased from freshwater to salt marshes, as a consequence of sedimentation patterns leading to decreasing clay contents. Moreover, SOC mineralizability increased with increasing salinity due to an increasing contribution of the fast C pool. Along the flooding gradient, SOC contents decreased with increasing flooding frequency which was closely linked to decreasing aboveground plant biomass. The effect of flooding on litter decomposition strongly depended on

litter quality, as higher flooding frequencies increased mass loss of labile litter, but decreased mass loss of recalcitrant litter. The mineralizability of SOC increased with increasing flooding which was indicated by a shorter mean residence time and could be related to elevated contributions of free particulate organic matter and dissolved organic carbon to total SOC with increasing flooding. Moreover, SOC protection within aggregates was negatively affected by increasing flooding and high soil water content.

In conclusion, SOC storage in estuarine marshes decreased with increasing salinity and flooding, which was attributed to a combination of biotic and abiotic drivers. The findings indicate that an increasing marine influence induced by climate change (sea-level rise and saltwater intrusion) is likely to change biogeochemical C cycling, reduce the SOC storage capacity, as well as hamper mechanisms of SOC stabilization in the estuarine marshes.

Zusammenfassung

Ästuarine Marschen sind für ihre beträchtlichen Kapazitäten zur Bindung und Speicherung von organischem Bodenkohlenstoff bekannt. Um die Auswirkungen des Klimawandels auf die Speicherung von organischem Bodenkohlenstoff in ästuarinen Marschen abschätzen zu können, ist ein umfassendes Verständnis der derzeitigen biotischen und abiotischen Kontrollfaktoren erforderlich. Das norddeutsche Elbeästuar wurde als Modellsystem gewählt, um den Einfluss der vorherrschenden Umweltbedingungen im Ästuar auf die Bodenkohlenstoff-speicherung und -dynamik zu untersuchen. Der Schwerpunkt lag dabei auf einer Verknüpfung der Effekte des Salzgehaltsgradienten und der räumlichen Variation der Überflutungshäufigkeit mit lokalen Bodenbedingungen und Einflüssen der Vegetation und Bodenmikrobiologie. Im Speziellen wurden die Einflüsse auf (I) den Abbau von Streu, (II) die Menge an gespeichertem Bodenkohlenstoff und dessen Stabilisierungsmechanismen (Einschluss in Aggregate, Mineralassoziation) sowie (III) den mikrobiellen Umsatz und die potenzielle Stabilität des Bodenkohlenstoffs gegenüber Mineralisierung untersucht.

Um die große Heterogenität von ästuarinen Marschen zu berücksichtigen, wurden drei Marschtypen entlang des Salinitätsgradienten (Salzmarsch, Brackmarsch und Süßwassermarsch) und drei Marschzonen mit unterschied-lichen Überflutungsregimen ausgewählt (Pionierzone = tägliche Überflutung, Untere Marsch = monatliche Überflutung und Obere Marsch = jährliche Überflutung). Die Zersetzung von Streu wurde anhand von standardisiertem Substrat (Tea Bag Index) und lokal heimischem Substrat untersucht. Die zugehörigen prokaryotischen Gemeinschaften wurden mittels 16S rRNA-Genamplikon-Sequenzierung bestimmt. Bodenproben wurden auf Kohlenstoff-gehalt, Kohlenstofffraktionen (Dichtefraktionierung zur Trennung von freier partikulärer, okkludierter partikulärer und mineralassoziierter organischer Substanz) sowie auf die Mineralisierbarkeit von Kohlenstoffpools (oxische Inkubation, Zwei-Pool-Modell-Anpassung zur Quantifizierung des schnellen Kohlenstoffpools, des langsamen Kohlenstoffpools und der *mean residence time*) untersucht. Lokale Umweltbedingungen (z.B. Bodentextur, pH-Wert, elektrische Leitfähigkeit, Redoxbedingungen und Pflanzenbiomasse) wurden charakterisiert, um die relevanten Einflussfaktoren der Bodenkohlenstoff-dynamik entlang der Gradienten im Ästuar zu identifizieren.

Mit zunehmendem Salzgehalt nahm der Kohlenstoffgehalt in den Marschböden des Elbästuars ab. Diese Abnahme ging mit einem Rückgang der oberirdischen Biomasse sowie mit zunehmenden Zersetzungsraten der Streu

aufgrund der geringeren Rekalzitranz der lokalen Vegetation einher. Darüber hinaus nahm der mineralassoziierte Kohlenstoff von der Süßwasser- zur Salzmarsch ab. Dies kann auf Sedimentationsmuster zurückgeführt werden, die sinkende Tongehalte im Boden zur Folge hatten. Die Mineralisierbarkeit des Bodenkohlenstoffs nahm mit zunehmendem Salzgehalt zu, was sich auf einen steigenden Beitrag des schnellen Kohlenstoffpools zurückführen lässt. Entlang des Überflutungsgradienten nahm der Bodenkohlenstoffgehalt mit zunehmender Überflutungshäufigkeit ab, was wiederum eng mit der abnehmenden Pflanzenbiomasse zusammenhing. Die Auswirkung der Überflutung auf die Zersetzung der Streu hing stark von deren chemischer Zusammensetzung ab, da höhere Überflutungshäufigkeiten einerseits den Massenverlust der labilen Streu erhöhten, andererseits jedoch den Massenverlust von schwer zersetzbarer Streu verringerten. Die Mineralisierbarkeit des Bodenkohlenstoffs nahm mit zunehmender Überflutung zu. Dies zeigte sich in einer kürzeren *mean residence time* und könnte mit erhöhten Anteilen an freier partikulärer organischer Substanz und gelöstem organischem Kohlenstoff am Gesamtbodenkohlenstoff bei zunehmender Überflutung zusammenhängen. Darüber hinaus wurde der Schutz des Bodenkohlenstoffes durch den Einschluss in Aggregate durch erhöhte Überflutungsraten und hohen Bodenwassergehalt negativ beeinflusst.

Zusammenfassend lässt sich sagen, dass die Bodenkohlenstoffspeicherung in ästuarinen Marschen durch eine Kombination aus biotischen und abiotischen Faktoren mit zunehmendem Salzgehalt und Überflutung abnahm. Die Ergebnisse deuten darauf hin, dass ein zunehmender mariner Einfluss aufgrund des Klimawandels (Anstieg des Meeresspiegels und zunehmender Salzgehalt) die biogeochemischen Prozessstrukturen verändern, und dadurch die Speicherkapazität für Bodenkohlenstoff und dessen Stabilisierungsmechanismen in Ästuaren verringern wird.

Manuscripts related to this Dissertation

Manuscript A:

Neiske F., Grüterich L., Eschenbach A., Wilson M., Streit W.R., Jensen K., Becker J.N.: Litter decomposition and prokaryotic decomposer communities along estuarine gradients.

FN: Conceptualization, Formal Analysis, Investigation, Writing – original draft, Visualization, Project administration. LG: Conceptualization, Formal Analysis, Investigation, Visualization, Writing – review & editing. AE: Conceptualization, Resources, Writing – review & editing, Supervision, Funding acquisition. MW: Investigation, Writing – review & editing. WRS: Conceptualization, Resources, Writing – review & editing, Supervision, Funding acquisition. KJ: Investigation, Resources, Writing – review & editing, Supervision, Funding acquisition. JNB: Conceptualization, Writing – review & editing, Supervision, Project administration.

Manuscript B:

Neiske F., Seedtke M., Eschenbach A., Wilson M., Jensen K., Becker J.N.: Soil organic carbon stocks and stabilization mechanisms in tidal marshes along estuarine gradients.

FN: Conceptualization, Formal Analysis, Investigation, Project administration, Visualization, Writing – original draft. MS: Investigation, Writing – review & editing. AE: Funding acquisition, Resources, Supervision, Conceptualization, Writing – review & editing. MW: Investigation, Writing – review & editing. KJ: Funding acquisition, Resources, Investigation, Supervision, Writing – review & editing. JNB: Conceptualization, Formal Analysis, Methodology, Project administration, Supervision, Writing – review & editing.

Manuscript C:

Neiske F., Beer C., Schwarze D., Seedtke M., Eschenbach A., Becker J.N.: Connecting organic matter fractions to mineralization dynamics in estuarine marsh soils.

FN: Conceptualization, Methodology, Formal Analysis, Investigation, Project administration, Visualization, Writing – original draft. CB: Formal Analysis. DS: Investigation, Writing – review & editing. MS: Investigation, Writing – review & editing. AE: Conceptualization, Methodology, Funding acquisition, Resources, Supervision, Writing – review & editing. JNB: Conceptualization, Formal Analysis, Methodology, Project administration, Supervision, Writing – review & editing.

Further Contributions to Manuscripts

Branoff B., Grüterich L., Wilson M., Tobias-Hünefeldt S.P., Saadaoui Y., Mittmann-Goetsch J., **Neiske F.**, Lexmond FN., Becker J.N., Grossart H.P., Porada P., Streit W.R., Eschenbach A., Kutzbach L., Jensen K. (in preparation). Partitioning biota along the Elbe River Estuary: Is there a brackish community? *Estuarine, Coastal & Shelf Science.*
Preprint: https://doi.org/10.1101/2024.05.13.593883

Lexmond FN.*, **Neiske F.***, Becker J.N., Grabellus B., Holl D., Jensen K., Kleinschmidt V., Kutzbach L., Mittmann-Goetsch J., Mueller P., Eschenbach A. (in preparation). Characterization of soil redox conditions along estuarine gradients. Characterization of soils and soil redox conditions along environmental gradients in the Elbe estuary (extended abstract in Appendix).

Saadaoui Y., Beer C., Mueller P., **Neiske F.**, Becker J.N., Eschenbach A., Porada P. (under review). Exploring effects of variation in plant root traits on carbon emissions from estuarine marshes. *EGUsphere*.
Preprint: https://doi.org/10.5194/egusphere-2024-1756

* equal contribution

Table of Contents

Manuscripts

List of Figures

Unifying Essay

Manuscript A

Manuscript B

Manuscript C

List of Tables

Unifying Essay

Manuscript B

Unifying Essay

1 Introduction

1.1 Background and Motivation

1.1.1 Estuaries and tidal marshes

Estuaries provide a wide range of important ecosystem services and functions, including flood regulation, the provision of raw materials, reproductive and nursery grounds for fish, breeding and resting habitats for birds, tourism, recreation, agriculture, and water purification particularly for pollutants (Barbier et al., 2011; Mitsch et al., 2015). The ecosystem service that has recently received significant attention in light of climate change is the large carbon (C) sequestration potential of vegetated coastal ecosystems, such as estuarine tidal marshes, which are termed as "blue carbon" (Chmura et al., 2003; Macreadie et al., 2019; IPCC, 2023). Despite covering only a small area globally, estuarine tidal marshes can store disproportionately large amounts of organic carbon in soil (SOC). Globally, tidal marsh soils store approximately 1.44 Pg C in the first meter, with average SOC stocks around 83.1 Mg C ha^{-1} (0 - 30 cm) and 185.3 Mg C ha^{-1} (30 - 100 cm) (Maxwell et al., 2023). Tidal marshes particularly stand out for their high annual C burial rates, reaching up to 2.2 t C ha^{-1} yr^{-1}, which is significantly higher than in terrestrial ecosystems (Mcleod et al., 2011). A reason for the high C sequestration potential of tidal marshes is the high rate of both autochthonous and allochthonous organic matter (OM) input, coupled with low OM output due to slow decomposition rates in flooded soils (Mcleod et al., 2011; Macreadie et al., 2019; Maxwell et al., 2023).

Estuarine tidal marshes are located at the interface of limnic, marine, and terrestrial ecosystems. The mixing of riverine freshwater with saline seawater leads to the formation of a salinity gradient - a defining feature of estuaries (Telesh and Khlebovich, 2010). In addition, tidal inundation is a significant factor influencing tidal marshes. The interaction of surface elevation with tidal regime leads to dynamic variations in the frequency and duration of tidal flooding (Broome et al., 2019). Variations in salinity and flooding significantly influence the distribution and composition of plant communities in estuarine marshes, resulting in distinct vegetation zones (Engels and Jensen, 2009; Struyf et al., 2009; Ellenberg et al., 2010). As a consequence, estuarine marshes are shaped by dynamic interactions between abiotic factors, such as sedimentation, tidal inundation and salinity, and biotic components, including vegetation and soil microorganisms, leading to high variability in biogeochemical processes affecting SOC dynamics (van de Broek et al., 2016; Seyfferth et al., 2020).

Today, tidal marshes are among the most threatened ecosystems globally, with an estimated area loss of more than 50% since the 1800s, due to global warming, sea-level rise, and anthropogenic activities such as agriculture, urban expansion, and diking (Kennish, 2002; Craft et al., 2009; Crosby et al., 2016; Macreadie et al., 2019). Sea-level rise is one of the most significant global-change factors that will influence the future of blue carbon ecosystems by potentially altering hydrodynamics and inducing saltwater intrusion, with severe consequences for their C storage capacity (Craft et al., 2009; Minick et al., 2019; Macreadie et al., 2019). The Intergovernmental Panel on Climate Change (IPCC) reported an accelerated sea-level rise from 1.3 mm per year (1901 - 1971) to 3.7 mm per year (2006 - 2018) (IPCC, 2023). It was predicted that sea-level rise can lead to the loss of 45% of the current global salt marsh area and 39% of the tidal freshwater marsh area by the end of the century (Craft et al., 2009). This will be accompanied by a reduction in the ability of tidal marshes to provide ecosystem services. For example, the loss of salt marshes globally between 2000 and 2019 caused an emission of 16.3 Tg CO_2-equivalent per year and reduced the annual C burial rate by 0.045 Tg CO_2-equivalent (Campbell et al., 2022).

Estuarine marshes are dynamic systems characterized by complex biogeochemistry that fluctuates over time and space leading to significant heterogeneity both within and between estuaries (van de Broek et al., 2016; Nelson et al., 2017; Seyfferth et al., 2020; Mazarrasa et al., 2023). Our understanding of the dynamic interactions among various environmental factors, such as salinity and hydrodynamics, which affect biogeochemical and biological processes, is insufficient to accurately estimate C sequestration capacity of estuarine marshes and assess their vulnerability to future changes.

1.1.2 Drivers of soil organic carbon storage in estuarine marshes

It is commonly assumed that the significant potential for SOC storage in tidal marshes results from reduced oxygen availability in prolonged water-logged soils, which in turn limits OM decomposition (Macreadie et al., 2019). When soils are water saturated, gas exchange becomes restricted, leading to oxygen depletion and the utilization of alternative electron acceptors by microorganisms, such as nitrate and sulfate, which yield less energy (Fiedler et al., 2007). This metabolic shift from aerobic to anaerobic processes affects OM breakdown, potentially reducing decomposition rates by up to tenfold compared to aerobic conditions (Keiluweit et al., 2017). However, oxygen availability in tidal marshes is influenced by surface elevation, inundation frequency, soil

properties, and their interactions with biota, resulting in exceptionally high spatial and temporal variability in redox conditions (Dorau and Mansfeldt, 2016). Consequently, water-logging, anoxic soils, and slowed OM decomposition are not universally characteristic for tidal marshes. For example, elevated marsh areas and topsoil may experience enhanced OM decomposition due to an optimal water balance (Yousefi Lalimi et al., 2018). Soil moisture below 50% volumetric water content can have a positive effect on C mineralization (Sierra et al., 2015; Basile-Doelsch et al., 2020). Further, increased flooding frequency can lead to reduced SOC stocks in tidal marshes, potentially due to lower primary production and thus lower OM input in these areas (Spohn and Giani, 2012; van de Broek et al., 2016; Hansen et al., 2017). Salinity is another critical factor influencing SOC storage in estuarine marshes (van de Broek et al., 2016; Hansen et al., 2017; Luo et al., 2019). Increasing salinity is often linked to a decline in SOC storage, likely due to decreased inputs of both autochthonous and allochthonous OM (Butzeck et al., 2015; Hansen et al., 2017). Generally, plant biomass production is higher in freshwater and brackish marshes compared to salt marshes, attributed to reduced salinity stress and greater nutrient availability in freshwater environments (Więski et al., 2010). Salinity can also directly impact OM decomposition by affecting microbial biomass, activity, and community structures, as well as the activity of extracellular enzymes (Setia et al., 2011; Morrissey et al., 2014; Zhang et al., 2021). Research has shown that elevated salinity levels can negatively impact microbial biomass, although many of these studies primarily focus on oxic soil conditions (Egamberdieva et al., 2010; Yan et al., 2015).

1.1.3 Organic matter input and litter decomposition

As long as C inputs exceed C outputs, ecosystems act as C sinks (Ontl and Schulte, 2012; Basile-Doelsch et al., 2020). Heterotrophic soil microorganisms, including bacteria, fungi, and archaea, play a crucial role in the turnover of SOC (Talbot and Treseder, 2011; Allison et al., 2013; Basile-Doelsch et al., 2020). The soil decomposer community utilizes a portion of the C for biomass synthesis, while another part is respired and released from the soil, primarily as CO_2 (or CH_4 under anaerobic conditions) (Hoffland et al., 2020). Organic matter entering the soil is predominantly derived from higher plants, either through root exudates and dead root material or as shoot litter (Kögel-Knabner, 2017). Root exudates consist of low-molecular-weight substances (e.g. sugars, amino acids, and organic acids), secondary metabolites (e.g. phenolics, tannins), and high-molecular-weight compounds (e.g. mucilage, proteins), while root and

shoot litter is mainly composed of structural compounds such as cellulose, hemicellulose, lignin, and proteins (Kögel-Knabner, 2017; Canarini et al., 2019).

The decomposition process of litter occurs in three distinct phases: the initial phase features rapid leaching of soluble components, followed by the breakdown of structural materials (notably cellulose), and concludes with the slow degradation of more resistant compounds like lignin (Valiela et al., 1985). The leaching phase is particularly pronounced in tidal wetlands, where inundation leads to high soil water contents (Marley et al., 2019; Trevathan-Tackett et al., 2021) and release of dissolved organic carbon (DOC). A combined laboratory and field experiment indicated that 93 - 100% of the initial mass loss of green and rooibos tea after 63 days was attributed to leaching of the water-soluble fraction (Marley et al., 2019). Litter decomposition is an essential ecosystem process, as it plays a central role in C and nutrient cycling (Aerts, 1997; Zhang et al., 2008). While climate is a global factor influencing OM decomposition (Aerts, 1997), local decomposition dynamics are shaped by complex interactions among multiple environmental factors, including redox conditions, pH, nutrient availability, microbial community composition, and substrate quality (Valiela et al., 1985; Hemminga et al., 1991; Craft, 2007; Makkonen et al., 2012; Yuan et al., 2020). Consequently, OM decomposition can exhibit strong spatio-temporal variations, particularly along environmental gradients (Becker and Kuzyakov, 2018; Stagg et al., 2018; Trevathan-Tackett et al., 2021).

Litter decomposition can be slowed down by oxygen limitations in frequently flooded soils (Hemminga et al., 1991; Yarwood, 2018), while other studies indicate a stimulating effect of flooding on decomposition (Zhai et al., 2021). The differences in litter decomposition between aerobic and anaerobic conditions are influenced by various factors, including the OM quality. For instance, the decomposition of lignin is significantly slower or even incomplete in the absence of oxygen, while labile OM decomposes at similar rates under both aerobic and anaerobic conditions (Benner et al., 1984; Kristensen et al., 1995; Hulthe et al., 1998). The reported impact of salinity on litter decomposition remains inconsistent, with some studies suggesting a positive correlation between salinity and decomposition rates in tidal wetlands (Craft, 2007; Morrissey et al., 2014; Stagg et al., 2018), while others report negative effects (Roache et al., 2006; Quintino et al., 2009; Bierschenk et al., 2012).

In addition to these abiotic factors, OM decomposition is driven by biotic ecosystem properties. The chemical and physical properties of plant materials, including N, lignin, and cellulose contents are recognized as key determinants of litter decomposition in various ecosystems (Valiela et al., 1985; Zhang et al., 2008; Stagg et al., 2018). Litter quality can strongly vary along estuarine

gradients due to variations in vegetation composition (Stagg et al., 2018; Schulte Ostermann et al., 2024). Moreover, plants can also influence microbial communities by promoting specific taxa capable of efficiently decomposing local vegetation (Wang et al., 2007; Bezemer et al., 2010) or by root exudation which can change the microbial gene transcription in wetlands (Grüterich et al., 2024). In addition, variations in flooding regimes and salinity can shape the composition and diversity of microbial communities in marsh soils (Yarwood, 2018; Trevathan-Tackett et al., 2021), as well as the predominant microbial metabolic pathways within these ecosystems (Yarwood, 2018; Grüterich et al., 2025). Climate is a crucial factor influencing litter decomposition (Aerts, 1997), a trend also evident in tidal wetlands (Mueller et al., 2018; Trevathan-Tackett et al., 2021). As a consequence, litter decomposition varies seasonally, generally increasing with higher temperatures and closely tied to soil moisture levels (Becker and Kuzyakov, 2018; Petraglia et al., 2019; Daebeler et al., 2022). In estuarine marshes, this relationship becomes more complex due to the interplay of tidal inundation and salinity. Considering the high sensitivity of litter decomposition to environmental influences, climate change could significantly impact OM decomposition in estuarine marshes, though predicting these effects can be difficult. It is vital to account for the complex interactions between abiotic and biotic system components to fully comprehend the dynamics of litter decomposition in estuarine marshes. The Tea Bag Index (TBI), introduced by Keuskamp et al. (2013), provides useful insights into the effect of external environmental drivers in litter decomposition. Nevertheless, it is also important to consider litter quality and the home-field advantage by including litter from local vegetation (Lopes et al., 2011; Franzitta et al., 2015). Understanding these relationships and the dynamics of litter decomposition is essential, as it significantly influences the C incorporation into soil while being highly responsive to environmental changes.

1.1.4 Soil organic carbon fractions, stability, and turnover

The SOC pool compromises a wide range of compounds at various stages of biotransformation and stability (Basile-Doelsch et al., 2020). This spectrum ranges from free particulate organic matter (POM), resembling fresh plant litter, to highly processed OM in the form of microbial products and organic monomers that are associated with minerals (MAOM) (Lützow et al., 2006; Wiesmeier et al., 2019; Basile-Doelsch et al., 2020). The free POM fraction has a turnover time of less than ten years and primarily contributes to the active C pool in soil (Lützow et al., 2008). Aside from fresh plant residues, the active

pool also includes root exudates, along with faunal and microbial residues (Smith and Paul, 2017). Stabilization within the free POM fraction primarily occurs through the selective preservation of recalcitrant compounds, especially during the early stages of litter decomposition (Lützow et al., 2006; Marschner et al., 2008). Currently it is assumed that the role of selective preservation is less important for the long-term storage of SOC. As OM decomposition progresses, selective preservation becomes less relevant due to the increased protection of labile OM within aggregates and by mineral associations (Lützow et al., 2008; Cotrufo et al., 2013). However, this assumption is primarily based on findings from terrestrial soils and has yet to be validated for estuarine ecosystems.

Microorganisms play a dual role in SOC dynamics, facilitating both decomposition and stabilization processes (Six et al., 2004; Wiesmeier et al., 2019). The occlusion of POM within aggregates is an important mechanism protecting OM against microbial decomposition and mineralization (Six et al., 2002; Zimmerman et al., 2004; Keiluweit et al., 2017). Occluded POM belongs to the intermediate pool with turnover times between 10 – 100 years (Lützow et al., 2008). Aggregates provide a physical barrier by spatially separating OM from microorganisms and their extracellular enzymes, as well as by reducing oxygen diffusion into the aggregates (Zimmerman et al., 2004; Keiluweit et al., 2017). The formation of soil aggregates is influenced by various factors, including the activity of soil biota (e.g. by microorganisms), as well as soil moisture, pH, and texture (Six et al., 2004). Aggregation in tidal marshes is significantly influenced by the processes of drying and rewetting, which affect the stability and composition of soil aggregates (Mao et al., 2018; Liu et al., 2021; Ran et al., 2021). The shrinking and swelling of clay minerals during dry-wet cycles and the compression of trapped air in capillary pores during rapid water infiltration potentially destabilize aggregates (Grant and Dexter, 1990). However, frequent drying and rewetting can also lead to a tighter arrangement of soil particles, potentially stabilizing the aggregates (Kemper and Rosenau, 1984). The effects of dry-wet cycles can vary widely depending on soil properties and management practices (Six et al., 2004). While such cycles may promote the formation of macroaggregates, they often do so at the expense of more stable microaggregates, which are critical for long-term OM stabilization (Najera et al., 2020). Much of the research on the effects of dry-wet cycles on aggregates has been conducted in terrestrial soils (Six et al., 2002; Najera et al., 2020), which may not represent the processes occurring in tidal marshes. Moreover, general studies on the role of aggregates in protecting OM in tidal wetlands are limited, partly because of the assumption that the conditions within tidal wetlands do not promote aggregate formation and persistence (Kirwan and

Megonigal, 2013). Indeed, studies have shown that inundation in regularly flooded ecosystems can disrupt soil aggregates (Mao et al., 2018; Liu et al., 2021; Ran et al., 2021). However, research on aggregation in tidal freshwater wetlands has also indicated that a significant portion of SOM can be occluded within large macroaggregates (Maietta et al., 2019). In addition to flooding, increased ionic strength in salt-affected soils can lead to the disruption of aggregates (Wong et al., 2010).

Organo-mineral interactions have emerged as a fundamental mechanism for stabilizing SOM across diverse soil types (Sollins et al., 1996; Schmidt et al., 2011; Wiesmeier et al., 2019). Density fractionation studies indicate that approximately 50 - 90% of SOC is associated with mineral surfaces, indicating that MAOM is the predominant OM fraction in mineral soils (John et al., 2005; Giannetta et al., 2018). Clay minerals are particularly effective in protecting OM as they include a variety of minerals with a high specific surface area, such as phyllosilicates (Lützow et al., 2006; Wiesmeier et al., 2019). Furthermore, metallic sesquioxides, comprising aluminum (Al) and iron (Fe) oxides, hydroxides, and oxyhydroxides, are crucial for the stabilization of OM in soils, as they exhibit a higher affinity for SOM compared to other mineral surfaces, including clay minerals (Sollins et al., 1996; Baldock and Skjemstad, 2000; Kaiser et al., 2012; Bramble et al., 2024). Mineral-associated OM belongs to the intermediate and passive C pool with turnover times > 100 years (Lützow et al., 2008). Typically, small molecules derived from microbial products and exudates (Simpson et al., 2007; Miltner et al., 2012) are associated with minerals via ligand exchange, polyvalent cation bridging, weak interactions, or co-precipitation (Lützow et al., 2006). The role of mineral association for SOC storage in tidal marshes has received limited attention, and further research is required to understand the role of organo-mineral interaction within these ecosystems (Macreadie et al., 2019; Spivak et al., 2019). There is growing evidence that mineral association plays a critical role in the preservation of SOM in tidal marshes. This is supported by studies that directly investigate SOC stabilization in tidal wetlands (Cui et al., 2014; van de Broek et al., 2018; Sun et al., 2019) and by research that provides indirect evidence through the identification of strong correlations between SOC content and clay content (Hansen et al., 2017; Xue et al., 2020). For example, it was demonstrated that approximately one-third of total SOC in marshes was mineral-associated (Sun et al., 2019). An important aspect of organo-mineral interaction in tidal wetlands is the dynamic flooding regime leading to fluctuating redox conditions, which can potentially destabilize MAOM through the reductive dissolution of oxides (Bailey et al., 2019; Spivak et al., 2019; Chen et al., 2020a). At the same time

it was also found that as soil moisture increases, Fe and Al hydroxides become increasingly important in SOC stabilization (Rasmussen et al., 2018).

Given the significant C sequestration potential of tidal marshes, it is crucial to address this knowledge gap. It is particularly important to consider the high spatio-temporal heterogeneity of biogeochemical controls in estuarine marshes, which arises from pronounced environmental gradients in salinity and flooding. While the fundamental biogeochemical controls on C accumulation in soils are well understood, the stability of C in tidal marshes soils remains unclear and particularly knowledge about mineral-associated OM in tidal marshes is particularly limited (Macreadie et al., 2019). To date, most research on SOC stabilization mechanisms has focused on grassland, forest, and agricultural soils, leaving tidal wetlands relatively understudied (Davidson and Janssens, 2006; Sun et al., 2019). Consequently, the understanding of how mineral associations and soil aggregation affect SOC stabilization and storage in estuarine marshes is limited.

1.2 Thesis Objectives and Outline

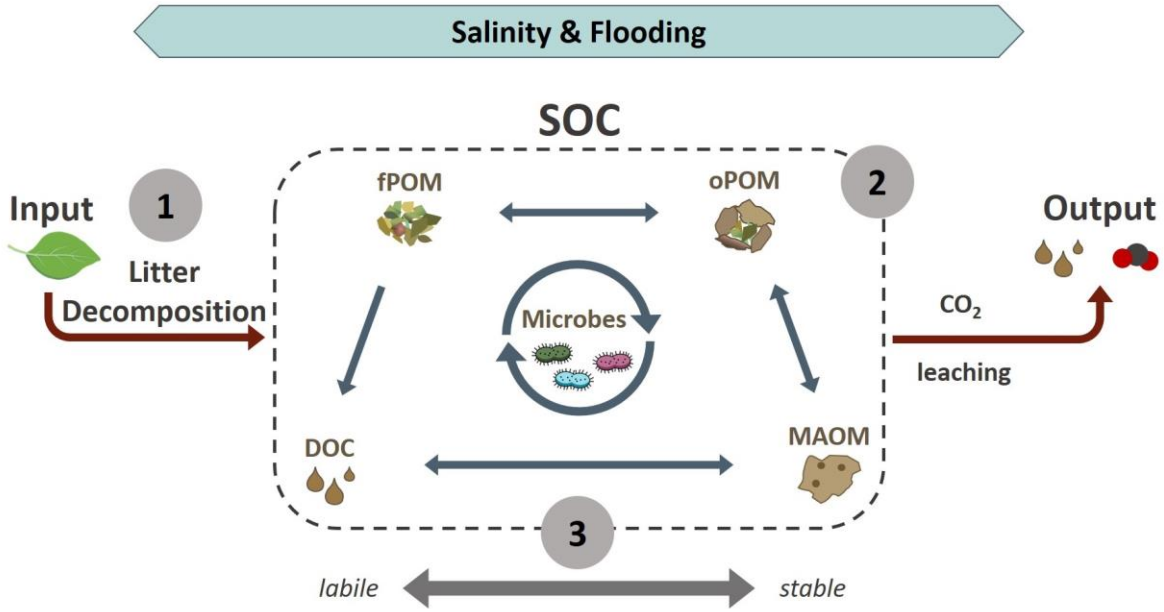

Figure 1: Scheme of the studied soil organic carbon (SOC) dynamics. Numbers indicate related studies in this dissertation (fPOM = free particulate organic matter, oPOM = occluded particulate organic matter, MAOM = mineral-associated organic matter, DOC = dissolved organic carbon).

The aim of this dissertation was to identify major drivers of SOC dynamics in estuarine marshes. The Elbe Estuary (Germany) was selected as a model system

to study effects of the salinity gradient and flooding gradients, reflecting major heterogeneity patterns within the system. Understanding SOC dynamics along estuarine gradients is an essential element for anticipating future changes in these blue carbon ecosystems. A particular focus was to assess how the interaction of the estuarine gradients with biological ecosystem components influences SOC storage. To contribute to a better understanding of SOC dynamics and its drivers in estuarine marshes, this dissertation is structured around three primary research objectives (Figure 1): (I) assessing mechanisms of OM input into marsh soils through litter decomposition (Study A), (II) investigating the SOC stabilization by aggregation and mineral associations (Study B), and (III) studying SOC mineralizability and turnover (Study C). The specific research objectives of the dissertation were:

Study A

The objective of Study A was to assess litter decomposition along the salinity and flooding gradients of the Elbe Estuary by: (I) quantifying litter decomposition rates and stabilization; (II) understanding the roles of environmental conditions and litter quality; (III) considering seasonality; and (IV) linking the prokaryotic communities associated with soil, native litter, and tea litter to litter decomposition.

Study B

The objective of Study B was to (I) quantify SOC stocks and to (II) assess the role of stabilization mechanisms (aggregate-occluded and mineral-associated OC) for SOC storage along the salinity and flooding gradients of the Elbe Estuary. Moreover, (III) findings were related to local site conditions (e.g. soil texture, pH, redox conditions, and vegetation properties) to identify the underlying drivers of SOC storage and stabilization along the estuary.

Study C

The objective of Study C was to assess the mineralizability of SOC pools (labile and stable SOC) along the salinity and flooding gradients and to link SOC turnover with SOC fractions (free, aggregate-occluded and mineral-associated OC) to derive information on the SOC stability along the Elbe Estuary. We hypothesized that SOC mineralizability would increase (I) from the freshwater to the salt marsh due to increasing salinity and reduced SOC stabilization; and (II) in frequently flooded marsh zones due the accumulation of labile SOC under

anoxic conditions. Moreover, we expected a link between C mineralizability and SOC stabilization mechanisms.

Embedment within the RTG 2530

This doctoral project is embedded in the collaborative research training group "Biota-mediated effects on Carbon cycling in Estuaries" (RTG 2530) Universität Hamburg and Leibniz-Institut für Gewässerökologie und Binnenfischerei im Forschungsverbund Berlin e.V. and is funded by the *Deutsche Forschungsgemeinschaft* (DFG, German Research Foundation). The shared research objective of RTG 2530 is to address current knowledge gaps concerning the impact of biota on C cycling in estuarine ecosystems. This initiative involves an interdisciplinary group of researchers with diverse scientific backgrounds, including terrestrial and marine ecology, geoscience, microbiology, and molecular plant and animal biology.

2 Material and Methods

2.1 Study Area: The Elbe Estuary

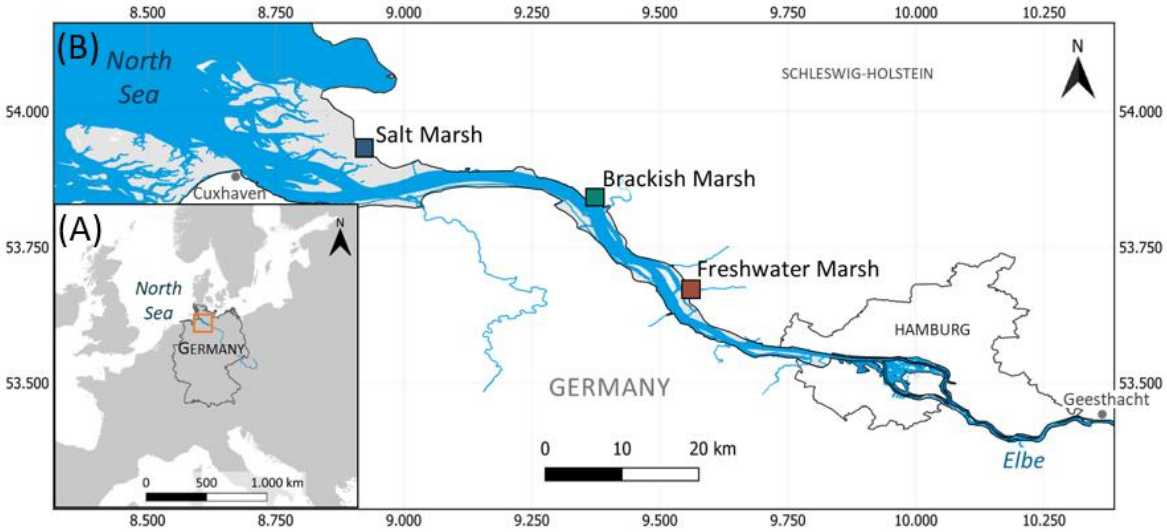

Figure 2: (A) Location of the Elbe Estuary in central Europe (orange rectangle) and (B) location of the marsh sites along the Elbe Estuary (salt marsh: 53°55'40.0"N 8°54'51.3"E/river-km: 710; brackish marsh: 53°50'03.0"N 9°22'15.6"E/river-km: 680; freshwater marsh: 53°39'56.3"N 9°33'11.5"E/river-km: 658) (Data sources: WSV, 2011; EEA, 2017; WSV, 2017).

The Elbe Estuary in Northern Germany was selected as a model system for all three studies of this dissertation (Figure 2). The Elbe Estuary extends approximately 140 kilometers downstream from a weir at Geesthacht, which limits tidal influence further upstream, to its mouth at Cuxhaven where the Elbe flows into the North Sea. The estuary has a semi-diurnal tidal regime that ranges from meso- to macrotidal, with mean tidal ranges between 2.0 m at the weir and 3.5 m at the port of Hamburg (Kappenberg and Grabemann, 2001; Kerner, 2007). The region is characterized by an oceanic climate with a mean annual temperature of 9.3 °C and mean annual rainfall of 812.8 mm (1991 - 2020, federal state of Schleswig-Holstein) (DWD, 2024). The variation in salinity of the river water and tidal flooding led to the formation of distinct marsh types along the shoreline of the estuary. These marsh types differ in their biogeochemical properties and plant species composition. For example, at the salt marsh, the low-lying marsh edge is characterized by salt-tolerant species such as *Spartina anglica* and *Salicornia europaea*. As elevation increases and flooding frequency decreases, *Atriplex portulacoides* and *Aster tripolium* become dominant at mid-marsh elevations, while *Elymus athericus* and *Festuca rubra* are prevalent at higher marsh elevations. Upstream of the estuary, where

salinity decreases, lowest marsh elevations are inhabited by *Bolboschoenus maritimus*, which is gradually replaced by *Phragmites australis* as elevation increases (Engels and Jensen, 2009).

2.2 Study Design: Marsh Research Stations

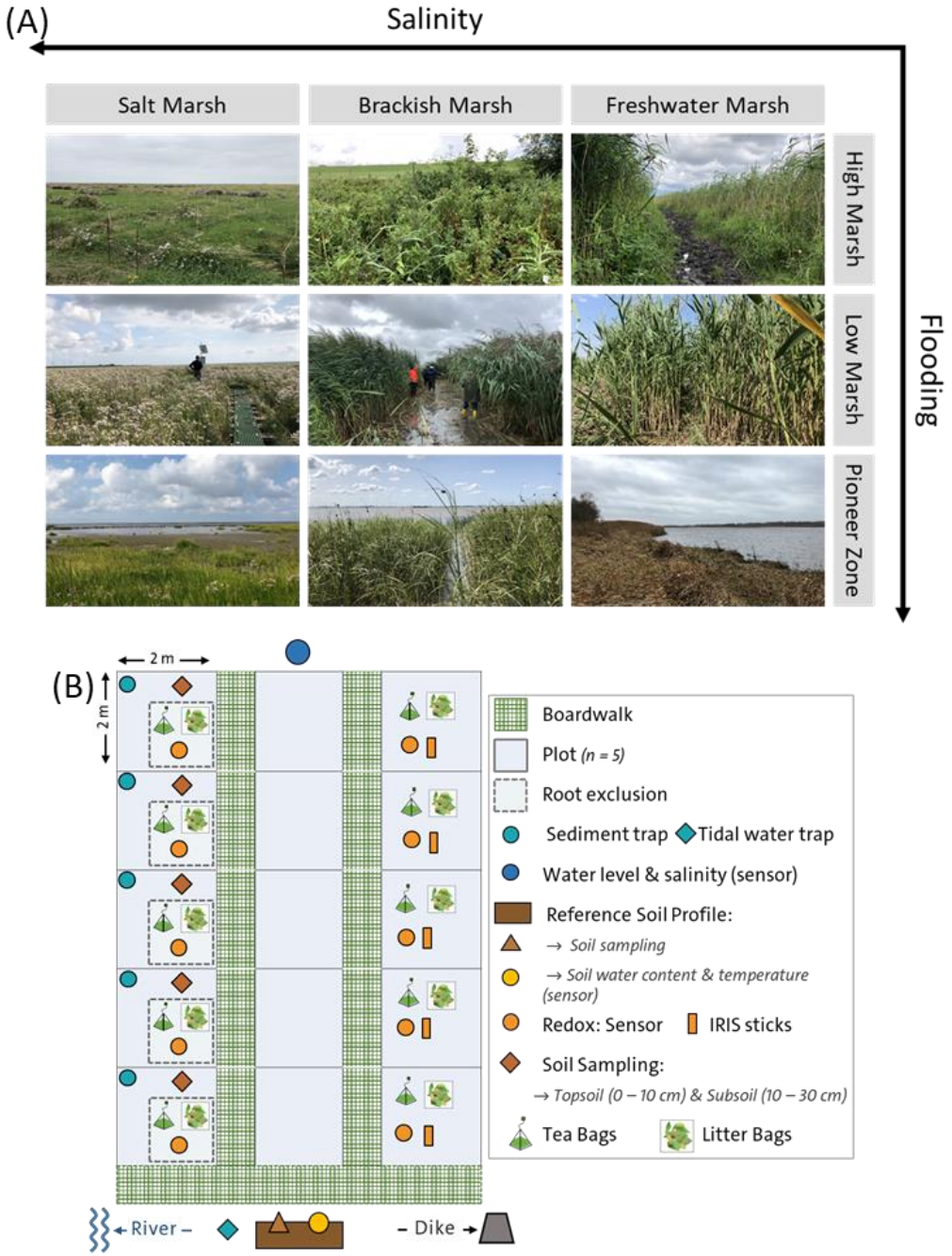

Figure 3: (A) Research sites along the salinity gradient (salt marsh, brackish marsh, and freshwater marsh) and flooding gradients (high marsh = yearly flooding, low marsh = monthly, pioneer zone = daily) and (B) scheme of research stations at each marsh location.

Three distinct marsh types were selected along the salinity gradient: a salt marsh at Kaiser-Wilhelm-Koog, located in the Schleswig-Holstein Wadden Sea National Park at the mouth of the estuary, a brackish marsh near Hollerwettern, and a freshwater marsh within the nature conservation area of Haseldorfer Binnenelbe, closest to Hamburg (Figure 2). At each of these marsh sites, research stations were established in three zones characterized by different flooding frequencies: Pioneer zones (PZ), located closest to the main channel of the Elbe river and flooded during high tide (twice per day); low marshes (LM), which are inundated during spring tides (occurring twice per month at new and full moons); and high marshes (HM), which are periodically flooded during storm tides (a few times per year) (Figure 3 (A)). Each of the nine research stations consisted of three different areas (sampling area, gas flux area, and undisturbed area) with each five adjacent replicate plots (2 x 2 m) (Figure 3 (B)). The selection of the marsh locations was based on dominant plant species typical for the respective salinity and flooding regimes (Engels and Jensen, 2009; Struyf et al., 2009; Branoff et al., 2024, preprint) (Table 1, list of all plant species available in supplement of Study A and B). All research sites are located on the seaward side of a dike and exhibit near-natural conditions.

Table 1: Plant species of each marsh location along the salinity gradient (salt marsh, brackish marsh, freshwater marsh) and flooding gradient (high marsh = yearly flooding, low marsh = monthly, pioneer zone = daily) with > 10% coverage.

Location		**Plant species**
Salt	High marsh	*Elymus athericus* (62%), *Atriplex prostrata* (16%), *Aster tripolium* (13%)
	Low marsh	*Puccinellia maritima* (41%), *Aster tripolium* (18%), *Triglochin maritima* (13%)
	Pioneer zone	*Spartina anglica* (59%)
Brackish	High marsh	*Calystegia sepium* (28%), *Epilobium hirsutum* (24%), *Phragmites australis* (11%)
	Low marsh	*Phragmites australis* (73%)
	Pioneer zone	*Bolboschoenus maritimus* (74%)
Freshwater	High marsh	*Phragmites australis* (54%), *Urtica dioica* (21%)
	Low marsh	*Phragmites australis* (93%)
	Pioneer zone	*Typha angustifolia* (46%), *Caltha palustris* (16%)

2.3 General Site Characterization

Field site monitoring and characterization

At each marsh location (n = 9), a pipe well was installed for continuous monitoring of groundwater levels, temperature, and salinity, as well as sensors for continuous measurement of soil volumetric water content (VWC) and temperature. Furthermore, reference soil profiles were characterized according to the World Reference Base for Soil Resources (WRB) (IUSS Working Group WRB, 2022) between December 2021 and February 2022.

Physico-chemical soil characterization

Topsoil (0 - 10 cm) and subsoil (10 - 30 cm) samples were collected from each marsh location for the general physico-chemical soil characterization, and for the analyses of Study B and Study C. Additionally, undisturbed soil cores for bulk density analysis were derived from each soil profile. Physico-chemical soil properties were characterized by measuring inorganic carbon (TIC), organic carbon (TOC), total carbon (TC), total nitrogen (N), soil texture (sieving and sedimentation method for mineral soils based on Müller et al., 2009), soil pH, and electrical conductivity (EC). For detailed description see Study B.

Soil Reduction Index

Reducing soil conditions were assessed using the "Indicator of Reduction in Soil" (IRIS) method, adapted from Castenson and Rabenhorst (2006) and Rabenhorst (2008). A modified method based on Mittmann-Goetsch et al. (2024) was used. PVC sticks coated with $FeCl_3$-paint were inserted into the soil for four weeks. After retrieval, a reduction index (RI) (0 to 1) was calculated based on the area of removed paint. Full paint removal (RI = 1) indicates more reducing conditions over the four-week period, while an RI of 0 indicates no reducing conditions. For detailed description see Study B.

Aboveground vegetation characteristics

Aboveground vegetation was characterized at the nine marsh locations by assessing the aboveground biomass, measuring C and N contents, identifying plant species, and estimating coverage of plant species. For detailed description see Study A and B.

2.4 Litter Decomposition and Prokaryotic Communities

Tea litter decomposition was assessed using the standardized Tea Bag Index (TBI) following the protocol by Keuskamp et al. (2013). Pairs of green and rooibos tea bags were deployed at each marsh location. After approximately 90 days all tea bags were replaced by new tea bags, to evaluate seasonal changes over four seasons throughout one year. Decomposition rate k_{TBI} and stabilization factor S_{TBI} were calculated based on the tea weight loss according to Keuskamp et al. (2013). In addition, self-made litter bags were used to include decomposition of native litter from each marsh location. Four mesh bags filled with a representative mixture of native aboveground vegetation were placed at the corresponding marsh location. One litter bag was retrieved from each plot after 1, 3, 6, and 12 months. The relative remaining dry mass of native litter over time was used to calculate the decomposition rate k_{LB} by fitting a single pool negative exponential model. Three litter subsamples of each marsh location were analyzed for contents of C, N, cellulose, and lignin. Two to three additional tea bag pairs and one native litter bag were incubated in the field, and together with soil samples, analyzed for their prokaryotic community by metabarcoding sequencing of the 16S rRNA gene variable regions. For detailed description see Study A.

2.5 Soil Organic Carbon Fractions, Pools, and Turnover

Density fractionation

Density fractionation was used to separate SOC fractions into free particulate organic matter (fPOM), occluded particulate organic matter (oPOM), and mineral-associated organic matter (MAOM), following the methods established by Golchin et al. (1994) and Viret and Grand (2019). After separation, the C and N contents of each density fraction was analyzed. Organic carbon associated with each fraction (C_{MAOM}, C_{oPOM}, C_{fPOM}) was expressed as total amounts (mg C g^{-1} soil) or as relative proportions of total SOC (% of total SOC). For detailed description see Study B.

Microbial biomass and dissolved organic carbon

Microbial biomass carbon (MBC) was determined using the chloroform fumigation extraction (CFE) method, adapted from Vance et al. (1987). The amount of MBC was determined by the difference between C concentrations in

chloroform-fumigated and non-fumigated soils. The C from the non-fumigated soils was accepted as extractable dissolved organic carbon (DOC) (Blagodatskaya et al., 2009; Pabst et al., 2013). For detailed description see Study C.

Soil organic carbon mineralization and pools

To quantify the potentially mineralizable C, soil samples were incubated for up to 465 days under optimum temperature and water content in sealed flasks. The cumulative mineralized CO_2 concentration was measured in the headspace over time. A two-pool model, which follows first-order kinetics of decomposition (Andrén and Kätterer, 1997) was employed to distinguish between a fast and a slow C pool and characterize the mean residence time (MRT) of fast, slow, and overall C pool. For detailed description see Study C.

Metabolic quotient and microbial substrate availability

The metabolic quotient (qCO_2) was calculated by dividing basal respiration (CO_2 efflux over one week of incubation) by MBC. Microbial substrate availability was assessed by the ratio of MBC to total SOC (MBC/SOC). For detailed description see Study C.

2.6 Statistical Analyses

Differences in target variables among marsh locations were evaluated by analysis of variance (ANOVA) with TukeyHSD post-hoc comparison or linear mixed-effects model (LME) for repeated measurements. Relationships between variables were explored using simple linear regression and Pearson correlation coefficients, as well as log regression and pearman rank correlation coefficients to account for potential non-linearity. Statistical significance was determined at p-values below 0.05, while p-values between 0.05 and 0.10 were considered to show a tendency towards significance. All statistical analyses were performed in R 4.2.0 (R Core Team, 2022), using "multcomp" (Hothorn et al., 2016) and "multcompView" (Graves et al., 2015) packages, as well as "ggplot2" (Wickham et al., 2016) for data visualization. For detailed description see Study A, B, and C.

3 Key Findings

Table 2: Overview of main objectives and key findings of each study related to this dissertation.

Study	Objective	Key Findings
Study A: *Litter decomposition and prokaryotic decomposer communities along estuarine gradients*	• Investigating the effect of estuarine gradients (i.e. salinity and flooding) on standardized and native litter decomposition • Evaluating the effect of litter quality on decomposition in relation to estuarine gradients • Assess seasonal patterns of litter decomposition • Connect litter decomposition to prokaryotic community composition and diversity	• Increasing salinity decreases tea decomposition, while flooding decreases rates and litter stabilization • Litter quality controls litter decomposition along the estuarine gradients, particularly lignin content • Litter quality drives effect of flooding on decomposition • Soil prokaryotic community adapted to local vegetation • Higher diversity of the prokaryotic soil community stimulates tea mass loss
Study B: *Soil organic carbon stocks and stabilization mechanisms in tidal marshes along estuarine gradients*	• Quantification of SOC stocks along the salinity and flooding gradient of the Elbe Estuary • Assess SOC fractions (free POM: fPOM, aggregate-occluded OM: oPOM, and mineral-associated OM: MAOM) as proxies for SOC stabilization • Identify drivers for SOC storage and SOC stabilization by including site conditions	• Decreasing SOC stocks with increasing salinity and flooding is related to decreasing OM input and SOC stabilization • MAOM is the dominant stabilization mechanism • MAOM decreased with increasing salinity • Clay drives SOC content, as well as SOC stabilization and reflects sedimentation patterns • Lower flooding frequency and salinity favor SOC protection by aggregates • Free POM proportion is higher under reducing soil conditions
Study C: *Connecting organic matter fractions to mineralization dynamics in estuarine marsh soils*	• Characterize SOC mineralizability and SOC pools (labile vs. stable) • Identify functional relationships between C mineralizability, incubation model parameters (SOC pools, MRT), and SOC fractions (fPOM, oPOM, MAOM, DOC) • Gain insights into SOC stability and its drivers	• Increasing SOC mineralizability with increasing salinity due to decreasing SOC stability • SOC turnover increases with increasing flooding and reducing soil conditions • SOC turnover decreases with increasing MAOM and decreasing fPOM and DOC

3.1 Soil Organic Carbon Dynamics along the Salinity Gradient

Litter decomposition

The salinity gradient had a significant effect on litter decomposition, reflecting an interplay of local site conditions and chemical litter quality. Tea litter decomposition decreased with increasing salinity, indicated by decreasing decomposition rates (k_{TBI}) along high marshes and increasing tea litter stabilization (S_{TBI}) across all flooding zones. This observation aligns with previous research indicating the negative impact of salinity on OM decomposition, likely due to reduced microbial activity and microbial biomass (Quintino et al., 2009; Bierschenk et al., 2012; Qu et al., 2019). While tea litter decomposition was negatively affected by higher salinity, native litter decomposed more rapidly (k_{LB}) in salt marshes (Figure 4). This observation was likely related to the chemical composition of the local vegetation, which exhibited increased lability (i.e., lower lignin, cellulose, lignin:N ratios, and C:N ratios) with greater salinity. Numerous studies have emphasized the significance of litter quality for litter decomposition, with lignin content and lignin:N ratios identified as key drivers (Wider and Lang, 1982; Aerts, 1997; Stagg et al., 2018), which was also observed in this study. Notably, the lignin content of freshwater-marsh vegetation was 1.8 times higher than the salt-marsh vegetation. In addition, salinity significantly influenced the structure and diversity of prokaryotic communities within the estuarine marshes, thereby indirectly affecting litter decomposition. Particularly, mass loss of tea litter was positively related to the diversity of soil prokaryotic communities. In contrast, the decomposition of native litter benefitted from soil prokaryotic communities that were adapted to the local litter, indicating a home-field advantage. Therefore, it is essential to consider different litter types in decomposition studies, especially in ecosystems like estuaries with variable OM input pathways (autochthonous and allochthonous). Soil conditions along the salinity gradient also affected litter decomposition. For instance, decomposition rates of both tea and native litter decreased with decreasing N contents in soils from the freshwater to the salt marsh (with the brackish pioneer zone excluded in the case of native litter). Additionally, soil texture influenced the decomposition of both litter types, with higher decomposition rates observed in soils with greater sand and lower clay contents.

Overall, the salinity gradient exerted significant direct and indirect effects on litter decomposition by influencing litter quality, decomposer communities, and soil properties. As a result, the salinity gradient also impacted the overall SOC storage in the estuarine marshes. Total SOC content showed a negative correlation with native litter decomposition, as indicated by decreasing SOC

contents and increasing rates of native litter decomposition from the freshwater to the salt marsh. Thus, litter decomposition is an important factor that drives SOC storage in the marshes of the Elbe Estuary.

SOC storage and stabilization

Soil organic carbon storage (stocks and contents) decreased from freshwater to salt marshes (Figure 4). This trend is commonly documented for estuaries (Kelleway et al., 2016; Kauffman et al., 2020; Gorham et al., 2021; Mazarrasa et al., 2023), and mainly related to decreasing inputs of both autochthonous and allochthonous OM (Butzeck et al., 2015; van de Broek et al., 2018). Accordingly, aboveground plant biomass decreased by 60 - 75% from freshwater to salt marshes in low marshes and pioneer zones. However, it was also shown that this trend was tightly linked to a decreasing degree of SOC stabilization towards the salt marsh (Figure 4). This is supported by a decrease of both mineral-associated (C_{MAOM}) and aggregate-occluded OM (C_{OPOM}) with higher salinity and a strong positive correlation of these fractions with SOC contents and stocks, as well as clay contents. Particularly C_{MAOM} played key role in stabilizing SOC in the Elbe marshes. This importance of mineral association for SOC storage was previously emphasized for salt marshes (Sun et al., 2019), and seems to further increase in the direction of freshwater marshes. Specifically, a higher clay content in freshwater marshes likely enhanced SOC storage and stabilization compared to salt and brackish sites (Kelleway et al., 2016; Gorham et al., 2021; Mazarrasa et al., 2023). The positive effect of clay on the formation of mineral-associated OM and aggregate-occluded OM has been demonstrated in several studies (Six et al., 2002; Lützow et al., 2006; Wiesmeier et al., 2019). With this, variation in soil texture was an important driver of SOC storage through promoting SOC stabilization and decreasing litter decomposition. The distribution of soil texture within estuarine marshes is closely related to sedimentation patterns along the estuary, as the contribution of fine minerogenic particles to sediment deposits is generally higher in freshwater marshes than in salt marshes (Butzeck et al., 2015). This decreasing degree of SOC stabilization with increasing salinity is also evident in SOC turnover.

SOC turnover

The amount of mineralized C (C_{min}) decreased from freshwater to salt marshes, probably linked to the overall reduction in SOC quantities along the salinity gradient and supported by a decreasing microbial biomass (Figure 4). In contrast to the absolute amounts of C_{min}, the proportion of C_{min} in relation to

total SOC (C_{min}/SOC) partly increased with rising salinity and exhibited a negative relationship with SOC contents. This suggests that mechanisms promoting SOC accumulation might have prevented its mineralization. Increasing quantities of relative mineralized C_{min}/SOC from freshwater to salt marshes appeared with enhanced proportions of the fast C pool and a tendency toward shorter mean residence times, indicating SOC contains a larger labile fraction downstream of the estuary. This increasing lability of SOC may be attributed to the previously mentioned decreasing degree of SOC stabilization, particularly by mineral association (Study B). The greater mineralization of this increasingly labile SOC could have been further stimulated by the positive effect of salinity on SOC mineralization (Craft, 2007; Morrissey et al., 2014; Wang et al., 2019). This finding is supported by a positive correlation between C_{min}/SOC and EC, as well as a partly shorter mean residence time (MRT) with increasing EC in topsoils. Overall, this enhanced SOC mineralizability, combined with a reduction in OM input and stabilization, results in decreased SOC storage downstream of the Elbe Estuary. In the context of climate change, saltwater intrusion into estuaries and the corresponding shift of increased salinity zones upstream poses a potential risk of enhanced C output through mineralization, further diminishing the SOC storage potential of estuarine marshes.

3.2 Soil Organic Carbon Dynamics along the Flooding Gradient

Litter decomposition

Tea litter decomposition rates k_{TBI} decreased with increasing flooding frequency at brackish and freshwater marshes (Figure 4). In contrast to many terrestrial ecosystems (Sarneel et al., 2024), these reduced decomposition rates were associated with lower tea litter stabilization factor S_{TBI}, which corresponds to trends observed in other tidal wetlands (Mueller et al., 2018). Differences in the quality of green and rooibos tea likely influenced these decomposition patterns; green tea, which is more nutrient-rich and contains a higher proportion of soluble compounds, was more susceptible to leaching and microbial decomposition, resulting in a decrease in S_{TBI} with increased flooding. In contrast, rooibos tea, characterized by higher lignin content and a lower fraction of water-soluble compounds (Keuskamp et al., 2013), was less appealing to microbial decomposers under oxygen-limited conditions, which contributed to a decline in the decomposition rate k_{TBI}. Previous research has shown that the effects of local conditions on OM decomposition are influenced by OM quality

(Fanin et al., 2020). For instance, labile materials tend to decompose at similar rates in both oxic and anoxic environments, whereas lignin breakdown is significantly slower and often incomplete in anoxic conditions (Kristensen et al., 1995; Hulthe et al., 1998). In case of native litter, increasing flooding decreased decomposition rates at brackish and freshwater marshes, while rates increased at the salt marsh, reflecting variations in the chemical recalcitrance of the vegetation with higher flooding levels. For example, brackish and freshwater pioneer zones showed lignin contents 1.5 times greater than the respective high marshes.

These dynamics were strongly dependent on seasonality with higher variation in less frequently flooded high marshes. Generally, tea decomposition rates k_{TBI} were higher in summer than in winter, while tea stabilization S_{TBI} displayed the opposite trend. Warmer temperatures generally enhance decomposition rates (Blagodatskaya et al., 2016; Mueller et al., 2018; Trevathan-Tackett et al., 2021), but seasonal variations in soil moisture also play a significant role for mediating the decomposer activity (Petraglia et al., 2019). For example, brackish and freshwater high marshes provided optimal conditions for litter decomposition during summer, resulting in the highest overall decomposition rates observed within the study. In contrast, low water availability and high salinity in rarely flooded areas of the salt marsh likely reduced litter decomposition at this location during summer.

SOC storage and stabilization

Flooding had a primarily negative effect on SOC storage, which aligns with previous research in tidal marshes (Spohn and Giani, 2012; Hansen et al., 2017; Kauffman et al., 2020; Mazarrasa et al., 2023) (Figure 4). Similar to the salinity gradient, the decline in SOC storage along the flooding gradient was likely related to a decrease in autochthonous OM inputs, evidenced by decreasing aboveground biomass, as well as decreased allochthonous OM inputs (Butzeck et al., 2015) with increasing flooding frequency. The amounts of C_{MAOM} and C_{oPOM} showed minimal response to flooding at the salt and freshwater marshes but were negatively impacted by increasing flooding at the brackish marsh (Figure 4). This pattern may be again associated with decreasing soil fine texture with more frequent flooding at the brackish marsh, thereby reducing the potential for mineral association and aggregation. Furthermore, higher quantities of C_{oPOM} in topsoils suggest that elevated soil water contents and increased dry-wet cycles may have adversely affected aggregate formation and stability (Six et al., 2004; Liu et al., 2021; Ran et al., 2021). In contrast, oxygen-limitation and reduced OM decomposition (Schmidt et al., 2011) may support the preservation

of C_{fPOM} in pioneer zones, as the contribution C_{fPOM} to total SOC increased towards the pioneer zones (Figure 4). This is further supported by a positive correlation between the proportions of C_{fPOM} and reducing soil conditions (as indicated by the reduction index, RI) of the sampling months.

SOC turnover

The flooding gradient did not demonstrate a clear effect on either absolute or relative quantities of mineralized C (C_{min} or C_{min}/SOC) or on proportions of the fast C pool. This finding contradicts the assumption that frequently flooded marsh zones would harbor greater quantities of (labile) SOC due to the preservation under anoxic conditions. Unlike the trends observed along the salinity gradient, the relationship between C_{min}/SOC and SOC stability (fast and slow C pools) and stabilization (mineral-associated and aggregate-occluded OM) did not exhibit a consistent trend along the flooding gradient, failing to explain the observed variations in relative quantities of mineralized C along the flooding gradient. Despite the lack of a clear trend in mineralized C or fast-pool C along the flooding gradient, the MRT of C decreased with increasing inundation (Figure 4). Specifically, the MRT of the fast C pool decreased across nearly all salinity zones, and the MRT of the overall and slow C pools declined in the freshwater marsh. Coupled with a negative correlation between the MRT of the fast-pool C and reducing soil conditions (as indicated by the RI), these findings suggested that frequent inundation and reducing soil conditions may have restricted SOC mineralization under field conditions. This is consistent with findings that under anaerobic conditions, the decomposition of OM occurs at slower rates, particularly of recalcitrant OM (Benner et al., 1984; Kristensen et al., 1995; Hulthe et al., 1998). Although the decomposition of fresh litter and the mineralization of SOC are distinct processes, findings from Study A indicated that the effect of flooding on tea litter decomposition is highly dependent on litter quality and can vary from a negative to positive influence. Therefore, the assumption that increasing anaerobic conditions would automatically lead to the accumulation of OM may be overly simplistic. Instead, the relationship between flooding and litter quality is leading to high complexity within the decomposition process.

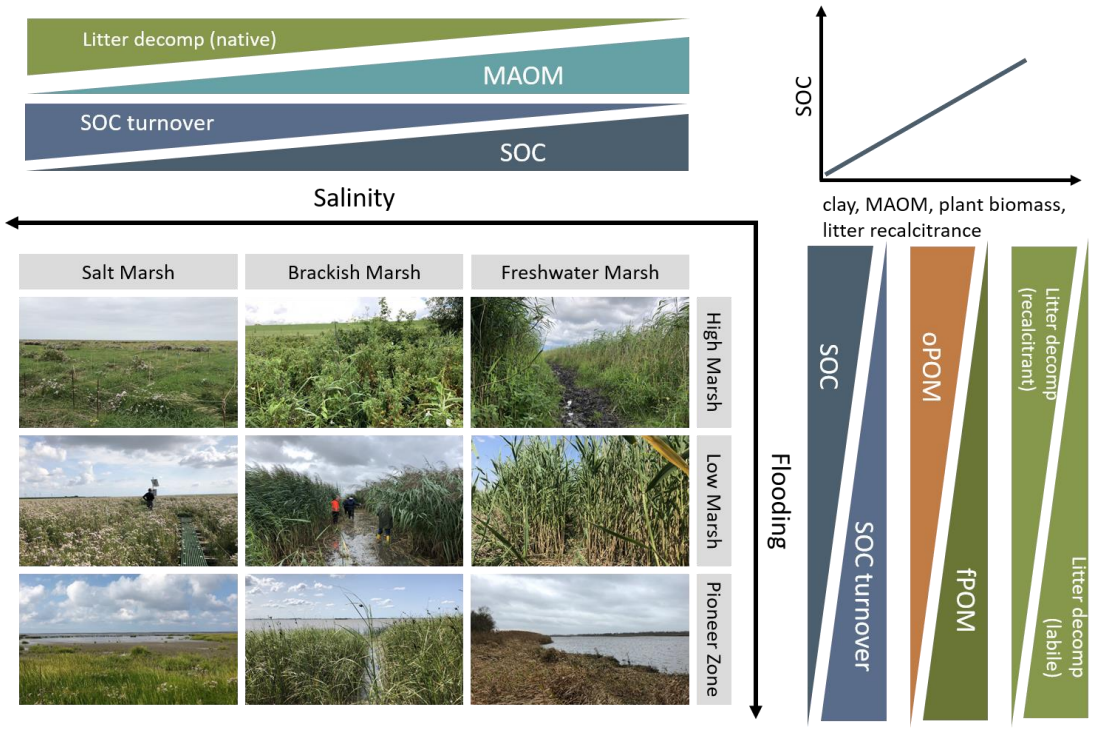

Figure 4: Schematic representation of soil organic carbon (SOC) dynamics (salt marsh, brackish marsh, and freshwater marsh) and flooding gradient (high marsh = yearly flooding, low marsh = monthly, pioneer zone = daily) (SOC = SOC content [%] and stocks [t ha^{-1}], MAOM = mineral-associated organic matter, litter decomp = native litter decomposition rates, oPOM = occluded particulate organic matter, fPOM = free particulate organic matter).

3.3 Which Mechanisms are driving Soil Organic Carbon Stability along the Estuarine Gradients?

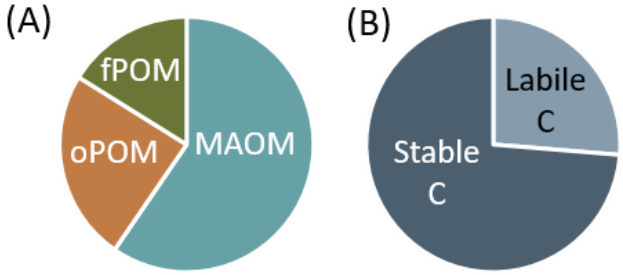

Figure 5: Proportions of (A) SOC fractions and (B) SOC pools as mean % of total SOC in marsh soils of the Elbe Estuary.

The observations on SOC storage, stabilization, and turnover in Study B and Study C underline the importance of critically assessing the mechanisms that control SOC stability in estuarine marshes. Nearly 85% of total SOC was protected by either mineral association (59%) or aggregate occlusion (24%)

(Study B) (Figure 5 (A)). This indicates that a substantial proportion of SOC is likely well protected and may be less susceptible to rapid mineralization. Indeed, results of Study C showed that the majority of SOC in the Elbe Estuary (nearly 75%) was attributed to the slow or stable C pool (Figure 5 (B)). Although MAOM and occluded POM are generally considered to be more stable than free POM (Lützow et al., 2006; Rocci et al., 2021), our data do not support a strict classification of SOC fractions into stability pools. Notably, the proportions of the fast C pool were positively correlated with the DOC concentration in relation to total SOC (DOC/SOC), while no correlation was observed with the relative proportions C_{fPOM}. A possible explanation might be that fPOM can contain a recalcitrant fraction (selective preservation principle) and can belong to the conceptual intermediate C pool (besides the active pool) (von Lützow et al., 2008). The recalcitrance of fPOM is influenced by factors such as its chemical composition, e.g. lignin-rich plant material has been shown to decompose more slowly, especially under anaerobic conditions (Kristensen et al., 1995; Baldock and Skjemstad, 2000; Stagg et al., 2018).

Although fPOM did not directly contribute to the fast C pool, the relative proportions of this SOC fraction were associated with a shorter MRT of the fast C pool, suggesting that a higher proportion of fPOM may have facilitated a faster turnover of labile C. Furthermore, higher DOC concentrations were associated with shorter MRT of all C pools, underlining the labile characteristic of DOC. The relative proportions of C_{MAOM} were positively correlated with amounts of the slow C pool, while the relative proportion of C_{fPOM} exhibited a negative effect; this supports findings of Study B regarding the importance of MAOM for SOC storage. Additionally, it was observed that the MRT of the overall and slow C pools were associated with increasing amounts of C_{oPOM} and C_{MAOM} in topsoils, indicating that enhanced SOC protection prolonged the MRT of C. While categorizing SOC fractions (fPOM, oPOM, MAOM) into C stability pools (fast and slow C) is not straightforward, the various SOC fractions clearly influences the rate of SOC turnover in the marsh soils.

3.4 Biota-Mediated Effects on Soil Organic Carbon Dynamics along Estuarine Gradients

Litter decomposition

Litter quality was the major factor controlling litter decomposition along the estuarine gradients. The chemical litter composition directly influenced both the

rate and extent of decomposition, while also defining how the estuarine gradients impacted this process. For instance, flooding increased the weight loss of labile green tea but decreased the weight loss of more recalcitrant rooibos tea. Additionally, litter decomposition was affected by the composition and diversity of the prokaryotic communities associated with soil, native litter, and tea litter along the estuarine gradients. Certain phyla (e.g. Bacillota, Proteobacteria, Bacteroidota) or order (e.g. Pseudomonadales, Rhizobiales, Flavobacteriales) were more dominant in prokaryotic communities associated with tea and native litter compared to soil communities, indicating that these taxa were involved in litter decomposition along the Elbe Estuary. The diversity and evenness of the prokaryotic community were higher in soil than in the communities associated with native and tea litter. This pattern suggests the selective colonization and a degree of specialization among prokaryotic taxa. The decomposition of foreign tea litter benefitted from a more diverse prokaryotic soil community, generally higher microbial biomass, and higher microbial efficiency (qCO_2) (Study A and Study C). In contrast, native litter decomposition was independent of soil prokaryotic community diversity but increased with microbial efficiency. The overlap between prokaryotic communities associated with native litter and soil suggests that the soil community may have specialized in decomposing litter from local vegetation and indicates a home-field advantage.

SOC storage, stabilization and turnover

The biomass and composition of the local vegetation had a major effect on SOC content, stabilization and mineralizability in the marshes of the Elbe Estuary. The SOC content was generally higher with greater aboveground biomass, higher lignin (excluding the brackish pioneer zone) and cellulose contents, and wider lignin:N ratio (excluding the brackish pioneer zone). Consequently, the reduction of SOC in response to increasing salinity likely resulted from the decline in both the amount and quality of OM input from the local vegetation. Increasing aboveground biomass also increased the amount of all three SOC fractions (fPOM, oPOM, MAOM). Besides the direct input of OM by the vegetation, plants and their roots can initiate and contribute to the formation of aggregate-occluded and mineral-associated OM (Six et al., 2002). Moreover, the quality of the local aboveground vegetation influenced SOC stabilization and mineralizability. Increased lignin and cellulose content, as well as a wider lignin:N ratio of the aboveground vegetation generally led to higher amounts and proportions of C_{MAOM}, and decreased the relative amount of C_{min}/SOC. These

findings indicate that the selective preservation of OM might play a role in the protection and long-term storage of SOC in tidal marshes.

In addition to the local vegetation, soil microbial biomass enhanced the proportions of C_{oPOM} and C_{MAOM}, indicating that microbial activity may have contributed to the formation of stabilized OM. Microorganisms are essential for creating long-term stabilized organic compounds (Miltner et al., 2012). Increased microbial activity can promote the development of soil aggregates, for instance, through the production of mucilages and other exudates (Six et al., 2004). Notably, microbial residues and exudates can account for up to 80% of C in stable SOM fractions (Simpson et al., 2007; Liang and Balser, 2011). In contrast, proportions of C_{fPOM} were negatively affected by the microbial biomass, with low levels of C_{fPOM} in brackish and freshwater high marshes characterized by elevated microbial and aboveground plant biomass. This suggests a rapid turnover of incoming OM at these marsh locations, a finding further supported by particularly fast decomposition rates of tea litter in these areas (Study A).

4 Conclusion and Outlook

4.1 Conclusion for Estuarine Soil Organic Carbon Storage

This dissertation contributed to a better understanding of SOC dynamics in the Elbe Estuary. Soil organic carbon dynamics and their underlying drivers were assessed with regard to abiotic and biotic controls along the salinity and flooding gradients within the estuary.

With increasing salinity, several factors negatively impacted SOC storage in the estuarine marshes. Firstly, there was a decrease in OM input due to the decline in local aboveground plant biomass. Second, the reduced recalcitrance of the local vegetation with increasing salinity resulted in higher litter decomposition rates, which in turn reduced SOC contents. Third, this suggests a greater loss of C during litter decomposition (as CO_2 or DOC) rather than a transformation of OM into more stable forms of SOC. This is reflected in partially decreasing quantities of mineral-associated OM and aggregate-occluded OM in topsoils with increasing salinity, as well as a negative correlation between the decomposition rates of native litter and the proportions of mineral-associated OM. Moreover, potential SOC output increased with rising salinity due to the increasing lability of SOC, leading to higher SOC mineralizability. Ultimately, the interplay between decreasing OM input and increasing OC outputs during decomposition of increasingly labile litter, along with greater mineralizability of increasingly labile SOC, contributes to a decline in SOC storage along the salinity gradient from freshwater to salt marsh.

Along the flooding gradient, SOC contents decreased with increasing flooding frequency at the salt and brackish marshes, whereas no significant changes were observed at the freshwater marsh. This trend was again closely linked to plant biomass. The role of litter decomposition in SOC storage varied along the flooding gradient, influenced by both the quantity and quality of the local vegetation. At the salt marsh, decreasing plant biomass, along with increased native litter decomposition due to lower litter recalcitrance, contributed to a decline in SOC contents as flooding frequency increased. At the brackish marsh, the increase in litter stability could not compensate for the decrease in biomass regarding SOC content. In addition to decreasing OM input by local vegetation with increasing flooding, the SOC mineralizability (reflected in short mean residence time) also increased with higher flooding frequencies, which may have further contributed to the decrease in SOC storage. The mean residence time of C was shortened by the growing contributions of free POM and DOC to total SOC. The proportions of free POM and DOC to total SOC not only

increased with rising flooding levels but also led to a decline in total SOC contents. These findings suggest that the negative effect of flooding on SOC storage in the Elbe Estuary is closely related to decreased OM input and the increasing mineralizability of SOC.

In conclusion, SOC contents decreased with increasing salinity and flooding, which is the result of the interacting effects between decreasing OM input, variations in the chemical composition of the local vegetation affecting litter decomposition, SOC stabilization related to sedimentation dynamics, and increasing SOC mineralizability. It can be expected that the adverse impact of increasing salinity and flooding on SOC storage is likely to be further amplified by climate change.

4.2 Implication for Climate-Change Effects on Soil Organic Carbon Dynamics

Based on observations from all three studies, climate change will likely have a significantly negative impact on SOC storage in the Elbe Estuary through sea-level rise and saltwater intrusion. Increasing salinity may lead to the inland migration of salt marshes at the expense of freshwater marshes, which will strongly affect local plant communities (Craft et al., 2009; Visser et al., 2013). Not only the amount of aboveground vegetation decreased with higher salinity, but the freshwater vegetation also exhibited greater recalcitrance compared to salt marsh vegetation (Study A and Study B). Consequently, shifts in salinity zones could lead to the expansion of areas with reduced aboveground plant biomass and less stable OM. The recalcitrance of local plant litter increased with rising flooding levels at the brackish and freshwater marsh (Study A), indicating that sea-level rise has the potential to elevate the proportion of recalcitrant OM in the estuary. However, a strong sea-level rise, combined with the restricted area of marshes due to dikes, could lead to the transformation of tidal marshes into unvegetated tidal flats and open water (Craft et al., 2009; Visser et al., 2013; Li et al., 2022). This transformation would result in decreased OM input due to reduced local plant biomass, as observed along the salt and brackish flooding gradient. Moreover, it was shown that the increasing recalcitrance of the local vegetation with increasing salinity did not automatically enhance overall SOC storage. In addition, current SOC stabilization in the Elbe Estuary is supported by the fluvial influence within the estuary that promote the accumulation of fine-textured sediments. However, this beneficial effect may be diminished by increased marine influence due to sea-level rise and storm

surges, which can increase the contribution of coarse sediment deposits and reduce the formation of mineral-associated and aggregate-occluded OM.

Ultimately, increasing marine influence may result in decreased OM input and enhanced litter decomposition, along with decreased SOC stabilization and increased SOC mineralizability, leading to an overall decline in SOC storage. Given these observations, it can be expected that climate change will reduce SOC storage in the Elbe Estuary. However, additional research is needed to explore the stability of OM under the ongoing influences of climate change.

4.3 Further Research Perspectives

This dissertation is one of the few comprehensive studies regarding SOC dynamics along environmental gradients within an estuary, addressing the significant heterogeneity in biogeochemical controls. It was demonstrated that mineral association, and to a lesser extent aggregation, are important mechanisms for SOC storage. Soil texture emerged as a key driver of SOC stabilization patterns. Findings also indicated that biota play a major role in SOC stabilization, with local vegetation influencing this process through the amount and chemical composition of OM inputs. Additionally, a strong correlation between microbial biomass and aggregate-occluded OC was observed. However, the mechanisms and processes through which biota mediate SOC stabilization remain unclear, and further research is necessary to elucidate the specific interactions and pathways involved. For example, the concept of selective preservation of recalcitrant OM as a mechanism for SOC stabilization is often questioned for terrestrial soils, while it is assumed that labile OM contributes to long-term SOC storage due to its ready availability to microorganisms and subsequent incorporation into the stable SOC pool (Cotrufo et al., 2013; Cotrufo et al., 2015; Basile-Doelsch et al., 2020). However, this dissertation indicates that the concept of selective preservation may still hold relevance under the unique conditions present in tidal wetlands. Specifically, increasing lignin content of the local vegetation correlates not only with an increase in overall SOC content but also enhances the contribution of mineral-associated OM to total SOC storage. More research is needed to distinguish these mechanisms from one another and assess their influence on SOC in tidal wetlands. To trace the fate of OM an integrated labelling approach could be applied. This could include OM from various sources with different stability e.g. root exudates, plant litter, or allochthonous OM and provide insights in their incorporation into microbial biomass, its transformation into stabilized forms

(e.g. mineral-associated OM), as well as potential destabilization processes leading to losses as DOC or CO_2.

While it is well established that biota significantly influence SOC storage, less is known about how the specific organisms found in intertidal environments affect SOC storage, and even less about their role in SOC stabilization. For example, phytobenthos are important biological communities that are attached to the sediment surface and can directly influence sediment properties through their biological activities e.g. the secretion of extracellular polymeric substances and other compounds, which can initiate the formation of soil aggregates (Winsborough, 2000; Chen et al., 2020b). Moreover, a portion of phytobenthic-derived OM may also directly bind to mineral surfaces in the sediment, leading to the formation of mineral-associated OM. In addition, the role of allochthonous OM for SOC storage and stabilization is not well understood. Studies have shown that allochthonous OM can dominate over autochthonous sources in tidal wetlands (Zhou et al., 2007; van de Broek et al., 2016). Within a modeling approach, it has been indicated that the tidal flats of the Elbe Estuary exhibit significant phytoplankton retention capacities (Steidle and Vennell, 2024) which represent a potential input of labile allochthonous OM into the marsh. Additionally, it has been demonstrated that the composition of suspended OM in the river water of the Elbe Estuary changes spatially and temporally (Tobias-Hünefeldt et al., 2024). Investigating the contribution of allochthonous OM to the overall C budget and to SOC stabilization, as well as its spatio-temporal variation could provide valuable insights into C dynamics that are specific to intertidal environments.

Most previous research, including this dissertation, focused on assessing the current state of SOC stability in estuarine marshes. However, to understand potential climate-change-related shifts in the steady state of the ecosystem, further manipulation experiments are required. Study B and Study C implied that alterations in sea level and increased saline intrusion in estuarine environments are likely to negatively affect SOC stabilization and enhance SOC degradability. A potential experiment could involve an extension of the oxic incubation experiment that was conducted in Study C. An incubation under optimal conditions was chosen to gain insights into the potential mineralizability of SOC along estuarine gradients. Conducting incubations with varying water levels and temperature would be a valuable method for understanding the effects of climate change on mineralization processes in tidal marshes. As sea levels continue to rise, tidal marshes may experience significant changes in their hydrology, potentially resulting in more frequent and prolonged inundation (Jiang et al., 2019). This shift could lead to enhanced anoxic conditions, even in high marshes. Conducting controlled experiments in mesocosms with

manipulated environmental conditions (e.g. increased temperature, salinity, or flooding, simulation of storm floods, changed plant species composition and diversity) and subsequent application of a density fraction or incubation could provide crucial insights into how environmental changes might impact C cycling in estuarine marshes.

Even though a growing body of research increased our knowledge on mechanisms of SOC storage in estuaries and other blue carbon ecosystems, these studies also show the high heterogeneity within and between these ecosystems. Unique biogeochemical conditions, hydrology, and ecological interactions present in tidal wetlands lead to different SOC dynamics. As a consequence, significant uncertainties exist, resulting in inconsistencies in research findings and complicating the ability to generalize and extrapolate results across different systems. In a global review of SOC stocks in tidal marshes, it was highlighted that the majority of the studies were located in the USA, UK, and Australia (Maxwell et al., 2023). Moreover, previous studies, including this thesis, often focused on temperate regions, while arctic and tropical areas, particularly in South America, remain understudied (Macreadie et al., 2019; Maxwell et al., 2023). In addition to focusing on understudied regions, we still lack information on SOC stabilization and its drivers in areas that have been more extensively studied in the past. For example, investigating SOC stabilization in organogenic marshes, as opposed to minerogenic marshes like those of the Elbe Estuary, would provide valuable insights into SOC stability of blue carbon ecosystem. Furthermore, exploring locations with different sediment mineralogy, such as those found in tropical regions, could enhance our understanding of SOC stabilization processes in tidal wetlands. Additionally, it would be worthwhile to consider the impacts of land use and marsh restoration on SOC stabilization. Previous research has demonstrated that natural marshes have different capacities than their restored counterparts to store C in aggregates (Maietta et al., 2019). Overall, this would enable the extrapolation of specific mechanisms and to draw conclusions regarding C storage mechanisms in the estuarine ecosystem on a global scale.

5 References

Aerts, R., 1997. Climate, Leaf Litter Chemistry and Leaf Litter Decomposition in Terrestrial Ecosystems: A Triangular Relationship. Oikos 79, 439.

Allison, S.D., Lu, Y., Weihe, C., Goulden, M.L., Martiny, A.C., Treseder, K.K., Martiny, J.B.H., 2013. Microbial abundance and composition influence litter decomposition response to environmental change. Ecology 94, 714–725.

Andrén, O., Kätterer, T., 1997. ICBM: THE INTRODUCTORY CARBON BALANCE MODEL FOR EXPLORATION OF SOIL CARBON BALANCES. Ecological Applications 7, 1226–1236.

Bailey, V.L., Pries, C.H., Lajtha, K., 2019. What do we know about soil carbon destabilization? Environmental Research Letters 14, 83004.

Baldock, J., Skjemstad, J., 2000. Role of the soil matrix and minerals in protecting natural organic materials against biological attack. Organic Geochemistry 31, 697–710.

Barbier, E.B., Hacker, S.D., Kennedy, C., Koch, E.W., Stier, A.C., Silliman, B.R., 2011. The value of estuarine and coastal ecosystem services. Ecological monographs 81, 169–193.

Basile-Doelsch, I., Balesdent, J., Pellerin, S., 2020. Reviews and syntheses: The mechanisms underlying carbon storage in soil. Biogeosciences 17, 5223–5242.

Becker, J.N., Kuzyakov, Y., 2018. Teatime on Mount Kilimanjaro: Assessing climate and land-use effects on litter decomposition and stabilization using the Tea Bag Index. Land Degradation & Development 29, 2321–2329.

Benner, R., Maccubbin, A.E., Hodson, R.E., 1984. Anaerobic biodegradation of the lignin and polysaccharide components of lignocellulose and synthetic lignin by sediment microflora. Applied and environmental microbiology 47, 998–1004.

Bezemer, T.M., Fountain, M.T., Barea, J.M., Christensen, S., Dekker, S.C., Duyts, H., van Hal, R., Harvey, J.A., Hedlund, K., Maraun, M., Mikola, J., Mladenov, A.G., Robin, C., Ruiter, P.C. de, Scheu, S., Setälä, H., Smilauer, P., van der Putten, W.H., 2010. Divergent composition but similar function of soil food webs of individual plants: plant species and community effects. Ecology 91, 3027–3036.

Bierschenk, A.M., Savage, C., Townsend, C.R., Matthaei, C.D., 2012. Intensity of Land Use in the Catchment Influences Ecosystem Functioning Along a Freshwater-Marine Continuum. Ecosystems 15, 637–651.

Blagodatskaya, E.V., Blagodatsky, S.A., Anderson, T.-H., Kuzyakov, Y., 2009. Contrasting effects of glucose, living roots and maize straw on microbial growth kinetics and substrate availability in soil. European Journal of Soil Science 60, 186–197.

Blagodatskaya, E., Blagodatsky, S., Khomyakov, N., Myachina, O., Kuzyakov, Y., 2016. Temperature sensitivity and enzymatic mechanisms of soil organic matter decomposition along an altitudinal gradient on Mount Kilimanjaro. Scientific Reports 6, 22240.

Bramble, D.S.E., Ulrich, S., Schöning, I., Mikutta, R., Brandt, L., Poll, C., Kandeler, E., Mikutta, C., Konrad, A., Siemens, J., Yang, Y., Polle, A., Schall, P., Ammer, C., Kaiser, K., Schrumpf, M., 2024. Formation of mineral-associated organic matter in

temperate soils is primarily controlled by mineral type and modified by land use and management intensity. Global Change Biology 30, e17024.

Branoff, B.B., Grüterich, L., Wilson, M., Tobias-Hunefeldt, S.P., Saadaoui, Y., Mittmann-Goetsch, J., Neiske, F., Lexmond, F., Becker, J.N., Grossart, H.-P., Porada, P., Streit, W.R., Eschenbach, A., Kutzbach, L., Jensen, K., 2024, preprint. Partitioning biota along the Elbe River estuary: where are the community transitions?

Broome, S.W., Craft, C.B., Burchell, M.R., 2019. Tidal Marsh Creation, in: Coastal Wetlands. Elsevier, pp. 789–816.

Butzeck, C., Eschenbach, A., Gröngröft, A., Hansen, K., Nolte, S., Jensen, K., 2015. Sediment Deposition and Accretion Rates in Tidal Marshes Are Highly Variable Along Estuarine Salinity and Flooding Gradients. Estuaries and Coasts 38, 434–450.

Campbell, A.D., Fatoyinbo, L., Goldberg, L., Lagomasino, D., 2022. Global hotspots of salt marsh change and carbon emissions. Nature 612, 701–706.

Canarini, A., Kaiser, C., Merchant, A., Richter, A., Wanek, W., 2019. Root exudation of primary metabolites: mechanisms and their roles in plant responses to environmental stimuli. Frontiers in plant science 10, 157.

Castenson, K.L., Rabenhorst, M.C., 2006. Indicator of reduction in soil (IRIS) evaluation of a new approach for assessing reduced conditions in soil. Soil Science Society of America Journal 70, 1222–1226.

Chen, C., Hall, S.J., Coward, E., Thompson, A., 2020a. Iron-mediated organic matter decomposition in humid soils can counteract protection. Nature communications 11, 2255.

Chen, D., Li, M., Zhang, Y., Zhang, L., Tang, J., Wu, H., Wang, Y.P., 2020b. Effects of diatoms on erosion and accretion processes in saltmarsh inferred from field observations of hydrodynamic and sedimentary processes. Ecohydrology 13.

Chmura, G.L., Anisfeld, S.C., Cahoon, D.R., Lynch, J.C., 2003. Global carbon sequestration in tidal, saline wetland soils. Global Biogeochemical Cycles 17.

Cotrufo, M.F., Soong, J.L., Horton, A.J., Campbell, E.E., Haddix, M.L., Wall, D.H., Parton, W.J., 2015. Formation of soil organic matter via biochemical and physical pathways of litter mass loss. Nature Geoscience 8, 776–779.

Cotrufo, M.F., Wallenstein, M.D., Boot, C.M., Denef, K., Paul, E., 2013. The Microbial Efficiency-Matrix Stabilization (MEMS) framework integrates plant litter decomposition with soil organic matter stabilization: do labile plant inputs form stable soil organic matter? Global Change Biology 19, 988–995.

Craft, C., 2007. Freshwater input structures soil properties, vertical accretion, and nutrient accumulation of Georgia and U.S tidal marshes. Limnology and Oceanography 52, 1220–1230.

Craft, C., Clough, J., Ehman, J., Joye, S., Park, R., Pennings, S., Guo, H., Machmuller, M., 2009. Forecasting the effects of accelerated sea-level rise on tidal marsh ecosystem services. Frontiers in Ecology and the Environment 7, 73–78.

Crosby, S.C., Sax, D.F., Palmer, M.E., Booth, H.S., Deegan, L.A., Bertness, M.D., Leslie, H.M., 2016. Salt marsh persistence is threatened by predicted sea-level rise. Estuarine, coastal and shelf science 181, 93–99.

Cui, J., Li, Z., Liu, Z., Ge, B., Fang, C., Zhou, C., Tang, B., 2014. Physical and chemical stabilization of soil organic carbon along a 500-year cultived soil chronosequence

originating from estuarine wetlands: Temporal patterns and land use effects. Agriculture, Ecosystems & Environment 196, 10–20.

Daebeler, A., Petrová, E., Kinz, E., Grausenburger, S., Berthold, H., Sandén, T., Angel, R., 2022. Pairing litter decomposition with microbial community structures using the Tea Bag Index (TBI). SOIL 8, 163–176.

Davidson, E.A., Janssens, I.A., 2006. Temperature sensitivity of soil carbon decomposition and feedbacks to climate change. Nature 440, 165–173.

Dorau, K., Mansfeldt, T., 2016. Comparison of redox potential dynamics in a diked marsh soil: 1990 to 1993 versus 2011 to 2014. Journal of Plant Nutrition and Soil Science 179, 641–651.

DWD, 2024. Time series and trends for the parameters temperature and precipitation. Reference period: 1991 - 2020. Federal State of Schleswig-Holstein. https://www.dwd.de/EN/ourservices/zeitreihen/zeitreihen.html#buehneTop, last accessed 20 Feb 2024.

EEA, 2017. EEA coastline for analysis (raw) - version 3.0. https://www.eea.europa.eu/data-and-maps/data/eea-coastline-for-analysis-2/gis-data/eea-coastline-polygon, last accessed 27 Feb 2024.

Egamberdieva, D., Renella, G., Wirth, S., Islam, R., 2010. Secondary salinity effects on soil microbial biomass. Biology and Fertility of Soils 46, 445–449.

Ellenberg, H., Leuschner, C., Dierschke, H., op. 2010. Vegetation Mitteleuropas mit den Alpen. In ökologischer, dyanmischer und historischer Sicht, 6th ed. Verlag Eugen Ulmer, Stuttgart.

Engels, J.G., Jensen, K., 2009. Patterns of wetland plant diversity along estuarine stress gradients of the Elbe (Germany) and Connecticut (USA) Rivers. Plant Ecology & Diversity 2, 301–311.

Fanin, N., Bezaud, S., Sarneel, J.M., Cecchini, S., Nicolas, M., Augusto, L., 2020. Relative Importance of Climate, Soil and Plant Functional Traits during the Early Decomposition Stage of Standardized Litter. Ecosystems 23, 1004–1018.

Fiedler, S., Vepraskas, M.J., Richardson, J.L., 2007. Soil Redox Potential: Importance, Field Measurements, and Observations, in: Elsevier, pp. 1–54.

Franzitta, G., Hanley, M.E., Airoldi, L., Baggini, C., Bilton, D.T., Rundle, S.D., Thompson, R.C., 2015. Home advantage? Decomposition across the freshwater-estuarine transition zone varies with litter origin and local salinity. Marine environmental research 110, 1–7.

Giannetta, B., Plaza, C., Vischetti, C., Cotrufo, M.F., Zaccone, C., 2018. Distribution and thermal stability of physically and chemically protected organic matter fractions in soils across different ecosystems. Biology and Fertility of Soils 54, 671–681.

Golchin, A., Oades, J.M., Skjemstad, J.O., Clarke, P., 1994. Study of free and occluded particulate organic matter in soils by solid state 13C Cp/MAS NMR spectroscopy and scanning electron microscopy. Soil Research 32, 285.

Gorham, C., Lavery, P., Kelleway, J.J., Salinas, C., Serrano, O., 2021. Soil Carbon Stocks Vary Across Geomorphic Settings in Australian Temperate Tidal Marsh Ecosystems. Ecosystems 24, 319–334.

Grant, C.D., Dexter, A.R., 1990. Air entrapment and differential swelling as factors in the mellowing of molded soil during rapid wetting. Soil Research 28, 361.

Graves, S., Piepho, H.-P., Selzer, M.L., 2015. Package 'multcompView'. Visualizations of paired comparisons.

Grüterich, L., Wilson, M., Jensen, K., Streit, W.R., Mueller, P., 2024. Transcriptomic response of wetland microbes to root influence. iScience, 110890. https://doi.org/10.1016/j.isci.2024.110890.

Grüterich, L., Woodhouse, J.N., Mueller, P., Tiemann, A., Ruscheweyh, H., Sunagawa, S., Grossart, H., Streit, W.R., 2025. Assessing environmental gradients in relation to dark CO2 fixation in estuarine wetland microbiomes. Applied Environmental Microbiology 91:e02177-24. https://doi.org/10.1128/aem.02177-24.

Hansen, K., Butzeck, C., Eschenbach, A., Gröngröft, A., Jensen, K., Pfeiffer, E.-M., 2017. Factors influencing the organic carbon pools in tidal marsh soils of the Elbe estuary (Germany). Journal of Soils and Sediments 17, 47–60.

Hemminga, M.A., Leeuw, J. de, Munek, W. de, Koutstaal, B.P., 1991. Decomposition in estuarine salt marshes: the effect of soil salinity and soil water content. Vegetatio 94, 25–33.

Hoffland, E., Kuyper, T.W., Comans, R.N.J., Creamer, R.E., 2020. Eco-functionality of organic matter in soils. Plant and Soil 455, 1–22.

Hothorn, T., Bretz, F., Westfall, P., Heiberger, R.M., Schuetzenmeister, A., Scheibe, S., Hothorn, M.T., 2016. Package 'multcomp'. Simultaneous inference in general parametric models. Project for Statistical Computing, Vienna, Austria.

Hulthe, G., Hulth, S., Hall, P.O., 1998. Effect of oxygen on degradation rate of refractory and labile organic matter in continental margin sediments. Geochimica et Cosmochimica Acta 62, 1319–1328.

IPCC, 2023. Sections, in: IPCC, 2023: Climate Change 2023: Synthesis Report. Contribution of Working Groups I, II and III to the Sixth Assessment Report of the Intergovernmental Panel on Climate Change [Core Writing Team, H. Lee and J. Romero (eds.)]. IPCC, Geneva, Switzerland. Intergovernmental Panel on Climate Change (IPCC).

IUSS Working Group WRB, 2022. World reference base for soil resources 2022. International soil classification system for naming soils and creating legends for soil maps, 4th ed. International Union of Soil Sciences (IUSS), Vienna, Austria.

Jiang, Z., Lu, Y., Xu, J., Li, M., Shan, G., Li, Q., 2019. Exploring the characteristics of dissolved organic matter and succession of bacterial community during composting. Bioresource technology 292, 121942.

John, B., Yamashita, T., Ludwig, B., Flessa, H., 2005. Storage of organic carbon in aggregate and density fractions of silty soils under different types of land use. Geoderma 128, 63–79.

Kaiser, M., Ellerbrock, R.H., Wulf, M., Dultz, S., Hierath, C., Sommer, M., 2012. The influence of mineral characteristics on organic matter content, composition, and stability of topsoils under long-term arable and forest land use. Journal of Geophysical Research: Biogeosciences 117.

Kappenberg, J., Grabemann, I., 2001. Variability of the mixing zones and estuarine turbidity maxima in the Elbe and Weser estuaries. Estuaries 24, 699–706.

Kauffman, J.B., Giovanonni, L., Kelly, J., Dunstan, N., Borde, A., Diefenderfer, H., Cornu, C., Janousek, C., Apple, J., Brophy, L., 2020. Total ecosystem carbon stocks at the marine-terrestrial interface: Blue carbon of the Pacific Northwest Coast, United States. Global Change Biology 26, 5679–5692.

Keiluweit, M., Wanzek, T., Kleber, M., Nico, P., Fendorf, S., 2017. Anaerobic microsites have an unaccounted role in soil carbon stabilization. Nature communications 8, 1771.

Kelleway, J.J., Saintilan, N., Macreadie, P.I., Ralph, P.J., 2016. Sedimentary Factors are Key Predictors of Carbon Storage in SE Australian Saltmarshes. Ecosystems 19, 865–880.

Kemper, W.D., Rosenau, R.C., 1984. Soil Cohesion as Affected by Time and Water Content. Soil Science Society of America Journal 48, 1001–1006.

Kennish, M.J., 2002. Environmental threats and environmental future of estuaries. Environmental Conservation 29, 78–107.

Kerner, M., 2007. Effects of deepening the Elbe Estuary on sediment regime and water quality. Estuarine, coastal and shelf science 75, 492–500.

Keuskamp, J.A., Dingemans, B.J.J., Lehtinen, T., Sarneel, J.M., Hefting, M.M., 2013. Tea Bag Index: a novel approach to collect uniform decomposition data across ecosystems. Methods in Ecology and Evolution 4, 1070–1075.

Kirwan, M.L., Megonigal, J.P., 2013. Tidal wetland stability in the face of human impacts and sea-level rise. Nature 504, 53–60.

Kögel-Knabner, I., 2017. The macromolecular organic composition of plant and microbial residues as inputs to soil organic matter: Fourteen years on. Soil Biology and Biochemistry 105, A3-A8.

Kristensen, E., Ahmed, S.I., Devol, A.H., 1995. Aerobic and anaerobic decomposition of organic matter in marine sediment: Which is fastest? Limnology and Oceanography 40, 1430–1437.

Li, F., Angelini, C., Byers, J.E., Craft, C., Pennings, S.C., 2022. Responses of a tidal freshwater marsh plant community to chronic and pulsed saline intrusion. Journal of Ecology 110, 1508–1524.

Liang, C., Balser, T.C., 2011. Microbial production of recalcitrant organic matter in global soils: implications for productivity and climate policy. Nature reviews. Microbiology 9, 75; author reply 75.

Liu, Y., Ma, M., Ran, Y., Yi, X., Wu, S., Huang, P., 2021. Disentangling the effects of edaphic and vegetational properties on soil aggregate stability in riparian zones along a gradient of flooding stress. Geoderma 385, 114883.

Lopes, M.L., Martins, P., Ricardo, F., Rodrigues, A.M., Quintino, V., 2011. In situ experimental decomposition studies in estuaries: A comparison of Phragmites australis and Fucus vesiculosus. Estuarine, coastal and shelf science 92, 573–580.

Luo, M., Huang, J.-F., Zhu, W.-F., Tong, C., 2019. Impacts of increasing salinity and inundation on rates and pathways of organic carbon mineralization in tidal wetlands: a review. Hydrobiologia 827, 31–49.

Lützow, M.v., Kögel-Knabner, I., Ekschmitt, K., Matzner, E., Guggenberger, G., Marschner, B., Flessa, H., 2006. Stabilization of organic matter in temperate soils: mechanisms and their relevance under different soil conditions – a review. European Journal of Soil Science 57, 426–445.

Lützow, M. von, Kögel-Knabner, I., Ludwig, B., Matzner, E., Flessa, H., Ekschmitt, K., Guggenberger, G., Marschner, B., Kalbitz, K., 2008. Stabilization mechanisms of organic matter in four temperate soils: Development and application of a conceptual model. Journal of Plant Nutrition and Soil Science 171, 111–124.

Macreadie, P.I., Anton, A., Raven, J.A., Beaumont, N., Connolly, R.M., Friess, D.A., Kelleway, J.J., Kennedy, H., Kuwae, T., Lavery, P.S., Lovelock, C.E., Smale, D.A., Apostolaki, E.T., Atwood, T.B., Baldock, J., Bianchi, T.S., Chmura, G.L., Eyre, B.D., Fourqurean, J.W., Hall-Spencer, J.M., Huxham, M., Hendriks, I.E., Krause-Jensen, D., Laffoley, D., Luisetti, T., Marbà, N., Masque, P., McGlathery, K.J., Megonigal, J.P., Murdiyarso, D., Russell, B.D., Santos, R., Serrano, O., Silliman, B.R., Watanabe, K., Duarte, C.M., 2019. The future of Blue Carbon science. Nature communications 10, 3998.

Maietta, C.E., Bernstein, Z.A., Gaimaro, J.R., Buyer, J.S., Rabenhorst, M.C., Monsaint-Queeney, V.L., Baldwin, A.H., Yarwood, S.A., 2019. Aggregation but Not Organo-Metal Complexes Contributed to C Storage in Tidal Freshwater Wetland Soils. Soil Science Society of America Journal 83, 252–265.

Makkonen, M., Berg, M.P., Handa, I.T., Hättenschwiler, S., van Ruijven, J., van Bodegom, P.M., Aerts, R., 2012. Highly consistent effects of plant litter identity and functional traits on decomposition across a latitudinal gradient. Ecology letters 15, 1033–1041.

Mao, R., Ye, S.-Y., Zhang, X.-H., 2018. Soil-Aggregate-Associated Organic Carbon along Vegetation Zones in Tidal Salt Marshes in the Liaohe Delta. CLEAN – Soil, Air, Water 46.

Marley, A.R., Smeaton, C., Austin, W.E., 2019. An Assessment of the Tea Bag Index Method as a Proxy for Organic Matter Decomposition in Intertidal Environments. Journal of Geophysical Research: Biogeosciences 124, 2991–3004.

Marschner, B., Brodowski, S., Dreves, A., Gleixner, G., Gude, A., Grootes, P.M., Hamer, U., Heim, A., Jandl, G., Ji, R., Kaiser, K., Kalbitz, K., Kramer, C., Leinweber, P., Rethemeyer, J., Schäffer, A., Schmidt, M.W.I., Schwark, L., Wiesenberg, G.L.B., 2008. How relevant is recalcitrance for the stabilization of organic matter in soils? Journal of Plant Nutrition and Soil Science 171, 91–110.

Maxwell, T.L., Rovai, A.S., Adame, M.F., Adams, J.B., Álvarez-Rogel, J., Austin, W.E.N., Beasy, K., Boscutti, F., Böttcher, M.E., Bouma, T.J., Bulmer, R.H., Burden, A., Burke, S.A., Camacho, S., Chaudhary, D.R., Chmura, G.L., Copertino, M., Cott, G.M., Craft, C., Day, J., Los Santos, C.B. de, Denis, L., Ding, W., Ellison, J.C., Ewers Lewis, C.J., Giani, L., Gispert, M., Gontharet, S., González-Pérez, J.A., González-Alcaraz, M.N., Gorham, C., Graversen, A.E.L., Grey, A., Guerra, R., He, Q., Holmquist, J.R., Jones, A.R., Juanes, J.A., Kelleher, B.P., Kohfeld, K.E., Krause-Jensen, D., Lafratta, A., Lavery, P.S., Laws, E.A., Leiva-Dueñas, C., Loh, P.S., Lovelock, C.E., Lundquist, C.J., Macreadie, P.I., Mazarrasa, I., Megonigal, J.P., Neto, J.M., Nogueira, J., Osland, M.J., Pagès, J.F., Perera, N., Pfeiffer, E.-M., Pollmann, T., Raw, J.L., Recio, M., Ruiz-Fernández, A.C., Russell, S.K., Rybczyk, J.M., Sammul, M., Sanders, C., Santos, R., Serrano, O., Siewert, M., Smeaton, C., Song, Z., Trasar-Cepeda, C., Twilley, R.R., van de Broek, M., Vitti, S., Antisari, L.V., Voltz, B., Wails, C.N., Ward, R.D., Ward, M., Wolfe, J., Yang, R., Zubrzycki, S., Landis, E., Smart, L., Spalding, M., Worthington, T.A., 2023. Global dataset of soil organic carbon in tidal marshes. Scientific data 10, 797.

Mazarrasa, I., Neto, J.M., Bouma, T.J., Grandjean, T., Garcia-Orellana, J., Masqué, P., Recio, M., Serrano, Ó., Puente, A., Juanes, J.A., 2023. Drivers of variability in Blue Carbon stocks and burial rates across European estuarine habitats. The Science of the total environment 886, 163957.

Mcleod, E., Chmura, G.L., Bouillon, S., Salm, R., Björk, M., Duarte, C.M., Lovelock, C.E., Schlesinger, W.H., Silliman, B.R., 2011. A blueprint for blue carbon: toward an improved understanding of the role of vegetated coastal habitats in sequestering CO 2. Frontiers in Ecology and the Environment 9, 552–560.

Miltner, A., Bombach, P., Schmidt-Brücken, B., Kästner, M., 2012. SOM genesis: microbial biomass as a significant source. Biogeochemistry 111, 41–55.

Minick, K.J., Mitra, B., Noormets, A., King, J.S., 2019. Saltwater reduces potential CO_2 and CH_4 production in peat soils from a coastal freshwater forested wetland. Biogeosciences 16, 4671–4686.

Mitsch, W.J., Bernal, B., Hernandez, M.E., 2015. Ecosystem services of wetlands. International Journal of Biodiversity Science, Ecosystem Services & Management 11, 1–4.

Mittmann-Goetsch, J., Wilson, M., Jensen, K., Mueller, P., 2024. Root-driven soil reduction in Wadden Sea salt marshes. Wetlands 44. https://doi.org/10.1007/s13157-024-01867-8.

Morrissey, E.M., Gillespie, J.L., Morina, J.C., Franklin, R.B., 2014. Salinity affects microbial activity and soil organic matter content in tidal wetlands. Global Change Biology 20, 1351–1362.

Mueller, P., Schile-Beers, L.M., Mozdzer, T.J., Chmura, G.L., Dinter, T., Kuzyakov, Y., Groot, A.V. de, Esselink, P., Smit, C., D'Alpaos, A., Ibáñez, C., Lazarus, M., Neumeier, U., Johnson, B.J., Baldwin, A.H., Yarwood, S.A., Montemayor, D.I., Yang, Z., Wu, J., Jensen, K., Nolte, S., 2018. Global-change effects on early-stage decomposition processes in tidal wetlands – implications from a global survey using standardized litter. Biogeosciences 15, 3189–3202.

Müller, H.-W., Dohrmann, R., Klosa, D., Rehder, S., Eckelmann, W., 2009. Comparison of two procedures for particle-size analysis: Köhn pipette and X-ray granulometry. Journal of Plant Nutrition and Soil Science 172, 172–179.

Najera, F., Dippold, M.A., Boy, J., Seguel, O., Koester, M., Stock, S., Merino, C., Kuzyakov, Y., Matus, F., 2020. Effects of drying/rewetting on soil aggregate dynamics and implications for organic matter turnover. Biology and Fertility of Soils 56, 893–905.

Nelson, N.G., Muñoz-Carpena, R., Neale, P.J., Tzortziou, M., Megonigal, J.P., 2017. Temporal variability in the importance of hydrologic, biotic, and climatic descriptors of dissolved oxygen dynamics in a shallow tidal-marsh creek. Water Resources Research 53, 7103–7120.

Ontl, T.A., Schulte, L.A., 2012. Soil carbon storage. Nature Education Knowledge 3.

Pabst, H., Kühnel, A., Kuzyakov, Y., 2013. Effect of land-use and elevation on microbial biomass and water extractable carbon in soils of Mt. Kilimanjaro ecosystems. Applied Soil Ecology 67, 10–19.

Petraglia, A., Cacciatori, C., Chelli, S., Fenu, G., Calderisi, G., Gargano, D., Abeli, T., Orsenigo, S., Carbognani, M., 2019. Litter decomposition: effects of temperature driven by soil moisture and vegetation type. Plant and Soil 435, 187–200.

Qu, W., Li, J., Han, G., Wu, H., Song, W., Zhang, X., 2019. Effect of salinity on the decomposition of soil organic carbon in a tidal wetland. Journal of Soils and Sediments 19, 609–617.

Quintino, V., Sangiorgio, F., Ricardo, F., Mamede, R., Pires, A., Freitas, R., Rodrigues, A.M., Basset, A., 2009. In situ experimental study of reed leaf decomposition along a full salinity gradient. Estuarine, coastal and shelf science 85, 497–506.

R Core Team, 2022. R. A language and environment for statistical computing. R Foundation for Statistical Computing, Vienna, Austria.

Rabenhorst, M.C., 2008. Protocol for using and interpreting IRIS tubes. Soil Survey Horizons 49, 74–77.

Ran, Y., Ma, M., Liu, Y., Zhou, Y., Sun, X., Wu, S., Huang, P., 2021. Hydrological stress regimes regulate effects of binding agents on soil aggregate stability in the riparian zones. CATENA 196, 104815.

Rasmussen, C., Heckman, K., Wieder, W.R., Keiluweit, M., Lawrence, C.R., Berhe, A.A., Blankinship, J.C., Crow, S.E., Druhan, J.L., Hicks Pries, C.E., Marin-Spiotta, E., Plante, A.F., Schädel, C., Schimel, J.P., Sierra, C.A., Thompson, A., Wagai, R., 2018. Beyond clay: towards an improved set of variables for predicting soil organic matter content. Biogeochemistry 137, 297–306.

Roache, M.C., Bailey, P.C., Boon, P.I., 2006. Effects of salinity on the decay of the freshwater macrophyte, Triglochin procerum. Aquatic Botany 84, 45–52.

Rocci, K.S., Lavallee, J.M., Stewart, C.E., Cotrufo, M.F., 2021. Soil organic carbon response to global environmental change depends on its distribution between mineral-associated and particulate organic matter: A meta-analysis. The Science of the total environment 793, 148569.

Sarneel, J.M., Hefting, M.M., Sandén, T., van den Hoogen, J., Routh, D., Adhikari, B.S., Alatalo, J.M., Aleksanyan, A., Althuizen, I.H.J., Alsafran, M.H.S.A., Atkins, J.W., Augusto, L., Aurela, M., Azarov, A.V., Barrio, I.C., Beier, C., Bejarano, M.D., Benham, S.E., Berg, B., Bezler, N.V., Björnsdóttir, K., Bolinder, M.A., Carbognani, M., Cazzolla Gatti, R., Chelli, S., Chistotin, M.V., Christiansen, C.T., Courtois, P., Crowther, T.W., Dechoum, M.S., Djukic, I., Duddigan, S., Egerton-Warburton, L.M., Fanin, N., Fantappiè, M., Fares, S., Fernandes, G.W., Filippova, N.V., Fliessbach, A., Fuentes, D., Godoy, R., Grünwald, T., Guzmán, G., Hawes, J.E., He, Y., Hero, J.-M., Hess, L.L., Hogendoorn, K., Høye, T.T., Jans, W.W.P., Jónsdóttir, I.S., Keller, S., Kepfer-Rojas, S., Kuz'menko, N.N., Larsen, K.S., Laudon, H., Lembrechts, J.J., Li, J., Limousin, J.-M., Lukin, S.M., Marques, R., Marín, C., McDaniel, M.D., Meek, Q., Merzlaya, G.E., Michelsen, A., Montagnani, L., Mueller, P., Murugan, R., Myers-Smith, I.H., Nolte, S., Ochoa-Hueso, R., Okafor, B.N., Okorkov, V.V., Onipchenko, V.G., Orozco, M.C., Parkhurst, T., Peres, C.A., Petit Bon, M., Petraglia, A., Pingel, M., Rebmann, C., Scheffers, B.R., Schmidt, I., Scholes, M.C., Sheffer, E., Shevtsova, L.K., Smith, S.W., Sofo, A., Stevenson, P.R., Strouhalová, B., Sundsdal, A., Sühs, R.B., Tamene, G., Thomas, H.J.D., Tolunay, D., Tomaselli, M., Tresch, S., Tucker, D.L., Ulyshen, M.D., Valdecantos, A., Vandvik, V., Vanguelova, E.I., Verheyen, K., Wang, X., Yahdjian, L., Yumashev, X.S., Keuskamp, J.A., 2024. Reading tea leaves worldwide: Decoupled drivers of initial litter decomposition mass-loss rate and stabilization. Ecology letters 27, e14415.

Schmidt, M.W.I., Torn, M.S., Abiven, S., Dittmar, T., Guggenberger, G., Janssens, I.A., Kleber, M., Kögel-Knabner, I., Lehmann, J., Manning, D.A.C., Nannipieri, P., Rasse, D.P., Weiner, S., Trumbore, S.E., 2011. Persistence of soil organic matter as an ecosystem property. Nature 478, 49–56.

Schulte Ostermann, T., Heuner, M., Fuchs, E., Temmerman, S., Schoutens, K., Bouma, T.J., Minden, V., 2024. Identifying Key Plant Traits and Ecosystem Properties

Affecting Wave Attenuation and the Soil Organic Carbon Content in Tidal Marshes. Estuaries and Coasts 47, 144–161.

Setia, R., Marschner, P., Baldock, J., Chittleborough, D., Smith, P., Smith, J., 2011. Salinity effects on carbon mineralization in soils of varying texture. Soil Biology and Biochemistry 43, 1908–1916.

Seyfferth, A.L., Bothfeld, F., Vargas, R., Stuckey, J.W., Wang, J., Kearns, K., Michael, H.A., Guimond, J., Yu, X., Sparks, D.L., 2020. Spatial and temporal heterogeneity of geochemical controls on carbon cycling in a tidal salt marsh. Geochimica et Cosmochimica Acta 282, 1–18.

Sierra, C.A., Trumbore, S.E., Davidson, E.A., Vicca, S., Janssens, I., 2015. Sensitivity of decomposition rates of soil organic matter with respect to simultaneous changes in temperature and moisture. Journal of Advances in Modeling Earth Systems 7, 335–356.

Simpson, A.J., Simpson, M.J., Smith, E., Kelleher, B.P., 2007. Microbially derived inputs to soil organic matter: are current estimates too low? Environmental Science & Technology 41, 8070–8076.

Six, J., Bossuyt, H., Degryze, S., Denef, K., 2004. A history of research on the link between (micro)aggregates, soil biota, and soil organic matter dynamics. Soil and Tillage Research 79, 7–31.

Six, J., Feller, C., Denef, K., Ogle, S.M., Moraes, J.C. de, Albrecht, A., 2002. Soil organic matter, biota and aggregation in temperate and tropical soils - Effects of no-tillage. Agronomie 22, 755–775.

Smith, J.L., Paul, E.A., 2017. The significance of soil microbial biomass estimations, in: Soil biochemistry. Routledge, pp. 357–398.

Sollins, P., Homann, P., Caldwell, B.A., 1996. Stabilization and destabilization of soil organic matter: mechanisms and controls. Geoderma 74, 65–105.

Spivak, A.C., Sanderman, J., Bowen, J.L., Canuel, E.A., Hopkinson, C.S., 2019. Global-change controls on soil-carbon accumulation and loss in coastal vegetated ecosystems. Nature Geoscience 12, 685–692.

Spohn, M., Giani, L., 2012. Carbohydrates, carbon and nitrogen in soils of a marine and a brackish marsh as influenced by inundation frequency. Estuarine, coastal and shelf science 107, 89–96.

Stagg, C.L., Baustian, M.M., Perry, C.L., Carruthers, T.J.B., Hall, C.T., 2018. Direct and indirect controls on organic matter decomposition in four coastal wetland communities along a landscape salinity gradient. Journal of Ecology 106, 655–670.

Steidle, L., Vennell, R., 2024. Phytoplankton retention mechanisms in estuaries: a case study of the Elbe estuary. Nonlinear Processes in Geophysics 31, 151–164.

Struyf, E., Jacobs, S., Meire, P., Jensen, K., Barendregt, A., 2009. Plant communities of European tidal freshwater wetlands, in: Tidal Freshwater Wetlands.

Sun, H., Jiang, J., Cui, L., Feng, W., Wang, Y., Zhang, J., 2019. Soil organic carbon stabilization mechanisms in a subtropical mangrove and salt marsh ecosystems. The Science of the total environment 673, 502–510.

Talbot, J.M., Treseder, K.K., 2011. Dishing the dirt on carbon cycling. Nature Climate Change 1, 144–146.

Telesh, I.V., Khlebovich, V.V., 2010. Principal processes within the estuarine salinity gradient: a review. Marine pollution bulletin 61, 149–155.

Tobias-Hünefeldt, S.P., van Beusekom, J.E.E., Russnak, V., Dähnke, K., Streit, W.R., Grossart, H.-P., 2024. Seasonality, rather than estuarine gradient or particle suspension/sinking dynamics, determines estuarine carbon distributions. The Science of the total environment 926, 171962.

Trevathan-Tackett, S.M., Kepfer-Rojas, S., Engelen, A.H., York, P.H., Ola, A., Li, J., Kelleway, J.J., Jinks, K.I., Jackson, E.L., Adame, M.F., Pendall, E., Lovelock, C.E., Connolly, R.M., Watson, A., Visby, I., Trethowan, A., Taylor, B., Roberts, T.N.B., Petch, J., Farrington, L., Djukic, I., Macreadie, P.I., 2021. Ecosystem type drives tea litter decomposition and associated prokaryotic microbiome communities in freshwater and coastal wetlands at a continental scale. The Science of the total environment 782, 146819.

Valiela, I., Teal, J.M., Allen, S.D., van Etten, R., Goehringer, D., Volkmann, S., 1985. Decomposition in salt marsh ecosystems: The phases and major factors affecting disappearance of above-ground organic matter. Journal of Experimental Marine Biology and Ecology 89, 29–54.

van de Broek, M., Temmerman, S., Merckx, R., Govers, G., 2016. Controls on soil organic carbon stocks in tidal marshes along an estuarine salinity gradient. Biogeosciences 13, 6611–6624.

van de Broek, M., Vandendriessche, C., Poppelmonde, D., Merckx, R., Temmerman, S., Govers, G., 2018. Long-term organic carbon sequestration in tidal marsh sediments is dominated by old-aged allochthonous inputs in a macrotidal estuary. Global Change Biology 24, 2498–2512.

Vance, E.D., Brookes, P.C., Jenkinson, D.S., 1987. An extraction method for measuring soil microbial biomass C. Soil Biology and Biochemistry 19, 703–707.

Viret, F., Grand, S., 2019. Combined Size and Density Fractionation of Soils for Investigations of Organo-Mineral Interactions. Journal of visualized experiments: JoVE.

Visser, J.M., Duke-Sylvester, S.M., Carter, J., Broussard, W.P., 2013. A Computer Model to Forecast Wetland Vegetation Changes Resulting from Restoration and Protection in Coastal Louisiana. Journal of Coastal Research 67, 51–59.

Wang, F., Kroeger, K.D., Gonneea, M.E., Pohlman, J.W., Tang, J., 2019. Water salinity and inundation control soil carbon decomposition during salt marsh restoration: An incubation experiment. Ecology and evolution 9, 1911–1921.

Wang, M., Chen, J.-K., LI, B., 2007. Characterization of Bacterial Community Structure and Diversity in Rhizosphere Soils of Three Plants in Rapidly Changing Salt Marshes Using 16S rDNA. Pedosphere 17, 545–556.

Wickham, H., Chang, W., Wickham, M.H., 2016. Package 'ggplot2'. Create elegant data visualisations using the grammar of graphics. Version 2, 1–189.

Wider, R.K., Lang, G.E., 1982. A Critique of the Analytical Methods Used in Examining Decomposition Data Obtained From Litter Bags. Ecology 63, 1636.

Więski, K., Guo, H., Craft, C.B., Pennings, S.C., 2010. Ecosystem Functions of Tidal Fresh, Brackish, and Salt Marshes on the Georgia Coast. Estuaries and Coasts 33, 161–169.

Wiesmeier, M., Urbanski, L., Hobley, E., Lang, B., Lützow, M. von, Marin-Spiotta, E., van Wesemael, B., Rabot, E., Ließ, M., Garcia-Franco, N., Wollschläger, U., Vogel, H.-J., Kögel-Knabner, I., 2019. Soil organic carbon storage as a key function of soils - A review of drivers and indicators at various scales. Geoderma 333, 149–162.

Winsborough, B.M., 2000. Diatoms and Benthic Microbial Carbonates, in: Riding, R.E., Awramik, S.M. (Eds.), Microbial Sediments. Springer Berlin Heidelberg, Berlin, Heidelberg, pp. 76–83.

Wong, V.N.L., Greene, R.S.B., Dalal, R.C., Murphy, B.W., 2010. Soil carbon dynamics in saline and sodic soils: a review. Soil Use and Management 26, 2–11.

WSV, 2011. MThw-Linie an der Unter- und Außenelbe. www.kuestendaten.de, last accessed 29 Sep 2023.

WSV, 2017. Vegetationskartierung / Biotoptypenkartierung 2017 Unterelbe. www.kuestendaten.de, last accessed 29 Sep 2023.

Xue, L., Jiang, J., Li, X., Yan, Z., Zhang, Q., Ge, Z., Tian, B., Craft, C., 2020. Salinity Affects Topsoil Organic Carbon Concentrations Through Regulating Vegetation Structure and Productivity. Journal of Geophysical Research: Biogeosciences 125.

Yan, N., Marschner, P., Cao, W., Zuo, C., Qin, W., 2015. Influence of salinity and water content on soil microorganisms. International Soil and Water Conservation Research 3, 316–323.

Yarwood, S.A., 2018. The role of wetland microorganisms in plant-litter decomposition and soil organic matter formation: a critical review. FEMS microbiology ecology 94.

Yousefi Lalimi, F., Silvestri, S., D'Alpaos, A., Roner, M., Marani, M., 2018. The Spatial Variability of Organic Matter and Decomposition Processes at the Marsh Scale. Journal of Geophysical Research: Biogeosciences 123, 3713–3727.

Yuan, Y., Li, X., Jiang, J., Xue, L., Craft, C.B., 2020. Distribution of organic carbon storage in different salt-marsh plant communities: A case study at the Yangtze Estuary. Estuarine, coastal and shelf science 243, 106900.

Zhai, J., Anderson, J.T., Yan, G., Cong, L., Wu, Y., Dai, L., Liu, J., Zhang, Z., 2021. Decomposition and nutrient dynamics responses of plant litter to interactive effects of flooding and salinity in Yellow River Delta wetland in northeastern China. Ecological Indicators 120, 106943.

Zhang, D., Hui, D., Luo, Y., Zhou, G., 2008. Rates of litter decomposition in terrestrial ecosystems: global patterns and controlling factors. Journal of Plant Ecology 1, 85–93.

Zhang, G., Bai, J., Tebbe, C.C., Zhao, Q., Jia, J., Wang, W., Wang, X., Yu, L., 2021. Salinity controls soil microbial community structure and function in coastal estuarine wetlands. Environmental microbiology 23, 1020–1037.

Zhou, J., Wu, Y., Kang, Q., Zhang, J., 2007. Spatial variations of carbon, nitrogen, phosphorous and sulfur in the salt marsh sediments of the Yangtze Estuary in China. Estuarine, coastal and shelf science 71, 47–59.

Zimmerman, A.R., Chorover, J., Goyne, K.W., Brantley, S.L., 2004. Protection of Mesopore-Adsorbed Organic Matter from Enzymatic Degradation. Environmental Science & Technology 38, 4542–4548.

Manuscripts

Study A:
Litter decomposition and prokaryotic decomposer communities along estuarine gradients

Friederike Neiske[a]*, Luise Grüterich[b], Annette Eschenbach[a], Monica Wilson[b], Wolfgang R. Streit[b], Kai Jensen[b], Joscha N. Becker[a]

[a] Institute of Soil Science, CEN Center for Earth System Research and Sustainability, Universität Hamburg, Allende-Platz 2, 20146 Hamburg, Germany

[b] Institute of Plant Science and Microbiology, Universität Hamburg, Ohnhorststrasse 18, 22609 Hamburg, Germany

*corresponding author

For the final publication, please refer to:

Neiske F., Grüterich L., Eschenbach A., Wilson M., Streit W.R., Jensen K., Becker J.N. (2025). Litter decomposition and prokaryotic decomposer communities along estuarine gradients. *Soil Biology and Biochemistry*. Volume 204, 109762. https://doi.org/10.1016/j.soilbio.2025.109762

A Abstract

Climate change driven sea-level rise and saltwater intrusion will impact carbon (C) cycling in estuarine marshes. To understand impacts of tidal inundation and changing salinity on microbial organic matter turnover, we investigated litter decomposition and the prokaryotic community in three marsh salinity and three flooding frequency zones of the Elbe Estuary.

Standardized litter (Tea Bag Index) was used to assess direct effects of the estuarine gradients on seasonal litter decomposition. Indirect effects of the estuarine gradients through mediating plant species composition and litter quality was studied using litter bags filled with native plant litter. 16S rRNA gene amplicon sequencing was used to identify the prokaryotic communities colonizing tea litter, native litter, and soil along the estuarine gradients.

Tea litter decomposition rates decreased with increasing salinity and flooding, with 2x faster rates in brackish and freshwater high marshes compared to the salt marsh pioneer zone. Native litter decomposition was significantly influenced by local vegetation properties, particularly higher lignin contents at the freshwater compared to salt marsh, as well as pioneer zones compared to high marshes contributed to a decreased litter decomposition. Greater diversity within the soil prokaryotic community increased tea litter mass loss, indicating indirect controls of salinity via changes in prokaryotic community composition and diversity.

Our results indicate that litter decomposition and prokaryotic communities are strongly influenced by estuarine gradients, and these processes are dependent upon local site conditions and litter quality. The complex interplay of these factors, will strongly affect C cycling in estuarine marsh soils under climate change.

Keywords

Flooding Gradient; Salinity Gradient; Tea Bag Index; Litter Bags; Litter Quality; Prokaryotic Community

Highlights

- Salinity decreases tea decomposition; flooding decreases rates and stabilization
- Litter quality controls litter decomposition along the estuarine gradients
- Soil prokaryotic community is adapted to local vegetation
- Increased diversity of the prokaryotic soil community stimulates tea mass loss

A1 Introduction

The breakdown of organic matter (OM), such as plant litter, is a fundamental ecosystem process, controlling the recycling of nutrients and carbon (C) (Swift et al., 1979) Plant litter decomposition is driven by the complex interplay of substrate quality, decomposer community, and environmental conditions including climate or local soil characteristics (e.g. oxygen availability, salinity) (Aerts, 1997; Makkonen et al., 2012). Therefore, litter turnover can vary strongly along environmental gradients (Stagg et al., 2018; Becker and Kuzyakov, 2018).

Estuarine marshes, located at the interface of aquatic and terrestrial as well as freshwater and marine ecosystems, are shaped by dynamic interactions between abiotic factors, such as tidal inundation and salinity, and biotic components, including vegetation and soil microorganisms (e.g. prokaryotic communities) (Engels and Jensen, 2009; Grüterich et al., 2025). Contradictory results have been reported regarding the effects of flooding and salinity on OM decomposition in tidal marshes (Hemminga et al., 1991; Craft, 2007; Morrissey et al., 2014; Stagg et al., 2018). In frequently flooded soils of tidal marshes, decomposition can be slowed down due to oxygen limitation (Yarwood, 2018; Macreadie et al., 2019). Variations in flooding regime and salinity have been shown to alter the composition and diversity of prokaryotic communities in marsh soils (Yarwood, 2018; Trevathan-Tackett et al., 2021; Schreckinger et al., 2021), as well as the predominant metabolic pathway (Yarwood, 2018; Grüterich et al., 2025). Although microbial diversity in soil has been linked to OM decomposition, the strength and direction remain debated (Nielsen et al., 2011). Salinity can also enhance OM decomposition by stimulating extracellular enzyme activities (Morrissey et al., 2014; Yang et al., 2022). Furthermore, direct effects of salinity and flooding on litter decomposition are accompanied by indirect ecosystem responses, such as modifications of vegetation composition and subsequent changes in litter quality (Stagg et al., 2018). The chemical and physical properties of plant materials, including nitrogen (N) content, lignin and cellulose concentrations, and C:N and lignin:N ratios, are recognized as key determinants of litter decomposition in different ecosystems (Valiela et al., 1985; Zhang et al., 2008; Djukic et al., 2018). Moreover, litter quality can impact the microbial community by promoting specific taxa that are adapted to decomposing local vegetation (Wang et al., 2007; Bezemer et al., 2010).

Climate is one of the most important regulators of litter decomposition (Aerts, 1997), which has been also observed for tidal wetlands (Mueller et al.,

2018; Trevathan-Tackett et al., 2021). In terrestrial ecosystems, litter decomposition varies seasonally, typically increasing with higher temperatures but strongly depending on soil water content (Becker and Kuzyakov, 2018; Petraglia et al., 2019; Daebeler et al., 2022). In estuarine marshes, the relationship can be more complex through the interaction of tidal inundation and salinity. Even though tidal marshes generally maintain high soil water contents, levels can drop in summer in infrequently flooded locations; this reduction, combined with elevated salinity, can adversely impact litter decomposition (Hemminga et al., 1991). Given the sensitivity of litter decomposition to environmental changes, climate change can significantly impact OM decomposition dynamics in estuarine marshes, but predicting the direction of these effects remains challenging. For instance, experimental warming has been shown to increase both the rate and amount of tea litter decomposition; while the effect of warming on decomposition rate appeared unaffected by flooding, the warming-effect on tea stabilization differed along a flooding gradient (Tang et al., 2023). Thus, it is essential to consider the complex interactions among flooding, salinity, climate, and litter quality in understanding litter decomposition dynamics in estuarine marshes. Moreover, sea-level rise due to climate change may alter local soil conditions by increasing salinity and modifying flooding dynamics, potentially shifting vegetation zones along estuaries and thereby affecting litter quality and decomposition (Craft et al., 2009; Li et al., 2022).

With respect to changing environmental conditions induced by climate change and the high C sequestration potential of tidal wetlands, understanding the controls of C cycling in these ecosystems is crucial. However, disentangling the importance of external abiotic conditions, such as salinity or flooding, from internal factors, such as litter quality, for litter decomposition and the prokaryotic decomposer community remains challenging. The Tea Bag Index (TBI), introduced by Keuskamp et al. (2013), can provide valuable insights into the role of environmental drivers for litter decomposition, excluding the interfering effect of litter quality across ecosystem gradients. The effectiveness of the TBI to compare litter break-down across ecosystems and along environmental gradients has been demonstrated in several studies (Mueller et al., 2018; Becker and Kuzyakov, 2018; Trevathan-Tackett et al., 2021). However, prior studies indicate that highest decomposition rates of plant material in tidal wetlands occur in proximity to its natural distribution (Lopes et al., 2011; Franzitta et al., 2015). Therefore, incorporating native litter into decomposition studies is essential to avoid misleading interpretations due to the home-field advantage.

The aim of this study was to identify the role of estuarine environmental conditions on litter decomposition, using the Elbe Estuary as a model system. Our specific research objectives were to investigate (i) the effect of estuarine gradients (i.e. salinity and flooding frequency) on decomposition of standardized and native litter, ii) seasonal patterns of litter decomposition, and (iii) prokaryotic community composition and diversity in soil, as well as standardized and native litter.

A2 Material and Methods

A2.1 Study Area

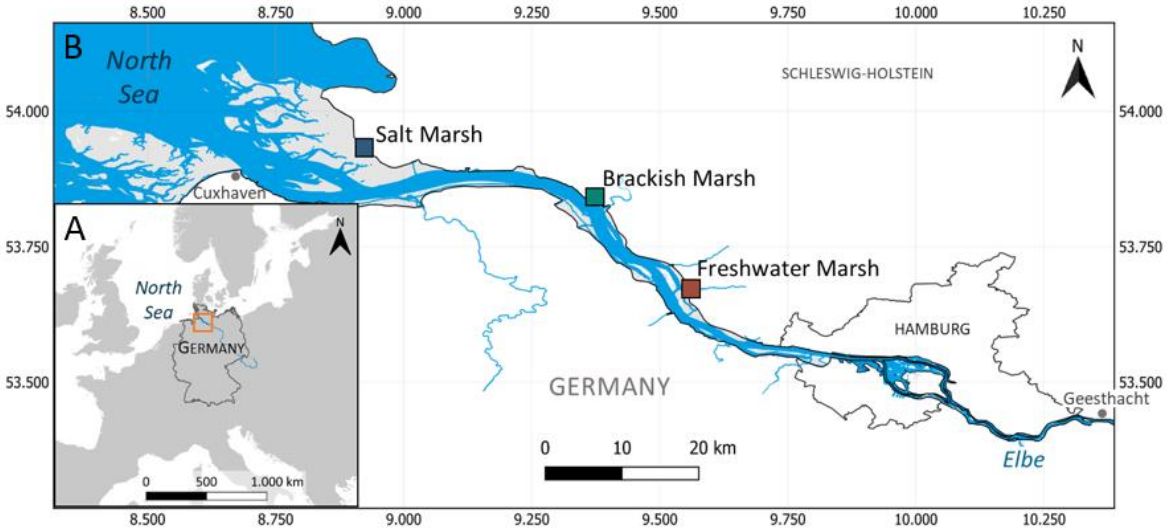

Figure A1: (A) Location of the Elbe Estuary in central Europe (orange rectangle) and (B) location of the marsh sites along the Elbe Estuary (salt marsh: 53°55'40.0"N 8°54'51.3"E/river-km: 710; brackish marsh: 53°50'03.0"N 9°22'15.6"E/river-km: 680; freshwater marsh: 53°39'56.3"N 9°33'11.5"E/river-km: 658) (Data sources: (WSV, 2011; EEA, 2017; WSV, 2017).

We conducted our study in the marshes of the Elbe Estuary (Northern Germany) (Figure A1). The regional climate is oceanic with a mean annual temperature of 9.3 °C and mean annual rainfall of 812.8 mm (1991 - 2020, federal state of Schleswig-Holstein) (DWD, 2024). The Elbe Estuary extends from the estuaries' mouth at Cuxhaven until a weir at Geesthacht, which restricts the tidal influence further upstream. The semi-diurnal tidal regime of the estuary is meso- to macrotidal (Boehlich and Strotmann, 2008).

Three sites were selected along the salinity gradient of the Elbe Estuary (Boehlich and Strotmann, 2008; Branoff et al., 2024 preprint). The salt marsh

at Kaiser-Wilhelm-Koog is situated in the Schleswig-Holstein Wadden Sea National Park at the estuarine mouth. For the brackish marsh, a site close to Hollerwettern and for the freshwater marsh, a site in the nature conservation area "Haseldorfer Binnenelbe" were chosen. Within each of these three marsh sites, we selected three locations along the flooding gradient: Pioneer zones (PZ) are located closest to the main channel and are flooded during high tide (twice per day), low marshes (LM) are inundated during spring tide (occurring twice per month at new and full moon), while high marshes (HM) are occasionally flooded during storm tides (few times per year). All sites are located on the seaward side of a dike and exhibit near-natural conditions. The selection of the marsh locations was based on dominant plant species that are typical for the respective salinity and flooding regime (Engels and Jensen, 2009) (Table S2). At each selected marsh location (n = 9), research stations were established consisting of five adjacent replicate plots (2 x 2 m).

A2.2 Litter decomposition

Tea Bag Index

The standardized Tea Bag Index (TBI) was applied following the protocol of Keuskamp et al. (2013). Five pairs of weighed green and rooibos tea bags were deployed at 8 cm depth in each of the five replicate plots of the nine research locations. After approximately 90 days, tea bags were exchanged with new tea bags. Tea bags were incubated during four periods over the course of one year to assess seasonal variation in litter decomposition (spring: March – June 2022, summer: June - September 2022, fall: September – December 2022, winter: December 2022 – March 2023). After retrieval, tea bags were dried at 60 °C until constant weight. The dried tea bags were opened, roots or other non-tea material was removed and the content of the tea bags was weighed. To account for sediment contamination, tea bags were additionally combusted at 550 °C and weight loss was corrected in comparison to initial ash contents.

Native litter decomposition

In addition to the TBI, self-made litter bags were used to include litter-quality effects in the assessment of litter decomposition. A representative mixture of native plants was collected in late fall 2021 from each of the nine marsh locations. The litter was cleaned and dried at 60 °C. Polyamide mesh bags with a mesh size of 1000 µm were filled with 5 g of the respective litter. Four litter bags were inserted into the soil to a depth of 0 - 15 cm in each of the five

replicate plots of the corresponding marsh location in March 2022. One litter bag was retrieved from each replicate plot after 1, 3, 6, and 12 months. After retrieval, the litter bag content was washed over a sieve (1 mm) to remove sediments, and separated from roots and other external debris. The remaining litter was dried at 60 °C until constant weight and the mass remaining relative to the initial mass was calculated.

A2.3 Analyses of prokaryotic community structures

An additional set of tea and litter bags was incubated in the field for the characterization of the prokaryotic community composition in spring 2023 (March - June). One litter bag (0 - 15 cm depth) and two (HM and LM) to three (PZ) pairs of green and rooibos tea bags (8 cm depth) were deployed in three replicate plots of each marsh location. Tea and litter bags were retrieved after three months, along with one soil sample from each replicate plot (taken in close proximity to the tea and litter bags). Tea bags, litter bags, and soil samples were cooled in the field and immediately frozen (- 20 °C) in the laboratory until further analyses. We also included tea and native litter materials that were not incubated in the field in our analysis as controls, allowing us to ascertain the community composition prior to incubation. DNA was extracted from 0.5 g of tea litter, native litter or soil using the NucleoSpin Soil Kit (Macherey-Nagel, Düren, Germany) according to the manufacturer's instructions and following standard DNA protocols for extraction of eDNAs (Refs). Concentration and quality of the isolated DNA was then analyzed using a Nanodrop spectrophotometer at a wavelength of 280 nm (NanoDrop 2000, Thermo Scientific, Waltham, USA). Metabarcoding sequencing of the 16S rRNA gene variable regions V3-4 was carried out at the Competence Centre for Genomic Analysis in Kiel, Germany. For this, the Illumina Nextera XT Index Kit, primers 341F (5'-CCTACGGGNGGCWGCAG-3') and 785R (5'-GACTACHVGGGTATCTAATCC-3'), and the MiSeq Reagent Kit v3, were used. For adaptor trimming of demultiplexed paired-end reads, BBDuk (v.38.8) was employed. The DADA2 pipeline (v.1.8) (Callahan et al., 2016) was used to filter reads and infer ASVs, with the following specific parameters (maxEE=2, maxN=0, truncQ=2, truncLen=270,230). Taxonomic assignment of the merged corrected reads was conducted using the SILVA database (v.138.1) (Quast et al., 2013). Raw reads of the 16S rRNA analysis were deposited at the European nucleotide archive ENA under project accession number PRJEB79857.

A2.4 Environmental parameters

Field site monitoring and characterization

At each research location, sensors for continuous measurement of soil volumetric water content (VWC) were installed (SMT100, Truebner GmbH, Neustadt, Germany). For physico-chemical soil characterization, soil samples (0 - 10 cm) were collected in February and March 2022 from each research location. Air-dried soil samples were sieved to 2 mm. Samples were dried at 105 °C and ground for measuring inorganic and organic C contents (soli TOC® cube, Elementar Analysensysteme GmbH, Langenselbold, Germany) and total C and N contents (vario Max cube, Elementar Analysensysteme GmbH, Langenselbold, Germany). Soil texture was assessed by the sieving and sedimentation method based on the Köhn-pipette fractionation for mineral soils (Müller et al., 2009). A vibratory sieve shaker (Retsch GmbH, Haan, Germany) and a Sedimat 4–12 (Umwelt-Geräte-Technik GmbH, Muencheberg, Germany) were used to analyze coarse (2.0 - 0.063 mm) and fine fractions (< 0.063 mm), respectively. Soil pH was measured with a pH meter (MP230 GLP, Mettler-Toledo GmbH, Gießen, Germany) in a suspension with 0.01 M $CaCl_2$-solution (pH_{CaCl2}) while the EC was determined in a soil-water-suspension with a conductivity meter (WTW Cond 330i with TetraCon 325, Xylem Analytics Germany Sales GmbH & Co. KG, Weilheim, Germany).

We analyzed reducing soil conditions by the "Indicator of Reduction in Soil" (IRIS) method (Castenson and Rabenhorst, 2006; Rabenhorst, 2008) based on the approach described by Mueller et al. (2020) and Mittmann-Goetsch et al. (2024). White PVC sticks (5 x 70 cm) covered with orange $FeCl_3$-paint were inserted into the soil of each replicate plot to a depth of 0 - 60 cm. Sticks were retrieved after four weeks and a reduction index (RI) (0 - 1) was calculated based on the area of removed orange $FeCl_3$-paint. Field incubation of IRIS sticks was conducted over the course of one year (12 x 4 weeks from May 2022 until April 2023). We calculated annual and seasonal RI values for depth increments 0 - 10 cm and 0 - 20 cm corresponding to the incubation of tea and litter bags.

Vegetation characteristics

Identification and coverage estimation of plant species were conducted in late July 2022 in two subplots (60 x 60 cm) of each replicate plot (n = 10) at the nine research locations. Three litter subsamples of each marsh location (collected for litter bags in fall 2021) were ground and dried for the analysis of total C and total N contents (vario Max cube, Elementar Analysensysteme GmbH, Langenselbold, Germany). Contents of cellulose and lignin (Naumann et

al., 1976) were measured at the "Professor Hellriegel Institut e.V." at Anhalt University of Applied Sciences.

A2.5 Data analyses

Decomposition rate and stabilization of tea litter

Median start and end weights of retrieved tea bags from one replicate plot (2 – 5 recovered tea bags per type and replicate plot) were calculated and used to derive the decomposition rate (k_{TBI}) and stabilization factor (S_{TBI}) following Keuskamp et al. (2013). For k_{TBI} the following equation was used:

$$W(t) = ae^{-kt} + (1 - a)$$

in which, *W(t)* is the remaining mass (median end weight) of rooibos tea after incubation time *t*, *a* is the labile fraction of rooibos tea, while *1 - a* reflects the recalcitrant fraction, *k* is the decomposition rate constants of the labile fraction.

Environmental factors can impede decomposition and lead to the incomplete decomposition of litter. The deviation of the potentially decomposable (hydrolyzable) fraction from the actual decomposed fraction is expressed in stabilization factor *S*:

$$S = 1 - \frac{a_g}{H_g}$$

where a_g represents the decomposable fraction and H_g the hydrolyzable fraction of green tea.

We calculated k_{TBI} and S_{TBI} for each season and as annual mean (mean over four seasons).

Decomposition of native litter

The relative remaining dry mass of native litter over time in litter bags was used to determine the decomposition rate k_{LB}. We fitted a single negative exponential model on the relative remaining mass over five time steps (0, 1, 3, 6, 12 months) for each replicate plot separately using the R package "litterfitter" (Cornwell and Weedon, 2014). The model type was selected based on the lowest values for the corrected Akaike's information criterion (AICc) (Figure S2). In case the remaining biomass increased to a later time step, we set the weight to the weight of the previous time step (Stagg et al., 2018).

Analyses of prokaryotic community structure and diversity

To test for differences in prokaryotic community composition among the different substrate types (tea, native litter, and soil) and along the estuarine

gradients, we applied a nonmetric multidimensional scaling (NMDS) based on Bray-Curtis distances at the genus level. Alpha diversity (indices richness, evenness, Shannon Diversity Index, and Inverse Simpson Index) were calculated at the phylum level. Multiple indices were used to derive a broader perspective on diversity estimates (Pioli et al., 2020; Daebeler et al., 2022). Both analyses were conducted using the vegan package in R (Oksanen et al., 2013).

Statistical analyses

Differences in litter decomposition (k_{TBI}, S_{TBI}, k_{LB}, and relative mass remaining of LB) and alpha diversity indices of the prokaryotic communities (richness, evenness, Shannon Diversity Index, and Inverse Simpson Index) along the estuarine gradients were assessed by analysis of variance (ANOVA) or linear mixed effect model (LME). The LME were applied including sampling location as random factor and either (I) season or (II) salinity, flooding and season as main factors. Assumptions of normality and variance homogeneity were checked by visual inspection of model residuals. Dixon's Q test was applied to check groups for potential outliers. Relationships between variables were assessed by linear regression and Pearson correlation, as well as Spearman rank correlation to account for potential non-linearity. Simple linear and log-linear fits were selected according to reduction in Akaike Information Criterion (AIC) values. Statistical differences were accepted as significant at p-level < 0.05 and p-levels between 0.10 and 0.05 were considered significant by tendency. Statistical analyses were conducted in R 4.2.0 (R Core Team, 2022), using "multcomp" (Hothorn et al., 2016) and "multcompView" (Graves et al., 2015) packages, as well as "ggplot2" (Wickham et al., 2016) for data visualization.

A3 Results

A3.1 Tea Bag Index

Effect of estuarine gradients on tea litter decomposition

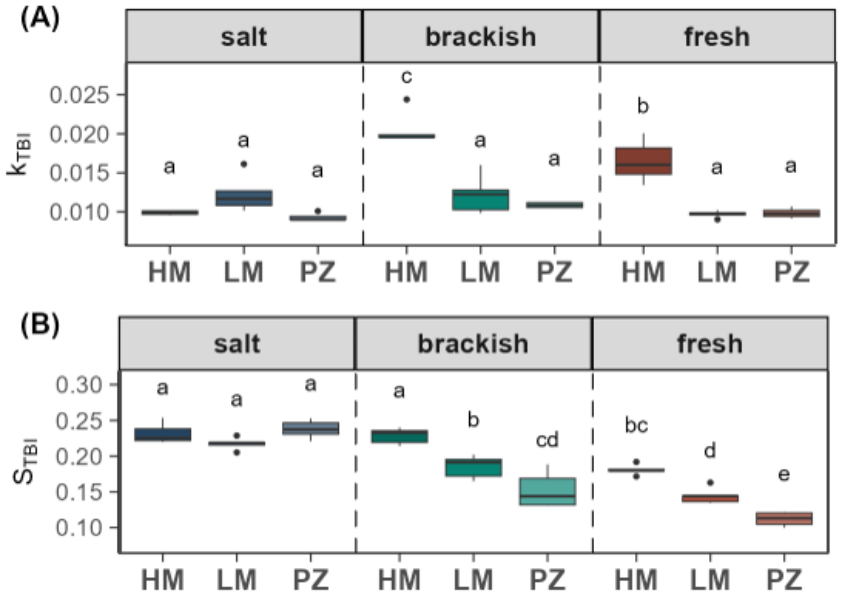

Figure A2: Annual means of (A) decomposition rate k_{TBI} and (B) stabilization factor S_{TBI} of tea litter along the salinity (salt marsh, brackish marsh, freshwater marsh) and flooding gradient (HM = high marsh, LM = low marsh, PZ = pioneer zone) of the Elbe Estuary (n = 5). Lowercase letters indicate significant differences ($p < 0.05$) derived from ANOVA with TukeyHSD post-hoc comparison.

The salinity and flooding gradient, as well as their interaction, had significant effects on annual k_{TBI} and S_{TBI} of tea litter (Figure A2). Highest annual k_{TBI} were found in high marshes of the brackish (0.021) and freshwater marsh (0.017), from where it decreased with increasing salinity and flooding towards salt marsh pioneer zones (0.009). In low marshes and pioneer zones, annual k_{TBI} did not change along the salinity gradient. Annual S_{TBI} increased with increasing salinity in all flooding zones by 20% - 50% and decreased with increasing flooding at the brackish and freshwater marsh by 35%.

Effect of seasons

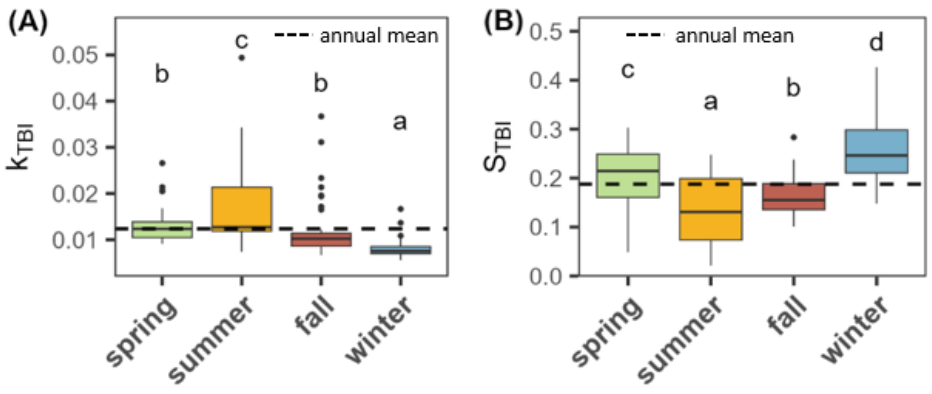

Figure A3: Effect of season on (A) decomposition rate k_{TBI} and (B) stabilization factor S_{TBI} of tea litter (n = 45). Lowercase letters indicate significant differences ($p < 0.05$) derived from linear mixed effect model.

Tea litter decomposition indices followed a strong seasonality (Figure A3, Figure S3). Average decomposition rate k_{TBI} was 100% higher in summer compared to winter (summer > spring = fall > winter) (Figure A3 (A)). Stabilization factor S_{TBI} was almost 50% higher in winter compared to summer (S_{TBI}: winter > spring > fall > summer) (Figure A3 (B)). Spring and fall are on the level of the annual average.

The seasonal variation of tea litter decomposition was affected by the estuarine gradients (Figure S3). Seasonal variation of k_{TBI} decreased with increasing salinity and flooding, while S_{TBI} showed a higher seasonality in pioneer zones. For k_{TBI}, the strongest seasonal effect was observed in the brackish and freshwater high marshes which also showed highest k_{TBI} during summer (0.024 and 0.033). Stabilization factor S_{TBI} was low in summer and high in winter especially in locations with higher flooding frequency (low marshes and pioneer zones). With decreasing flooding, less seasonal variation was observed. Strongest effects of the salinity gradient on k_{TBI} were observed for high marshes and in summer. The strongest effect of the flooding gradient on k_{TBI} and S_{TBI} occurred in summer.

A3.2 Native litter decomposition

Effect of estuarine gradients on native litter decomposition

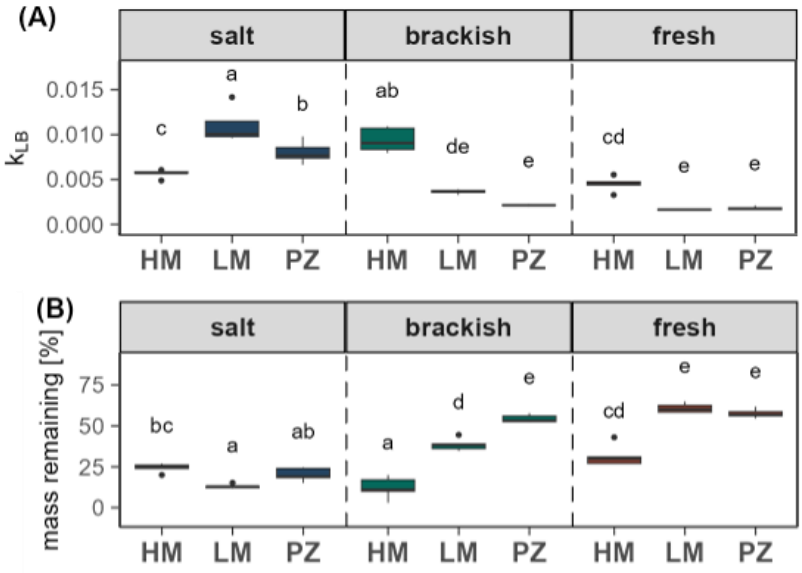

Figure A4: Annual (A) decomposition rate k_{LB} and (B) relative mass remaining of native litter after one year along the salinity (salt marsh, brackish marsh, freshwater marsh) and flooding gradient (HM = high marsh, LM = low marsh, PZ = pioneer zone) of the Elbe Estuary. Lowercase letters indicate significant differences ($p < 0.05$) derived from ANOVA with TukeyHSD post-hoc comparison.

Decomposition rate of native litter k_{LB} was lowest at the low marsh and pioneer zone of the freshwater marsh (both 0.002), while highest k_{LB} values occurred at the low marsh (0.011) and pioneer zone (0.008) of the salt marsh and the brackish high marsh (0.009) (Figure A4 (A)). Decomposition rate k_{LB} increased with increasing salinity at pioneer zones and low marshes or was highest at the brackish marsh (high marshes). Increasing flooding decreased k_{LB} at the brackish marsh and freshwater marsh and increased k_{LB} at the salt marsh. Relative remaining mass of native litter after one year showed the reverse trend along the estuarine gradients (Figure A4 (B)).

A3.3 Structure and diversity of prokaryotic communities

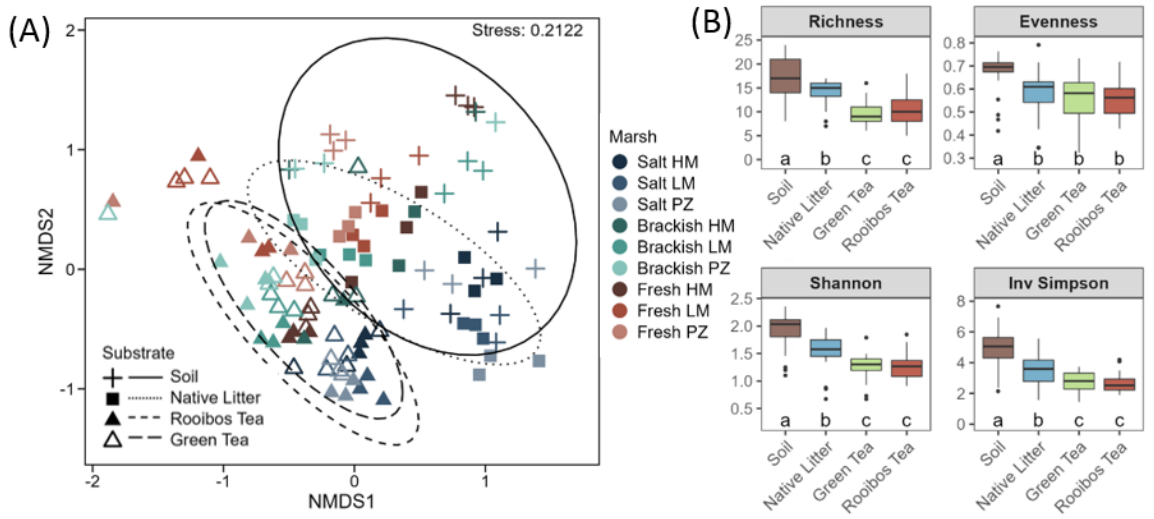

Figure A5: (A) NMDS based on Bray-Curtis dissimilarity of the prokaryotic community associated with tea, native litter and soil at genus level along the salinity (salt marsh, brackish marsh, freshwater marsh) and flooding gradient (HM = high marsh, LM = low marsh, PZ = pioneer zone) of the Elbe Estuary. Ellipses indicate 90% confidence area per substrate type. (B) Alpha diversity (richness, evenness, Shannon Diversity Index, and Inverse Simpson Index) of the prokaryotic community at phylum level in the different substrate types (soil, native litter, green tea, rooibos tea).

Prokaryotic community structure and diversity

The estuarine gradients and the substrate type (soil, native litter, green tea, and rooibos tea) had a strong effect on the structure and alpha diversity (richness, evenness, Shannon Diversity Index, and Inverse Simpson Index) of the prokaryotic community (Figure A5 (A) + (B)). We observed a partial overlap of communities associated with soil and native litter and a strong overlap between the communities associated with green tea and rooibos tea, whereas communities associated with tea showed distinct differences compared to communities associated with soil and native litter (Figure A5 (A)). Highest alpha diversity of the prokaryotic community was observed in soil, followed by native litter, while communities associated with green and rooibos tea showed similar alpha diversity. The assemblage of communities associated with tea and native litter differed from their non-incubated controls (Figure S6). Across all substrate types, the communities at the salt marsh showed a different assemblage and lower alpha diversity than the brackish and freshwater marsh communities.

Prokaryotic taxa

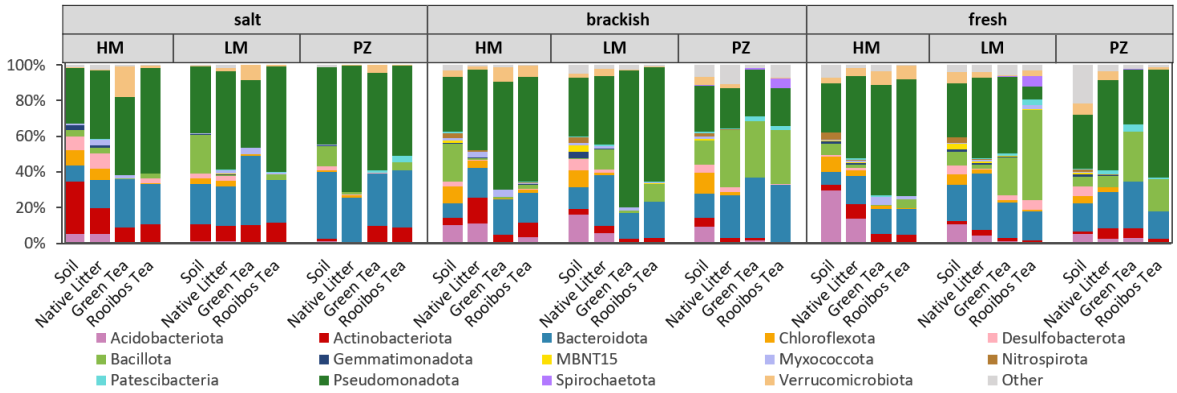

Figure A6: Prokaryotic community composition in soil, native litter, green tea, and rooibos tea (relative abundance of phyla) along the salinity (salt marsh, brackish marsh, freshwater marsh) and flooding gradient (HM = high marsh, LM = low marsh, PZ = pioneer zone) of the Elbe Estuary. Each bar reflects the average of three biological replicates.

The most abundant phyla (> 1%) were Pseudomonadota (43.8%), Bacteroidota (21.2%), Bacillota (10.1%), Actinomycetota (6.1%), Acidobacteriotaa (4.1%), Verrucomicrobiota (2.7%), Chloroflexota (2.6%), Desulfobacterota (1.9%), Campylobacterota (1.3%), and Myxococcota (1.1%), which made up 95% of the total prokaryotic community (Figure A6). The estuarine gradients and substrate type affected the relative occurrence of certain prokaryotic phyla. Pseudomonadota, Bacteroidota, Bacillota, and Patescibacteria were more dominant in tea and native litter than in soil in several marshes. Lower abundance in tea compared to soil was observed for Acidobacteriota and Chloroflexota. Increasing salinity led to a reduced abundance of Bacillota, Acidobacteriota, Nitrospirota, and Spirochaetota while the abundance of Bacteroidota, Actinomycetota, and Patescibacteria was higher. The occurrence of Actinomycetota and Acidobacteriota increased with frequent flooding while Bacillota and Bacteroidota decreased in their abundance.

A3.4 Relationships between litter decomposition and environmental variables

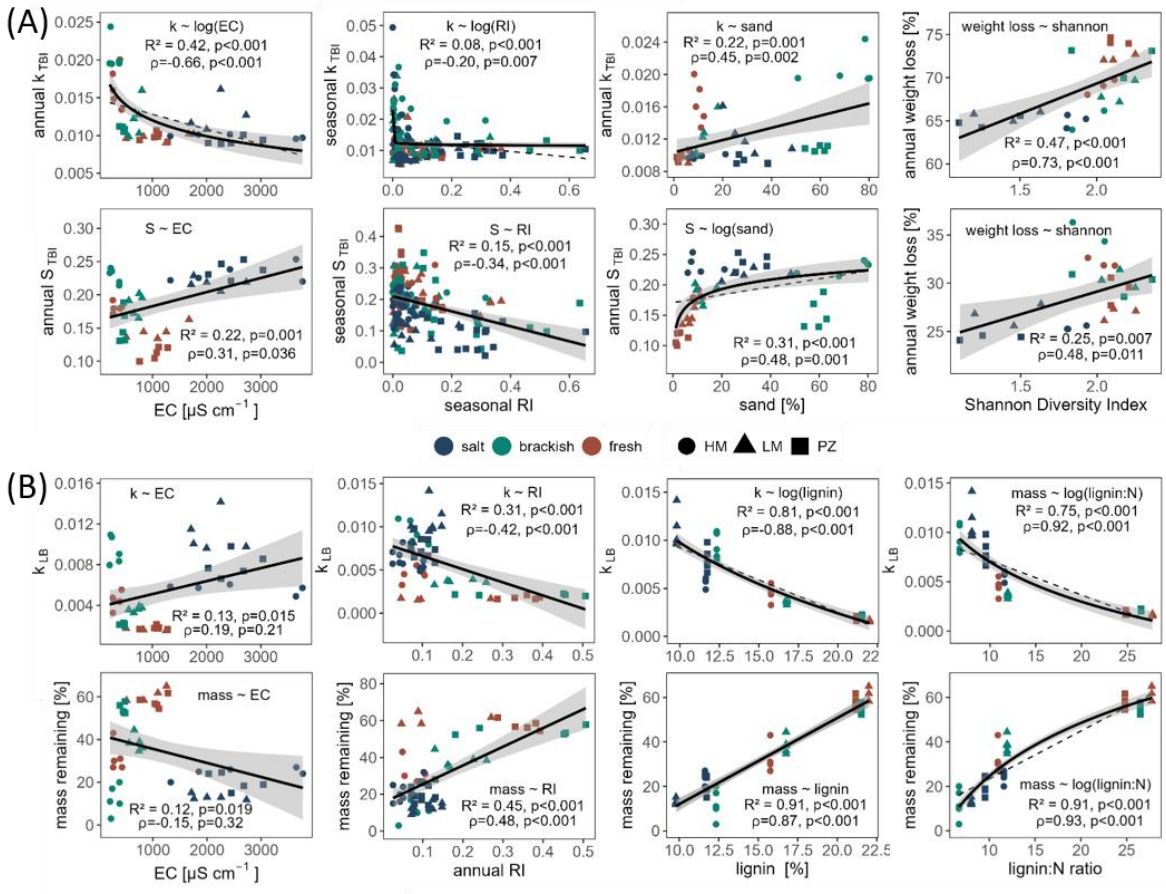

Figure A7: Relationship between decomposition indices of (A) tea litter (decomposition rate k_{TBI}, stabilization factor S_{TBI}, relative weight loss of green tea (upper panel) and rooibos tea (lower panel)) and (B) native litter (decomposition rate k_{LB}, relative mass remaining after one year) and selected site characteristics (soil EC, soil reduction index (RI), soil sand content, Shannon Diversity Index of the prokaryotic soil community, litter lignin content, litter lignin:N ratio) with Spearman rank correlation coefficients (ρ). Black solid lines indicate linear or logarithmic regression lines with 95% confidence bands and respective coefficients of determination (R^2). Additional dashed lines indicate significant simple linear relationship in case logarithmic regression was used.

Annual tea litter k_{TBI} correlated negatively with the EC and clay content of the soil, while it was positively affected by the sand content (Figure A7 (A), Figure S4). Annual S_{TBI} increased with increasing EC and sand content while it decreased with increasing clay content. Seasonal k_{TBI} and S_{TBI} were negatively affected by the seasonal RI of the soil. Relative weight loss of green and rooibos tea was positively linked to the richness and diversity (Shannon Diversity Index, Inverse Simpson Index) of the prokaryotic soil community. We found a positive correlation between native litter k_{LB} and the sand content, as well as EC of the soil, while k_{LB} was negatively correlated with clay content and annual RI of the

soil (Figure A7 (B), Figure S4). The relative native litter mass remaining after one year showed the opposite trend regarding sand content, clay content, EC, and annual RI. Decomposition of native litter (k_{LB}, relative mass remaining after one year) was strongly affected by litter quality indices of the aboveground vegetation (contents of lignin, cellulose, N, C, and ratios of C:N, lignin:N) (Figure A7 (B), Figure S4). In this context, litter quality varied along the estuarine gradients (Figure S5).

A4 Discussion

A4.1 Effect of estuarine gradients on litter decomposition

Effect of estuarine gradients on tea litter decomposition

We observed two different trends in tea litter decomposition rates along the salinity gradient: First, increasing salinity slowed down tea litter decomposition rates in high marshes; second, salinity did not affect decomposition rates in low marshes and pioneer zones. Therefore, fastest tea litter decomposition occurred in high marshes of the brackish and freshwater marsh. Tea litter stabilization benefitted from increasing salinity in all flooding zones leading to highest tea litter stabilization in the salt marsh and brackish high marsh. We observed decreasing tea litter decomposition rates and increasing tea litter stabilization with increasing EC of the soil. In accordance with our findings, previous studies reported direct negative effects of salinity on OM decomposition or found higher OM decomposition rates in freshwater compared to marine environments (Hemminga et al., 1991; Mendelssohn et al., 1999; Quintino et al., 2009; Bierschenk et al., 2012; Qu et al., 2019). These trends might be related to reduced microbial activities, microbial biomass, and enzyme activities with increasing salinity (Roache et al., 2006; Yan et al., 2015). However, the literature on OM decomposition in relation to salinity in tidal wetlands presents inconsistent results, with studies reporting higher OM decomposition rates in marshes with elevated salinities compared to freshwater marshes (Craft, 2007; Stagg et al., 2018). Moreover, research indicates that extracellular enzyme activities and bacterial abundance can increase with rising salinity from freshwater to oligohaline tidal wetlands (Morrissey et al., 2014). These inconsistent trends suggest that the effect of salinity on OM decomposition is not straightforward but rather influenced by several interacting factors, such as litter quality, exposure time, OM decay stage, salinity levels and nutrient

availability (Mendelssohn et al., 1999; Quintino et al., 2009; Lopes et al., 2011; Franzitta et al., 2015).

In our study, tea litter decomposition rates decreased with increasing flooding from high marshes to pioneer zones at the brackish and freshwater marshes. Reduced oxygen availability induced by increasing flooding might have slowed down microbial litter decomposition (Day and Megonigal, 1993). This is supported by a negative correlation between seasonal tea litter decomposition rates and reducing soil conditions (measured as Reduction Index RI; Figure A7 (A)). However, a high soil water content can have a dual role for OM decomposition as it can also increase mass low due to strong leaching of OM which plays a particularly large role in intertidal ecosystems (Aerts, 1997; Marley et al., 2019; Trevathan-Tackett et al., 2021). This might be the reason why the reduced tea litter decomposition rates were not accompanied by higher litter stabilization. In contrast, tea litter stabilization was also largely negatively affected by increasing flooding leading to a positive correlation between k_{TBI} and S_{TBI} at the brackish and freshwater marsh. Similar trends were previously reported in tidal wetlands (Mueller et al., 2018). The different qualities of green and rooibos tea might lead to the varying patterns of tea decomposition along the flooding gradient. Green tea is more nutrient-rich and contains a higher fraction of soluble compounds compared to rooibos tea which has less nutrients, fewer soluble compounds, and is rich in lignin (Keuskamp et al., 2013). Consequently, rooibos tea may be less susceptible to leaching than green tea and less appealing to microbial decomposers, as its breakdown is energetically less favorable under oxygen-limited conditions. It was demonstrated that the decomposition of rooibos tea is more strongly influenced by soil conditions than that of green tea, likely due to differences in litter quality (Fanin et al., 2020). This finding aligns with previous studies demonstrating that the effects of oxygen availability on OM decomposition depend on OM quality. Labile materials generally decompose at similar rates in both oxic and anoxic environments while the breakdown of lignin occurs more slowly and incompletely in the absence of oxygen (Benner et al., 1984; Kristensen et al., 1995; Hulthe et al., 1998; Basile-Doelsch et al., 2020). As a result, the mass loss of rooibos tea decreased with increasing flooding frequency, leading to a lower decomposition rate k, whereas the mass loss of green tea increased with increasing flooding, resulting in a lower stabilization factor S. An underlying assumption of the TBI is that stabilization factor S is the same for green and rooibos tea. Certain environmental conditions (strong leaching in our case) can lead to a deviation from this assumption resulting in a decoupling and seemingly positive correlation between k and S (Mori et al., 2022; Sarneel et al., 2024). This

observation underlines the importance to consider litter quality in decomposition studies.

Tea vs. native litter decomposition along estuarine gradients

Native litter decomposition was also affected by the estuarine gradients but showed partly different responses than tea litter. For example, while decomposition rates of tea litter were not affected by the salinity gradient, decomposition rates of native litter increased with increasing salinity in low marshes and pioneer zones. Increasing flooding at the salt marsh did not affect tea litter decomposition rates but increased native litter decomposition rates. These findings suggest that litter quality might have caused differences in native and tea litter decomposition. It is important to note that decomposition indices of both methods cannot be compared directly due to differences in the methodological approach (e.g. mesh size, volume of litter material, incubation period and time). Nevertheless, it can be used to derive some general trends. Several studies have shown the direct link between litter quality and litter decomposition (Stagg et al., 2018; Carrasco-Barea et al., 2022). Thereby, high initial N contents of litter are known to favor microbial decomposition and leaching (Valiela et al., 1985) while higher cellulose and lignin contents, as well as higher ratios of C:N and lignin:N are indicators of recalcitrant litter with low degradability (Wider and Lang, 1982; Aerts, 1997). In our study, decomposition of native litter was strongly affected by litter quality parameters, as the decomposition rate of native litter decreased with indices of recalcitrant litter and increased with labile litter components. The lignin content was the strongest overall predictor for native litter decomposition, followed by the lignin:N ratio which was also highlighted in other studies (Stagg et al., 2018). Moreover, rates of native litter decomposition followed the trend of increasingly labile aboveground litter with increasing salinity and less flooding (Figure S5). This supports previous findings that estuarine gradients indirectly control litter decomposition by shaping the local plant community (Schulte Ostermann et al., 2024). Our findings therefore support existing literature on the importance of litter quality in driving litter decomposition (Zhang et al., 2008).

However, external conditions induced by estuarine gradients for litter decomposition cannot be completely neglected. Decomposition rates of both tea and native litter decreased with increasing flooding at the brackish and freshwater marsh and were negatively influenced by reducing soil conditions. Therefore, the effect of flooding on native litter decomposition at this location might be the combined result of litter quality and environmental conditions induced by the flooding gradient. The estuarine gradients can directly affect

litter decomposition by increasing salinity and flooding, or indirectly through controlling other site conditions. For example, we found that tea and native litter decomposition rates were negatively affected by the clay content, while it was positively affected by the sand content of the soil. The soil texture of estuarine marshes can be the result of the sedimentation dynamics along the estuarine gradients as freshwater marshes often receive finer textured sediments compared to their marine counterparts (Butzeck et al., 2015). A higher sand content in soil might increase drainage and the aeration of the soil which might have enhanced litter decomposition (Carrasco-Barea et al., 2022). But higher contents of sand were not always related to higher decomposition rates (and vice versa for the clay content) which indicates that the effect of soil texture also depends on the interplay with other factors.

Based on these observations, climate change is likely to influence litter decomposition through various pathways. If inland migration of marshes is restricted, the area of freshwater marshes may decline due to increased salinity associated with sea-level rise (Craft et al., 2009). This shift may lead to increased labile plant material, potentially enhancing decomposition rates. Our study also demonstrated that flooding, which may be also enhanced with sea-level rise, can impede or increase litter decomposition depending on litter quality. Therefore, the overall impact of climate change on litter decomposition will be influenced by the complex interplay of multiple factors within tidal ecosystems.

A4.2 Effect of season

Climate has been identified as a major driver of OM decomposition (Aerts, 1997). We therefore expected strong seasonal variations in litter decomposition. Indeed, we observed high tea litter decomposition rates and low tea litter stabilization in summer, while winter showed the opposite trend. Seasonal maxima of k_{TBI}-values in our study occurred during summer and reached or exceeded upper values reported by Keuskamp et al. (2013) and Mueller et al. (2018) (Figure S1). Annual and seasonal values of stabilization factor S_{TBI} were in the lower to mid-range of S-values found by Keuskamp et al. (2013) and Mueller et al. (2018). This seasonal pattern is typical for temperate regions (Daebeler et al., 2022; Sarneel et al., 2024). Decomposition of OM increases with temperature, which has also been demonstrated for tidal wetlands (Mueller et al., 2018; Trevathan-Tackett et al., 2021). In addition to temperature, litter decomposition is affected by soil moisture which also varies seasonally (Petraglia et al., 2019). In winter, higher soil water content induced by a lower

evaporation and increased storm floods might also limit decomposition. In summer, low water availability can hamper decomposition in rarely flooded locations of marshes, particularly when co-occurring with high salinities (Hemminga et al., 1991). This might have been the case in the high salt marsh, being the only location with lowest tea litter decomposition rates during summer. In contrast, tea litter decomposition rates at the brackish and freshwater high marshes exceeded k-values found by Keuskamp et al. (2013) and Mueller et al. (2018) during summer. This indicates that brackish and freshwater high marshes provided optimal conditions for tea litter decomposition in summer.

The strength of seasonal variation in tea litter decomposition decreased with increasing flooding as high marshes showed a stronger seasonal variation than pioneer zones. The high and relatively constant soil water content in pioneer zones throughout the year might diminish seasonal variations in litter decomposition. The soil water content at the freshwater high marsh (10 cm depth) showed a significant stronger seasonal fluctuation than the pioneer zone (Table S4). Variations in soil water content might also explain the varying effects of estuarine gradients on tea litter decomposition throughout the year. A high and more similar soil water content in all flooding zones during winter might reduce the flooding effect. The overall high water content and cold temperature might reduce microbial decomposition and leaching, leading to the low decomposition rates and high stabilization in winter. In warmer seasons, the soil water content showed a stronger differentiation along the flooding gradient and therefore tidal inundation might have had a stronger impact on decomposition.

Projected climate warming has the potential to enhance litter decomposition in the Elbe Estuary. Although rising sea levels may lead to increased soil moisture and promote anoxic conditions, this does not necessarily result in reduced OM decomposition rates as tea litter decomposition rates were highest during the summer months, also in wet pioneer zones. Experiments have demonstrated that warming can increase tea litter decomposition rates in salt marshes, regardless of flooding frequency. However, the response of tea litter stabilization to warming were found to be inhibited by increasing reducing soil conditions (Tang et al., 2023).

A4.3 Prokaryotic communities and litter decomposition

Effect of substrate on prokaryotic community structure

The substrate type (soil, native litter, and tea litter) had a strong effect on the composition and diversity of the prokaryotic communities. This was mainly observed by a different composition of the prokaryotic communities associated with green and rooibos tea, while the native litter and soil communities showed a strong overlap with each other. Similar to other studies (Pioli et al., 2020; Trevathan-Tackett et al., 2021; Daebeler et al., 2022), the soil-associated community had the highest diversity and evenness compared to the communities associated with native litter and tea. Together with a different assemblage of the non-incubated tea and native litter controls, these findings indicate the selective colonization of tea and native litter with prokaryotic taxa originating from the soil pool (Figure S7) (Pioli et al., 2020). The taxa that benefited from or were better adapted to the specific substrate became dominant, whereby a certain degree of diversity and evenness was lost compared to the surrounding soil. The strong overlap of native litter and soil-associated communities reflected the adaptation of the soil prokaryotic community to the local litter. In contrast, the foreign tea litter provided new substrate and created a specific ecological niche that not all microbial groups can equally exploit and therefore different prokaryotic taxa were selected. Further, green tea and rooibos tea contain compounds with antimicrobial properties, which might lead to the observed decrease in the diversity of the prokaryotic community colonizing the tea compared to communities associated with native litter and soil (Friedman, 2007; Simpson et al., 2013). Plants influence the soil microbial communities not only through the supply of litter material but also by releasing root exudates into the rhizosphere. Root exudation creates redox oscillations by either inducing reducing conditions through OM input or promote oxidation in an otherwise anoxic environments by releasing O_2 to which the microbial community reacts (Grüterich et al., 2024; Rolando et al., 2024). The introduction of non-native litter (green tea or rooibos tea) leads to shifts in the prokaryotic community composition as different taxa respond to the altered availability of resources and environmental conditions, which were well adapted to both the native litter and root exudates before.

Estuarine gradients and prokaryotic community structure

Besides substrate type, the prokaryotic communities were influenced by the estuarine gradients. The composition of the prokaryotic community at the salt marsh showed a clear distinction from the brackish and freshwater marsh and

was characterized by a lower diversity. Salinity is known to strongly affect prokaryotic communities by reducing biomass and diversity as not all taxa can cope with the osmotic stress induced by increased salinity (Lozupone and Knight, 2007; Chen et al., 2022). The lower diversity of the salt marsh community is supported by a negative correlation between soil EC and alpha diversity indices of the soil community. Flooding also negatively affected the diversity of the prokaryotic communities in soil and native litter at the salt marsh (Figure S8). This might also be related to the enhanced input of saltwater with increasing inundation frequency as we did not observe this negative effect at the brackish and freshwater marsh. At the brackish and freshwater marsh, we observed a slight increase (not significant) with increasing flooding in alpha diversity indices of the communities associated with native litter and soil which might be the result of increased input of different prokaryotic taxa with regular inundation. As this is only a slight tendency, this requires further investigation. The observed patterns in alpha diversity of the prokaryotic soil community along the estuarine gradient are less pronounced in communities associated with native litter and tea. Particularly the tea-associated communities often deviate from patterns in the soil community. This observation underlines the importance of the substrate type and litter quality for the prokaryotic community.

Relative abundance of prokaryotic taxa

16S rRNA offers the benefit of allowing simultaneous observation of shifts in multiple functional groups. Nonetheless, linking phylogenetic groups to specific functions can be difficult due to microbial plasticity and functional redundancy. There is still limited understanding of how microbial composition affects community-level physiological profiles (Yarwood, 2018) Nonetheless, some phylogenetic groups are recognized for specific functions. While these characteristics may not be universally applicable to every member of this group, they provide insight into the general capabilities associated with many members within that group.

The prokaryotic taxa found in tea, native litter and soil are typical for marine and estuarine sediments (Baker et al., 2015; Zhang et al., 2021; Chen et al., 2022). The substrate type and the estuarine gradients had strong effects on the relative abundance of dominant prokaryotic taxa. The clearest distinction in dominant taxa was observed between communities associated with soil and tea, while communities associated native litter often had an intermediate position. This observation suggests the adaptation of the local prokaryotic community to the local litter. Similar to a previous study (Daebeler et al., 2022), green and

rooibos tea showed similar patterns regarding dominant prokaryotic taxa (Figure A5 (A), Figure A6).

On phylum level, Bacillota, Pseudomonadota, and Bacteroidota showed an increased abundance in tea and native litter compared to soil, indicating that these phyla take over an important role in the breakdown of litter and proliferate rapidly on the rich substrates provided by the tea and native litter. Bacteroidota are known for their ability to break down complex organic compounds, which could explain their prevalence in both substrates (Bauer et al., 2006). Thignificant increase of Bacillota in tea litter, especially in the freshwater low marsh and in pioneer zones, suggests that Bacillota are particularly efficient at degrading the tea litter and that the conditions in these zones favor their growth. Bacillota are often involved in the decomposition of organic material (Wegner and Liesack, 2016; Jiang et al., 2019). Several orders of these phyla, such as Pseudomonadales (Pseudomonadota), Rhizobiales (Pseudomonadota) Flavobacteriales (Bacteroidota), Sphingobacteriales (Bacteroidota), together with Micrococcales (Actinomycetota) also showed a larger abundance in litter compared to soil which was also observed in other studies with tea bags (Daebeler et al., 2022) or straw (Yan et al., 2024). The phyla Acidobacteriota and Chloroflexota had a lower abundance in tea compared to soil. The decline in Acidobacteriota abundance when colonizing tea litter suggests that this prokaryotic group may not thrive under the conditions or resource availability provided by the tea litter. Acidobacteriota are often found in nutrient-poor soils and can effectively use scarce resources which provide an advantage compared to other taxa (Ward et al., 2009) and might explain their higher abundance in soil. With regard to tea, Acidobacteriota may struggle to adapt to the chemical composition or physical properties of the tea substrate. The minimal occurrence of Chloroflexota in tea indicates that this group of bacteria may be reduced by the secondary metabolites present in the tea (Friedman, 2007; Simpson et al., 2013), as it is a common phylum in soils and usually known for its diverse role in C metabolism (Hug et al., 2013).

Litter decomposition and prokaryotic community diversity

Previous studies have highlighted the role of microbial diversity for litter decomposition (Hättenschwiler et al., 2005; Maron et al., 2018; Liu et al., 2023). In this study, the decomposition of tea litter (weight loss of both tea types and k_{TBI}) was positively affected by the diversity of the prokaryotic soil community, while the stabilization factor S_{TBI} was negatively affected. This observation indicates that a diverse pool of prokaryotes in soil is important for the successful colonization of the foreign tea litter by taxa capable of utilizing

this substrate. We found highest green tea mass loss with increasing flooding at the brackish and freshwater marshes, which coincided with a slight (but not significant) increase in soil prokaryotic richness and diversity with increasing flooding. A higher diversity with increasing flooding might be beneficial to increase the functional diversity of the community while environmental conditions become more adverse (e.g. oxygen limitation) (Maron et al., 2018). The green tea might be usable by a wider set of microorganisms and therefore benefits directly from a diverse soil pool. In contrast, the diversity of the prokaryotic community associated with the tea litter was less important for tea decomposition and native litter mass loss was negatively correlated with increasing soil diversity. These observations suggest that diversity is not necessarily predictive for the effectiveness of the prokaryotic community to decompose the specific litter under the local conditions. In general, a high microbial diversity promotes ecosystem functioning, but at the same time, the species identity and community composition are essential for adaptation to specific environments (Peter et al., 2011).

A5 Conclusion

In this study, we provided insights into litter decomposition and associated prokaryotic communities in marsh soils of the Elbe Estuary. Significant spatio-temporal variations in litter decomposition were observed, driven by the dynamic interaction of estuarine gradients, local conditions, climate, and litter quality. Litter quality is thereby a key parameter driving litter decomposition along the estuary. The recalcitrant nature of rooibos, leads to reduced mass loss under frequent flooding, while the more labile green tea experiences enhanced mass loss. The chemical composition of local native litter, particularly the lignin content, drove its decomposition along the estuarine gradients. Seasonal variation in litter decomposition was affected by estuarine gradients, with optimal conditions in less frequently flooded areas of the brackish and freshwater marsh during summer, while simultaneously salt marshes exhibited low decomposition rates due to high salinity and dry soil. Salinity also strongly shaped the prokaryotic community involved in decomposition, affecting both community structure and diversity. With this the estuarine gradient indirectly influence litter decomposition, particularly the foreign tea litter. The prokaryotic soil community demonstrated a strong overlap with the community associated with native litter, suggesting an adaptation to the local vegetation. Based on

our findings, climate change could have substantial effects on OM decomposition dynamics in estuarine marshes but predicting the potential effects is challenging due to the numerous interacting factors. The impact of climate change on litter decomposition will be determined by the complex interplay of salinity, flooding, temperature, soil conditions, and litter quality. Warmer temperatures may lead to higher litter decomposition but only as long as sufficient soil water is available. This highlights the necessity for further research to consider this complexity to fully comprehend litter decomposition dynamics in estuarine ecosystems.

Authors' contributions

Friederike Neiske: Conceptualization, Formal Analysis, Investigation, Writing - original draft, Visualization, Project administration. **Luise Grüterich:** Conceptualization, Formal Analysis, Investigation, Visualization, Writing – review & editing. **Annette Eschenbach:** Conceptualization, Resources, Writing - review & editing, Supervision, Funding acquisition. **Monica Wilson:** Investigation, Writing - review & editing. **Wolfgang R. Streit:** Conceptualization, Resources, Writing - review & editing, Supervision, Funding acquisition. **Kai Jensen:** Investigation, Resources, Writing - review & editing, Supervision, Funding acquisition. **Joscha N. Becker:** Conceptualization, Writing - review & editing, Supervision, Project administration.

Acknowledgement

This study was funded by the *Deutsche Forschungsgemeinschaft* (DFG, German Research Foundation) within the Research Training Group 2530: "Biota-mediated effects on Carbon cycling in Estuaries" (project number 407270017; contribution to *Universität Hamburg* and *Leibniz-Institut für Gewässerökologie und Binnenfischerei im Forschungsverbund Berlin e.V.*) and further supported by the DFG Research Infrastructure NGS_CC (project 407495230) as part of the Next Generation Sequencing Competence Network (project 423957469). We thank Volker Kleinschmidt, Deborah Harms, Sumita Rui, Annika Naumann, Julian Mittmann-Goetsch, Fay Lexmond and all involved student assistants for their help during field and lab work, as well as technical support. We further thank all persons involved in the planning, establishment and maintenance of the RTG 2530 marsh research facilities.

A6 References

Aerts, R., 1997. Climate, Leaf Litter Chemistry and Leaf Litter Decomposition in Terrestrial Ecosystems: A Triangular Relationship. Oikos 79, 439.

Baker, B.J., Lazar, C.S., Teske, A.P., Dick, G.J., 2015. Genomic resolution of linkages in carbon, nitrogen, and sulfur cycling among widespread estuary sediment bacteria. Microbiome 3, 14.

Basile-Doelsch, I., Balesdent, J., Pellerin, S., 2020. Reviews and syntheses: The mechanisms underlying carbon storage in soil. Biogeosciences 17, 5223–5242.

Bauer, M., Kube, M., Teeling, H., Richter, M., Lombardot, T., Allers, E., Würdemann, C.A., Quast, C., Kuhl, H., Knaust, F., Woebken, D., Bischof, K., Mussmann, M.,

Choudhuri, J.V., Meyer, F., Reinhardt, R., Amann, R.I., Glöckner, F.O., 2006. Whole genome analysis of the marine Bacteroidetes'Gramella forsetii' reveals adaptations to degradation of polymeric organic matter. Environmental microbiology 8, 2201–2213.

Becker, J.N., Kuzyakov, Y., 2018. Teatime on Mount Kilimanjaro: Assessing climate and land-use effects on litter decomposition and stabilization using the Tea Bag Index. Land Degradation & Development 29, 2321–2329.

Benner, R., Maccubbin, A.E., Hodson, R.E., 1984. Anaerobic biodegradation of the lignin and polysaccharide components of lignocellulose and synthetic lignin by sediment microflora. Applied and environmental microbiology 47, 998–1004.

Bezemer, T.M., Fountain, M.T., Barea, J.M., Christensen, S., Dekker, S.C., Duyts, H., van Hal, R., Harvey, J.A., Hedlund, K., Maraun, M., Mikola, J., Mladenov, A.G., Robin, C., Ruiter, P.C. de, Scheu, S., Setälä, H., Smilauer, P., van der Putten, W.H., 2010. Divergent composition but similar function of soil food webs of individual plants: plant species and community effects. Ecology 91, 3027–3036.

Bierschenk, A.M., Savage, C., Townsend, C.R., Matthaei, C.D., 2012. Intensity of Land Use in the Catchment Influences Ecosystem Functioning Along a Freshwater-Marine Continuum. Ecosystems 15, 637–651.

Boehlich, M.J., Strotmann, T., 2008. The Elbe Estuary. Die Küste 74, 288–306.

Branoff, B.B., Grüterich, L., Wilson, M., Tobias-Hunefeldt, S.P., Saadaoui, Y., Mittmann-Goetsch, J., Neiske, F., Lexmond, F., Becker, J.N., Grossart, H.-P., Porada, P., Streit, W.R., Eschenbach, A., Kutzbach, L., Jensen, K., 2024. Partitioning biota along the Elbe River estuary: where are the community transitions?

Butzeck, C., Eschenbach, A., Gröngröft, A., Hansen, K., Nolte, S., Jensen, K., 2015. Sediment Deposition and Accretion Rates in Tidal Marshes Are Highly Variable Along Estuarine Salinity and Flooding Gradients. Estuaries and Coasts 38, 434–450.

Callahan, B.J., McMurdie, P.J., Rosen, M.J., Han, A.W., Johnson, A.J.A., Holmes, S.P., 2016. DADA2: High-resolution sample inference from Illumina amplicon data. Nature methods 13, 581–583.

Carrasco-Barea, L., Llorens, L., Romaní, A.M., Gispert, M., Verdaguer, D., 2022. Litter decomposition of three halophytes in a Mediterranean salt marsh: Relevance of litter quality, microbial activity and microhabitat. The Science of the total environment 838, 155743.

Castenson, K.L., Rabenhorst, M.C., 2006. Indicator of reduction in soil (IRIS) evaluation of a new approach for assessing reduced conditions in soil. Soil Science Society of America Journal 70, 1222–1226.

Chen, H., Ma, K., Huang, Y., Fu, Q., Qiu, Y., Yao, Z., 2022. Significant response of microbial community to increased salinity across wetland ecosystems. Geoderma 415, 115778.

Cornwell, W.K., Weedon, J.T., 2014. Decomposition trajectories of diverse litter types: a model selection analysis. Methods in Ecology and Evolution 5, 173–182.

Craft, C., 2007. Freshwater input structures soil properties, vertical accretion, and nutrient accumulation of Georgia and U.S tidal marshes. Limnology and Oceanography 52, 1220–1230.

Craft, C., Clough, J., Ehman, J., Joye, S., Park, R., Pennings, S., Guo, H., Machmuller, M., 2009. Forecasting the effects of accelerated sea-level rise on tidal marsh ecosystem services. Frontiers in Ecology and the Environment 7, 73–78.

Daebeler, A., Petrová, E., Kinz, E., Grausenburger, S., Berthold, H., Sandén, T., Angel, R., 2022. Pairing litter decomposition with microbial community structures using the Tea Bag Index (TBI). SOIL 8, 163–176.

Day, F.P., Megonigal, J.P., 1993. The relationship between variable hydroperiod, production allocation, and belowground organic turnover in forested wetlands. Wetlands 13, 115–121.

Djukic, I., Kepfer-Rojas, S., Schmidt, I.K., Larsen, K.S., Beier, C., Berg, B., Verheyen, K., 2018. Early stage litter decomposition across biomes. The Science of the total environment 628-629, 1369–1394.

DWD, 2024. Time series and trends for the parameters temperature and precipitation. Reference period: 1991 - 2020. Federal State of Schleswig-Holstein. https://www.dwd.de/EN/ourservices/zeitreihen/zeitreihen.html#buehneTop, last accessed 20 Feb 2024.

EEA, 2017. EEA coastline for analysis (raw) - version 3.0. https://www.eea.europa.eu/data-and-maps/data/eea-coastline-for-analysis-2/gis-data/eea-coastline-polygon, last accessed 27 Feb 2024.

Engels, J.G., Jensen, K., 2009. Patterns of wetland plant diversity along estuarine stress gradients of the Elbe (Germany) and Connecticut (USA) Rivers. Plant Ecology & Diversity 2, 301–311.

Fanin, N., Bezaud, S., Sarneel, J.M., Cecchini, S., Nicolas, M., Augusto, L., 2020. Relative Importance of Climate, Soil and Plant Functional Traits During the Early Decomposition Stage of Standardized Litter. Ecosystems 23, 1004–1018.

Franzitta, G., Hanley, M.E., Airoldi, L., Baggini, C., Bilton, D.T., Rundle, S.D., Thompson, R.C., 2015. Home advantage? Decomposition across the freshwater-estuarine transition zone varies with litter origin and local salinity. Marine environmental research 110, 1–7.

Friedman, M., 2007. Overview of antibacterial, antitoxin, antiviral, and antifungal activities of tea flavonoids and teas. Molecular nutrition & food research 51, 116–134.

Graves, S., Piepho, H.-P., Selzer, M.L., 2015. Package 'multcompView'.

Grüterich, L., Wilson, M., Jensen, K., Streit, W., Müller, P., 2024. Transcriptomic response of wetland microbes to root influence. *iScience*. https://doi.org/10.1016/j.isci.2024.110890.

Grüterich, L., Woodhouse, J.N., Mueller, P., Tiemann, A., Ruscheweyh, H., Sunagawa, S., Grossart, H., Streit, W.R., 2025. Assessing environmental gradients in relation to dark CO_2 fixation in estuarine wetland microbiomes. Applied Environmental Microbiology 91:e02177-24. https://doi.org/10.1128/aem.02177-24.

Hättenschwiler, S., Tiunov, A.V., Scheu, S., 2005. Biodiversity and Litter Decomposition in Terrestrial Ecosystems. Annual Review of Ecology, Evolution, and Systematics 36, 191–218.

Hemminga, M.A., Leeuw, J. de, Munek, W. de, Koutstaal, B.P., 1991. Decomposition in estuarine salt marshes: the effect of soil salinity and soil water content. Vegetatio 94, 25–33.

Hothorn, T., Bretz, F., Westfall, P., Heiberger, R.M., Schuetzenmeister, A., Scheibe, S., Hothorn, M.T., 2016. Package 'multcomp'.

Hug, L.A., Castelle, C.J., Wrighton, K.C., Thomas, B.C., Sharon, I., Frischkorn, K.R., Williams, K.H., Tringe, S.G., Banfield, J.F., 2013. Community genomic analyses

constrain the distribution of metabolic traits across the Chloroflexi phylum and indicate roles in sediment carbon cycling. Microbiome 1, 22.

Hulthe, G., Hulth, S., Hall, P.O., 1998. Effect of oxygen on degradation rate of refractory and labile organic matter in continental margin sediments. Geochimica et Cosmochimica Acta 62, 1319–1328.

Jiang, Z., Lu, Y., Xu, J., Li, M., Shan, G., Li, Q., 2019. Exploring the characteristics of dissolved organic matter and succession of bacterial community during composting. Bioresource technology 292, 121942.

Keuskamp, J.A., Dingemans, B.J.J., Lehtinen, T., Sarneel, J.M., Hefting, M.M., 2013. Tea Bag Index: a novel approach to collect uniform decomposition data across ecosystems. Methods in Ecology and Evolution 4, 1070–1075.

Kristensen, E., Ahmed, S.I., Devol, A.H., 1995. Aerobic and anaerobic decomposition of organic matter in marine sediment: Which is fastest? Limnology and Oceanography 40, 1430–1437.

Li, F., Angelini, C., Byers, J.E., Craft, C., Pennings, S.C., 2022. Responses of a tidal freshwater marsh plant community to chronic and pulsed saline intrusion. Journal of Ecology 110, 1508–1524.

Liu, S., Plaza, C., Ochoa-Hueso, R., Trivedi, C., Wang, J., Trivedi, P., Zhou, G., Piñeiro, J., Martins, C.S.C., Singh, B.K., Delgado-Baquerizo, M., 2023. Litter and soil biodiversity jointly drive ecosystem functions. Global change biology 29, 6276–6285.

Lopes, M.L., Martins, P., Ricardo, F., Rodrigues, A.M., Quintino, V., 2011. In situ experimental decomposition studies in estuaries: A comparison of Phragmites australis and Fucus vesiculosus. Estuarine, Coastal and Shelf Science 92, 573–580.

Lozupone, C.A., Knight, R., 2007. Global patterns in bacterial diversity. Proceedings of the National Academy of Sciences of the United States of America 104, 11436–11440.

Macreadie, P.I., Anton, A., Raven, J.A., Beaumont, N., Connolly, R.M., Friess, D.A., Kelleway, J.J., Kennedy, H., Kuwae, T., Lavery, P.S., Lovelock, C.E., Smale, D.A., Apostolaki, E.T., Atwood, T.B., Baldock, J., Bianchi, T.S., Chmura, G.L., Eyre, B.D., Fourqurean, J.W., Hall-Spencer, J.M., Huxham, M., Hendriks, I.E., Krause-Jensen, D., Laffoley, D., Luisetti, T., Marbà, N., Masque, P., McGlathery, K.J., Megonigal, J.P., Murdiyarso, D., Russell, B.D., Santos, R., Serrano, O., Silliman, B.R., Watanabe, K., Duarte, C.M., 2019. The future of Blue Carbon science. Nature communications 10, 3998.

Makkonen, M., Berg, M.P., Handa, I.T., Hättenschwiler, S., van Ruijven, J., van Bodegom, P.M., Aerts, R., 2012. Highly consistent effects of plant litter identity and functional traits on decomposition across a latitudinal gradient. Ecology letters 15, 1033–1041.

Marley, A.R., Smeaton, C., Austin, W.E., 2019. An Assessment of the Tea Bag Index Method as a Proxy for Organic Matter Decomposition in Intertidal Environments. Journal of Geophysical Research: Biogeosciences 124, 2991–3004.

Maron, P.-A., Sarr, A., Kaisermann, A., Lévêque, J., Mathieu, O., Guigue, J., Karimi, B., Bernard, L., Dequiedt, S., Terrat, S., Chabbi, A., Ranjard, L., 2018. High Microbial Diversity Promotes Soil Ecosystem Functioning. Applied and environmental microbiology 84.

Mendelssohn, I.A., Sorrell, B.K., Brix, H., Schierup, H.-H., Lorenzen, B., Maltby, E., 1999. Controls on soil cellulose decomposition along a salinity gradient in a Phragmites australis wetland in Denmark. Aquatic Botany 64, 381–398.

Mittmann-Goetsch, J., Wilson, M., Jensen, K., Mueller, P., 2024. Root-driven soil reduction in Wadden Sea salt marshes. Wetlands 44. https://doi.org/10.1007/s13157-024-01867-8.

Mori, T., Nakamura, R., Aoyagi, R., 2022. Risk of misinterpreting the Tea Bag Index: Field observations and a random simulation. Ecological Research 37, 381–389.

Morrissey, E.M., Gillespie, J.L., Morina, J.C., Franklin, R.B., 2014. Salinity affects microbial activity and soil organic matter content in tidal wetlands. Global change biology 20, 1351–1362.

Mueller, P., Granse, D., Nolte, S., Weingartner, M., Hoth, S., Jensen, K., 2020. Unrecognized controls on microbial functioning in Blue Carbon ecosystems: The role of mineral enzyme stabilization and allochthonous substrate supply. Ecology and evolution 10, 998–1011.

Mueller, P., Schile-Beers, L.M., Mozdzer, T.J., Chmura, G.L., Dinter, T., Kuzyakov, Y., Groot, A.V. de, Esselink, P., Smit, C., D'Alpaos, A., Ibáñez, C., Lazarus, M., Neumeier, U., Johnson, B.J., Baldwin, A.H., Yarwood, S.A., Montemayor, D.I., Yang, Z., Wu, J., Jensen, K., Nolte, S., 2018. Global-change effects on early-stage decomposition processes in tidal wetlands – implications from a global survey using standardized litter. Biogeosciences 15, 3189–3202.

Müller, H.-W., Dohrmann, R., Klosa, D., Rehder, S., Eckelmann, W., 2009. Comparison of two procedures for particle-size analysis: Köhn pipette and X-ray granulometry. Journal of Plant Nutrition and Soil Science 172, 172–179.

Naumann, C., Bassler, R., Seibold, R., Barth, C., Buchholz, H., 1976. Methodenbuch: Die chemische Untersuchung von Futtermitteln. Band III. VDLUFA - Verlag.

Nielsen, U.N., Ayres, E., Wall, D.H., Bardgett, R.D., 2011. Soil biodiversity and carbon cycling: a review and synthesis of studies examining diversity–function relationships. European Journal of Soil Science 62, 105–116.

Oksanen, J., Blanchet, F.G., Kindt, R., Legendre, P., Minchin, P.R., O'hara, R.B., Simpson, G.L., Solymos, P., Stevens, M.H.H., Wagner, H., 2013. Package 'vegan'.

Peter, H., Beier, S., Bertilsson, S., Lindström, E.S., Langenheder, S., Tranvik, L.J., 2011. Function-specific response to depletion of microbial diversity. The ISME journal 5, 351–361.

Petraglia, A., Cacciatori, C., Chelli, S., Fenu, G., Calderisi, G., Gargano, D., Abeli, T., Orsenigo, S., Carbognani, M., 2019. Litter decomposition: effects of temperature driven by soil moisture and vegetation type. Plant and Soil 435, 187–200.

Pioli, S., Sarneel, J., Thomas, H.J., Domene, X., Andrés, P., Hefting, M., Reitz, T., Laudon, H., Sandén, T., Piscová, V., Aurela, M., Brusetti, L., 2020. Linking plant litter microbial diversity to microhabitat conditions, environmental gradients and litter mass loss: Insights from a European study using standard litter bags. Soil Biology and Biochemistry 144, 107778.

Qu, W., Li, J., Han, G., Wu, H., Song, W., Zhang, X., 2019. Effect of salinity on the decomposition of soil organic carbon in a tidal wetland. Journal of Soils and Sediments 19, 609–617.

Quast, C., Pruesse, E., Yilmaz, P., Gerken, J., Schweer, T., Yarza, P., Peplies, J., Glöckner, F.O., 2013. The SILVA ribosomal RNA gene database project: improved data processing and web-based tools. Nucleic acids research 41, D590-6.

Quintino, V., Sangiorgio, F., Ricardo, F., Mamede, R., Pires, A., Freitas, R., Rodrigues, A.M., Basset, A., 2009. In situ experimental study of reed leaf decomposition along a full salinity gradient. Estuarine, Coastal and Shelf Science 85, 497–506.

R Core Team, 2022. R. A language and environment for statistical computing. R Foundation for Statistical Computing, Vienna, Austria.

Rabenhorst, M.C., 2008. Protocol for using and interpreting IRIS tubes. Soil Survey Horizons 49, 74–77.

Roache, M.C., Bailey, P.C., Boon, P.I., 2006. Effects of salinity on the decay of the freshwater macrophyte, Triglochin procerum. Aquatic Botany 84, 45–52.

Rolando, J.L., Kolton, M., Song, T., Liu, Y., Pinamang, P., Conrad, R., Morris, J.T., Konstantinidis, K.T., Kostka, J.E., 2024. Sulfur oxidation and reduction are coupled to nitrogen fixation in the roots of the salt marsh foundation plant Spartina alterniflora. Nature communications 15, 3607.

Sarneel, J.M., Hefting, M.M., Sandén, T., van den Hoogen, J., Routh, D., Adhikari, B.S., Alatalo, J.M., Aleksanyan, A., Althuizen, I.H.J., Alsafran, M.H.S.A., Atkins, J.W., Augusto, L., Aurela, M., Azarov, A.V., Barrio, I.C., Beier, C., Bejarano, M.D., Benham, S.E., Berg, B., Bezler, N.V., Björnsdóttir, K., Bolinder, M.A., Carbognani, M., Cazzolla Gatti, R., Chelli, S., Chistotin, M.V., Christiansen, C.T., Courtois, P., Crowther, T.W., Dechoum, M.S., Djukic, I., Duddigan, S., Egerton-Warburton, L.M., Fanin, N., Fantappiè, M., Fares, S., Fernandes, G.W., Filippova, N.V., Fliessbach, A., Fuentes, D., Godoy, R., Grünwald, T., Guzmán, G., Hawes, J.E., He, Y., Hero, J.-M., Hess, L.L., Hogendoorn, K., Høye, T.T., Jans, W.W.P., Jónsdóttir, I.S., Keller, S., Kepfer-Rojas, S., Kuz'menko, N.N., Larsen, K.S., Laudon, H., Lembrechts, J.J., Li, J., Limousin, J.-M., Lukin, S.M., Marques, R., Marín, C., McDaniel, M.D., Meek, Q., Merzlaya, G.E., Michelsen, A., Montagnani, L., Mueller, P., Murugan, R., Myers-Smith, I.H., Nolte, S., Ochoa-Hueso, R., Okafor, B.N., Okorkov, V.V., Onipchenko, V.G., Orozco, M.C., Parkhurst, T., Peres, C.A., Petit Bon, M., Petraglia, A., Pingel, M., Rebmann, C., Scheffers, B.R., Schmidt, I., Scholes, M.C., Sheffer, E., Shevtsova, L.K., Smith, S.W., Sofo, A., Stevenson, P.R., Strouhalová, B., Sundsdal, A., Sühs, R.B., Tamene, G., Thomas, H.J.D., Tolunay, D., Tomaselli, M., Tresch, S., Tucker, D.L., Ulyshen, M.D., Valdecantos, A., Vandvik, V., Vanguelova, E.I., Verheyen, K., Wang, X., Yahdjian, L., Yumashev, X.S., Keuskamp, J.A., 2024. Reading tea leaves worldwide: Decoupled drivers of initial litter decomposition mass-loss rate and stabilization. Ecology letters 27, e14415.

Schreckinger, J., Mutz, M., Mendoza-Lera, C., Frossard, A., 2021. Attributes of Drying Define the Structure and Functioning of Microbial Communities in Temperate Riverbed Sediment. Frontiers in microbiology 12, 676615.

Schulte Ostermann, T., Heuner, M., Fuchs, E., Temmerman, S., Schoutens, K., Bouma, T.J., Minden, V., 2024. Identifying Key Plant Traits and Ecosystem Properties Affecting Wave Attenuation and the Soil Organic Carbon Content in Tidal Marshes. Estuaries and Coasts 47, 144–161.

Simpson, M.J., Hjelmqvist, D., López-Alarcón, C., Karamehmedovic, N., Minehan, T.G., Yepremyan, A., Salehani, B., Lissi, E., Joubert, E., Udekwu, K.I., Alarcon, E.I., 2013. Anti-peroxyl radical quality and antibacterial properties of rooibos infusions and

their pure glycosylated polyphenolic constituents. Molecules (Basel, Switzerland) 18, 11264–11280.

Stagg, C.L., Baustian, M.M., Perry, C.L., Carruthers, T.J.B., Hall, C.T., 2018. Direct and indirect controls on organic matter decomposition in four coastal wetland communities along a landscape salinity gradient. Journal of Ecology 106, 655–670.

Swift, M.J., Heal, O.W., Anderson, J.M., 1979. Decomposition in terrestrial ecosystems. University of California Press, Berkeley.

Tang, H., Nolte, S., Jensen, K., Rich, R., Mittmann-Goetsch, J., Mueller, P., 2023. Warming accelerates belowground litter turnover in salt marshes – insights from a Tea Bag Index study. Biogeosciences 20, 1925–1935.

Trevathan-Tackett, S.M., Kepfer-Rojas, S., Engelen, A.H., York, P.H., Ola, A., Li, J., Kelleway, J.J., Jinks, K.I., Jackson, E.L., Adame, M.F., Pendall, E., Lovelock, C.E., Connolly, R.M., Watson, A., Visby, I., Trethowan, A., Taylor, B., Roberts, T.N.B., Petch, J., Farrington, L., Djukic, I., Macreadie, P.I., 2021. Ecosystem type drives tea litter decomposition and associated prokaryotic microbiome communities in freshwater and coastal wetlands at a continental scale. The Science of the total environment 782, 146819.

Valiela, I., Teal, J.M., Allen, S.D., van Etten, R., Goehringer, D., Volkmann, S., 1985. Decomposition in salt marsh ecosystems: The phases and major factors affecting disappearance of above-ground organic matter. Journal of Experimental Marine Biology and Ecology 89, 29–54.

Wang, M., Chen, J.-K., LI, B., 2007. Characterization of Bacterial Community Structure and Diversity in Rhizosphere Soils of Three Plants in Rapidly Changing Salt Marshes Using 16S rDNA. Pedosphere 17, 545–556.

Ward, N.L., Challacombe, J.F., Janssen, P.H., Henrissat, B., Coutinho, P.M., Wu, M., Xie, G., Haft, D.H., Sait, M., Badger, J., Barabote, R.D., Bradley, B., Brettin, T.S., Brinkac, L.M., Bruce, D., Creasy, T., Daugherty, S.C., Davidsen, T.M., DeBoy, R.T., Detter, J.C., Dodson, R.J., Durkin, A.S., Ganapathy, A., Gwinn-Giglio, M., Han, C.S., Khouri, H., Kiss, H., Kothari, S.P., Madupu, R., Nelson, K.E., Nelson, W.C., Paulsen, I., Penn, K., Ren, Q., Rosovitz, M.J., Selengut, J.D., Shrivastava, S., Sullivan, S.A., Tapia, R., Thompson, L.S., Watkins, K.L., Yang, Q., Yu, C., Zafar, N., Zhou, L., Kuske, C.R., 2009. Three genomes from the phylum Acidobacteria provide insight into the lifestyles of these microorganisms in soils. Applied and environmental microbiology 75, 2046–2056.

Wegner, C.-E., Liesack, W., 2016. Microbial community dynamics during the early stages of plant polymer breakdown in paddy soil. Environmental microbiology 18, 2825–2842.

Wickham, H., Chang, W., Wickham, M.H., 2016. Package 'ggplot2'. Create elegant data visualisations using the grammar of graphics. Version 2, 1–189.

Wider, R.K., Lang, G.E., 1982. A Critique of the Analytical Methods Used in Examining Decomposition Data Obtained From Litter Bags. Ecology 63, 1636.

WSV, 2011. MThw-Linie an der Unter- und Außenelbe. www.kuestendaten.de, last accessed 29 Sep 2023.

WSV, 2017. Vegetationskartierung / Biotoptypenkartierung 2017 Unterelbe. www.kuestendaten.de, last accessed 29 Sep 2023.

Yan, C., Zhao, S., Wu, H., Yang, D., Hou, Z., Shan, F., Yan, S., Lyu, X., Ma, C., Gong, Z., 2024. Nitrogen release and microbial community characteristics during the

decomposition of field-incorporated corn straw in Northeast China. Land Degradation & Development 35, 3897–3910.

Yan, N., Marschner, P., Cao, W., Zuo, C., Qin, W., 2015. Influence of salinity and water content on soil microorganisms. International Soil and Water Conservation Research 3, 316–323.

Yang, Y., Moorhead, D.L., Craig, H., Luo, M., Chen, X., Huang, J., Olesen, J.E., Chen, J., 2022. Differential Responses of Soil Extracellular Enzyme Activities to Salinization: Implications for Soil Carbon Cycling in Tidal Wetlands. Global Biogeochemical Cycles 36.

Yarwood, S.A., 2018. The role of wetland microorganisms in plant-litter decomposition and soil organic matter formation: a critical review. FEMS microbiology ecology 94.

Zhang, D., Hui, D., Luo, Y., Zhou, G., 2008. Rates of litter decomposition in terrestrial ecosystems: global patterns and controlling factors. Journal of Plant Ecology 1, 85–93.

Zhang, G., Bai, J., Tebbe, C.C., Zhao, Q., Jia, J., Wang, W., Wang, X., Yu, L., 2021. Salinity controls soil microbial community structure and function in coastal estuarine wetlands. Environmental microbiology 23, 1020–1037.

A7 Supplementary Material

TBI: k vs. S

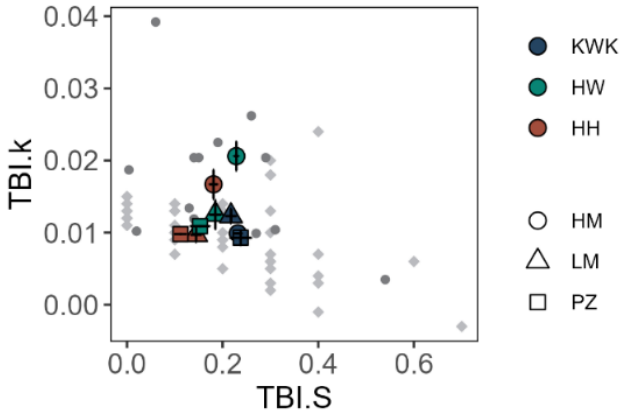

Figure S1: (A) Annual means of decomposition rates k_{TBI} versus stabilization factor S_{TBI} of tea litter along the salinity and flooding gradient of the Elbe Estuary. Light grey diamonds indicate global marshes taken from Mueller et al. (2018), darker grey dots indicate global data taken from Keuskamp et al. (2013). Whiskers indicate standard error of the mean based on five pairs of tea bags and four seasons at each site.

Model fit

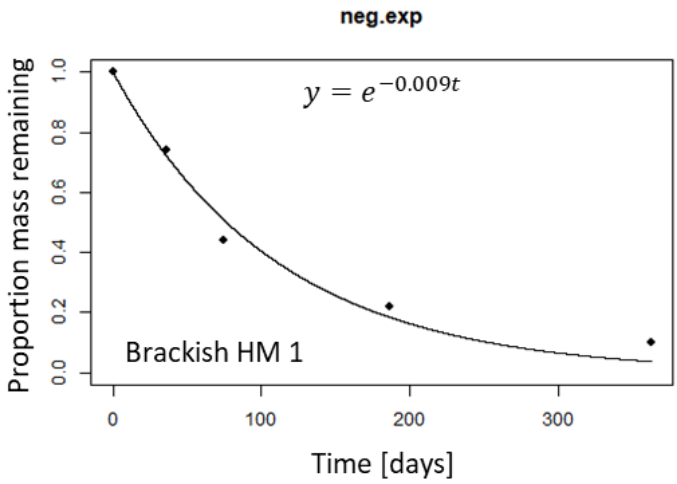

Figure S2: Example model fit (negative exponential) using the R package "litterfitter". Based on relative remaining mass over five time steps.

Seasonal tea litter decomposition

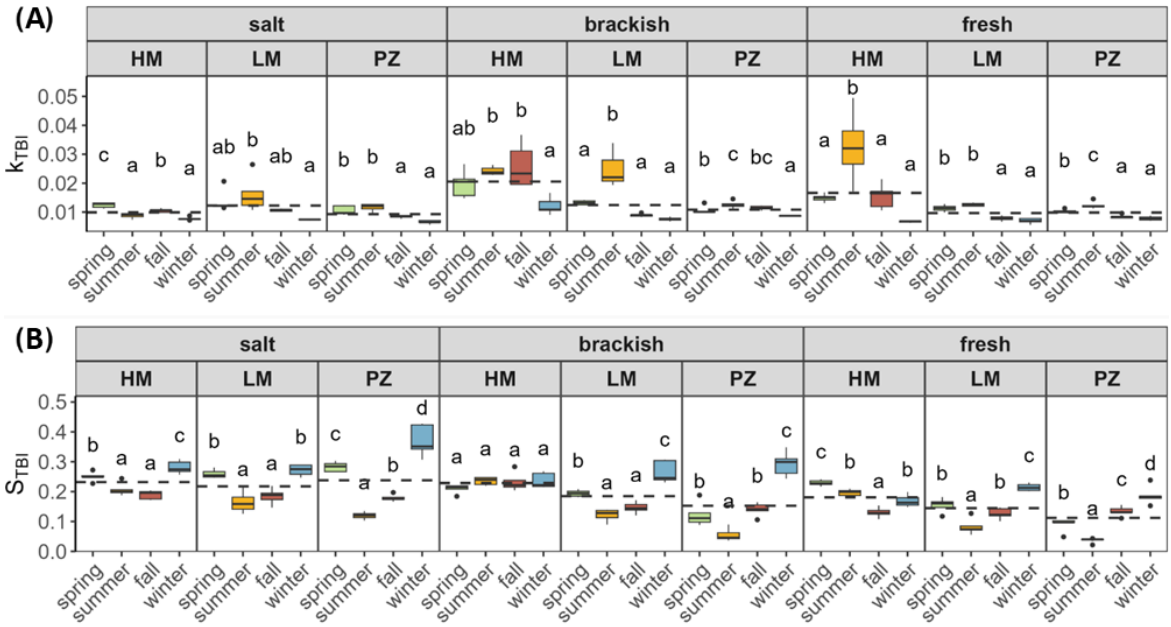

Figure S3: Seasonal variation in (A) decomposition rate k_{TBI} and (B) stabilization factor S_{TBI} of tea litter along the salinity (salt marsh, brackish marsh, freshwater marsh) and flooding gradient (HM = high marsh, LM = low marsh, PZ = pioneer zone) of the Elbe Estuary (n = 5). Lowercase letters indicate significant differences ($p < 0.05$) derived from linear mixed effect model applied on each marsh location separately (n = 5). Dashed lines indicate mean annual decomposition rate k_{TBI} or stabilization factor S_{TBI}.

Correlation Matrix

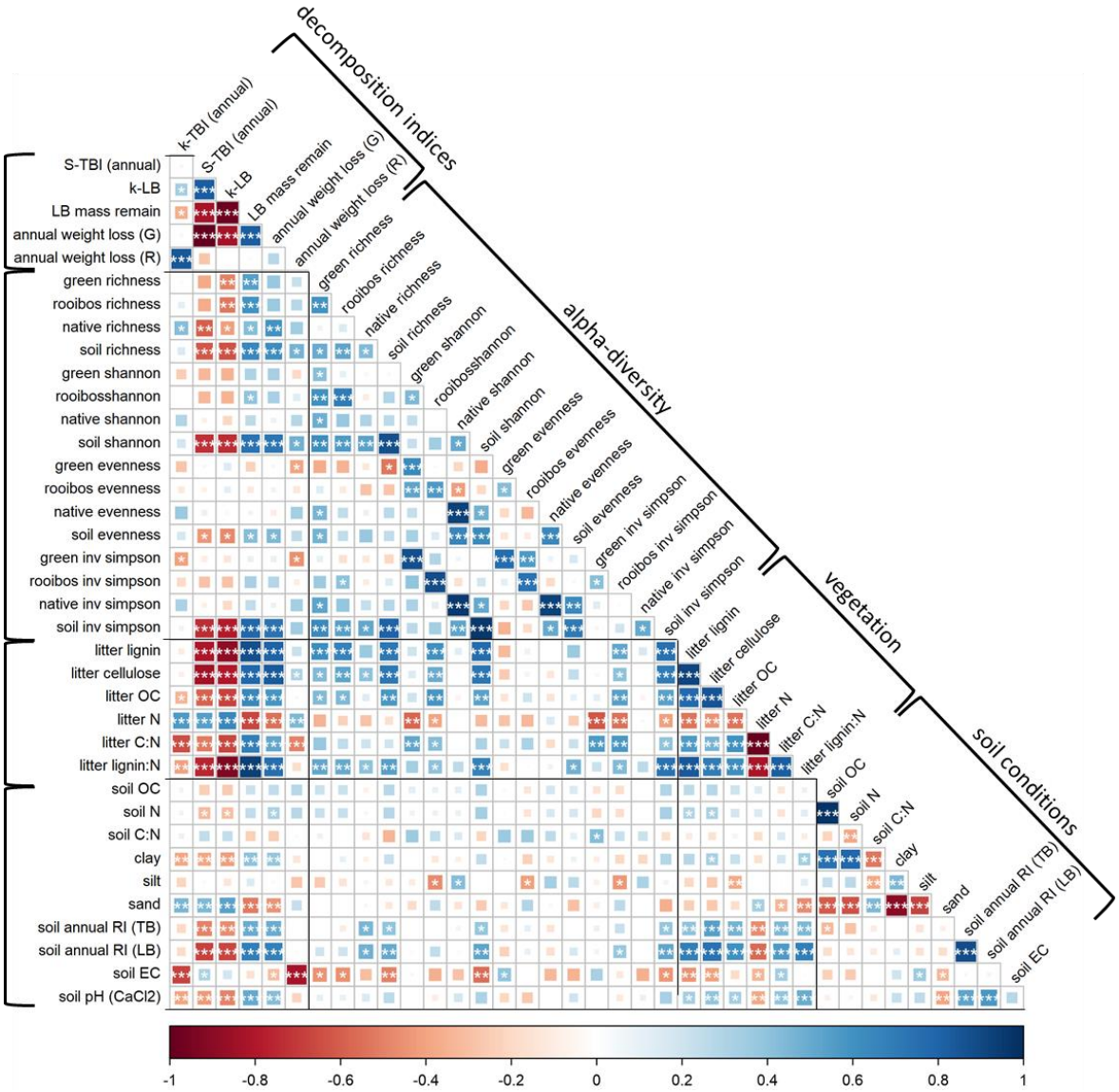

Figure S4: Spearman correlation matrix between litter decomposition indices and selected site characteristics. Asterisk indicate significant correlation at: * $p < 0.05$, ** $p < 0.005$, and *** $p < 0.001$.

Litter quality

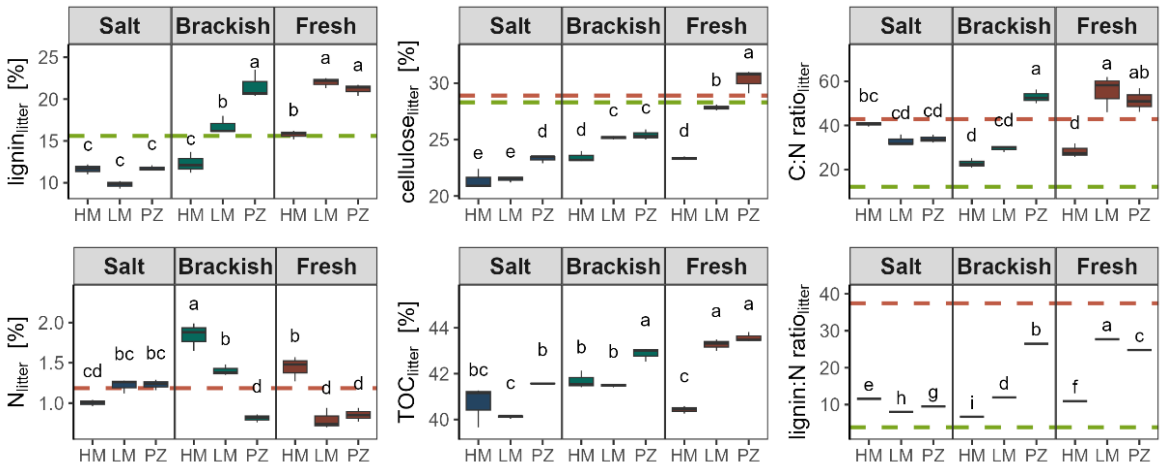

Figure S5: Litter quality indices along the salinity (salt marsh, brackish marsh, freshwater marsh) and flooding gradient (HM = high marsh, LM = low marsh, PZ = pioneer zone) of the Elbe Estuary (n = 3). Lowercase letters indicate significant differences ($p < 0.05$) derived from ANOVA with TukeyHSD post-hoc comparison. Dashed horizontal lines indicate values for green tea (green) and rooibos tea (red) based on values in Keuskamp et al. 2013.

Annual weight loss tea

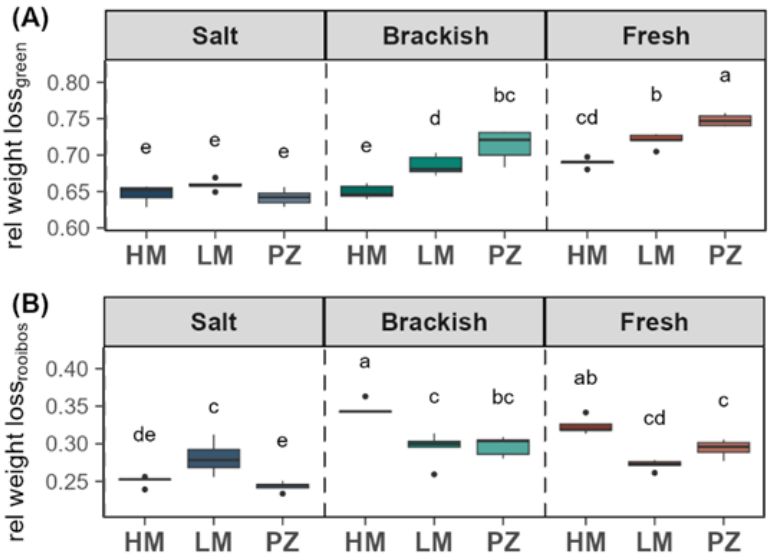

Figure S6: Annual weight loss of (A) green tea and (B) rooibos tea along the salinity (salt marsh, brackish marsh, freshwater marsh) and flooding gradient (HM = high marsh, LM = low marsh, PZ = pioneer zone) of the Elbe Estuary (n = 5). Lowercase letters indicate significant differences ($p < 0.05$) derived from ANOVA with TukeyHSD post-hoc comparison.

Prokaryotic communities (NMDS)

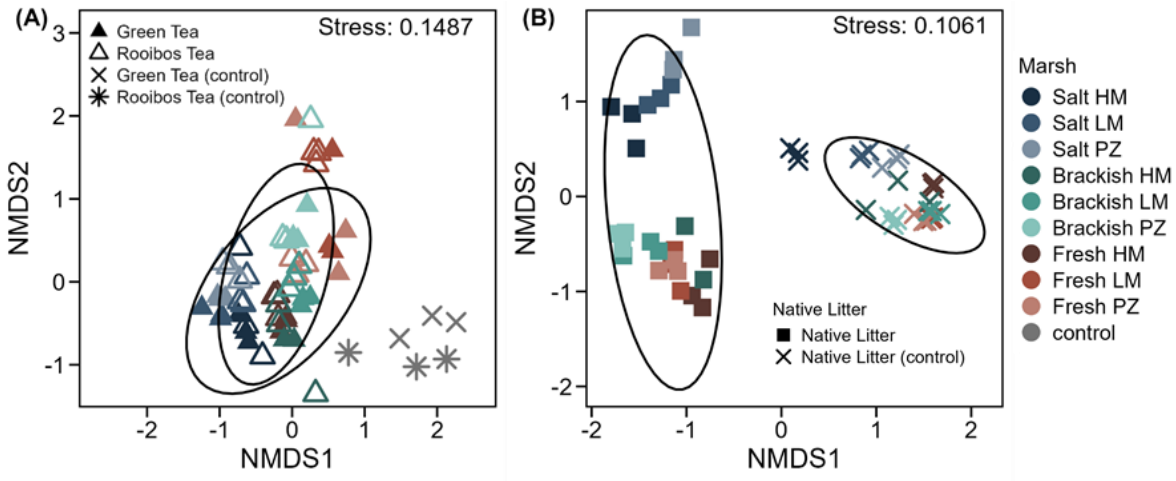

Figure S7: NMDS based on Bray-Curtis dissimilarity of the prokaryotic community associated with (A) tea litter and (B) native litter at genus level along the salinity (salt marsh, brackish marsh, freshwater marsh) and flooding gradient (HM = high marsh, LM = low marsh, PZ = pioneer zone) of the Elbe Estuary and their non-incubated controls. Ellipses indicate 90% confidence area per litter type.

Alpha diversity along estuarine gradients

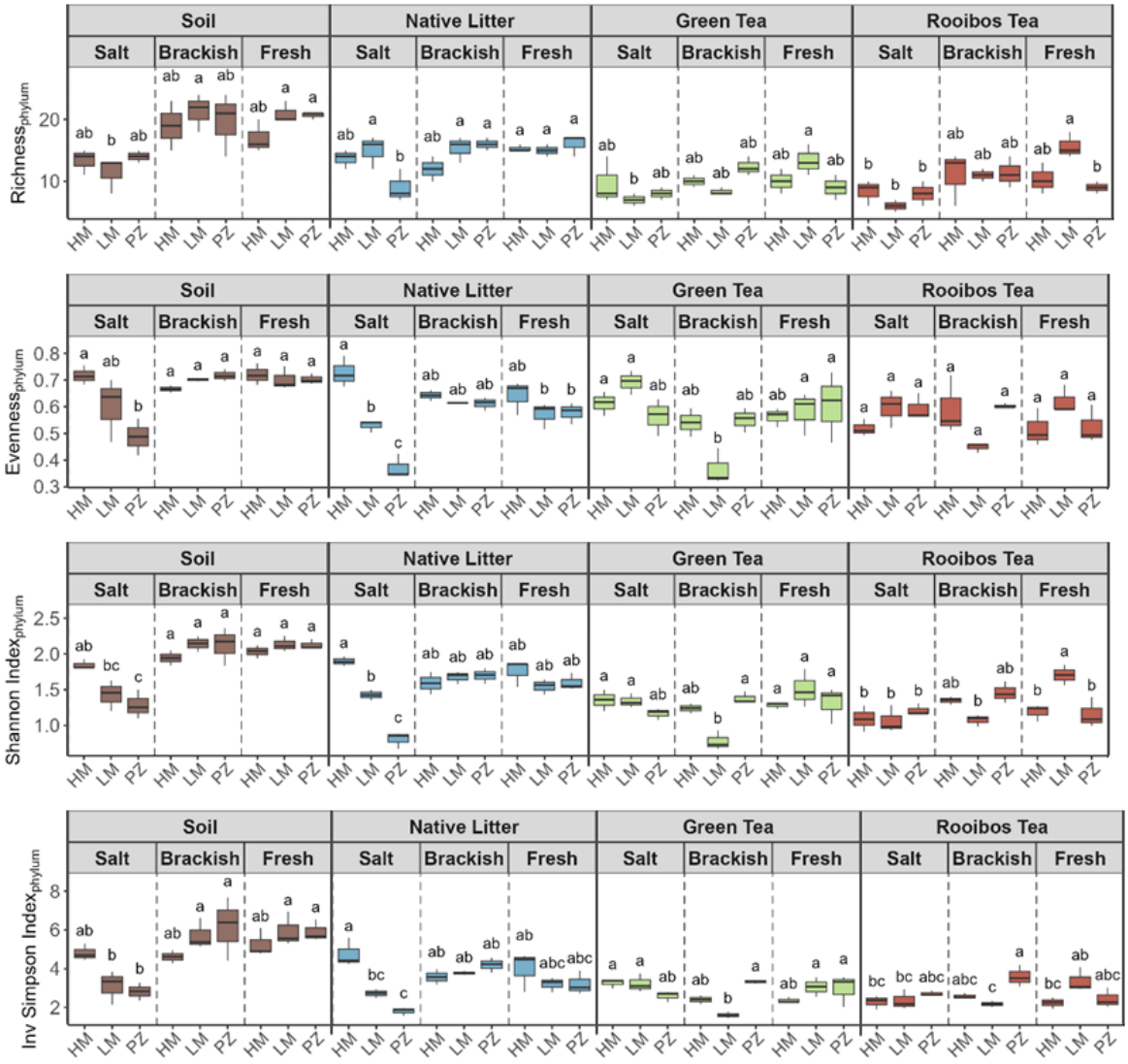

Figure S8: Alpha diversity (richness, evenness, Shannon Diversity Index, and Inverse Simpson Index) of the prokaryotic community at phylum level in the different substrate types along the salinity (salt marsh, brackish marsh, freshwater marsh) and flooding gradient (HM = high marsh, LM = low marsh, PZ = pioneer zone) of the Elbe Estuary (n = 3). Lowercase letters indicate significant differences ($p < 0.05$) derived from ANOVA with TukeyHSD post-hoc comparison applied on each substrate type separately.

Table TBI

Table S1: Decomposition indices of tea and native litter along the salinity and flooding gradient of the Elbe Estuary.

Salinity Gradient	Flooding Gradient	Season	Tea litter								Native litter			
			k (TBI)		S (TBI)		rel weight loss (G)		rel weight loss (R)		k (LB)		rel mass remaining (LB)	
			mean	sde	mean	sde	mean	sde	mean	sde	mean	sde	mean	sde
Salt Marsh	HM	spring	0.012	± 0.0004	0.25	± 0.01	0.63	± 0.01	0.28	± 0.01				
		summer	0.009	± 0.0004	0.21	± 0.01	0.67	± 0.01	0.24	± 0.01				
		fall	0.011	± 0.0003	0.19	± 0.01	0.68	± 0.01	0.28	± 0.00				
		winter	0.008	± 0.0003	0.28	± 0.01	0.61	± 0.01	0.21	± 0.00				
		annual	0.010	± 0.0000	0.23	± 0.01	0.65	± 0.01	0.25	± 0.01	0.006	± 0.00	0.24	± 0.01
	LM	spring	0.014	± 0.0017	0.26	± 0.01	0.62	± 0.01	0.28	± 0.02				
		summer	0.016	± 0.0028	0.17	± 0.02	0.70	± 0.01	0.34	± 0.02				
		fall	0.011	± 0.0002	0.18	± 0.01	0.69	± 0.01	0.28	± 0.00				
		winter	0.007	± 0.0001	0.27	± 0.01	0.61	± 0.01	0.20	± 0.00				
		annual	0.012	± 0.0010	0.22	± 0.01	0.66	± 0.01	0.28	± 0.01	0.011	± 0.00	0.13	± 0.01
	PZ	spring	0.011	± 0.0007	0.28	± 0.01	0.60	± 0.01	0.25	± 0.01				
		summer	0.012	± 0.0006	0.12	± 0.01	0.74	± 0.00	0.32	± 0.01				
		fall	0.008	± 0.0002	0.18	± 0.01	0.69	± 0.00	0.24	± 0.00				
		winter	0.007	± 0.0003	0.37	± 0.02	0.53	± 0.02	0.16	± 0.01				
		annual	0.009	± 0.0010	0.24	± 0.02	0.64	± 0.02	0.24	± 0.01	0.008	± 0.00	0.20	± 0.02
Brackish Marsh	HM	spring	0.020	± 0.0021	0.21	± 0.01	0.67	± 0.01	0.36	± 0.01				
		summer	0.024	± 0.0007	0.24	± 0.01	0.64	± 0.00	0.37	± 0.00				
		fall	0.026	± 0.0034	0.23	± 0.01	0.65	± 0.01	0.38	± 0.01				
		winter	0.012	± 0.0013	0.24	± 0.01	0.64	± 0.01	0.28	± 0.02				
		annual	0.021	± 0.0020	0.23	± 0.01	0.65	± 0.00	0.35	± 0.01	0.009	± 0.00	0.12	± 0.03
	LM	spring	0.013	± 0.0003	0.19	± 0.00	0.68	± 0.00	0.30	± 0.00				
		summer	0.025	± 0.0034	0.12	± 0.01	0.74	± 0.01	0.44	± 0.02				
		fall	0.009	± 0.0002	0.15	± 0.01	0.72	± 0.01	0.27	± 0.00				
		winter	0.008	± 0.0003	0.27	± 0.02	0.62	± 0.01	0.19	± 0.01				
		annual	0.012	± 0.0020	0.18	± 0.01	0.69	± 0.01	0.30	± 0.02	0.004	± 0.00	0.38	± 0.02
	PZ	spring	0.011	± 0.0006	0.12	± 0.02	0.74	± 0.01	0.32	± 0.01				
		summer	0.013	± 0.0006	0.06	± 0.01	0.80	± 0.01	0.35	± 0.01				
		fall	0.011	± 0.0003	0.14	± 0.01	0.72	± 0.01	0.31	± 0.01				
		winter	0.009	± 0.0001	0.29	± 0.02	0.60	± 0.02	0.21	± 0.01				
		annual	0.011	± 0.0000	0.15	± 0.02	0.71	± 0.02	0.30	± 0.01	0.002	± 0.00	0.54	± 0.01
Fresh-water Marsh	HM	spring	0.015	± 0.0006	0.23	± 0.00	0.65	± 0.00	0.31	± 0.01				
		summer	0.033	± 0.0060	0.20	± 0.01	0.68	± 0.00	0.42	± 0.02				
		fall	0.016	± 0.0019	0.13	± 0.01	0.73	± 0.01	0.36	± 0.02				
		winter	0.007	± 0.0001	0.17	± 0.01	0.70	± 0.01	0.21	± 0.00				
		annual	0.017	± 0.0020	0.18	± 0.01	0.69	± 0.01	0.32	± 0.02	0.004	± 0.00	0.32	± 0.03
	LM	spring	0.011	± 0.0005	0.15	± 0.01	0.71	± 0.01	0.30	± 0.01				
		summer	0.013	± 0.0003	0.08	± 0.01	0.77	± 0.01	0.34	± 0.00				
		fall	0.008	± 0.0004	0.13	± 0.01	0.74	± 0.01	0.25	± 0.01				
		winter	0.007	± 0.0004	0.21	± 0.01	0.66	± 0.00	0.20	± 0.01				
		annual	0.010	± 0.0010	0.14	± 0.01	0.72	± 0.01	0.27	± 0.01	0.002	± 0.00	0.61	± 0.02
	PZ	spring	0.010	± 0.0003	0.09	± 0.01	0.77	± 0.01	0.32	± 0.01				
		summer	0.012	± 0.0006	0.04	± 0.00	0.81	± 0.00	0.36	± 0.01				
		fall	0.008	± 0.0003	0.13	± 0.01	0.73	± 0.01	0.26	± 0.01				
		winter	0.008	± 0.0003	0.19	± 0.01	0.68	± 0.01	0.22	± 0.00				
		annual	0.010	± 0.0000	0.11	± 0.01	0.75	± 0.01	0.29	± 0.01	0.002	± 0.00	0.58	± 0.01

Plant Species

Table S2: Plant species with area coverage [%] and Ellenberg Indicator Values for salinity (EIV-S) (Ellenberg et al., 1991) along the salinity and flooding gradient of the Elbe Estuary in July 2022.

Salt High Marsh	[%]	**Brackish High Marsh**	[%]	**Fresh High Marsh**	[%]
Agrostis stolonifera	<0.1	*Agrostis stolonifera*	0.1	*Agrostis stolonifera*	0.8
Aster tripolium	13.4	*Berula erecta*	0.3	*Calystegia sepium*	7.2
Atriplex littoralis	0.2	*Calystegia sepium*	28.3	*Equisetum palustre*	0.1
Atriplex prostrata	15.8	*Dactylis glomerata*	<0.1	*Phalaris arundinacea*	7.6
Elymus athericus	62.3	*Epilobium hirsutum*	24.1	*Phragmites australis*	54.0
Salicornia europaea	<0.1	*Galeopsis sp.*	<0.1	*Urtica dioica*	21.1
Suaeda maritima	0.5	*Galium palustre*	0.2	*Valeriana officinalis*	0.6
		Phalaris arundinacea	4.9		
		Phragmites australis	10.9		
		Poa trivalis	0.2		
		Rosa sp.	2.3		
		Urtica dioica	6.7		
		Valeriana officinalis	<0.1		
		Vicia cracca	0.3		
EIV-S: 5.4		EIV-S: 0.3		EIV-S: 0.0	
Salt Low Marsh	[%]	**Brackish Low Marsh**	[%]	**Fresh Low Marsh**	[%]
Agrostis stolonifera	0.2	*Agrostis stolonifera*	0.2	*Bidens sp.*	0.1
Aster tripolium	18.2	*Berula erecta*	6.9	*Caltha palustris*	0.1
Atriplex littoralis	<0.1	*Caltha palustris*	0.3	*Myosotis palustris*	0.1
Atriplex prostrata	5.6	*Calystegia sepium*	9.5	*Nasturtium officinale*	0.1
Elymus athericus	<0.1	*Lycopus europaeus*	0.9	*Phragmites australis*	92.6
Festuca rubra	8.3	*Phragmites australis*	73.0		
Halimione portulacoides	1.4				
Plantago maritima	<0.1				
Puccinellia maritima	40.8				
Salicornia europaea	1.7				
Spartina anglica	2.3				
Spergularia media	0.1				
Suaeda maritima	3.4				
Triglochin maritima	13.2				
EIV-S: 7.0		EIV-S: 0.1		EIV-S: 0.0	
Salt Pioneer Zone	[%]	**Brackish Pioneer Zone**	[%]	**Fresh Pioneer Zone**	[%]
Aster tripolium	3.2	*Bolboschoenus maritimus*	73.5	*Alisma plantago-aquatica*	1.8
Atriplex prostrata	2.0	*Nasturtium officinale*	0.2	*Caltha palustris*	16.0
Halimione portulacoides	0.01			*Mentha aquatica*	0.1
Puccinellia maritima	4.1			*Myosotis palustris*	0.1
Salicornia europaea	<0.1			*Typha angustifolia*	46.0
Spartina anglica	59.1				
Suaeda maritima	2.6				
Triglochin maritima	0.8				
EIV-S: 7.8		EIV-S: 2.0		EIV-S: 0.7	

Site characteristics

Table S3: Selected soil properties of the different marsh types along the salinity (salt marsh, brackish marsh, freshwater marsh) and flooding gradient (HM = high marsh, LM = low marsh, PZ = pioneer zone) of the Elbe Estuary (mean ± standard error, n = 5). Mean of five replicates.

Marsh type & zone		Depth [cm]	SOC [%]	pH_{CaCl_2}	EC *[µS/cm]*	clay *[%]*	silt *[%]*	sand *[%]*
Salt Marsh	HM	0 - 10	2.9 ± 0.6	7.2 ± 0.3	2606 ± 1081	21.1 ± 4.3	68.1 ± 3.5	10.8 ± 6.1
	LM	0 - 10	1.6 ± 0.2	7.2 ± 0.1	2093 ± 418	14.5 ± 5.1	54.4 ± 7.0	31.1 ± 10.8
	PZ	0 - 10	1.8 ± 0.3	7.2 ± 0.1	2494 ± 387	20.0 ± 7.8	48.4 ± 4.5	31.6 ± 6.4
Brackish Marsh	HM	0 - 10	3.8 ± 1.0	7.1 ± 0.1	292 ± 87	10.4 ± 6.2	18.2 ± 6.4	71.4 ± 12.5
	LM	0 - 10	2.7 ± 0.4	7.3 ± 0.1	704 ± 96	24.4 ± 4.1	63.4 ± 1.2	12.2 ± 3.5
	PZ	0 - 10	0.2 ± 0.0	7.3 ± 0.1	456 ± 39	3.4 ± 0.9	37.5 ± 3.3	59.2 ± 3.7
Freshwater Marsh	HM	0 - 10	5.2 ± 0.6	7.1 ± 0.0	330 ± 79	26.4 ± 1.7	63.3 ± 1.1	10.2 ± 1.6
	LM	0 - 10	5.8 ± 0.7	7.2 ± 0.0	1074 ± 436	39.8 ± 5.7	53.6 ± 4.6	6.6 ± 1.9
	PZ	0 - 10	4.6 ± 0.2	7.4 ± 0.1	1053 ± 188	39.9 ± 12.5	57.4 ± 11.4	2.8 ± 2.1

Table S4: Mean volumetric water content (VWC) of the soil profile at freshwater marsh (HM = high marsh, LM = low marsh, PZ = pioneer zone) corresponding to the incubation periods of the tea bags (n = 1).

Marsh type & zone		Depth [cm]	VWC_{spring} *[%]*	VWC_{summer} *[%]*	VWC_{fall} *[%]*	VWC_{winter} *[%]*
Freshwater Marsh	HM	10	41.9	27.4	43.0	55.5
	LM	10	59.6	56.9	59.6	60.9
	PZ	10	70.1	72.7	75.4	76.1

Study B:

Soil organic carbon stocks and stabilization mechanisms in tidal marshes along estuarine gradients

Friederike Neiske[a]*, Maria Seedtke[a], Annette Eschenbach[a], Monica Wilson[b], Kai Jensen[b], Joscha N. Becker[a]

[a] Institute of Soil Science, CEN Center for Earth System Research and Sustainability, Universität Hamburg, Allende-Platz 2, 20146 Hamburg, Germany

[b] Institute of Plant Science and Microbiology, Universität Hamburg, Ohnhorststrasse 18, 22609 Hamburg, Germany

*corresponding author

For the final publication, please refer to:

Neiske F., Seedtke M., Eschenbach A., Wilson M., Jensen K., Becker J.N. (2025). Soil organic carbon stocks and stabilization mechanisms in tidal marshes along estuarine gradients. *Geoderma*. Volume 456, 117274. https://doi.org/10.1016/j.geoderma.2025.117274

B Abstract

Tidal marshes store large amounts of soil organic carbon (SOC), however, little is known on SOC stabilization mechanisms in these ecosystems. In estuarine marshes, SOC storage is dominated by a complex interaction of tidal inundation and salinity with biotic ecosystem components, leading to strong spatio-temporal variations within estuaries. Our aim was to assess (i) SOC stocks, (ii) SOC stabilization mechanisms (aggregation and mineral-association), and (iii) their environmental drivers along estuarine gradients. We analyzed SOC stocks and SOC density fractions in topsoil (0 - 10 cm) and subsoil (10 - 30 cm) of three marsh zones representing three flooding regimes (daily, monthly, yearly) in three marsh types along the salinity gradient (salt, brackish, freshwater) of the Elbe Estuary, Germany.

Increasing salinity and flooding reduced SOC stocks 0-30 cm (9.3-74.6 t ha^{-1}), which was related to decreasing plant biomass and soil texture. Mineral-associated organic matter (C_{MAOM}) was the largest SOC fraction (59% of total SOC), followed by aggregate-occluded organic matter (C_{oPOM}) (24%) and free particulate organic matter (C_{fPOM}) (16%). The C_{MAOM} amount in topsoils decreased downstream with increasing salinity, reflecting decreasing fine-texture along the estuary. The amount of C_{oPOM} was higher in topsoils and high marshes, indicating negative effects of flooding on aggregation. The relative proportion of C_{fPOM} (% of total SOC) increased with increasing flooding frequency and reducing soil conditions.

Our results underline the importance of estuarine gradients as drivers of SOC storage and stabilization. Climate-change induced sea-level rise and variations in salinity might reduce SOC storage and stabilization in estuaries.

Graphical Abstract

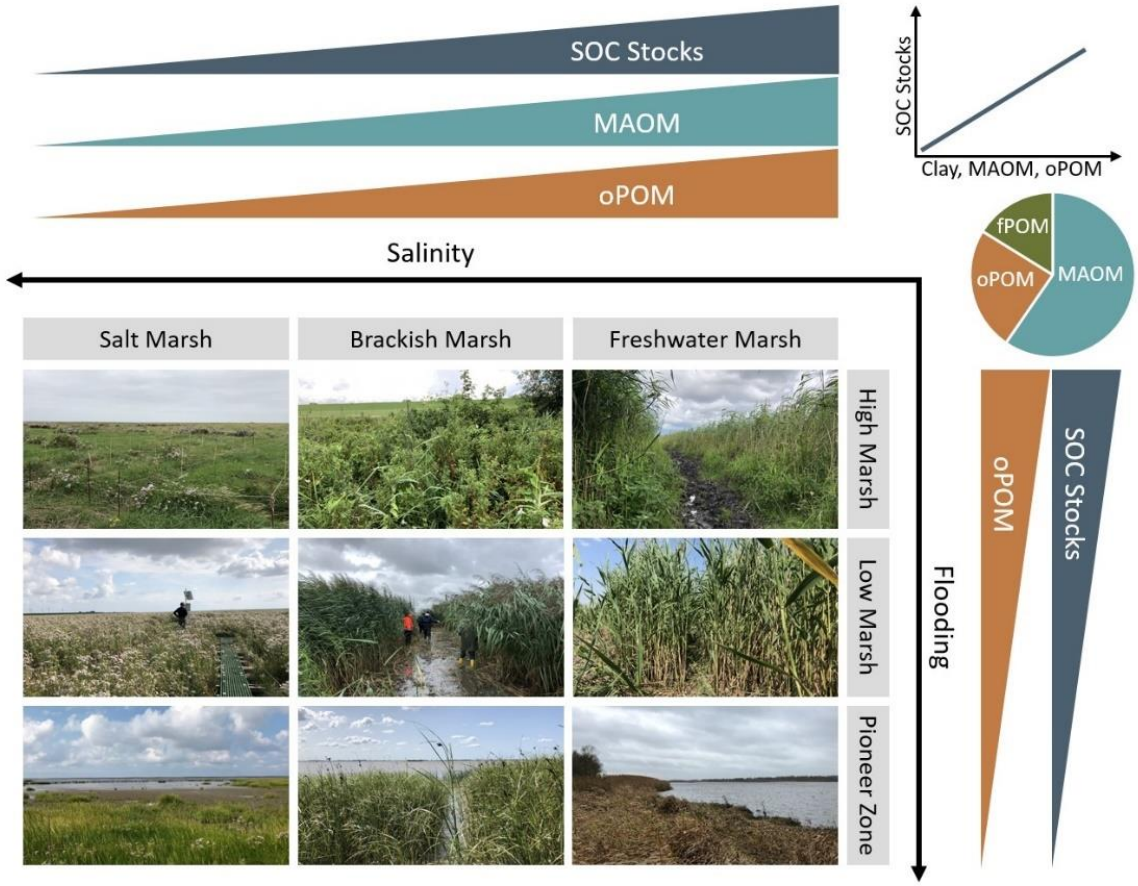

Keywords

Elbe Estuary; salinity; flooding; density fractionation; particulate organic matter; aggregate-occluded organic matter; mineral-associated organic matter

Highlights

- Decreasing SOC stocks from freshwater to salt marsh
- Mineral-association dominant stabilization mechanism in the Elbe Estuary
- Clay is important driver of SOC stabilization and reflects sedimentation dynamics
- Lower flooding frequency and salinity favor SOC protection by aggregates
- Higher free POM proportion under reducing soil conditions

B1 Introduction

Intertidal wetlands play a critical role as carbon (C) sinks on a global scale (Mcleod et al., 2011). They are known for their exceptional capacity to sequester and store significant amounts of soil organic carbon (SOC) (Mcleod et al., 2011; Chmura et al., 2003; Macreadie et al., 2019). Such tidal marshes form the interface of marine and terrestrial ecosystems and are thus shaped by strong environmental gradients. These gradients are particularly pronounced for estuarine marshes with intersecting limnic and marine influence. Increasing salinity towards the coast results in an estuarine salinity gradient forming distinct marsh types along the course of the estuary (salt marshes, brackish marshes, freshwater marshes). Additionally, the elevation of the marsh surface rises from the river inland, leading to a flooding gradient. Both gradients are also reflected in vegetation composition in estuaries (Engels and Jensen, 2009). The interplay of abiotic gradients and biotic communities determine the biogeochemical control of SOC storage in tidal marshes (Seyfferth et al., 2020; Schulte Ostermann et al., 2021) and might be affected by environmental changes (Ruiz-Fernández et al., 2018; Barry et al., 2023; Tang et al., 2023).

Due to their coastal location, tidal marshes and their SOC storage potential are highly vulnerable to climate change (Macreadie et al., 2019; Lovelock and Reef, 2020). In estuaries, a rising sea-level can increase overall saline conditions and lead to the expansion of salt marshes and the displacement of brackish or freshwater marshes (Craft et al., 2009; Visser et al., 2013). Furthermore, a rising sea-level along with an altered flooding regime might force wetlands to move further inland, which is often impeded due to human activities such as embanking (Kirwan and Megonigal, 2013; Enwright et al., 2016). These shifts can have a negative effect on SOC stocks, as previous research indicates that SOC contents decrease with increasing salinity and flooding frequency (Craft, 2007; Spohn et al., 2013; van de Broek et al., 2016). However, previous studies on SOC storage in tidal marshes were mainly conducted in salt marshes (e.g.: Drake et al., 2015; Yuan et al., 2020; Human et al., 2022), while much less is known about tidal freshwater marshes and even less about brackish marshes (e.g.: Spohn and Giani, 2012; van de Broek et al., 2016; Hansen et al., 2017). Considering the pronounced vulnerability of these ecosystems, we need to better understand C dynamics along estuarine gradients and the underlying processes of SOC storage.

In general, SOC storage is regulated by the relation of C inputs and outputs (Lützow et al., 2006). This is particularly important for tidal marshes, which receive large amounts of allochthonous C through flooding-induced deposition

and autochthonous OC input through high primary productivity (Mcleod et al., 2011). In contrast, atmospheric CO_2 outputs are typically low due to limited microbial C mineralization, resulting from anaerobic conditions in regularly flooded soils (Kirwan and Megonigal, 2013; Chapman et al., 2019). This circumstance, together with the recalcitrance of organic matter (OM) itself, has long been considered as the measures for OC protection in wetland soils. Little attention has been paid to alternative mechanisms protecting OC through the interaction with other soil components (van de Broek et al., 2018; Sun et al., 2019; Maietta et al., 2019; Ran et al., 2021). For terrestrial soils, it is well known that the occlusion of OM in aggregates or the association of OM with mineral surfaces (MAOM) increases the accumulation and preservation of OM (Six et al., 2002a; Lützow et al., 2006; Wiesmeier et al., 2019). There is rising evidence that in terrestrial soils, pedogenic stabilization mechanisms are more important for the long-term storage of OC than the recalcitrance of the OM itself. Mineral-associated OM is older, has longer turnover times, and is less responsive to environmental changes than free particulate organic matter (fPOM) (Lützow et al., 2006; Rocci et al., 2021).

For intertidal wetlands, knowledge on effects of mineral association and soil aggregation for SOC stabilization is surprisingly limited and previous studies have reported contradictory results. Maietta et al. (2019) showed that aggregation contributed to stabilization of SOC, while organo-metal oxide complexes were negligible in tidal freshwater marshes of the Patuxent River (Maryland, USA). In contrast, Cui et al. (2014) found that aggregation played a minor role in soils of the subtropical Chongming Island (Yangtze Estuary, China) and the majority of SOC was bound to iron and aluminum oxyhydrates, as well as silt and clay minerals. A reason for these confounding findings may be the high spatio-temporal heterogeneity of biogeochemical properties in estuarine marshes, resulting from strong environmental gradients in salinity and flooding (van de Broek et al., 2016; Seyfferth et al., 2020). The dynamic flooding regime leads to fluctuating redox conditions and can potentially destabilize SOC by the reductive dissolution of iron oxides (Kleber et al., 2015; Chen et al., 2020). Moreover, dry-wet cycles have a strong but opposing effect on aggregate formation and stability which is strongly dependent on soil properties, management practices, or intensities of the dry-wet periods (Six et al., 2004). Dry-wet cycles may increase OM turnover due to the increasing formation of macroaggregates at the expense of more stable microaggregates (Najera et al., 2020). Moreover, inundation may destroy aggregates in soils of regularly flooded ecosystems (Mao et al., 2018; Liu et al., 2021; Ran et al., 2021).

The objectives of our study were to (i) quantify OC stocks along a salinity and flooding gradient of the Elbe Estuary, (ii) estimate SOC stabilization

mechanisms (aggregate-occluded and mineral-associated OC), and (iii) relate the SOC storage to site characteristics. Therefore, we quantified SOC stocks and applied a density fractionation to separate OC associated with minerals (C_{MAOM}), OC occluded in aggregates (C_{oPOM}), and OC in free particulate OM (C_{fPOM}). We related our findings to soil conditions (texture, pH, redox conditions) and vegetation properties (aboveground biomass) to identify drivers for SOC storage and SOC stabilization.

B2 Methods

B2.1 Study Area

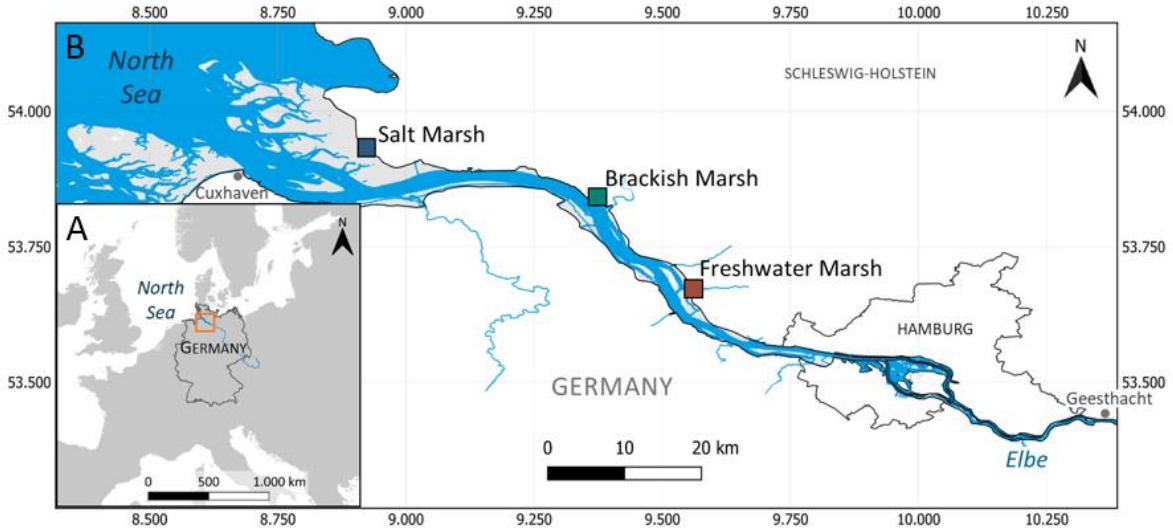

Figure B1: (A) Location of the Elbe Estuary in central Europe (orange rectangle) and (B) location of the marsh sites along the Elbe Estuary (salt marsh: 53°55'40.0"N 8°54'51.3"E/river-km: 710; brackish marsh: 53°50'03.0"N 9°22'15.6"E/river-km: 680; freshwater marsh: 53°39'56.3"N 9°33'11.5"E/river-km: 658) (Data sources: WSV, 2011, 2017; EEA, 2017).

The study was conducted in the Elbe Estuary, Northern Germany (Figure B1). The region is characterized by an oceanic climate with a mean annual temperature of 9.3 °C and mean annual rainfall of 812.8 mm (1991 - 2020, federal state of Schleswig-Holstein) (DWD, 2024). Upstream tidal influence of the Elbe Estuary is restricted by a weir at Geesthacht approximately 140 km inland from the estuaries mouth at Cuxhaven (Boehlich and Strotmann, 2008). The estuary experiences a semi-diurnal meso- to macrotidal regime (Carstens et al., 2004; Boehlich and Strotmann, 2008) with a mean tidal range between

2 m (weir at Geesthacht) and 3.5 m (port of Hamburg) (Kappenberg and Grabemann, 2001). The Elbe Estuary can be subdivided into different salinity zones forming distinct marsh types along the salinity gradient of the estuary (Engels and Jensen, 2009).

We selected three marsh types along the salinity gradient of the Elbe Estuary (salt marsh, brackish marsh, freshwater marsh). Kaiser-Wilhelm-Koog represents a salt marsh and is located in the Schleswig-Holstein Wadden Sea National Park at the mouth of the estuary. As brackish marsh, a site close to Hollerwettern was chosen and the selected freshwater marsh is located in the nature conservation area "Haseldorfer Binnenelbe" closest to the city of Hamburg. Within each of these marsh types, we selected three locations along the flooding gradient: Pioneer zones (PZ) are located closest to the main channel and experience flooding during high tide (twice per day), low marshes (LM) are flooded during spring tides with new and full moon (occurring twice per month), and high marshes (HM) undergo few inundations per year during storm tides. The different marsh zones and types were defined by dominant plant species that are typical for the respective salinity and flooding regime (Engels and Jensen, 2009) (Table S1). All locations are situated on the seaward side of a dike and exhibit near-natural conditions. Soils were formed on marine and fluvial sediments and classified as Eutric or Fluvic Gleysols and Solonchaks (IUSS Working Group WRB, 2022).

B2.2 Field sampling and site characterization

Sampling and field site monitoring

Soil samples were collected in February and March 2022 from each marsh type along the salinity gradient (salt marsh, brackish marsh, freshwater marsh) and marsh zone along the flooding gradient (pioneer zone, low marsh, high marsh). Soil samples were taken from five adjacent replicate plots (2 x 2 m) and directly separated into topsoil (0 - 10 cm) and subsoil (10 - 30 cm) samples. At each marsh location, a pipe well was installed for continuous monitoring of (ground-)water level, temperature and salinity (CTD-Diver, vanEssen Instruments, Delft, The Netherlands). Undisturbed soil cores (volume: 100 cm^3) for bulk density analysis were taken from soil profiles (n = 5) at depths of 5, 10, 30, and 60 cm. Aboveground plant biomass was harvested from two 20 x 20 cm squares in each of the five replicate plots in late July 2022.

Soil Reduction Index

Reducing soil conditions at each replicate plot were investigated using the "Indicator of Reduction in Soil" (IRIS) (Castenson and Rabenhorst, 2006; Rabenhorst, 2008). In this study, the method was modified based on Mueller et al. (2020) and Mittmann-Goetsch et al. (2024). In short, PVC sticks (5 x 70 cm) were covered with $FeCl_3$-paint and inserted into the soil down to a depth of 60 cm for four weeks. After retrieval of the sticks, a reduction index (RI) (0 - 1) was calculated based on the area where the $FeCl_3$-paint was removed from the PVC sticks. Field incubation of IRIS sticks were conducted over the course of almost one year (11 x 4 weeks). We calculated the reduction index over the whole period (RI_{year}) and for the soil sampling period in February and March (RI_{march}) for depth increments corresponding to the soil sampling depths (0 - 10 cm, 10 - 30 cm).

B2.3 Laboratory analyses

Laboratory analyses were conducted at the Institute of Soil Science, University of Hamburg unless indicated otherwise. Soil samples were air-dried at room temperature until constant weight and sieved to 2 mm.

Density fractionation

A density fractionation was applied on the soil samples to separate the SOC into the free light fraction (which corresponds to free particulate organic matter = fPOM), occluded light fraction (organic matter occluded in aggregates = oPOM), and heavy fraction (mineral-associated organic matter = MAOM) based on Golchin et al. (1994) and Viret and Grand (2019). A sodium polytungstate (SPT) ($3\ Na_2WO_4 \cdot 9\ WO_3 \cdot H_2O$) solution ($\rho$ = 1.62 g cm^{-3}) was added to the air-dried and sieved soil samples. The suspensions were carefully mixed and, after resting for 30 minutes, centrifuged at 3000 rpm for 60 minutes. The supernatants were filtered (cellulose acetate filter, 0.45 µm) under vacuum. The filtrates, consisting of fPOM, were washed with distilled water to remove the SPT solution until the supernatants reached an electrical conductivity (EC) of < 50 µS cm^{-1}. Afterwards, the fPOM was dried at 65 °C. In order to separate the oPOM from the remaining soil deposits, the sample was mixed again with SPT solution and treated with ultrasound (171 W ml^{-1}) for 11 minutes to disrupt soil aggregates. The suspended samples were centrifuged at 3000 rpm for 60 minutes, supernatants (consisting of oPOM) were vacuum filtered, and filtrates were washed with distilled water and dried at 65 °C. The remaining soil (containing

MAOM) was washed with distilled water and centrifuged (3000 rpm for 60 minutes) until the supernatant's EC was < 50 µS cm^{-1}. The obtained MAOM was dried at 105 °C until constant weight.

Determination of C and N contents (soil)

The MAOM and bulk soil samples were ground and dried at 105 °C, before they were analyzed for their inorganic and organic C contents with an elemental analyzer (soli TOC® cube, Elementar Analysensysteme GmbH, Langenselbold, Germany) and total C and N contents (vario Max cube, Elementar Analysensysteme GmbH, Langenselbold, Germany). Samples of fPOM and oPOM were ground and as sample volumes were very low, OC and N contents were analyzed during isotope ratio mass spectrometry (Delta XP, Thermo Electron, Bremen Germany; with a preconnected elemental analyzer Flash EA 1112, Thermo Electron, Rodano, Milano, Italy) at the Centre for Stable Isotope Research and Analysis (KOSI) at the University of Goettingen. Organic carbon associated with each fraction (C_{MAOM}, C_{oPOM}, C_{fPOM}) was expressed as total amounts (mg C g^{-1} soil) or as relative proportions of total SOC (% of total SOC).

Calculation of C Stocks

Soil organic carbon stocks (t ha^{-1}) were calculated with the following equation:

Eq. (1): SOC stock=OC x thickness x BD

where OC is the OC content (%), thickness is the thickness of the soil layer (cm) and BD is the bulk density of the soil layer (g soil cm^{-3}).

General soil characterization

Soil texture was determined using the sieving and sedimentation method for mineral soils (Müller et al., 2009). Soil samples were freed from organic matter (samples with OC content > 1%) and carbonates (samples with carbonate content > 0.4%) by treatment with 30% H_2O_2 and hydrochloric acid (10% HCl solution), respectively. After dispersion with sodium pyrophosphate ($Na_4P_2O_7 \cdot 10\ (H_2O)$), the sand fraction (63 µm - 2000 µm) was assessed with a vibratory sieve shaker (Retsch GmbH, Haan, Germany). The fine fraction was analyzed based on the Köhn-pipette fractionation method in a Sedimat 4–12 (Umwelt-Geräte-Technik GmbH, Muencheberg, Germany). Soil pH was measured with a pH meter (MP230 GLP, Mettler-Toledo GmbH, Gießen, Germany) in a 0.01 M $CaCl_2$ solution (pH_{CaCl_2}) and in H_2O (pH_{H_2O}). The soil-water-suspension was used to determine the EC with a conductivity meter

(WTW Cond 330i with TetraCon 325, Xylem Analytics Germany Sales GmbH & Co. KG, Weilheim, Germany).

Aboveground plant biomass

Plant samples were washed with water to remove adhered sediments and dried at 60 °C for at least 48 h until constant weight. After drying, plant samples were weighed to estimate the dry weight. Dried plant samples were ground and analyzed for total C and total N content (vario Max cube, Elementar Analysensysteme GmbH, Langenselbold, Germany).

B2.4 Data analysis

Differences between marsh locations were assessed by analysis of variance (ANOVA) followed by TukeyHSD post-hoc comparison. Depth effects were assessed separately for each marsh location using a linear mixed effect model (LME) for paired comparison with depth as a main factor and sampling location as random factor. Assumptions of normality and variance homogeneity were checked by visual inspection of model residuals. When necessary, Dixon's Q test was applied to check groups for potential outliers. Relationships between measurement variables were assessed by linear regression and Pearson correlation. Additionally, Spearman rank correlation coefficients were included to account for potential non-linearity. Statistical differences were accepted as significant at p-level < 0.05 and p-levels between 0.10 and 0.05 were considered as significance by tendency. Statistical analyses were conducted in R 4.2.0 (R Core Team, 2022), using "multcomp" (Hothorn et al., 2016) and "multcompView" (Graves et al., 2015) packages, as well as "ggplot2" (Wickham et al., 2016) for data visualization.

B3 Results

B3.1 Effect of estuarine gradients on SOC storage

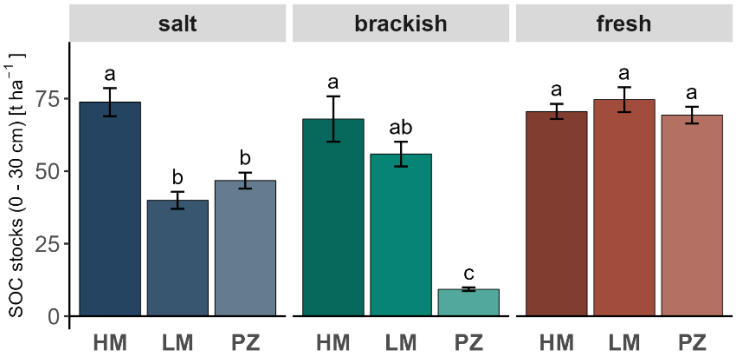

Figure B2: Soil organic carbon (SOC) stocks [t ha^{-1}] (0 – 30 cm) of the different marsh types and zones along the salinity (salt marsh, brackish marsh, freshwater marsh) and flooding gradient (HM = high marsh, LM = low marsh, PZ = pioneer zone) of the Elbe Estuary. Error bars indicate standard error of the mean (n = 5). Lowercase letters indicate significant differences ($p < 0.05$) derived from ANOVA with TukeyHSD post-hoc comparison.

Soil organic carbon storage (SOC stocks and contents) were affected by the estuarine gradients and depth (Figure B2, Table S2 + S3). The SOC stocks in 0 - 30 cm depth ranged from 9.3 to 74.6 t ha^{-1} across the examined marshes in the Elbe Estuary and were partly negatively affected by increasing salinity and flooding (Figure B2). The highest SOC stocks were found in the freshwater marsh (69.2 - 74.6 t ha^{-1}) and in all high marshes (67.6 - 73.7 t ha^{-1}), while the brackish pioneer zone had the lowest SOC stocks (9.3 ± 1.4 t ha^{-1}). The SOC stocks in the pioneer zones and low marshes decreased by 33% and 46% from freshwater to salt marsh conditions, respectively, while the high marshes were not affected by the salinity gradient. The SOC stocks generally decreased with more frequent flooding, but the decrease was absent in the freshwater marsh. The strongest decline along the flooding gradient occurred in the brackish marsh, with a reduction of 86% from the high marsh to pioneer zone. The SOC contents in bulk soil varied between 0.23% and 5.8% in the different marshes and depths (Table S2). The SOC contents decreased with increasing salinity (except for high marsh subsoils) and with increasing flooding at the salt and brackish marsh (Table S3). At the freshwater marsh, the SOC contents did not change along the flooding gradient. Effects of the estuarine gradients on SOC contents were more pronounced in topsoils compared to subsoils.

B3.2 Effect of estuarine gradients on total amounts of SOC fractions

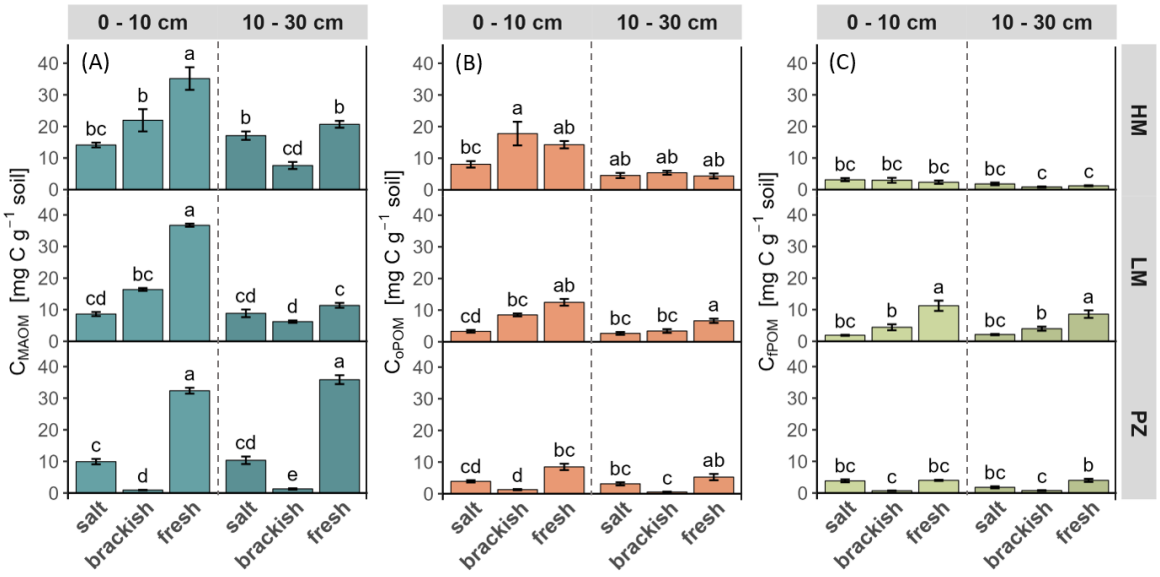

Figure B3: Amount (mg C g^{-1} soil) of mineral-associated OC (C_{MAOM}) (A), aggregate-occluded OC (C_{oPOM}) (B), and OC in free particulate organic matter (C_{fPOM}) (C) of the different marsh types and zones along the salinity (salt marsh, brackish marsh, freshwater marsh) and flooding gradient (HM = high marsh, LM = low marsh, PZ = pioneer zone) of the Elbe Estuary. Error bars indicate standard error of the mean (n = 5). Lowercase letters indicate significant differences ($p < 0.05$) among marsh types and zones per SOC fraction and per depth derived from ANOVA with TukeyHSD post-hoc comparison.

Mineral-associated OC (C_{MAOM}) made up the largest SOC fraction in terms of total amount in the investigated marshes with an average amount of 15.4 ± 11.7 mg C g^{-1} (Figure B3 (A)). The amount of C_{MAOM} decreased with increasing salinity with a more pronounced effect in topsoils and varied along the flooding gradient with no consistent trend. In topsoils, high amounts of C_{MAOM} were found in the freshwater marsh (28.7 ± 10.4 mg C g^{-1}) and decreased by -56% towards the salt marsh with the strongest decline in pioneer zones (-69%). In subsoils, the C_{MAOM} amount significantly decreased with increasing salinity only in the pioneer zones (-71%). Overall, the brackish pioneer zones had the lowest amounts of C_{MAOM} with 0.9 ± 0.2 mg C g^{-1} in topsoil and 1.3 ± 0.5 mg C g^{-1} in subsoil. The amount of C_{MAOM} decreased along the flooding gradient from the high marsh to the pioneer zone in the brackish topsoil (-96%) and subsoil (-83%), as well as in the subsoil of the salt marsh (-40%).

Occluded POM in aggregates (C_{oPOM}) represents the second largest SOC fraction with 5.6 ± 4.6 mg C g^{-1} (Figure B3 (B)). The estuarine gradients had no clear effect on the amount of C_{oPOM} but in some marshes the C_{oPOM} amount showed a negative response to increasing salinity and flooding frequency. The highest amounts of C_{oPOM} were found in topsoils of the brackish high marsh

(17.8 ± 8.4 mg C g^{-1}), freshwater high marsh (14.3 ± 2.6 mg C g^{-1}) and freshwater low marsh (12.5 ± 2.4 mg C g^{-1}), while the lowest amounts were detected in subsoil of the brackish pioneer zone (0.5 ± 0.3 mg C g^{-1}). The amount of C_{oPOM} showed a significant decrease along the salinity gradient from the freshwater to the salt marsh in low marsh topsoils (-73%) and subsoils (-60%). The flooding gradient also tended to have a negative effect but this was only significant in the brackish marsh with a reduction from high marshes to pioneer zones by -93% in topsoils and -90% in subsoils. Overall, topsoils (8.7 ± 5.4 mg C g^{-1}) had more than twice the C_{oPOM} amount of subsoils (4.0 ± 1.8 mg C g^{-1}) but a significant decrease with increasing depth was only observed in parts of the brackish and freshwater marsh.

Free POM was the smallest SOC fraction with 3.17 ± 2.7 mg C g^{-1} (Figure B3 (C)). The amount of C_{fPOM} decreased with increasing salinity in low marshes while the flooding gradient did not exhibit a clear effect. Highest amounts of C_{fPOM} were found in topsoil (11.2 ± 3.6 mg C g^{-1}) and subsoil (8.6 ± 2.6 mg C g^{-1}) of the freshwater low marsh, from where it decreased along the salinity gradient towards the salt marsh by -83% (topsoil) and -75% (subsoils). The flooding gradient did not exhibit a clear trend on the amount of C_{fPOM}: The amount of C_{fPOM} remained relatively constant along the flooding gradient at the salt marsh while it decreased in the brackish topsoil by -93% from the high marsh to the pioneer zone. In contrast, the amount of C_{fPOM} was positively influenced by increasing flooding in the freshwater subsoil (+16%).

B3.3 Effect of estuarine gradients on relative proportions of SOC fractions

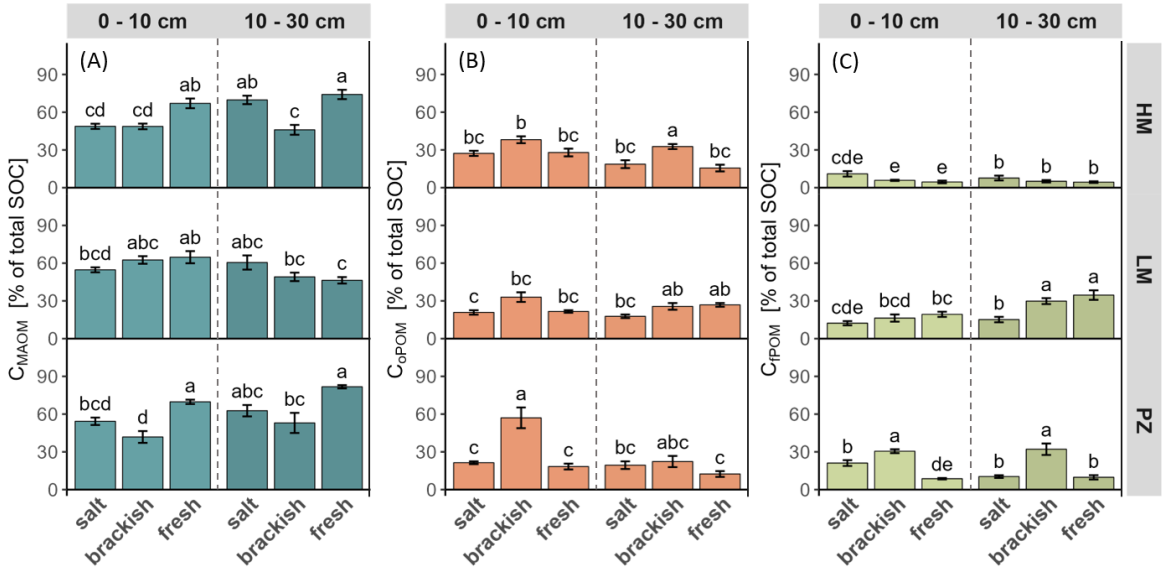

Figure B4: Relative proportions of mineral-associated OC (C_{MAOM}) (A), aggregate-occluded OC (C_{oPOM}) (B), and OC in free particulate organic matter (C_{fPOM}) (C) of total SOC (% of total SOC) of the different marsh types and zones along the salinity (salt marsh, brackish marsh, freshwater marsh) and flooding gradient (HM = high marsh, LM = low marsh, PZ = pioneer zone) of the Elbe Estuary. Error bars indicate standard error of the mean (n = 5). Lowercase letters indicate significant differences ($p < 0.05$) among marsh types and zones per SOC fraction and per depth derived from ANOVA with TukeyHSD post-hoc comparison.

Proportions of C_{MAOM} constituted the largest proportion of total SOC (59.2 ± 11.2% of total SOC) ranging between 42% and 82% of total SOC (Figure B4 (A)). Proportions of C_{MAOM} decreased with increasing salinity in topsoils while the flooding did not exhibit an overall trend on C_{MAOM} proportions. Maximum proportions of C_{MAOM} were found in freshwater soils (67.3 ± 11.2%). Topsoil proportions of C_{MAOM} decreased from the freshwater to the salt marsh along the salinity gradient by -27% in high marshes and -22% in pioneer zones. The brackish marsh tended to have lower C_{MAOM} proportions (49.9 ± 11.2% in topsoil and subsoil combined) compared to salt and freshwater marshes.

Occluded POM presented the second largest proportion of total SOC (24.2 ± 10.3%) with the highest values in the brackish marsh (Figure B4 (B)). Proportions of C_{oPOM} did not show a uniform trend along the estuarine gradients. The brackish marsh exhibited the highest C_{oPOM} proportions (32.1 ± 10.3%) with maximum values in the topsoil of the brackish pioneer zone (57.0 ± 18.4%) while lowest proportions were found in subsoil of the freshwater pioneer zone (12.4 ± 5.1%). Overall, proportions of C_{oPOM} decreased from top- to subsoil (29.5 ± 12.2% to 21.2 ± 6.3%).

Free POM had the lowest proportion of SOC (15.8 ± 10.2%) (Figure B4 (B)). The salinity gradient did not display a uniform effect, while increasing flooding frequency exhibited a positive effect on C_{fPOM} proportions. The highest proportions of C_{fPOM} were found in subsoils of the freshwater low marsh (34.6 ± 8.4%), brackish low marsh (29.8 ± 5.2%), and in the brackish pioneer zone (30.5 ± 3.4% - 32.1 ± 10.2%). While C_{fPOM} proportions in most marshes remained largely unaffected by the salinity gradient, the proportions doubled along the salinity gradient from the freshwater to the salt marsh in topsoils of pioneer zones and were reduced by 50% in the subsoils of low marshes. The lowest proportions of C_{fPOM} occurred in high marshes (6.2 ± 2.5%) and increased along the flooding gradient towards pioneer zones (18.3 ± 10.7%). The strongest increase along the flooding gradient occurred at the brackish marsh, where C_{fPOM} proportions were five (topsoils) to six times (subsoils) higher in the pioneer zone compared to the high marsh. Proportions of C_{fPOM} also nearly doubled along the flooding gradient from the high marsh to the pioneer zone in topsoil of the salt marsh.

B3.4 Soil properties

The soil texture was affected by estuarine gradients but trends were not uniform along the estuary (Table B1). The highest clay contents were found in the freshwater low marsh (topsoil: 39.8%) and freshwater pioneer zone (topsoil: 39.9%; subsoil: 37.0%). The brackish marsh tended to have lower clay (3.3% - 24.4%) and silt (11.8% - 63.4%) but higher sand contents (12.2% - 82.0%). The EC increased along the salinity gradient from the freshwater marsh (104 – 1119 µS cm^{-1}) to the salt marsh (2080 - 3134 µS cm^{-1}). Pronounced differences in redox conditions (RI_{year} and RI_{march}) were observed with respect to soil depth and the estuarine gradients. The average RI_{year} over the year (0.2) decreased downstream with increasing salinity in pioneer zones. Highest values of RI_{year} were found in subsoil of pioneer zones (0.23 - 0.66), while topsoils of low and high marshes exhibited the lowest RI_{year} (0.03 - 0.09). The average RI for the soil sampling period (RI_{march}) was 0.2 and showed a less pronounced trend than RI_{year}.

Table B1: Soil characteristics (pH_{CaCl2} = soil pH measured in $CaCl_2$-solution; EC = soil electric conductivity; BD = soil bulk density; RI (year) = mean soil reduction index of one year derived from IRIS method; RI (march) = soil reduction index for the sampling period in February and March derived from the IRIS method) of the different marsh types and zones along the salinity (salt marsh, brackish marsh, freshwater marsh) and flooding gradient (HM = high marsh, LM = low marsh, PZ = pioneer zone) of the Elbe Estuary (mean ± standard error, n = 5).

Marsh		Depth [cm]	pH_{CaCl2}	EC *[µS/cm]*	clay *[%]*	silt *[%]*	sand *[%]*	BD† *[g cm^{-3}]*	RI (year)	RI (march)
Salt Marsh	HM	0 - 10	7.2 ± 0.3	2606 ± 1081	21.1 ± 4.3	68.1 ± 3.5	10.8 ± 6.1	0.98 ± 0.03	0.04 ± 0.02	0.02 ± 0.00
		10 - 30	7.4 ± 0.0	2080 ± 372	26.0 ± 4.6	68.2 ± 3.6	5.7 ± 2.0	0.92 ± 0.03	0.16 ± 0.02	0.00 ± 0.00
	LM	0 - 10	7.2 ± 0.1	2093 ± 418	14.5 ± 5.1	54.4 ± 7.0	31.1 ± 10.8	0.93 ± 0.08	0.09 ± 0.02	0.01 ± 0.00
		10 - 30	7.4 ± 0.1	2512 ± 222	16.6 ± 3.2	59.8 ± 2.1	23.6 ± 4.9	0.87 ± 0.07	0.21 ± 0.01	0.04 ± 0.02
	PZ	0 - 10	7.2 ± 0.1	2494 ± 387	20.0 ± 7.8	48.4 ± 4.5	31.6 ± 6.4	0.79 ± 0.03	0.05 ± 0.01	0.02 ± 0.01
		10 - 30	7.4 ± 0.1	3134 ± 637	16.6 ± 5.0	47.8 ± 3.6	35.7 ± 7.4	0.98 ± 0.05	0.23 ± 0.02	0.14 ± 0.02
Brackish Marsh	HM	0 - 10	7.1 ± 0.1	292 ± 87	10.4 ± 6.2	18.2 ± 6.4	71.4 ± 12.5	0.68 ± 0.05	0.04 ± 0.02	0.01 ± 0.00
		10 - 30	6.8 ± 0.3	91 ± 13	6.3 ± 2.2	11.8 ± 2.0	82.0 ± 4.0	1.12 ± 0.04	0.21 ± 0.01	0.03 ± 0.01
	LM	0 - 10	7.3 ± 0.1	704 ± 96	24.4 ± 4.1	63.4 ± 1.2	12.2 ± 3.5	0.87 ± 0.04	0.09 ± 0.02	0.08 ± 0.03
		10 - 30	6.7 ± 0.1	328 ± 63	11.3 ± 2.8	41.8 ± 3.9	47.0 ± 4.9	1.26 ± 0.06	0.38 ± 0.05	0.43 ± 0.10
	PZ	0 - 10	7.3 ± 0.1	456 ± 39	3.4 ± 0.9	37.5 ± 3.3	59.2 ± 3.7	1.28 ± 0.11	0.15 ± 0.04	0.47 ± 0.08
		10 - 30	6.9 ± 0.1	282 ± 63	3.3 ± 0.4	31.8 ± 2.3	64.9 ± 2.1	1.33 ± 0.09	0.62 ± 0.06	0.45 ± 0.09
Fresh-water Marsh	HM	0 - 10	7.1 ± 0.0	330 ± 79	26.4 ± 1.7	63.3 ± 1.1	10.2 ± 1.6	0.58 ± 0.03	0.03 ± 0.00	0.01 ± 0.01
		10 - 30	6.9 ± 0.2	104 ± 10	15.7 ± 1.4	65.7 ± 1.2	18.6 ± 2.1	0.72 ± 0.04	0.21 ± 0.02	0.02 ± 0.01
	LM	0 - 10	7.2 ± 0.0	1074 ± 436	39.8 ± 5.7	53.6 ± 4.6	6.6 ± 1.9	0.56 ± 0.02	0.04 ± 0.01	0.22 ± 0.09
		10 - 30	6.0 ± 0.1	573 ± 154	14.4 ± 1.9	42.9 ± 2.4	42.8 ± 2.3	0.86 ± 0.09	0.35 ± 0.05	0.45 ± 0.10
	PZ	0 - 10	7.4 ± 0.1	1053 ± 188	39.9 ± 12.5	57.4 ± 11.4	2.8 ± 2.1	0.48 ± 0.09	0.17 ± 0.01	0.13 ± 0.06
		10 - 30	7.2 ± 0.3	1119 ± 265	37.0 ± 8.2	60.0 ± 8.3	3.0 ± 1.3	0.56 ± 0.10	0.66 ± 0.01	0.35 ± 0.13

† mean of five replicates taken from the reference soil profiles.

B3.5 Aboveground plant biomass

The highest aboveground plant biomass was found in the freshwater marsh and the brackish high marsh (Table B2). The aboveground plant biomass decreased downstream with increasing salinity in low marshes (-75%) and pioneer zones (-62%). No clear trends in the C:N ratio of the aboveground plant biomass along the estuary were observed (Table B2). Ratios decreased downstream with increasing salinity in pioneer zones, while ratios did not change along high and low marshes. A decrease in C:N ratio with increasing flooding frequency was detected at the salt marsh while the C:N ratios increased with increasing flooding frequency at the brackish marsh.

Table B2: Total biomass (g DW m^{-2}) and C:N ratio of the aboveground vegetation present at the different marsh types and zones along the salinity (salt marsh, brackish marsh, freshwater marsh) and flooding gradient (HM = high marsh, LM = low marsh, PZ = pioneer zone) of the Elbe Estuary (mean ± standard error, n = 5).

Marsh		aboveground vegetation	
		biomass *[g DW m^{-2}]*	*C:N ratio*
Salt Marsh	HM	1427.5 ± 174	39.9 ± 4.4
	LM	860.4 ± 42	38.8 ± 7.1
	PZ	960.2 ± 55	26.8 ± 3.2
Brackish Marsh	HM	2421.0 ± 365	37.1 ± 4.2
	LM	2213.6 ± 314	52.2 ± 6.1
	PZ	1367.9 ± 140	48.3 ± 2.2
Fresh-water Marsh	HM	1999.0 ± 421	43.3 ± 6.9
	LM	3404.4 ± 234	43.9 ± 2.7
	PZ	2504.3 ± 235	49.0 ± 5.7

B3.6 Relationships between environmental variables and SOC storage and stabilization

Soil organic carbon storage (SOC stocks and contents) showed a strong positive correlation with proportions of C_{MAOM} and the amount of all three SOC fractions (C_{MAOM}, C_{oPOM}, C_{fPOM}) (Figure B5 (A) + (B)). The clay content was a good predictor for SOC storage, for the amount of C_{MAOM} in topsoil and subsoil, and the amount of C_{oPOM} in topsoil. Proportions of C_{MAOM} also showed a positive correlation with clay content in topsoil and subsoil. The amounts and proportions of C_{oPOM} were negatively correlated with EC with the exception of the C_{oPOM} amount in subsoil. The SOC storage in topsoils correlated negatively with the RI_{year}, while RI_{march} positively affected amounts and proportions of C_{fPOM}. Aboveground biomass was positively correlated with SOC storage in topsoil as well as the amount of C_{MAOM} in topsoil, C_{oPOM} in topsoil and subsoil and C_{fPOM} in topsoil and subsoil. The majority of the fraction proportions were unaffected by aboveground plant biomass. The C:N ratio of the aboveground plant biomass had negligible effects on SOC stocks, SOC contents, and SOC fractions.

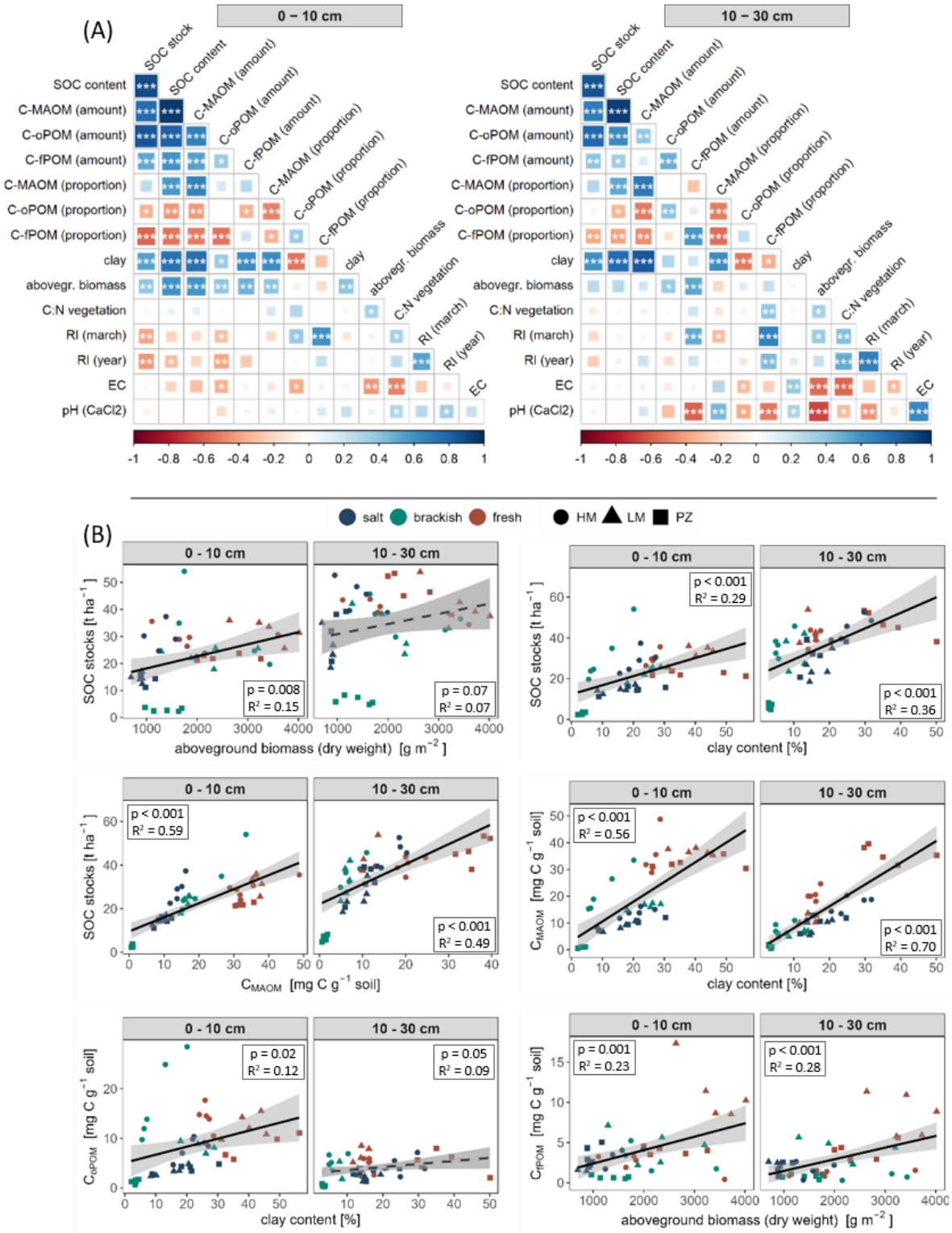

Figure B5: (A) Pearson correlation matrices for topsoil (0 - 10 cm) and subsoil (10 - 30 cm) (n = 45). Asterisk indicate significant correlation at * $p < 0.05$, ** $p < 0.005$, and *** $p < 0.001$. (B) Linear regression between SOC stocks, SOC fractions (C_{MAOM} = mineral-associated OC, C_{oPOM} = OC associated with aggregate-occluded OC, C_{fPOM} = OC in free particulate organic matter), and selected site characteristics (n = 45).

B4 Discussion

B4.1 Effect of estuarine gradients on SOC storage

The SOC stocks (0 - 30 cm) in the Elbe Estuary varied between 9.3 - 74.6 t ha^{-1}. This is at the lower end of previously described global medians of 79.2 ± 38.1 t ha^{-1} SOC in tidal marshes (0 - 30 cm) (Maxwell et al., 2023). Previous research on North Sea estuaries found SOC stocks between 99 – 217 t ha^{-1} (0 - 60 cm, Scheldt Estuary) (van de Broek et al., 2016), 40 - 134 t ha^{-1} (0 - 80 cm, Elbe Estuary) (Schulte Ostermann et al., 2021), or 31 - 153 t ha^{-1} (0 - 30 cm, Elbe Estuary) (Hansen et al., 2017). The SOC storage (SOC stocks and contents) in our study were predominantly negatively affected by higher salinity and flooding frequency, which is in line with previously reported research from Europe (van de Broek et al., 2016; Hansen et al., 2017; Mazarrasa et al., 2023), temperate USA (Craft, 2007; Kauffman et al., 2020), Australia (Kelleway et al., 2016; Gorham et al., 2021), or China (Yuan et al., 2020). These trends are likely related to differences in OM inputs and preservation capacity along estuarine gradients. As estuarine tidal marshes form the interface of marine, riverine, and terrestrial ecosystems, soils experience a quantitative and qualitative change of autochthonous (local biomass) and allochthonous (flood deposits and sedimentation) OC input along the salinity and flooding gradients (Abril et al., 2002; Hansen et al., 2017). In accordance with the decreasing SOC stocks, autochthonous OM inputs and OC contents in deposited sediments generally decrease from freshwater to salt marshes and with higher flooding frequency (Butzeck et al., 2015). Moreover, higher SOC contents in high marshes might be also attributed to a progressed soil development with continuous C accumulation (Spohn et al., 2013).

The aboveground plant biomass, along with its potential autochthonous OC input, decreased downstream with increasing salinity at the Elbe Estuary and was positively correlated to SOC stocks, as well as SOC contents. Due to the high primary productivity in tidal marshes, the local plant biomass can strongly contribute to SOC storage in marshes (Mcleod et al., 2011; Yuan et al., 2020). The plant biomass production is generally greater at freshwater and brackish marshes than at salt marshes due to reduced salinity stress and higher nutrient availability in freshwater marshes (Więski et al., 2010; Hansen et al., 2017). Consistent with these findings, a higher contribution of tidal marsh vegetation to SOC stocks in fluvial compared to marine settings were found in estuarine marshes of temperate Australia (Gorham et al., 2021). The aboveground biomass of the Elbe Estuary also tended to decrease with increasing flooding frequency at the salt and brackish marsh ($p < 0.1$), which could have

contributed to the observed negative trends of SOC stocks with increasing flooding frequency. However, not all our sites expressed a positive relationship between aboveground plant biomass and SOC storage. Other controlling factors, such as local geomorphology, allochthonous OC inputs, or the OC preservation capacity need to be considered as well (van de Broek et al., 2016; Kelleway et al., 2016; van de Broek et al., 2018). Allochthonous OC inputs can exceed the amount of autochthonous OC input in marshes (Zhou et al., 2007; van de Broek et al., 2016), and can dominate the long-term SOC storage in these soils (van de Broek et al., 2018). The allochthonous OC input into the marsh is determined by the concentration of suspended sediments and associated OM in the river water, both of which show high spatio-temporal variations along the course of estuaries (Abril et al., 2002; Butzeck et al., 2015; Kelleway et al., 2016). It was found that the sediment concentration in the channel of the Elbe Estuary declines downstream (Abril et al., 2002) which might result in a reduced deposition of sediments and accompanied OC into the marsh (Butzeck et al., 2015; van de Broek et al., 2018). Therefore, lower SOC stocks in the salt marsh of the Elbe Estuary are mainly coinciding with low autochthonous and allochthonous OC inputs. Moreover, it was found that freshwater marshes exhibit a greater SOC preservation capacity compared to marine settings due to their fine-grained texture (Kelleway et al., 2016; van de Broek et al., 2018; Gorham et al., 2021). Accordingly, we found larger SOC stocks with higher clay contents. Fine texture can increase SOC storage due to lower drainage and oxygen exchange, leading to lower redox potentials and mineralization rates (Kirwan and Megonigal, 2013; Chapman et al., 2019). However, we found only a weak negative relationship between SOC storage and proxies of inhibited OC mineralization e.g. the reduction index calculated for the whole year (R^2 < 9% for SOC content and R^2 < 20% for SOC stocks). Oxygen limitation seems therefore not to explain the observed patterns of SOC storage along the estuarine gradients of the Elbe Estuary. Fine minerogenic particles also have a strong potential to protect OC against mineralization by building organo-mineral interactions or by the occlusion in aggregates (Wiesmeier et al., 2019; Six et al., 2002a; Six et al., 2002b). Therefore, the positive effect of clay on SOC contents might indicate that SOC stabilization mechanisms by mineral association or aggregation play important roles for SOC storage in the Elbe Estuary.

B4.2 SOC stabilization mechanisms along estuarine gradients

The majority of SOC in the Elbe marshes was associated to minerals (C_{MAOM}: 59%), indicating that organo-mineral interaction plays a key role in the Elbe Estuary. Other SOC fractions (C_{oPOM}: 24% and C_{fPOM}: 16%) were less abundant. This is in contrast to a study in tidal freshwater marshes of the Patuxent River in Maryland (USA) where SOC was predominantly stored in aggregates and not in organo-mineral complexes (Maietta et al., 2019). However, the importance of mineral association for SOC storage in salt marshes was also emphasized (Sun et al., 2019). These contrasting results indicate that SOC stabilization mechanisms undergo strong spatial variability between estuaries as well as along estuarine gradients.

We found highest amounts of C_{MAOM} at the freshwater marsh of the Elbe Estuary and a partially decreasing trend along the salinity gradient from the freshwater to the salt marsh. These trends, for the most part, were positively related to aboveground biomass and clay content. The important role of clay for SOC stabilization is well established due to the provision of surface area for OM adsorption and organo-mineral interactions (Six et al., 2002a; Lützow et al., 2006; Wiesmeier et al., 2019). The contribution of fine minerogenic particles (< 63 µm) and OC to the amount of deposited sediments in the Elbe Estuary is generally higher in the freshwater compared to the salt marsh (Butzeck et al., 2015). This decreasing input of fine particles and OM downstream of the estuary reduces the input of new mineral surface areas for mineral association of OC and might indicate a decreased input of already mineral-associated OC. Therefore, the decreasing trend of C_{MAOM} downstream of the estuary from the freshwater to the salt marsh might be the combined effect of decreasing input of OC (autochthonous and allochthonous) and mineral surfaces by sedimentation along the gradient. This is supported by a maximum occurrence of C_{MAOM} in topsoils and a strongly expressed effect of the salinity gradient in pioneer zones, which are more affected by recent sedimentation. The contribution of C_{MAOM} to total SOC in pioneer zones and high marshes decreased downstream with increasing salinity, while proportions of C_{fPOM} partly increased. This underlines the decreasing formation and relevance of mineral association for SOC storage from the freshwater to the salt marsh of the Elbe Estuary. Similar to C_{MAOM}, the amount of C_{oPOM} was also largely related to aboveground biomass and clay content, and showed a decreasing trend from the freshwater to the salt marsh. Fine mineral particles play an import role in the formation of aggregates (Six et al., 2002b; Lützow et al., 2006). Thus, the decreasing trend of C_{oPOM} with increasing salinity might be attributed to the decreased availability of clay for aggregation due to a reduced deposition of fine mineral particles in

salt marshes compared to freshwater marshes. These observed negative trends downstream of the estuary in aggregation might be further amplified by the direct adverse effect of salt on aggregate stability (Wong et al., 2010). This is supported by a negative correlation between EC of the marsh soils and the amounts and proportions of C_{oPOM}. The high amounts of C_{fPOM} in the freshwater marsh and its decreasing trend downstream of the estuary with increasing salinity is strongly linked to the local aboveground plant biomass. In contrast, the increasing contribution of C_{fPOM} to total SOC downstream with increasing salinity in pioneer zones and high marshes highlights the shift from protected SOC in mineral association in the freshwater marsh towards pedogenically unprotected free POM in the salt marsh.

The flooding gradient had no clear effect on the amount of C_{MAOM} and C_{oPOM}. This indicates that the flooding gradient pose no overall effect on C_{MAOM} and C_{oPOM} but interacts with the salinity gradient and other factors leading to local variability. The OC in mineral association and aggregates occlusion at the salt marsh might be less affected by the flooding gradient due to generally smaller sedimentation rates, which also contain less clay (Butzeck et al., 2015). The negative effect of increasing flooding at the brackish marsh can be attributed to differences in the texture of the deposited sediments along the gradient that resulted in different soil textures. The brackish pioneer zone was characterized by high sand and very low clay contents, while the brackish low marsh had higher silt and clay contents with a larger potential for mineral association and aggregate formation (Table 1). However, high sand or clay contents were not always associated with low or high amounts of C_{MAOM} and C_{oPOM}, such as in topsoil of the brackish high marsh and the freshwater marsh. Besides soil texture, the soil water content and dry-wet cycles are controlling aggregate dynamics and associated OM turnover in soil (Six et al., 2002b; Six et al., 2004; Najera et al., 2020). Aggregate formation and stability in soil can decrease with increasing flooding intensity and increasing soil water content in strongly flood-effected soils (Mao et al., 2018; Liu et al., 2021; Ran et al., 2021). This indicates that the conditions in the less inundated high marshes favor aggregation. In addition, the amounts of C_{oPOM} tended to be higher in topsoils compared to subsoils, which might also be related to less favorable conditions for aggregate formation in the predominantly wet subsoils. This is underlined by the observation that the amount of C_{oPOM} did not correlate with the clay content in subsoil. This supports the assumption that the conditions in less frequently flooded high marshes and topsoils promote the stabilization of OM in aggregates more effectively than the frequently inundated and overall wetter low marshes, pioneer zones and subsoils. Despite large aboveground biomass, high marshes did not show enriched C_{fPOM} pools. On the contrary, the contribution of C_{fPOM} to total SOC

increased with increasing flooding at the salt and brackish marsh. This suggests that high marsh soils, due to their better aeration, are likely characterized by a faster turnover of plant litter, by which the OM is either lost by mineralization or is protected by mineral-association or in aggregates. The latter assumption is supported by the higher amount of C_{oPOM} and generally higher SOC contents in high marshes. In pioneer zones, the preservation of C_{fPOM} might benefit from the constant sedimentation and flooding, inducing oxygen-limitation and restricted mineralization (Schmidt et al., 2011). This is supported by a positive correlation between proportions of C_{fPOM} and the reduction index for the sampling month (RI_{march}) while C_{fPOM} proportions were unrelated to the aboveground biomass.

B4.3 Implications for climate change effects on SOC storage and stabilization in estuarine marshes

Various climatic- and non-climatic controls have led to a substantial loss in global wetland area. Sea-level rise and storm surges associated with climate change will pose a major impact on coastal ecosystems and their C storage capacity (IPCC, 2022). Landward expansion of marshes, vertical accretion, elevated atmospheric CO_2, and increasing temperatures can enhance C sequestration in coastal ecosystems (Kirwan and Mudd, 2012; Macreadie et al., 2019; Lovelock and Reef, 2020). However, in our study we found decreasing SOC storage with increasing salinity and flooding along the estuarine gradients of the Elbe Estuary. This indicates the special role of estuaries at the aquatic-terrestrial interface. Particularly changes in SOC stabilization mechanisms should be considered when addressing implications of sea-level rise on C storage in these ecosystems. Submergence, burial, and erosion can pose a threat on coastal C storage if marshes cannot keep pace with sea-level rise (Macreadie et al., 2019; Lovelock and Reef, 2020; IPCC, 2022). The ability of landward migration is often limited by anthropogenic infrastructure (e.g. construction of dikes and weirs) (Lovelock and Reef, 2020; IPCC, 2022). In the Elbe Estuary this might not only limits the expansion of marshes but may also decrease SOC sequestration due to decreasing OC inputs and reduced SOC stabilization. Currently, SOC storage and stabilization in the freshwater marsh of the Elbe Estuary benefits from the strong fluvial influence, increasing biomass production, and the input of allochthonous OC and fine textured sediments. This beneficial fluvial influence might be reduced by sea-level rise and increased storm surges which enhance salinity and the contribution of coarse material in sediment deposits. Moreover, more frequent drought spells might reduce river

discharge (IPCC, 2022), further reducing fine particle deposition and freshwater input. It was also shown that increasing inundation frequency and higher water content may have negative effects on aggregate formation and stability (Najera et al., 2020; Liu et al., 2021). Increasing dry-wet cycles can lead to the formation of macroaggregates at the expense of microaggregates with a strong implication for SOC turnover (Najera et al., 2020). How these effects control the SOC budget and stability in estuarine soils remains subject of future investigations.

B5 Conclusion

In this study, we investigated effects of estuarine gradients (salinity and flooding) on SOC storage and potential stabilization mechanisms, indicated by SOC density fractions. Our results show that SOC stocks decrease from freshwater to salt marshes within the Elbe Estuary, which is likely related to decreasing autochthonous and allochthonous OC input downstream of the river. Mineral-association was the dominant stabilization mechanisms in the Elbe Estuary, followed by aggregation, reflected by a strong correlation between SOC stocks, MAOM, aggregate-occluded OC, and the clay content of the marsh soils. This indicates that the sedimentation dynamic is an important driver of SOC storage and stabilization mechanisms. Higher clay content led to higher potential of SOC preservation and stabilization at the freshwater marsh compared to salt and brackish sites. On the local scale, the actual degree of protection of SOC depends on the interaction of the estuarine gradients with each other and other local conditions; towards terrestrial influence (less flooding and lower salinity) the protection of SOC by aggregation increases. In contrast, free POM is more relevant for SOC storage in frequently-flooded parts of the marsh induced by reducing soil conditions.

Our data also highlights the strong spatial heterogeneity in SOC storage and stabilization, as well as environmental drivers within the estuary. Comparing our results with studies from other estuaries, indicated a strong variation in SOC storage and in the importance of controlling factors from one estuary to the other. Therefore, it is crucial to consider this heterogeneity in the assessment of SOC storage and stabilization to understand potential effects of climate change.

Authors' contributions

Friederike Neiske: Conceptualization, Formal Analysis, Investigation, Project administration, Visualization, Writing - original draft. **Maria Seedtke:** Investigation, Writing - review & editing. **Annette Eschenbach:** Funding acquisition, Resources, Supervision, Conceptualization, Writing - review & editing. **Monica Wilson:** Investigation, Writing - review & editing. **Kai Jensen:** Funding acquisition, Resources, Investigation, Supervision, Writing - review & editing. **Joscha N. Becker:** Conceptualization, Formal Analysis, Methodology, Project administration, Supervision, Writing - review & editing.

Acknowledgement

This study was funded by the Deutsche Forschungsgemeinschaft (DFG, German Research Foundation) within the Research Training Group 2530: "Biota-mediated effects on Carbon cycling in Estuaries" (project number 407270017; contribution to Universität Hamburg and Leibniz-Institut für Gewässerökologie und Binnenfischerei im Forschungsverbund Berlin e.V.). We thank Volker Kleinschmidt, Deborah Harms, Sumita Rui, Annika Naumann, Julian Mittmann-Goetsch, Fay Lexmond and involved student assistants for their help during field and lab work, as well as technical support.

B6 References

Abril, G., Nogueira, M., Etcheber, H., Cabeçadas, G., Lemaire, E., Brogueira, M., 2002. Behaviour of Organic Carbon in Nine Contrasting European Estuaries. Estuarine, coastal and shelf science 54 (2), 241–262.

Barry, A., Ooi, S.K., Helton, A.M., Steven, B., Elphick, C.S., Lawrence, B.A., 2023. Carbon Dynamics Vary Among Tidal Marsh Plant Species in a Sea-level Rise Experiment. Wetlands 43 (7).

Boehlich, M.J., Strotmann, T., 2008. The Elbe Estuary. Die Küste 74 (1), 288–306.

Butzeck, C., Eschenbach, A., Gröngröft, A., Hansen, K., Nolte, S., Jensen, K., 2015. Sediment Deposition and Accretion Rates in Tidal Marshes Are Highly Variable Along Estuarine Salinity and Flooding Gradients. Estuaries and Coasts 38 (2), 434–450.

Carstens, M., Claussen, U., Bergemann, M., Gaumert, T., 2004. Transitional waters in Germany: the Elbe estuary as an example. Aquatic Conservation: Marine and Freshwater Ecosystems 14 (S1), S81-S92.

Castenson, K.L., Rabenhorst, M.C., 2006. Indicator of reduction in soil (IRIS) evaluation of a new approach for assessing reduced conditions in soil. Soil Science Soc of Amer J 70 (4), 1222–1226.

Chapman, S.K., Hayes, M.A., Kelly, B., Langley, J.A., 2019. Exploring the oxygen sensitivity of wetland soil carbon mineralization. Biology letters 15 (1), 20180407.

Chen, C., Hall, S.J., Coward, E., Thompson, A., 2020. Iron-mediated organic matter decomposition in humid soils can counteract protection. Nature communications 11 (1), 2255.

Chmura, G.L., Anisfeld, S.C., Cahoon, D.R., Lynch, J.C., 2003. Global carbon sequestration in tidal, saline wetland soils. Global Biogeochemical Cycles 17 (4).

Craft, C., 2007. Freshwater input structures soil properties, vertical accretion, and nutrient accumulation of Georgia and U.S tidal marshes. Limnology & Oceanography 52 (3), 1220–1230.

Craft, C., Clough, J., Ehman, J., Joye, S., Park, R., Pennings, S., Guo, H., Machmuller, M., 2009. Forecasting the effects of accelerated sea-level rise on tidal marsh ecosystem services. Frontiers in Ecol & Environ 7 (2), 73–78.

Cui, J., Li, Z., Liu, Z., Ge, B., Fang, C., Zhou, C., Tang, B., 2014. Physical and chemical stabilization of soil organic carbon along a 500-year cultived soil chronosequence originating from estuarine wetlands: Temporal patterns and land use effects. Agriculture, Ecosystems & Environment 196, 10–20.

Drake, K., Halifax, H., Adamowicz, S.C., Craft, C., 2015. Carbon Sequestration in Tidal Salt Marshes of the Northeast United States. Environmental management 56 (4), 998–1008.

Duarte, C.M., Losada, I.J., Hendriks, I.E., Mazarrasa, I., Marbà, N., 2013. The role of coastal plant communities for climate change mitigation and adaptation. Nature Clim Change 3 (11), 961–968.

DWD, 2024. Time series and trends for the parameters temperature and precipitation: Reference period: 1991 - 2020. Federal State of Schleswig-Holstein. Deutscher Wetterdienst. https://www.dwd.de/EN/ourservices/zeitreihen/zeitreihen.html#buehneTop.

Engels, J.G., Jensen, K., 2009. Patterns of wetland plant diversity along estuarine stress gradients of the Elbe (Germany) and Connecticut (USA) Rivers. Plant Ecology & Diversity 2 (3), 301–311.

Enwright, N.M., Griffith, K.T., Osland, M.J., 2016. Barriers to and opportunities for landward migration of coastal wetlands with sea-level rise. Frontiers in Ecol & Environ 14 (6), 307–316.

Golchin, A., Oades, J.M., Skjemstad, J.O., Clarke, P., 1994. Study of free and occluded particulate organic matter in soils by solid state 13C Cp/MAS NMR spectroscopy and scanning electron microscopy. Soil Res. 32 (2), 285.

Gorham, C., Lavery, P., Kelleway, J.J., Salinas, C., Serrano, O., 2021. Soil Carbon Stocks Vary Across Geomorphic Settings in Australian Temperate Tidal Marsh Ecosystems. Ecosystems 24 (2), 319–334.

Graves, S., Piepho, H.-P., Selzer, M.L., 2015. Package 'multcompView'. Visualizations of paired comparisons.

Hansen, K., Butzeck, C., Eschenbach, A., Gröngröft, A., Jensen, K., Pfeiffer, E.-M., 2017. Factors influencing the organic carbon pools in tidal marsh soils of the Elbe estuary (Germany). J Soils Sediments 17 (1), 47–60.

Hothorn, T., Bretz, F., Westfall, P., Heiberger, R.M., Schuetzenmeister, A., Scheibe, S., Hothorn, M.T., 2016. Package 'multcomp'. Simultaneous inference in general parametric models. Project for Statistical Computing, Vienna, Austria.

Human, L.R.D., Els, J., Wasserman, J., Adams, J.B., 2022. Blue carbon and nutrient stocks in salt marsh and seagrass from an urban African estuary. The Science of the total environment 842, 156955.

IPCC (Ed.), 2022. Climate Change 2022 – Impacts, Adaptation and Vulnerability: Contribution of Working Group II to the Sixth Assessment Report of the Intergovernmental Panel on Climate Change. [H.-O. Pörtner, D.C. Roberts, M. Tignor, E.S. Poloczanska, K. Mintenbeck, A. Alegría, M. Craig, S. Langsdorf]. Cambridge University Press, Cambridge, UK and New York, NY, USA, 3056 pp.

IUSS Working Group WRB, 2022. World Reference Base for Soil Resources. International soil classification system for naming soils and creating legends for soil maps. 4th edition. International Union of Soil Sciences (IUSS), Vienna, Austria.

Kappenberg, J., Grabemann, I., 2001. Variability of the mixing zones and estuarine turbidity maxima in the Elbe and Weser estuaries. Estuaries 24, 699–706.

Kauffman, J.B., Giovanonni, L., Kelly, J., Dunstan, N., Borde, A., Diefenderfer, H., Cornu, C., Janousek, C., Apple, J., Brophy, L., 2020. Total ecosystem carbon stocks at the marine-terrestrial interface: Blue carbon of the Pacific Northwest Coast, United States. Global Change Biology 26 (10), 5679–5692.

Kelleway, J.J., Saintilan, N., Macreadie, P.I., Ralph, P.J., 2016. Sedimentary Factors are Key Predictors of Carbon Storage in SE Australian Saltmarshes. Ecosystems 19 (5), 865–880.

Kirwan, M.L., Megonigal, J.P., 2013. Tidal wetland stability in the face of human impacts and sea-level rise. Nature 504 (7478), 53–60.

Kirwan, M.L., Mudd, S.M., 2012. Response of salt-marsh carbon accumulation to climate change. Nature 489 (7417), 550–553.

Kleber, M., Eusterhues, K., Keiluweit, M., Mikutta, C., Mikutta, R., Nico, P.S., 2015. Mineral–Organic Associations: Formation, Properties, and Relevance in Soil Environments, vol. 130. Advances in Agronomy. Elsevier, pp. 1–140.

Liu, Y., Ma, M., Ran, Y., Yi, X., Wu, S., Huang, P., 2021. Disentangling the effects of edaphic and vegetational properties on soil aggregate stability in riparian zones along a gradient of flooding stress. Geoderma 385, 114883.

Lovelock, C.E., Reef, R., 2020. Variable Impacts of Climate Change on Blue Carbon. One Earth 3 (2), 195–211.

Lützow, M.v., Kögel-Knabner, I., Ekschmitt, K., Matzner, E., Guggenberger, G., Marschner, B., Flessa, H., 2006. Stabilization of organic matter in temperate soils: mechanisms and their relevance under different soil conditions – a review. European J Soil Science 57 (4), 426–445.

Macreadie, P.I., Anton, A., Raven, J.A., Beaumont, N., Connolly, R.M., Friess, D.A., Kelleway, J.J., Kennedy, H., Kuwae, T., Lavery, P.S., Lovelock, C.E., Smale, D.A., Apostolaki, E.T., Atwood, T.B., Baldock, J., Bianchi, T.S., Chmura, G.L., Eyre, B.D., Fourqurean, J.W., Hall-Spencer, J.M., Huxham, M., Hendriks, I.E., Krause-Jensen, D., Laffoley, D., Luisetti, T., Marbà, N., Masque, P., McGlathery, K.J., Megonigal, J.P., Murdiyarso, D., Russell, B.D., Santos, R., Serrano, O., Silliman, B.R., Watanabe, K., Duarte, C.M., 2019. The future of Blue Carbon science. Nature communications 10 (1), 3998.

Maietta, C.E., Bernstein, Z.A., Gaimaro, J.R., Buyer, J.S., Rabenhorst, M.C., Monsaint-Queeney, V.L., Baldwin, A.H., Yarwood, S.A., 2019. Aggregation but Not Organo-

Metal Complexes Contributed to C Storage in Tidal Freshwater Wetland Soils. Soil Science Soc of Amer J 83 (1), 252–265.

Mao, R., Ye, S.-Y., Zhang, X.-H., 2018. Soil-Aggregate-Associated Organic Carbon Along Vegetation Zones in Tidal Salt Marshes in the Liaohe Delta. CLEAN Soil Air Water 46 (4).

Maxwell, T.L., Rovai, A.S., Adame, M.F., Adams, J.B., Álvarez-Rogel, J., Austin, W.E.N., Beasy, K., Boscutti, F., Böttcher, M.E., Bouma, T.J., Bulmer, R.H., Burden, A., Burke, S.A., Camacho, S., Chaudhary, D.R., Chmura, G.L., Copertino, M., Cott, G.M., Craft, C., Day, J., Los Santos, C.B. de, Denis, L., Ding, W., Ellison, J.C., Ewers Lewis, C.J., Giani, L., Gispert, M., Gontharet, S., González-Pérez, J.A., González-Alcaraz, M.N., Gorham, C., Graversen, A.E.L., Grey, A., Guerra, R., He, Q., Holmquist, J.R., Jones, A.R., Juanes, J.A., Kelleher, B.P., Kohfeld, K.E., Krause-Jensen, D., Lafratta, A., Lavery, P.S., Laws, E.A., Leiva-Dueñas, C., Loh, P.S., Lovelock, C.E., Lundquist, C.J., Macreadie, P.I., Mazarrasa, I., Megonigal, J.P., Neto, J.M., Nogueira, J., Osland, M.J., Pagès, J.F., Perera, N., Pfeiffer, E.-M., Pollmann, T., Raw, J.L., Recio, M., Ruiz-Fernández, A.C., Russell, S.K., Rybczyk, J.M., Sammul, M., Sanders, C., Santos, R., Serrano, O., Siewert, M., Smeaton, C., Song, Z., Trasar-Cepeda, C., Twilley, R.R., van de Broek, M., Vitti, S., Antisari, L.V., Voltz, B., Wails, C.N., Ward, R.D., Ward, M., Wolfe, J., Yang, R., Zubrzycki, S., Landis, E., Smart, L., Spalding, M., Worthington, T.A., 2023. Global dataset of soil organic carbon in tidal marshes. Scientific data 10 (1), 797.

Mazarrasa, I., Neto, J.M., Bouma, T.J., Grandjean, T., Garcia-Orellana, J., Masqué, P., Recio, M., Serrano, Ó., Puente, A., Juanes, J.A., 2023. Drivers of variability in Blue Carbon stocks and burial rates across European estuarine habitats. The Science of the total environment 886, 163957.

Mcleod, E., Chmura, G.L., Bouillon, S., Salm, R., Björk, M., Duarte, C.M., Lovelock, C.E., Schlesinger, W.H., Silliman, B.R., 2011. A blueprint for blue carbon: toward an improved understanding of the role of vegetated coastal habitats in sequestering CO 2. Frontiers in Ecol & Environ 9 (10), 552–560.

Mittmann-Goetsch, J., Wilson, M., Jensen, K., Mueller, P., 2024. Root-driven soil reduction in Wadden Sea salt marshes. Wetlands 44. https://doi.org/10.1007/s13157-024-01867-8.

Mueller, P., Granse, D., Nolte, S., Weingartner, M., Hoth, S., Jensen, K., 2020. Unrecognized controls on microbial functioning in Blue Carbon ecosystems: The role of mineral enzyme stabilization and allochthonous substrate supply. Ecology and evolution 10 (2), 998–1011.

Müller, H.-W., Dohrmann, R., Klosa, D., Rehder, S., Eckelmann, W., 2009. Comparison of two procedures for particle-size analysis: Köhn pipette and X-ray granulometry. Z. Pflanzenernähr. Bodenk. 172 (2), 172–179.

Najera, F., Dippold, M.A., Boy, J., Seguel, O., Koester, M., Stock, S., Merino, C., Kuzyakov, Y., Matus, F., 2020. Effects of drying/rewetting on soil aggregate dynamics and implications for organic matter turnover. Biol Fertil Soils 56 (7), 893–905.

R Core Team, 2022. R. A language and environment for statistical computing. R Foundation for Statistical Computing, Vienna, Austria.

Rabenhorst, M.C., 2008. Protocol for using and interpreting IRIS tubes. Soil Survey Horizons 49 (3), 74–77.

Ran, Y., Ma, M., Liu, Y., Zhou, Y., Sun, X., Wu, S., Huang, P., 2021. Hydrological stress regimes regulate effects of binding agents on soil aggregate stability in the riparian zones. CATENA 196, 104815.

Rocci, K.S., Lavallee, J.M., Stewart, C.E., Cotrufo, M.F., 2021. Soil organic carbon response to global environmental change depends on its distribution between mineral-associated and particulate organic matter: A meta-analysis. The Science of the total environment 793, 148569.

Ruiz-Fernández, A.C., Carnero-Bravo, V., Sanchez-Cabeza, J.A., Pérez-Bernal, L.H., Amaya-Monterrosa, O.A., Bojórquez-Sánchez, S., López-Mendoza, P.G., Cardoso-Mohedano, J.G., Dunbar, R.B., Mucciarone, D.A., Marmolejo-Rodríguez, A.J., 2018. Carbon burial and storage in tropical salt marshes under the influence of sea level rise. The Science of the total environment 630, 1628–1640.

Schmidt, M.W.I., Torn, M.S., Abiven, S., Dittmar, T., Guggenberger, G., Janssens, I.A., Kleber, M., Kögel-Knabner, I., Lehmann, J., Manning, D.A.C., Nannipieri, P., Rasse, D.P., Weiner, S., Trumbore, S.E., 2011. Persistence of soil organic matter as an ecosystem property. Nature 478 (7367), 49–56.

Schulte Ostermann, T., Kleyer, M., Heuner, M., Fuchs, E., Temmerman, S., Schoutens, K., Bouma, J., Minden, V., 2021. Hydrodynamics affect plant traits in estuarine ecotones with impact on carbon sequestration potentials. Estuarine, coastal and shelf science 259, 107464.

Seyfferth, A.L., Bothfeld, F., Vargas, R., Stuckey, J.W., Wang, J., Kearns, K., Michael, H.A., Guimond, J., Yu, X., Sparks, D.L., 2020. Spatial and temporal heterogeneity of geochemical controls on carbon cycling in a tidal salt marsh. Geochimica et Cosmochimica Acta 282, 1–18.

Six, J., Bossuyt, H., Degryze, S., Denef, K., 2004. A history of research on the link between (micro)aggregates, soil biota, and soil organic matter dynamics. Soil and Tillage Research 79 (1), 7–31.

Six, J., Conant, R.T., Paul, E.A., Paustian, K., 2002a. Stabilization mechanisms of soil organic matter: Implications for C-saturation of soils. Plant and Soil 241 (2), 155–176.

Six, J., Feller, C., Denef, K., Ogle, S.M., Moraes, J.C. de, Albrecht, A., 2002b. Soil organic matter, biota and aggregation in temperate and tropical soils - Effects of no-tillage. Agronomie 22 (7-8), 755–775.

Spohn, M., Babka, B., Giani, L., 2013. Changes in soil organic matter quality during sea-influenced marsh soil development at the North Sea coast. CATENA 107, 110–117.

Spohn, M., Giani, L., 2012. Carbohydrates, carbon and nitrogen in soils of a marine and a brackish marsh as influenced by inundation frequency. Estuarine, coastal and shelf science 107, 89–96.

Sun, H., Jiang, J., Cui, L., Feng, W., Wang, Y., Zhang, J., 2019. Soil organic carbon stabilization mechanisms in a subtropical mangrove and salt marsh ecosystems. The Science of the total environment 673, 502–510.

Tang, H., Nolte, S., Jensen, K., Rich, R., Mittmann-Goetsch, J., Mueller, P., 2023. Warming accelerates belowground litter turnover in salt marshes – insights from a Tea Bag Index study. Biogeosciences 20 (10), 1925–1935.

van de Broek, M., Temmerman, S., Merckx, R., Govers, G., 2016. Controls on soil organic carbon stocks in tidal marshes along an estuarine salinity gradient. Biogeosciences 13 (24), 6611–6624.

van de Broek, M., Vandendriessche, C., Poppelmonde, D., Merckx, R., Temmerman, S., Govers, G., 2018. Long-term organic carbon sequestration in tidal marsh sediments is dominated by old-aged allochthonous inputs in a macrotidal estuary. Global Change Biology 24 (6), 2498–2512.

Viret, F., Grand, S., 2019. Combined Size and Density Fractionation of Soils for Investigations of Organo-Mineral Interactions. Journal of visualized experiments: JoVE (144).

Visser, J.M., Duke-Sylvester, S.M., Carter, J., Broussard, W.P., 2013. A Computer Model to Forecast Wetland Vegetation Changes Resulting from Restoration and Protection in Coastal Louisiana. Journal of Coastal Research 67, 51–59.

Wickham, H., Chang, W., Wickham, M.H., 2016. Package 'ggplot2'. Create elegant data visualisations using the grammar of graphics. Version 2 (1), 1–189.

Więski, K., Guo, H., Craft, C.B., Pennings, S.C., 2010. Ecosystem Functions of Tidal Fresh, Brackish, and Salt Marshes on the Georgia Coast. Estuaries and Coasts 33 (1), 161–169.

Wiesmeier, M., Urbanski, L., Hobley, E., Lang, B., Lützow, M. von, Marin-Spiotta, E., van Wesemael, B., Rabot, E., Ließ, M., Garcia-Franco, N., Wollschläger, U., Vogel, H.-J., Kögel-Knabner, I., 2019. Soil organic carbon storage as a key function of soils - A review of drivers and indicators at various scales. Geoderma 333, 149–162.

Wong, V.N.L., Greene, R.S.B., Dalal, R.C., Murphy, B.W., 2010. Soil carbon dynamics in saline and sodic soils: a review. Soil Use and Management 26 (1), 2–11.

Yuan, Y., Li, X., Jiang, J., Xue, L., Craft, C.B., 2020. Distribution of organic carbon storage in different salt-marsh plant communities: A case study at the Yangtze Estuary. Estuarine, coastal and shelf science 243, 106900.

Zhou, J., Wu, Y., Kang, Q., Zhang, J., 2007. Spatial variations of carbon, nitrogen, phosphorous and sulfur in the salt marsh sediments of the Yangtze Estuary in China. Estuarine, coastal and shelf science 71 (1-2), 47–59.

B7 Supplementary Material

Table S1: Plant species with area coverage [%] and Ellenberg Indicator Values for salinity (EIV-S) along the salinity and flooding gradient of the Elbe Estuary in July 2022.

Salt High Marsh	[%]	**Brackish High Marsh**	[%]	**Fresh High Marsh**	[%]
Agrostis stolonifera	<0.1	*Agrostis stolonifera*	0.1	*Agrostis stolonifera*	0.8
Aster tripolium	13.4	*Berula erecta*	0.3	*Calystegia sepium*	7.2
Atriplex littoralis	0.2	*Calystegia sepium*	28.3	*Equisetum palustre*	0.1
Atriplex prostrata	15.8	*Dactylis glomerata*	<0.1	*Phalaris arundinacea*	7.6
Elymus athericus	62.3	*Epilobium hirsutum*	24.1	*Phragmites australis*	54.0
Salicornia europaea	<0.1	*Galeopsis sp.*	<0.1	*Urtica dioica*	21.1
Suaeda maritima	0.5	*Galium palustre*	0.2	*Valeriana officinalis*	0.6
		Phalaris arundinacea	4.9		
		Phragmites australis	10.9		
		Poa trivalis	0.2		
		Rosa sp.	2.3		
		Urtica dioica	6.7		
		Valeriana officinalis	<0.1		
		Vicia cracca	0.3		
EIV-S: 5.4		EIV-S: 0.3		EIV-S: 0.0	
Salt Low Marsh	[%]	**Brackish Low Marsh**	[%]	**Fresh Low Marsh**	[%]
Agrostis stolonifera	0.2	*Agrostis stolonifera*	0.2	*Bidens sp.*	0.1
Aster tripolium	18.2	*Berula erecta*	6.9	*Caltha palustris*	0.1
Atriplex littoralis	<0.1	*Caltha palustris*	0.3	*Myosotis palustris*	0.1
Atriplex prostrata	5.6	*Calystegia sepium*	9.5	*Nasturtium officinale*	0.1
Elymus athericus	<0.1	*Lycopus europaeus*	0.9	*Phragmites australis*	92.6
Festuca rubra	8.3	*Phragmites australis*	73.0		
Halimione portulacoides	1.4				
Plantago maritima	<0.1				
Puccinellia maritima	40.8				
Salicornia europaea	1.7				
Spartina anglica	2.3				
Spergularia media	0.1				
Suaeda maritima	3.4				
Triglochin maritima	13.2				
EIV-S: 7.0		EIV-S: 0.1		EIV-S: 0.0	
Salt Pioneer Zone	[%]	**Brackish Pioneer Zone**	[%]	**Fresh Pioneer Zone**	[%]
Aster tripolium	3.2	*Bolboschoenus maritimus*	73.5	*Alisma plantago-aquatica*	1.8
Atriplex prostrata	2.0	*Nasturtium officinale*	0.2	*Caltha palustris*	16.0
Halimione portulacoides	0.01			*Mentha aquatica*	0.1
Puccinellia maritima	4.1			*Myosotis palustris*	0.1
Salicornia europaea	<0.1			*Typha angustifolia*	46.0
Spartina anglica	59.1				
Suaeda maritima	2.6				
Triglochin maritima	0.8				
EIV-S: 7.8		EIV-S: 2.0		EIV-S: 0.7	

Table S2: SOC stocks (t ha^{-1}), SOC contents (%), amount of SOC fractions (mg C g^{-1} soil) and proportions of SOC fractions (% of total SOC) (C_{MAOM} = mineral-associated OC, C_{oPOM} = aggregate-occluded OC, and C_{fPOM} = OC in free particulate organic matter) of the different marsh types and zones along the salinity (salt marsh, brackish marsh, freshwater marsh) and flooding gradient (HM = high marsh, LM = low marsh, PZ = pioneer zone) of the Elbe Estuary (mean ± standard error, n = 5).

Marsh type & zone		Depth [cm]	SOC		C_{MAOM}		C_{oPOM}		C_{fPOM}	
			stocks	stocks	contents	amount	proportion	amount	proportion	amount	proportion
Salt Marsh	HM	0 - 10	28.7 ± 2.6	73.7 ± 4.9	2.9 ± 0.6	14.1 ± 1.7	48.8 ± 4.6	8.1 ± 2.3	27.3 ± 4.6	3.1 ± 1.1	11.0 ± 4.8
		10 - 30	45.0 ± 2.6		2.4 ± 0.3	17.1 ± 3.0	69.8 ± 7.5	4.6 ± 1.8	18.7 ± 6.9	1.8 ± 0.9	7.7 ± 4.3
	LM	0 - 10	14.6 ± 0.7	39.9 ± 2.9	1.6 ± 0.2	8.6 ± 1.4	54.7 ± 4.4	3.3 ± 1.0	20.8 ± 4.0	1.9 ± 0.4	12.3 ± 3.8
		10 - 30	25.3 ± 2.8		1.5 ± 0.4	8.8 ± 2.7	60.4 ± 12.8	2.6 ± 1.0	17.7 ± 3.2	2.1 ± 0.4	15.2 ± 4.8
	PZ	0 - 10	14.4 ± 0.9	46.7 ± 2.7	1.8 ± 0.3	9.9 ± 1.9	54.4 ± 6.5	3.9 ± 0.8	21.3 ± 2.5	3.8 ± 1.0	21.1 ± 5.1
		10 - 30	32.3 ± 3.3		1.6 ± 0.4	10.3 ± 2.6	62.8 ± 10.3	3.1 ± 1.1	19.4 ± 6.8	1.8 ± 0.7	10.4 ± 2.4
Brackish Marsh	HM	0 - 10	31.4 ± 6.2	68.0 ± 7.8	3.8 ± 1.0	21.9 ± 7.9	48.6 ± 5.0	17.8 ± 8.4	38.1 ± 6.1	3.0 ± 1.7	5.9 ± 1.1
		10 - 30	36.6 ± 2.7		1.6 ± 0.3	7.6 ± 2.5	46.0 ± 8.7	5.4 ± 1.4	32.7 ± 4.5	0.8 ± 0.3	5.1 ± 2.1
	LM	0 - 10	23.1 ± 1.5	55.9 ± 4.2	2.7 ± 0.4	16.4 ± 1.0	62.5 ± 6.8	8.5 ± 1.0	33.0 ± 8.6	4.4 ± 2.1	16.3 ± 6.5
		10 - 30	32.8 ± 3.4		1.3 ± 0.3	6.2 ± 0.9	49.1 ± 7.6	3.4 ± 1.3	25.6 ± 5.9	4.0 ± 1.4	29.8 ± 5.2
	PZ	0 - 10	2.9 ± 0.3	9.3 ± 0.6	0.2 ± 0.0	0.9 ± 0.2	41.6 ± 10.4	1.3 ± 0.4	57.0 ± 18.4	0.7 ± 0.2	30.5 ± 3.4
		10 - 30	6.4 ± 0.6		0.2 ± 0.1	1.3 ± 0.5	52.9 ± 17.4	0.5 ± 0.3	22.3 ± 9.9	0.8 ± 0.3	32.1 ± 10.2
Freshwater Marsh	HM	0 - 10	30.2 ± 1.5	70.5 ± 2.6	5.2 ± 0.6	35.2 ± 8.0	67.0 ± 8.7	14.3 ± 2.6	27.9 ± 6.8	2.3 ± 1.2	4.5 ± 2.4
		10 - 30	40.3 ± 1.7		2.8 ± 0.3	20.7 ± 2.4	74.1 ± 8.2	4.4 ± 1.8	15.6 ± 6.0	1.2 ± 0.4	4.4 ± 1.5
	LM	0 - 10	32.3 ± 1.9	74.6 ± 4.3	5.8 ± 0.7	36.7 ± 1.1	64.8 ± 10.8	12.5 ± 2.4	21.6 ± 2.4	11.2 ± 3.6	19.3 ± 4.6
		10 - 30	42.3 ± 3.0		2.5 ± 0.4	11.4 ± 1.7	46.4 ± 5.8	6.6 ± 1.5	26.8 ± 3.3	8.6 ± 2.7	34.6 ± 8.4
	PZ	0 - 10	22.3 ± 0.5	69.3 ± 2.9	4.6 ± 0.2	32.4 ± 2.1	69.7 ± 3.9	8.5 ± 2.2	18.3 ± 5.2	4.0 ± 0.4	8.7 ± 1.3
		10 - 30	47.0 ± 2.8		4.2 ± 0.5	35.9 ± 3.1	81.8 ± 2.9	5.2 ± 2.2	12.4 ± 5.1	4.0 ± 1.1	9.8 ± 3.8

Table S3: Effects of estuarine gradients on SOC stocks (t ha^{-1}), SOC contents (%), amounts (mg C g^{-1} soil) and proportions of SOC fractions (% of total SOC) (C_{MAOM} = mineral-associated OC, C_{oPOM} = aggregate-occluded OC, and C_{fPOM} = OC in free particulate organic matter). P- and F-values are derived from ANOVA and asterisk indicate significant differences (* $p < 0.05$; ** $p < 0.005$; *** $p < 0.001$) (df = degree of freedom).

Gradient	Depth [cm]		SOC		C_{MAOM}		C_{oPOM}		C_{fPOM}	
			stock	content	amount	proportion	amount	proportion	amount	proportion
Salinity	0 - 10	p	< 0.001	< 0.001	< 0.001	< 0.001	< 0.001	< 0.001	< 0.001	< 0.001
		F	13.6	188.2	166.7	22.9	16.0	30.9	16.8	12.4
		df	2	2	2	2	2	2	2	2
	10 - 30	p	< 0.001	< 0.001	< 0.001	< 0.001	< 0.001	< 0.001	< 0.001	< 0.001
		F	33.8	142.1	215.3	12.7	10.7	9.7	27.0	27.0
		df	2	2	2	2	2	2	2	2
Flooding	0 - 10	p	< 0.001	< 0.001	< 0.001	0.061 .	< 0.001	0.04 *	< 0.001	< 0.001
		F	35.9	42.5	21.6	3.0	28.1	3.4	17.2	35.7
		df	2	2	2	2	2	2	2	2
	10 - 30	p	< 0.001	< 0.001	< 0.001	0.002 **	0.006 **	0.050 .	< 0.001	< 0.001
		F	15.4	9.7	41.1	7.4	5.9	3.3	38.4	38.4
		df	2	2	2	2	2	2	2	2
Salinity: Flooding	0 - 10	p	< 0.001	< 0.001	< 0.001	0.004	< 0.001	< 0.001	< 0.001	< 0.001
		F	7.6	17.3	10.2	4.7	5.9	6.0	16.1	16.1
		df	4	4	4	4	4	4	4	4
	10 - 30	p	< 0.001	< 0.001	< 0.001	0.002 **	< 0.001	0.007 **	< 0.001	< 0.001
		F	19.0	30.1	63.5	5.3	6.5	4.2	12.1	12.1
		df	4	4	4	4	4	4	4	4

Study C:
Connecting organic matter fractions to mineralization dynamics in estuarine marsh soils

in preparation

Friederike Neiske[a], Christian Beer[a], Daniel Schwarze[a], Maria Seedtke[a], Annette Eschenbach[a], Joscha N. Becker[a]

[a] Institute of Soil Science, CEN Center for Earth System Research and Sustainability, Universität Hamburg, Allende-Platz 2, 20146 Hamburg, Germany

C Abstract

Tidal marshes are critical carbon (C) sinks with high soil organic carbon (SOC) storage potential. Currently the vulnerability of SOC in tidal marshes with regard to threats from anthropogenic disturbances and climate change is unknown. To increase understanding of controlling mechanisms for C cycling in tidal marshes, we examined SOC mineralization in tidal marshes of the Elbe Estuary, Germany. We incubated topsoil (0 - 10 cm) and subsoil (10 - 30 cm) samples from three marsh types along the salinity gradient (salt, brackish, freshwater) and three flooding zones (high marsh, low marsh, pioneer zone) under oxic conditions to assess the C mineralization potential. A two-pool model was applied to quantify C pools (fast versus slow C) and their mean residence times (MRT). Model parameters were connected to SOC storage, SOC density fractions, dissolved organic carbon (DOC), microbial biomass (MBC), and local soil properties to gain insight into SOC stability and its drivers.

We found increasing amounts of mineralized C in relation to total SOC from the freshwater to the salt marsh, indicating a less stable SOC pool downstream of the salinity gradient. Effects of flooding on SOC mineralization were less clear, but shorter MRT in frequently flooded marshes indicated a higher proportion of easily available SOC. While direct relationships between SOC mineralization dynamics and SOC fractions could not be established, specific SOC fractions influenced the turnover of SOC pools. Free particulate organic matter (fPOM) was linked to decreased MRT, while mineral-associated organic matter (MAOM) was connected to a prolonged MRT. As a consequence, increasing marine influence in estuaries due to climate change (sea-level rise and saltwater intrusion) has the potential to decrease the SOC stability in the Elbe Estuary and reduce its overall SOC storage capacity.

Keywords

Elbe Estuary; soil organic carbon pools; mean residence time; soil organic carbon mineralizability; mineral-associated organic matter

C1 Introduction

Tidal marshes provide important ecosystem functions and are particularly recognized for their carbon (C) sequestration and storage potential (Chmura et al., 2003; Mcleod et al., 2011). Anthropogenic disturbances, particularly those linked to climate change, potentially undermine the function of tidal marshes within estuaries as C sinks. One of the primary threats to coastal ecosystems is sea-level rise, which potentially alters hydrodynamics (Jiang et al., 2019) and induces saltwater intrusion, negatively affecting their C storage capacity (Minick et al., 2019). However, uncertainty exists regarding the decomposability of soil organic carbon (SOC) in estuarine marshes resulting from the high heterogeneity in the amount and properties of SOC within these ecosystems.

Tidal marshes receive significant allochthonous C input due to flooding-related deposition, alongside autochthonous C contributions from high primary productivity (Mcleod et al., 2011). Additionally, the output of C through microbial mineralization is restricted by anaerobic conditions that arise from high soil moisture levels, leading to a net accumulation of C (Chmura et al., 2003; Mcleod et al., 2011). Estuarine marshes experience significant spatio-temporal fluctuations in soil water content due to the interaction of surface elevation changes and tidal inundation, which can significantly affect SOC mineralization and storage (Spohn and Giani, 2012; Mazarrasa et al., 2023; Study B). Salinity is another key factor influencing SOC storage and mineralization in estuarine soils (Yarwood, 2018; Luo et al., 2019). Estuaries exhibit a salinity gradient, with salinity levels gradually increasing toward the mouth of the estuary. Even though the effects of salinity on SOC mineralization have been widely studied, the findings remain inconsistent (Luo et al., 2019). Salinity can decrease microbial biomass and slow down the activity of microorganisms and enzymes (Lozupone and Knight, 2007; Setia et al., 2011; Chen et al., 2022). However, several studies in tidal marshes also indicated accelerated SOC mineralization in the context of increased salinity, for example due to enhanced microbial and enzymatic activities or sulfate availability (Craft, 2007; Weston et al., 2011; Chambers et al., 2013; Morrissey et al., 2014). Overall, the variability in microbial responses to salinity and its influence on SOC mineralization underscores the complexity of SOC dynamics in estuarine marshes and the need for comprehensive studies.

Soil organic carbon mineralization is also affected by the quality of the SOC itself (Lützow et al., 2006; Basile-Doelsch et al., 2020). Soil organic matter can be separated into different functional pools that are stabilized through specific mechanisms and exhibit distinct turnover rates. To predict variations in SOM

storage (e.g. by mechanistic models), it is essential to quantify and characterize these C pools (Lützow et al., 2007). Moreover, to improve existing models and to enhance our knowledge of SOC stability, it would be beneficial to combine conceptual SOC pools and measurable SOM fractions (Sollins et al., 1996; Lützow et al., 2006). For example, it is widely accepted that the fast or labile C pool, which is readily decomposed and characterized by a short turnover time, includes dissolved organic carbon (DOC), fresh plant detritus, or microbial biomass (MBC) (Lützow et al., 2007; Lützow et al., 2008; Smith and Paul, 2017). The stable or slow C pool is more resistant to microbial breakdown reflected in a longer turnover time and is often attributed to mineral-associated OM (Fang et al., 2005; Lützow et al., 2008). However, large uncertainties exist regarding the incorporation of certain SOC fractions into SOC pools (Lützow et al., 2007). Despite some shortcomings, laboratory soil incubation is one of few methods providing insight into the turnover of C pools (Schwendenmann and Pendall, 2008). Characterizing conceptual C pools and their turnover can provide valuable information on the decomposability of SOC. Density fractionation can be useful in identifying SOC stabilization mechanisms (Golchin et al., 1994; Cerli et al., 2012). Fractions of SOC can be divided into light density fractions, comprising particulate organic matter (POM) from plant detritus, and heavy density fractions, mainly mineral-associated organic matter (MAOM). The light fraction can be further differentiated into free light fraction (free POM) and occluded light fraction (occluded POM), the latter being protected within soil aggregates (Wagai et al., 2009). Previous research identified soil texture, oxygen availability, and C input as crucial factors for SOC stabilization in terrestrial soils (Basile-Doelsch et al., 2020). However, the relationship between these factors and SOC stabilization remains unclear for tidal ecosystems. For examples, SOC stabilization by mineral-association and aggregate-occlusion varies within the Elbe Estuary. Mineral-associated OM decreased downstream of the Elbe Estuary which could be related to decreasing clay content from freshwater to salt marsh (Study B). Characterizing SOC pools and fractions is essential because, a larger pool of labile C can lead to more C being mineralized with less MBC, due to its easier accessibility for microorganisms (Pabst et al. 2016). At the same time, stress and disturbances, such as flooding, can reduce microbial activity and efficiency in C utilization (Anderson and Domsch, 1993; Anderson, 2003; Rinklebe and Langer, 2006).

Our objective was to characterize variation in mineralization dynamics of SOC along the salinity and flooding gradients of the Elbe Estuary. By identifying functional relationships between C mineralizability, incubation model parameters (SOC pools, MRT), SOC fractions, and soil properties we aim to gain insights into SOC stability and its drivers in the estuary. We hypothesize

increasing SOC mineralizability (i) from the freshwater to the salt marsh due to increasing salinity and less SOC protection by mineral association; and (ii) with increasing flooding due to the accumulation of labile SOC under anoxic conditions. Moreover, (iii) we expect that model parameters will be reflected in SOC fractions.

C2 Methods

C2.1 Study area

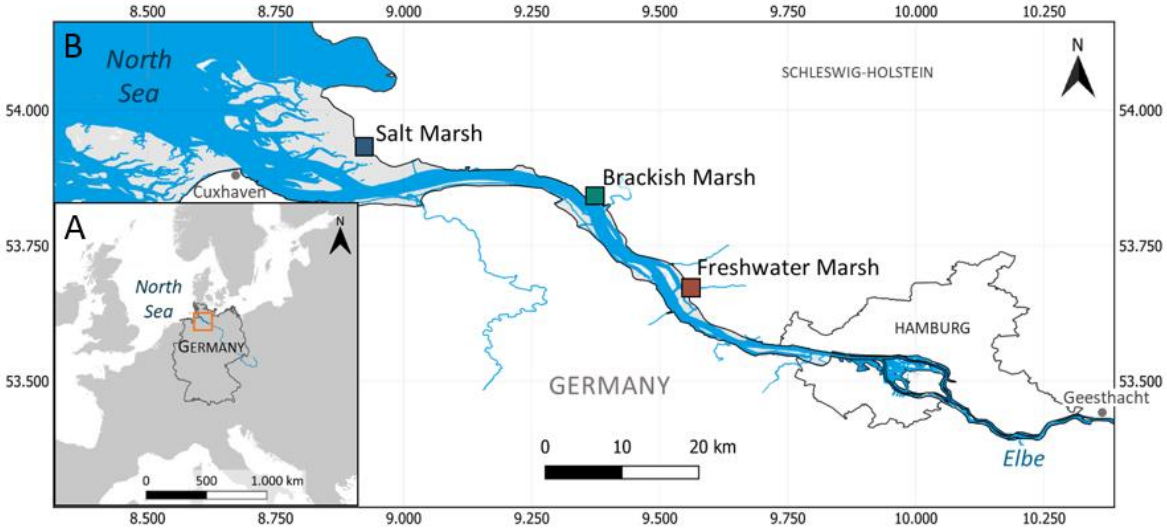

Figure C1: (A) Location of the Elbe Estuary in central Europe (orange rectangle) and (B) location of the marsh sites along the Elbe Estuary (salt marsh: 53°55'40.0"N 8°54'51.3"E/river-km: 710; brackish marsh: 53°50'03.0"N 9°22'15.6"E/river-km: 680; freshwater marsh: 53°39'56.3"N 9°33'11.5"E/river-km: 658) (WSV, 2011, 2017; EEA, 2017).

The study was conducted in the Elbe Estuary, Germany (Figure C1). The region is characterized by an oceanic climate, with a mean annual temperature of 9.3 °C and mean annual rainfall of 812.8 mm (DWD, 2024). The estuary experiences a semi-diurnal meso- to macrotidal regime with a mean tidal rage between 2.0 m (at weir Geesthacht) and 3.5 m (port of Hamburg) (Kappenberg and Grabemann, 2001; Kerner, 2007), and can be divided into distinct salinity zones based on vegetation (Engels and Jensen, 2009). Along this salinity gradient, we selected three research sites: a salt marsh (Kaiser-Wilhelm-Koog), a brackish marsh (Hollerwettern), and a freshwater marsh (Haseldorfer Binnenelbe) (Figure C1 (B)) (Branoff et al., 2024, preprint). At

each site, three research stations were established, representing a flooding frequency gradient: Pioneer zones (PZ), located closest to the main channel, experience flooding during high tide (twice per day), low marshes (LM) are flooded during spring tides (twice per month), and high marshes (HM) are flooded during storm tides (a few times per year). Each research station consists of five adjacent replicate plots (2 x 2 m). These marsh locations were defined according to plant species associated with the respective salinity and flooding regime (Engels and Jensen, 2009) (Table S1). All locations are located on the seaward side of a dike and exhibit near-natural conditions.

C2.2 Field sampling and site characterization

Soil sampling

At each marsh location along the salinity gradient (salt marsh, brackish marsh, and freshwater marsh) and flooding gradient (pioneer zone, low marsh, and high marsh), soil samples were collected from each replicate plot (n = 5) between February and March 2022, and separated into topsoil (0 - 10 cm) and subsoil (10 - 30 cm) samples. Soil samples were transported to the laboratory at Institute of Soil Science, University of Hamburg, and separated into three aliquots for further analysis; one aliquot was stored at -20 °C, a second one was air-dried at room temperature, and third one dried at 105 °C.

Soil reduction index

Reducing soil conditions were assessed at each replicate plot using a modified "Indicator of Reduction in Soil" (IRIS) method (Castenson and Rabenhorst, 2006; Rabenhorst, 2008; Mueller et al., 2020; Mittmann-Goetsch et al., 2024). PVC sticks (5 x 70 cm) were coated with $FeCl_3$-paint and inserted into the soil to a depth of 60 cm for four weeks. Upon retrieval, a reduction index (RI) ranging from 0 to 1 was calculated based on the area where the paint was removed. We incubated IRIS sticks over the course of nearly one year (11 x 4 weeks), and calculated the annual reduction index (RI_{year}), as well as the index for the soil sampling period in February and March (RI_{march}) corresponding to the specific soil depths (0 - 10 cm and 10 - 30 cm).

C2.3 Laboratory analyses

Carbon mineralization and decomposition model

We conducted an oxic incubation under optimal conditions to derive information on the potentially mineralizable SOC. After thawing and sieving (2 mm), soil samples (20 g dry mass equivalent) were adjusted to 60% water holding capacity. Water-adjusted samples were filled in 1000 ml flasks and incubated in the dark at 20 °C for up to 465 days. The mineralization rate of SOC was measured as the headspace accumulation of CO_2 over time in each flask. At regular time intervals, headspace samples (1 ml) were collected for CO_2 measurements by gas chromatography (GC) (JAS 6890N, Germany). Sampling interval was daily in the first week of incubation, and decreased with progressing incubation. In order to maintain a higher pressure within the flasks compared to ambient air and to avoid respiration-limiting oxygen deficiency by high CO_2 concentrations (> 2.5% in headspace), flasks were evacuated and flushed with synthetic air.

To assess the final amount of mineralized C, we calculated the amount of cumulative mineralized C C_{cum} at the end of the experiment, expressed as absolute amounts of mineralized C (C_{min}) per initial soil dry mass [mg C_{CO2} g^{-1} soil] or as relative proportions per initial SOC (C_{min}/SOC) [mg C_{CO2} g^{-1} SOC]. A two-pool model following first-order kinetics of decomposition (Andrén and Kätterer, 1997) was calibrated against observed CO_2 production. The two C pools represent more available and easily decomposable material (fast pool) and more stabilized OM or OM that is more difficult to decompose (slow pool). The decomposition rate constants of both C pools, the initial fast C pool proportion, and the stabilization constant were optimized. We apply a least-squares gradient decent method (MATLAB function lsqnonlin). The model was fitted against the cumulative produced C_{cum} from each sample. Mean residence time is defined as the reciprocal of the decomposition rate constant. A log transformation was applied to estimate the mean turnover time of all samples (methodological details can be found in Knoblauch et al. (2013) and Beer et al. (2022)).

Density fractionation

Data on soil density fractionation were derived from Study B, where a more detailed method description can be found. In brief, sodium polytungstate (at ρ = 1.62 g cm^{-3}) was mixed with air-dried soil samples to quantify free particulate organic matter (fPOM) and occluded particulate organic matter (oPOM), as well as mineral-associated organic matter (MAOM) based on Golchin

et al. (1994) and Viret and Grand (2019). Organic carbon associated with each fraction were expressed as total amount [mg C g^{-1} soil] or as proportion relative to total SOC [% of total SOC].

Physico-chemical soil analyzes

Air dried bulk soil samples were sieved (2 mm), dried at 105 °C, and ground for analyzing their inorganic and organic C contents with an elemental analyzer (soliTOC® cube, Elementar Analyzensysteme GmbH, Germany), and total C and N contents (vario Max cube, Elementar Analyzensysteme GmbH, Germany). Soil texture was determined using the sieving and sedimentation method for mineral soils (DIN ISO 11277) using a vibratory sieve shaker (Retsch GmbH, Germany) and a Sedimat 4-12 (Umwelt-Geräte-Technik GmbH, Germany) based on the Köhn pipette fractionation. Soil pH was measured in a 0.01 M $CaCl_2$ solution (pH_{CaCl2}) and in H_2O (pH_{H2O}), the latter suspension was also used for measuring the electric conductivity (EC). Detailed method descriptions are available Study B.

Microbial biomass and dissolved organic carbon

Microbial biomass C (MBC) was determined by chloroform fumigation extraction (CFE) adapted from Vance et al. (1987). Fumigated and non-fumigated soil samples were extracted with 0.05 M K_2SO_4 (Werth and Kuzyakov, 2010; Halbritter et al., 2020). Concentrations of C in the extracts were measured with a TOC/TN Analyzer (Shimadzu Corporation, Kyoto, Japan). The amount of MBC was determined by the difference between C concentrations in fumigated and non-fumigated soils, with a correction factor of 0.45 (Joergensen and Mueller, 1996). The K_2SO_4-extractable C from the non-fumigated samples was accepted as extractable dissolved organic carbon (DOC) (Blagodatskaya et al., 2009; Pabst et al., 2013). The DOC is either expressed as DOC [mg C g^{-1} soil] or as DOC/SOC [mg C g^{-1} SOC].

Metabolic quotient and substrate availability

For calculating the metabolic quotient (qCO_2), we first assessed the basal respiration rate [mg C_{CO2} g^{-1} h^{-1}]. Basal respiration rates were measured after one week of incubation, as CO_2 efflux over one-week intervals. For each interval, the CO_2 efflux rate was assessed for linearity. A threshold of $R^2 \geq 0.99$ was used to determine acceptable linearity. If the efflux rate did not meet this criterion, subsequent one-week intervals were analyzed until the R^2 value met or exceeded 0.99. Across all intervals, the mean R^2 value for the CO_2 efflux rate

was found to be 0.9985, indicating a highly linear relationship throughout the measurement periods. The metabolic quotient (qCO_2) was calculated by dividing basal respiration by MBC. Substrate availability was determined by dividing MBC by total SOC (MBC/SOC).

C2.4 Data analyzes

To analyze differences in target variables among marsh locations, analysis of variance (ANOVA) with TukeyHSD post-hoc comparison was applied. The effect of depth was evaluated using a linear mixed-effects model (LME) for paired comparison, with depth as the main factor and sampling location as a random factor. We assessed assumptions of normality and homogeneity of variance through visual inspection of the model residuals. Dixon's Q test was utilized to identify potential outliers within groups. Relationships between variables were analyzed using linear regression and Pearson correlation coefficients. Additionally, Spearman rank correlation coefficients were used to account for potential non-linearity. Simple linear and log-linear fits were selected according to reduction in Akaike Information Criterion (AIC) values. Statistical significance was determined at a p-value of less than 0.05, while p-values between 0.10 and 0.05 were considered to show a tendency towards significance. All statistical analyses were performed using R 4.2.0 (R Core Team, 2022), using "multcomp" (Hothorn et al., 2016) and "multcompView" (Graves et al., 2015) packages, as well as "ggplot2" (Wickham et al., 2016) for data visualization.

C3 Results

C3.1 Incubation parameter

Cumulative mineralized C

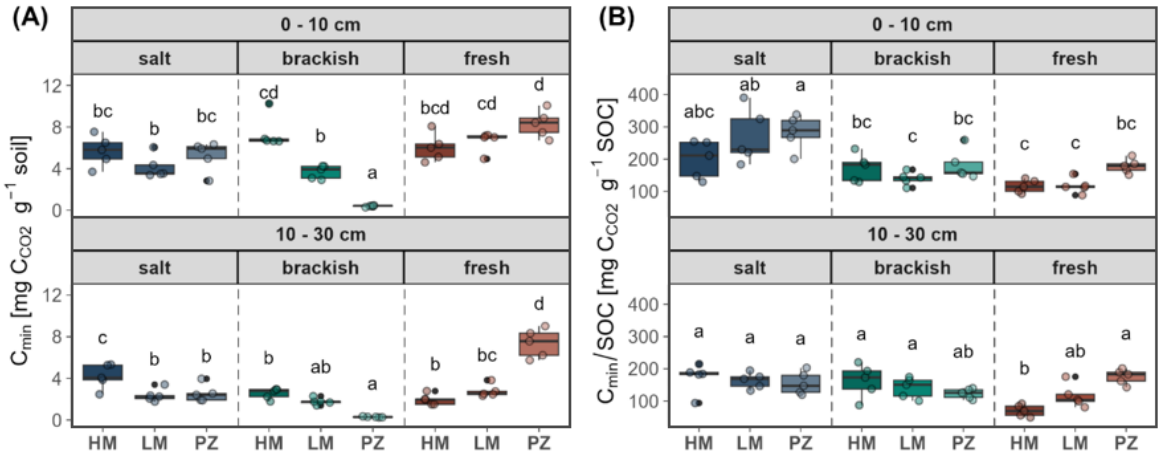

Figure C2: Cumulative mineralized C (C_{min}) as (A) absolute amounts [mg C_{CO2} g^{-1} soil] and (B) relative proportions (C_{min}/SOC) [mg C_{CO2} g^{-1} SOC] along the salinity (salt marsh, brackish marsh, freshwater marsh) and flooding gradient (HM = high marsh, LM = low marsh, PZ = pioneer zone) of the Elbe Estuary. Lowercase letters indicate significant differences ($p < 0.05$) derived from ANOVA with TukeyHSD post-hoc comparison applied on each depth separately.

The absolute amounts (C_{min}) [mg C_{CO2} g^{-1} soil] and relative proportions (C_{min}/SOC) [mg C_{CO2} g^{-1} SOC] of mineralized C varied along the estuarine gradients and with depth (Figure C2, Figure S2). Along the salinity gradient from the freshwater to the salt marsh, the absolute C_{min} decreased significantly in low marshes (topsoil) and pioneer zones while C_{min}/SOC increased in several flooding zones. Increasing flooding reduced absolute C_{min} at the salt marsh (subsoil) and brackish marsh, while it enhanced C_{min} at the freshwater marsh. Relative C_{min}/SOC increased with higher flooding frequency at the salt marsh (topsoil) and freshwater marsh, while it tended to decrease in brackish subsoil. Topsoils showed larger C_{min} and C_{min}/SOC than subsoils (Figure S2). The amount of mineralized C_{min} increased with increasing SOC content, fast and slow C pool size, MBC (topsoil), DOC, the amount of all three SOC fractions (C_{oPOM}, C_{fPOM}, C_{MAOM}), and decreasing relative proportions of fast C (topsoil), C_{oPOM}, and C_{fPOM}. The relative proportion of mineralized C (C_{min}/SOC) decreased with increasing SOC content (topsoil), amounts of all three SOC fractions and decreasing EC and qCO_2 (subsoil) (Figure C6, Figure S5).

Fast and slow C pool

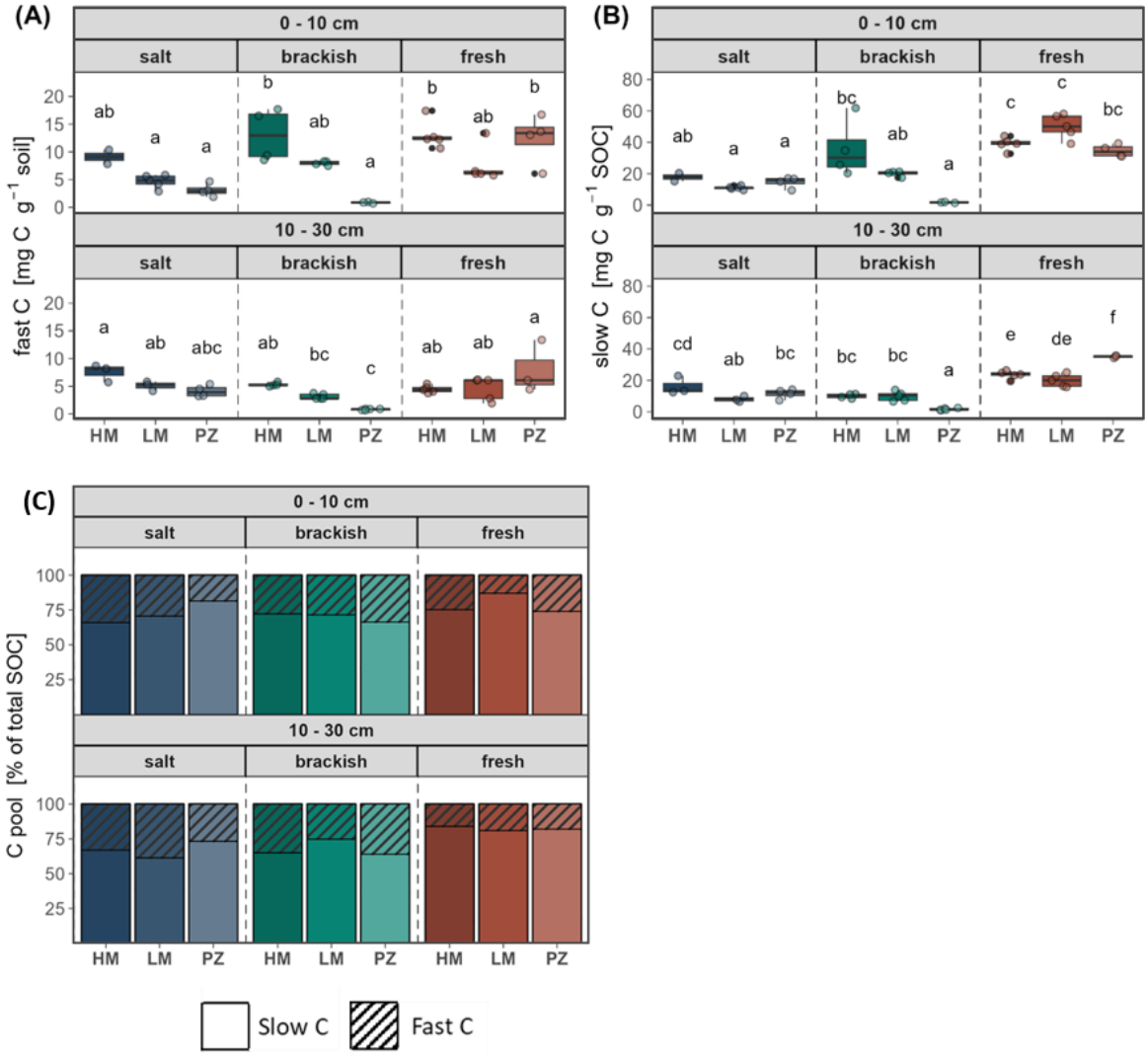

Figure C3: (A) Absolute amounts of fast C [mg C g^{-1} soil], (B) absolute amounts of slow C [mg C g^{-1} soil], and (C) relative proportions of the fast and slow C pool [% of total SOC], in topsoil (0 - 10 cm) and subsoil (10 - 30 cm) along the salinity (salt marsh, brackish marsh, freshwater marsh) and flooding gradient (HM = high marsh, LM = low marsh, PZ = pioneer zone). Lowercase letters in (A) and (B) indicate significant differences ($p < 0.05$) derived from ANOVA with TukeyHSD post-hoc comparison applied on each depth separately.

Based on the model outcome, the majority of SOC in the marshes of the Elbe Estuary was attributed to the slow C pool, with 73.7% ± 1.0 (topsoil: 74.8% ± 1.2; subsoil: 73.1% ± 1.6) (Figure C3 (A), Figure S3). Along the salinity gradient, the relative proportion of fast C [% of total SOC] increased or tended to increase from the freshwater to the salt marsh in high marshes, low marshes, and subsoil of pioneer zones, while slow C decreased. In topsoil of pioneer zones, the relative proportion of fast C tended to decrease from freshwater and brackish to the salt marsh (-30% to -45%, respectively) (slow C tended to

increase). The flooding gradient did not have a clear effect on the relative proportion of fast and slow C. Along the flooding gradient, increasing flooding tended to decrease the proportions of fast C at the salt marsh or tended to increase fast C at the brackish topsoil, while at some marshes the low marsh showed higher fast C proportions (brackish subsoil, freshwater topsoil) (slow C showed the opposite trend). Absolute amounts of fast C decreased along the salinity gradient from the freshwater to the salt marsh in pioneer zones and low marsh topsoils, while slow C amounts decreased in almost all flooding zones along the salinity gradient (Figure C3 (B) + (C)). The flooding gradient did not have a clear effect on the absolute amounts of fast and slow C. Fast C amounts were reduced or tended to be reduced with increasing flooding at the salt and brackish marsh while slow C amounts also decreased with increasing flooding at the brackish marsh but increased at the freshwater marsh. The fast C proportion increased with increasing DOC/SOC (subsoil) and decreasing SOC contents and clay content (the slow C proportion showed the opposite relationship). The fast C amount increased with increasing SOC content, C_{oPOM} amount, C_{MAOM} amount, and decreasing EC (topsoil), and qCO_2 (topsoil). The slow C amount increased with increasing SOC content, C_{oPOM} amount, C_{fPOM} amount, C_{MAOM} amount, C_{MAOM} proportions, and decreasing C_{fPOM} proportions (Figure C6, Figure S5).

Mean residence time

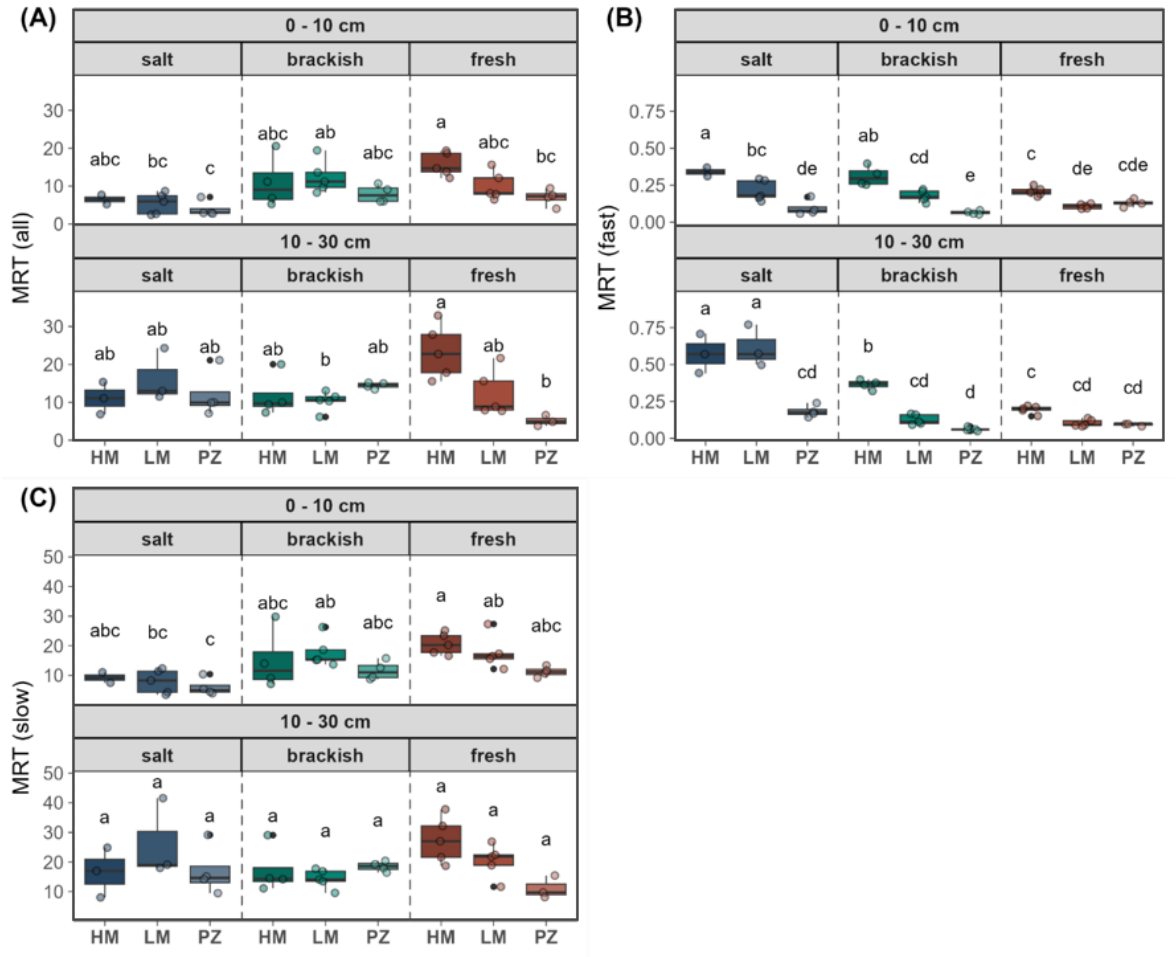

Figure C4: Mean residence time (MRT) of the (A) overall C pool, (B) fast C pool, and (C) slow C pool in topsoil (0 - 10 cm) and subsoil (10 - 30 cm) along the salinity (salt marsh, brackish marsh, freshwater marsh) and flooding gradient (HM = high marsh, LM = low marsh, PZ = pioneer zone) of the Elbe Estuary. Lowercase letters indicate significant differences ($p < 0.05$) derived from ANOVA with TukeyHSD post-hoc comparison applied on each depth separately.

The MRT of overall SOC tended to decrease with increasing salinity from the freshwater (5.1 - 23.4), over the brackish (7.9 - 14.5) to the salt marsh (4.0 - 16.3). This trend was more pronounced in topsoils, and with decreasing flooding (Figure C4). The overall MRT decreased with increasing flooding at the freshwater marsh from the high marsh (15.7 - 23.4), over the low marsh (10.1 - 12.4) to the pioneer zone (5.1 - 7.0). The MRT of the fast C pool (0.1 - 0.6) increased with increasing salinity in high marshes (1.5 - 3 times longer at the salt marsh compared to the freshwater marsh) and low marshes (2 - 6 times longer at the salt marsh compared to the freshwater marsh). Increasing flooding decreased the MRT of the fast C pool in almost all salinity zones. The MRT of the slow C pool followed the trend of the overall MRT and was not significantly affected by the estuarine gradients but tended to decrease

with increasing salinity in high marshes, low marshes (topsoil), and pioneer zones (subsoil). Increasing flooding tended to decrease the MRT of the slow C pool at the freshwater marsh. We found a negative correlation between the MRT of the overall C pool and EC, DOC, and qCO_2 and a positive correlation with amounts of C_{MAOM} and C_{oPOM} in topsoil. The MRT of the slow C pool correlated negatively with increasing DOC, EC, and qCO_2 (topsoil) and positively with amounts of C_{MAOM} and C_{oPOM} in topsoil. The MRT of the fast C pool increased with decreasing RI_{year} and RI_{March}, as well as relative proportions of C_{fPOM}, DOC/SOC, and qCO_2 (topsoil) (Figure C6, Figure S5).

C3.2 Microbial biomass

Soil microbial biomass (MBC) was affected by the estuarine gradients and depth as amounts of MBC were highest in topsoil of brackish and freshwater high marshes (1.11 ± 0.08 mg g^{-1} and 1.23 ± 0.11 mg g^{-1}, respectively) while the brackish pioneer zone (0.12 ± 0.01 mg g^{-1}) showed lowest amounts (Figure C5). Amounts of MBC decreased or tended to decrease along the salinity gradient from the freshwater to the salt marsh. Flooding negatively affected MBC at the brackish and freshwater marsh. Topsoils (0.60 ± 0.05 mg g^{-1}) had 40% higher amounts of MBC than subsoils (0.36 ± 0.03 mg g^{-1}).

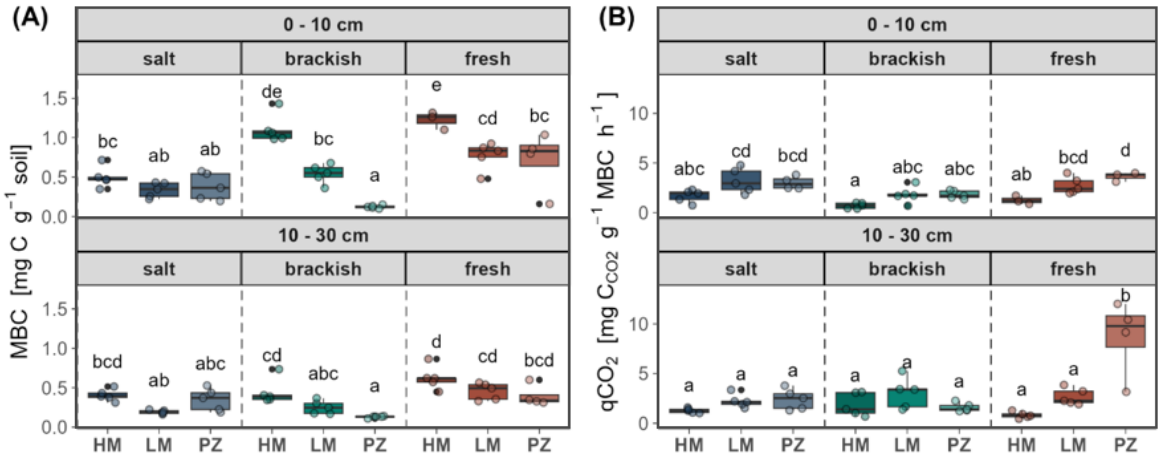

Figure C5: (A) Amount microbial biomass (MBC) [mg C g^{-1} soil] and (B) metabolic quotient qCO_2 [mg C_{CO2} g^{-1} MBC h^{-1}] in topsoil (0 - 10 cm) and subsoil (10 - 30 cm) along the salinity (salt marsh, brackish marsh, freshwater marsh) and flooding gradient (HM = high marsh, LM = low marsh, PZ = pioneer zone) of the Elbe Estuary. Lowercase letters indicate significant differences ($p < 0.05$) derived from ANOVA with TukeyHSD post-hoc comparison applied on each depth separately.

C3.3 Microbial metabolic quotient (qCO_2)

Along the salinity gradient, qCO_2 tended to be lower in brackish topsoils (0.7 - 1.8 mg C_{CO2} g^{-1} MBC h^{-1}) compared to freshwater (1.2 - 3.6 mg C_{CO2} g^{-1} MBC h^{-1}) and salt marshes (1.7 - 3.2 mg C_{CO2} g^{-1} MBC h^{-1}) (Figure C5 (B)). Along the flooding gradient, we observed that qCO_2 tended to increase from high marshes to pioneer zones in all salinity zones. In subsoils, qCO_2 varied little (0.8 - 3.0 mg C_{CO2} g^{-1} MBC h^{-1}) along the estuarine gradient with the exception of highest values in the freshwater pioneer zone (8.7 ± 1.7 mg C_{CO2} g^{-1} MBC h^{-1}). The qCO_2 was positively linked to EC, as well as C:N ratios of free POM and occluded POM but negatively affected by amount of C in the fast pool and relative proportions of C_{oPOM} (Figure C6, Figure S5).

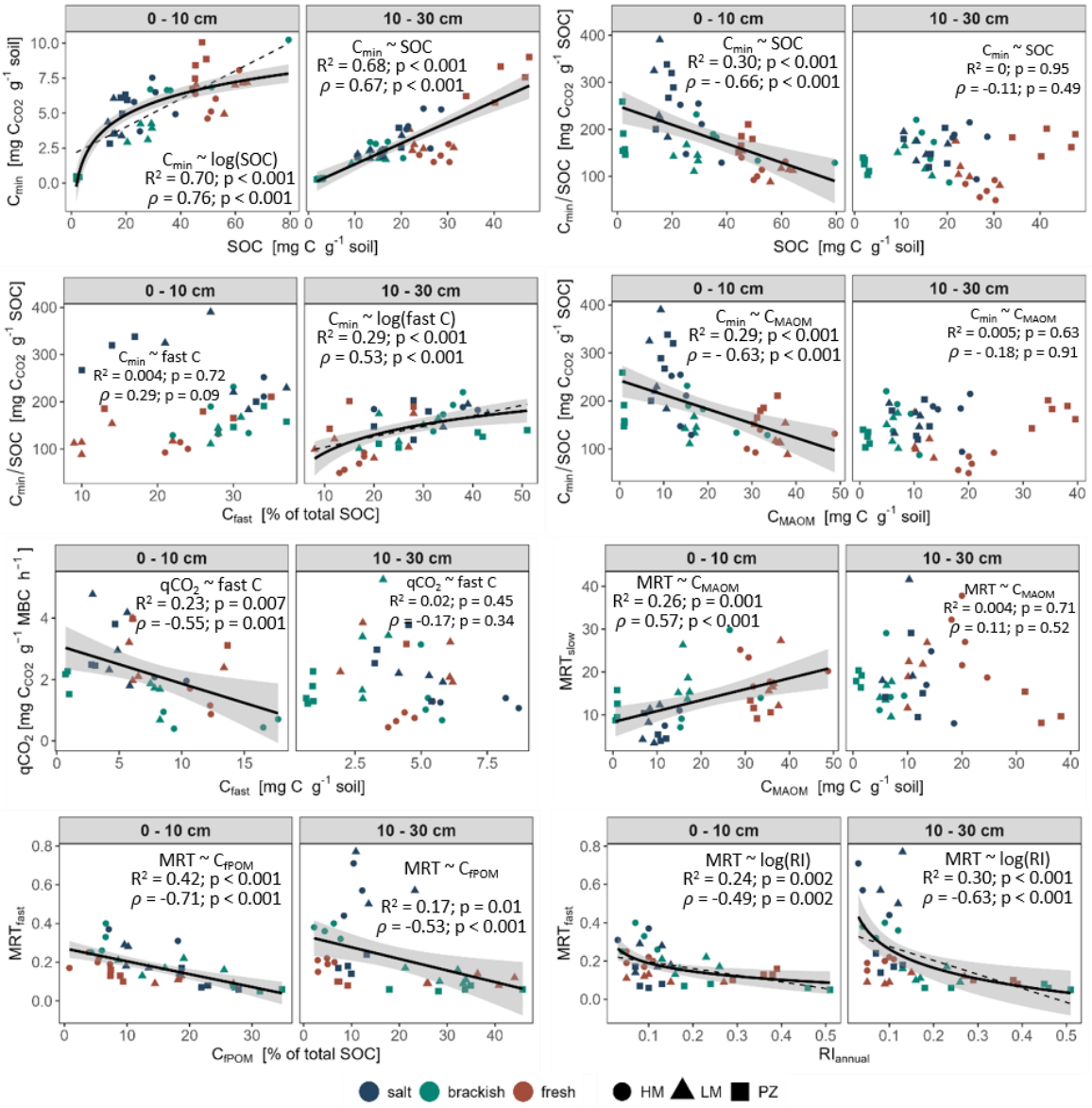

Figure C6: Relationship between selected variables with Spearman rank correlation coefficients (ρ). Black solid lines indicate linear or logarithmic regression lines with 95% confidence bands and respective coefficients of determination (R^2). Additional dashed lines indicate significant simple linear relationship in case logarithmic regression was used.

C4 Discussion

C4.1 Carbon mineralization along estuarine gradients

Salinity gradient

We observed two trends in mineralized C (C_{min}) along the salinity gradient of the Elbe Estuary. While absolute amounts of C_{min} decreased from freshwater to salt marshes, the relative proportions C_{min}/SOC increased in most flooding zones. The latter observation fits to our hypothesis that SOC mineralizability increases along the salinity gradient from the freshwater to the salt marsh.

Mineralization of SOC is primarily influenced by its quantity and quality (Middelburg et al., 1996). The decline in amounts of C_{min} downstream of the estuary was directly attributed to decreasing SOC contents. The SOC contents of estuaries often show a decreasing trend from freshwater toward salt marshes (Kelleway et al., 2016; van de Broek et al., 2016; Study B), due to a decline in allochthonous and autochthonous OC inputs (Craft, 2007; Więski et al., 2010; Butzeck et al., 2015). Moreover, we found a positive correlation between C_{min} and DOC concentrations in subsoils, suggesting that higher DOC levels enhanced SOC degradability. However, this relationship did not entirely explain the trend in C_{min} along the salinity gradients, as DOC concentrations did not exhibit the same tendencies along the gradient. In addition, the amount of C_{min} was positively linked to microbial biomass (MBC). Therefore, the decreasing MBC from the freshwater to the salt marsh might have contributed to a decreased amount of mineralized C. An adverse effect of salinity on microbial biomass has been also observed in other studies (Egamberdieva et al., 2010; Yang et al., 2017).

In contrast to the absolute amounts of mineralized C, the proportion of mineralized C in relation to total SOC (C_{min}/SOC) increased or tended to increase with increasing salinity and exhibited a negative relationship with SOC contents. This suggests that mechanisms promoting SOC accumulation potentially hinder its mineralization. The increasing C_{min}/SOC from the freshwater to the salt marsh coincided with elevated relative proportions of the fast C pool, indicating that SOC becomes increasingly labile downstream of the estuary. Further supporting this, the MRT of the overall and slow C pools tended to be shorter downstream of the estuary, although not significantly. The increasing SOC degradability might be attributed to variations in the quality of the autochthonous and allochthonous OM entering the marsh along the estuary. It was shown that the aboveground vegetation - and with this the potential autochthonous OC input - became more labile from the freshwater to the salt marsh of the Elbe Estuary,

reflected in decreased contents of lignin and cellulose, as well as lowered ratios of C:N and lignin:N (Study A). Moreover, in summer labile phytoplankton-derived OC contributed less to deposits in freshwater marshes compared to salt marsh of the Scheldt Estuary (van de Broek et al., 2018). In addition to the chemical stability of the SOC itself, the amount of OC protected within mineral-association and aggregates decreased from the freshwater to the salt marsh (Study B), which might have additionally led to the decline in the relative amount of mineralized C. This assumption was supported by a negative correlation between C_{min}/SOC and the amounts of C_{MAOM} and C_{oPOM}. The increased mineralization of the increasingly labile SOC could be further enhanced by the stimulating effect of salinity on SOC mineralization (Morrissey et al., 2014; Wang et al., 2019). This was supported by a positive correlation between C_{min}/SOC and EC, as well as a negative correlation between EC and MRTs of the overall and slow C pools in topsoils. These findings support our hypothesis that SOC mineralizability would increase from the freshwater to the salt marsh. This enhanced SOC mineralizability, combined with a reduction in OM input, has led to decreased SOC storage downstream of the Elbe Estuary. In the context of climate change, saltwater intrusion into estuaries and the subsequent shift of increased salinity zones upstream poses a potential risk of enhanced C output through mineralization, further diminishing the SOC storage potential of the estuary.

Flooding gradient

In our study, the flooding gradient did not show a clear effect on the quantities of mineralized C (C_{min} and C_{min}/SOC) nor on the fast C pool (relative and absolute quantities). This did not support our assumption that soils from frequently flooded marsh zones would contain larger proportions of labile SOM due to preservation under anoxic conditions.

Relative proportions of the fast C pool tended to decrease along the flooding gradient from the high marsh to the pioneer zone at the salt marsh and tended to increase at the brackish marsh (not significant). The relative proportion of mineralized C (C_{min}/SOC) also exhibited variable responses to the flooding gradient, ranging from negative over neutral to positive. Moreover, the relationship between relative mineralized C and SOC stability (fast and slow C pool) and stabilization (C_{MAOM} and C_{oPOM}) did not exhibit a consistent trend along the flooding gradient which could explain the observed variations. Despite no clear trend in quantities of mineralized C or labile C along the flooding gradient, SOC turnover increased with increasing flooding, reflected in shorter MRT. Particularly, the MRT of the fast C pool decreased in almost all salinity zones

while the MRT of the overall and slow C pool decreased at the freshwater marsh. Moreover, we observed a negative correlation between MRT of the fast C pool and reducing soil conditions (RI_{year} and RI_{March}). These findings indicate, that frequent inundation and reducing soil conditions may have suppressed SOC mineralization under field conditions and led to the accumulation of C with higher degradability. This aligns with the finding that the decomposition of recalcitrant OM is considerably slower and incomplete under anaerobic conditions (Benner et al., 1984; Kristensen et al., 1995; Hulthe et al., 1998).

C4.2 Connecting SOC pools, fractions, and MRT along gradients

From our observations, we cannot clearly classify C_{MAOM} and C_{oPOM} as stable C and C_{fPOM} as labile C to confirm our third hypothesis that C mineralization dynamics will be reflected in SOC fractions. Free POM is often regarded as labile C reflected in a higher microbial utilization potential, rapid turnover, and sensitivity to environmental changes while occluded POM and mineral-associated OM are considered to be more stable forms of SOC (Lützow et al., 2006; Wiesmeier et al., 2019; Rocci et al., 2021). We expected that a higher degree of SOC protection in mineral-association and aggregate-occlusion would be reflected in a lower C mineralization and a larger slow C pool while a larger occurrence of free POM would lead to the opposite pattern. However, amounts of the fast C pool were unrelated to C_{fPOM}. Relative proportions of the fast C pool were positively correlated with relative concentrations of DOC (DOC/SOC), while no correlation was found with relative C_{fPOM} proportions. This suggests that the labile C pool may be more closely related to DOC than to free POM. Although free POM is often associated with the labile C pool, it can still contain a recalcitrant fraction. The degree of recalcitrance of free POM is influenced by factors such as its chemical composition and age (Lützow et al., 2006; Basile-Doelsch et al., 2020). For example, lignin-rich plant material was shown to decompose slower (Stagg et al., 2018), particularly under anaerobic conditions (Benner et al., 1984). Even though the selective preservation of SOC has been questioned for terrestrial soils (Lützow et al., 2006; Schmidt et al., 2011; Basile-Doelsch et al., 2020) it might play a role under the unique conditions in tidal wetlands. It has been shown that the quality of the local vegetation, including its lignin content, varied along estuarine gradients (Stagg et al., 2018; Schulte Ostermann et al., 2024; Study A). As estuarine marshes receive OM from various sources (allochthonouse and autochthonouse), it can be assumed that this OM is characterized by high heterogeneity with varying qualities (Abril et al., 2002; Spohn et al., 2013; Butzeck et al., 2015). Moreover, it was shown

that a high microbial availability of OM does not automatically indicate rapid mineralization into CO_2 but its incorporation into microbial biomass (Cotrufo et al., 2013). Although free POM did not seem to directly contribute to the fast C pool, relative proportions of this SOC fraction were associated with a shorter MRT of the fast C pool, indicating that free POM may have enhanced the turnover of the labile C pool. Additionally, DOC was also found to contribute to a decrease in MRT across all C pools.

In contrast, mineral-associated organic matter was found to decrease SOC turnover. Relative proportions of C_{MAOM} were positively correlated with amounts of C in the slow pool, while relative proportion of C_{fPOM} exhibited a negative effect. Moreover, the MRT of the overall and slow C pools were associated with increasing amounts of C_{MAOM} and C_{oPOM} in topsoil, suggesting that greater protection by mineral association and aggregate occlusion resulted in a prolonged MRT. Even though it is not straightforward to categorize the SOC fractions (MAOM, oPOM, fPOM) into the SOC pools (fast vs. slow), the fractions influenced the speed of SOC turnover in the marsh soils during oxic incubation.

C4.3 Microbial efficiency and substrate availability

Our observations suggest that reduced microbial efficiency enhanced C mineralization and C turnover in the marsh soil. The metabolic quotient (qCO_2) serves as an indicator for the efficiency of microbial communities to metabolize C, with lower values indicating more efficient resource usage (Anderson and Domsch, 1993).

We found that increasing qCO_2 increased C_{min}/SOC, and decreased the MRTs of the fast C pool (topsoil), slow C pool (topsoil), and overall C pool (both depths). This relationship aligns with the assumption that a reduced microbial efficiency results in a larger fraction of C being respired as CO_2 instead of being incorporated into microbial biomass (Kaiser, 1992). Microbial community dynamics and their C mineralization potential are strongly affected by soil salinity and moisture (Lozupone and Knight, 2007; Yarwood, 2018; Chen et al., 2022). In our study, microbial efficiency did not display a clear trend along the salinity gradient; however, a positive correlation between qCO_2 and EC in topsoils suggested that increased salinity may have adversely affected microbial efficiency along the estuary. In contrast to the salinity gradient, we observed a higher qCO_2 with increasing flooding levels, particularly in topsoils. This aligns with the concept that environmental disturbances or stress negatively impact soil microbial properties, including microbial efficiency (Pabst et al., 2016; Feng et al., 2021; Ashraf et al., 2022). The microbial community may have been

adversely affected by oxygen scarcity as the flooding frequency increased. A similar effect has been documented in floodplain soils of the Elbe, where soil samples from frequently flooded locations had a higher qCO_2 than from locations that are less often flooded (Rinklebe and Langer, 2006). Moreover, the lower qCO_2 values observed in soils from less flooded marsh locations may indicate advanced soil development, as a decline in qCO_2 is often associated with progressive ecosystem succession and improved microbial stability (Insam and Haselwandter, 1989; Anderson and Domsch, 1993). The more pronounced trend in qCO_2 in topsoils along the flooding gradient compared to subsoils may be attributed to the more direct effect of flooding on topsoils, while subsoils typically maintain consistently high water content due to the high water table.

Microbial efficiency was driven by microbial substrate availability. The ratio of microbial biomass to total SOC (MBC/SOC) serves as an indicator of microbial substrate availability (Anderson, 2003). Negative correlations between MBC/SOC and SOC, as well as between MBC/SOC and qCO_2 suggested that a proportion of SOC was not accessible to microbes, which, in turn, reduced microbial efficiency. This trend was also observed in other studies (Pabst et al., 2016; Iqbal et al., 2016). We found that substrate availability and microbial efficiency depends on the quantity of the fast C pool and the quality of free POM. An increase in the amount of C_{fPOM} was associated with reduced substrate availability, particularly in the freshwater low marsh. This marsh location is characterized by relatively recalcitrant aboveground vegetation (high lignin content, cellulose content, lignin:N ratio, C:N ratio) which might have reduced the microbial usability of the incoming OM. In contrast, relative proportions of C_{fPOM} increased substrate availability, predominantly in topsoils. Moreover, the C:N ratio of free POM showed a positive correlation with qCO_2. These observations support our previous findings that free POM can enhance C mineralization by providing available substrates for microbes but can also contain recalcitrant fractions protecting the OM from microbial decomposition. We found that relative proportions of C_{oPOM} increased microbial efficiency and substrate availability while C_{MAOM} proportions decreased microbial substrate availability. This suggested that aggregates may have provided less protection for OM compared OM in mineral association. Particularly under the oxic incubation conditions, aggregates might have been less stable as they could not reduce microbial substrate availability, microbial efficiency, nor the amount of mineralized C. Similar to free POM, though to a lesser degree, the C:N ratio of occluded POM was positively linked to qCO_2, implying that microbial efficiency was influenced by the quality of both free and occluded POM. Conversely, the negative correlation between C_{MAOM} proportions and substrate availability

(MBC/SOC) underlined our observation that mineral association is a critical mechanism protecting SOC from microbial decomposition.

C5 Conclusion

Our study demonstrates the large spatial heterogeneity in OM decomposability in estuarine marshes and provided insight into underlying drivers of SOC turnover. Our hypothesis that increasing salinity would enhance SOC mineralization was partially supported, as we observed an increase in the proportion of mineralized C in relation to total SOC from freshwater to salt marshes. Increasing salinity may have enhanced the mineralization of an increasingly labile SOC pool along the salinity gradient. The increasing SOC mineralizability was associated to less protection of SOC in mineral associations. The enhanced SOC degradability, together with a reduced OM input, lowered SOC storage with increasing salinity along the Elbe Estuary. Contrary to our second hypothesis, we found no clear effect of the flooding gradient on the enrichment of labile C or increased SOC mineralizability. However, the shorter mean residence time of SOC along the flooding gradient indicated that frequent inundation may have suppressed SOC turnover under field conditions and led to the accumulation of SOC with higher degradability.

Against our assumption, the SOC mineralization was not clearly reflected in SOC density fractions. Nonetheless, our findings revealed that the SOC fractions influenced SOC turnover and microbial substrate availability. Free POM increased the SOC degradability by reducing the mean residence time of SOC and by acting as substrate for microbial utilization. Our findings indicate that aggregation provided intermediate protection for OM. Aggregate-occluded OM could contribute to a longer mean residence time but did not reduce the amount of mineralized C nor microbial substrate availability. In contrast, mineral-association decreased SOC degradability reflected in higher amounts of stable C, longer SOC turnover, and reduced microbial efficiency.

With respect to climate change, salt water intrusion, a shift of increased salinity further upstream, and altered sedimentation pattern within estuaries have the potential to increase SOC degradability, potentially enhancing C output and reducing the capacity of estuarine marshes to function as a C sink.

Authors' contributions

Friederike Neiske: Conceptualization, Methodology, Formal Analysis, Investigation, Project administration, Visualization, Writing - original draft. **Christian Beer**: Formal Analysis. **Daniel Schwarze**: Investigation, Writing - review & editing. **Maria Seedtke**: Investigation, Writing - review & editing. **Annette Eschenbach**: Conceptualization, Methodology, Funding acquisition, Resources, Supervision, Writing - review & editing. **Joscha N. Becker**: Conceptualization, Formal Analysis, Methodology, Project administration, Supervision, Writing – review & editing.

Acknowledgement

This study was funded by the *Deutsche Forschungsgemeinschaft* (DFG, German Research Foundation) within the Research Training Group 2530: "Biota-mediated effects on Carbon cycling in Estuaries" (project number 407270017; contribution to *Universität Hamburg* and *Leibniz-Institut für Gewässerökologie und Binnenfischerei im Forschungsverbund Berlin e.V.*). We thank Volker Kleinschmidt, Deborah Harms, Sumita Rui, Annika Naumann, Julian Mittmann-Goetsch, Fay Lexmond and all involved student assistants for their help during field and lab work, as well as technical support. We further thank all persons involved in the planning, establishment and maintenance of the RTG 2530 marsh research facilities.

C6 References

Abril, G., Nogueira, M., Etcheber, H., Cabeçadas, G., Lemaire, E., Brogueira, M., 2002. Behaviour of Organic Carbon in Nine Contrasting European Estuaries. Estuarine, coastal and shelf science 54, 241–262.

Anderson, T.-H., 2003. Microbial eco-physiological indicators to assess soil quality. Agriculture, Ecosystems & Environment 98, 285–293.

Anderson, T.-H., Domsch, a.K.H., 1993. The metabolic quotient for CO2 (q CO2) as a specific activity parameter to assess the effects of environmental conditions, such as pH, on the microbial biomass of forest soils.

Andrén, O., Kätterer, T., 1997. ICBM: The Intoductory Carbon Balance Model For Exploration Of Soil Carbon Balances. Ecological Applications 7, 1226–1236.

Ashraf, M.N., Waqas, M.A., Rahman, S., 2022. Microbial Metabolic Quotient is a Dynamic Indicator of Soil Health: Trends, Implications and Perspectives (Review). Eurasian Soil Science 55, 1794–1803.

Basile-Doelsch, I., Balesdent, J., Pellerin, S., 2020. Reviews and syntheses: The mechanisms underlying carbon storage in soil. Biogeosciences 17, 5223–5242.

Beer, C., Knoblauch, C., Hoyt, A.M., Hugelius, G., Palmtag, J., Mueller, C.W., Trumbore, S., 2022. Vertical pattern of organic matter decomposability in cryoturbated permafrost-affected soils. Environmental Research Letters 17, 104023.

Benner, R., Maccubbin, A.E., Hodson, R.E., 1984. Anaerobic biodegradation of the lignin and polysaccharide components of lignocellulose and synthetic lignin by sediment microflora. Applied and environmental microbiology 47, 998–1004.

Blagodatskaya, E.V., Blagodatsky, S.A., Anderson, T.-H., Kuzyakov, Y., 2009. Contrasting effects of glucose, living roots and maize straw on microbial growth kinetics and substrate availability in soil. European Journal of Soil Science 60, 186–197.

Branoff, B.B., Grüterich, L., Wilson, M., Tobias-Hunefeldt, S.P., Saadaoui, Y., Mittmann-Goetsch, J., Neiske, F., Lexmond, F., Becker, J.N., Grossart, H.-P., Porada, P., Streit, W.R., Eschenbach, A., Kutzbach, L., Jensen, K., 2024, preprint. Partitioning biota along the Elbe River estuary: where are the community transitions?

Butzeck, C., Eschenbach, A., Gröngröft, A., Hansen, K., Nolte, S., Jensen, K., 2015. Sediment Deposition and Accretion Rates in Tidal Marshes Are Highly Variable Along Estuarine Salinity and Flooding Gradients. Estuaries and Coasts 38, 434–450.

Castenson, K.L., Rabenhorst, M.C., 2006. Indicator of reduction in soil (IRIS) evaluation of a new approach for assessing reduced conditions in soil. Soil Science Society of America Journal 70, 1222–1226.

Cerli, C., Celi, L., Kalbitz, K., Guggenberger, G., Kaiser, K., 2012. Separation of light and heavy organic matter fractions in soil — Testing for proper density cut-off and dispersion level. Geoderma 170, 403–416.

Chambers, L.G., Osborne, T.Z., Reddy, K.R., 2013. Effect of salinity-altering pulsing events on soil organic carbon loss along an intertidal wetland gradient: a laboratory experiment. Biogeochemistry 115, 363–383.

Chen, H., Ma, K., Huang, Y., Fu, Q., Qiu, Y., Yao, Z., 2022. Significant response of microbial community to increased salinity across wetland ecosystems. Geoderma 415, 115778.

Chmura, G.L., Anisfeld, S.C., Cahoon, D.R., Lynch, J.C., 2003. Global carbon sequestration in tidal, saline wetland soils. Global Biogeochemical Cycles 17.

Cotrufo, M.F., Wallenstein, M.D., Boot, C.M., Denef, K., Paul, E., 2013. The Microbial Efficiency-Matrix Stabilization (MEMS) framework integrates plant litter decomposition with soil organic matter stabilization: do labile plant inputs form stable soil organic matter? Global Change Biology 19, 988–995.

Craft, C., 2007. Freshwater input structures soil properties, vertical accretion, and nutrient accumulation of Georgia and U.S tidal marshes. Limnology and Oceanography 52, 1220–1230.

DWD, 2024. Time series and trends for the parameters temperature and precipitation. Reference period: 1991 - 2020. Federal State of Schleswig-Holstein. https://www.dwd.de/EN/ourservices/zeitreihen/zeitreihen.html#buehneTop, last accessed 20 Feb 2024.

EEA, 2017. EEA coastline for analysis (raw) - version 3.0. https://www.eea.europa.eu/data-and-maps/data/eea-coastline-for-analysis-2/gis-data/eea-coastline-polygon, last accessed 27 Feb 2024.

Egamberdieva, D., Renella, G., Wirth, S., Islam, R., 2010. Secondary salinity effects on soil microbial biomass. Biology and Fertility of Soils 46, 445–449.

Engels, J.G., Jensen, K., 2009. Patterns of wetland plant diversity along estuarine stress gradients of the Elbe (Germany) and Connecticut (USA) Rivers. Plant Ecology & Diversity 2, 301–311.

Fang, C., Smith, P., Moncrieff, J.B., Smith, J.U., 2005. Similar response of labile and resistant soil organic matter pools to changes in temperature. Nature 433, 57–59.

Feng, J., Zeng, X.-M., Zhang, Q., Zhou, X.-Q., Liu, Y.-R., Huang, Q., 2021. Soil microbial trait-based strategies drive metabolic efficiency along an altitude gradient. ISME communications 1, 71.

Golchin, A., Oades, J.M., Skjemstad, J.O., Clarke, P., 1994. Study of free and occluded particulate organic matter in soils by solid state 13C Cp/MAS NMR spectroscopy and scanning electron microscopy. Soil Research 32, 285.

Graves, S., Piepho, H.-P., Selzer, M.L., 2015. Package 'multcompView'. Visualizations of paired comparisons.

Halbritter, A.H., Boeck, H.J. de, Eycott, A.E., Reinsch, S., Robinson, D.A., Vicca, S., Berauer, B., Christiansen, C.T., Estiarte, M., Grünzweig, J.M., Gya, R., Hansen, K., Jentsch, A., Lee, H., Linder, S., Marshall, J., Peñuelas, J., Kappel Schmidt, I., Stuart-Haëntjens, E., Wilfahrt, P., Vandvik, V., 2020. The handbook for standardized field and laboratory measurements in terrestrial climate change experiments and observational studies (ClimEx). Methods in Ecology and Evolution 11, 22–37.

Hothorn, T., Bretz, F., Westfall, P., Heiberger, R.M., Schuetzenmeister, A., Scheibe, S., Hothorn, M.T., 2016. Package 'multcomp'. Simultaneous inference in general parametric models. Project for Statistical Computing, Vienna, Austria.

Hulthe, G., Hulth, S., Hall, P.O., 1998. Effect of oxygen on degradation rate of refractory and labile organic matter in continental margin sediments. Geochimica et Cosmochimica Acta 62, 1319–1328.

Insam, H., Haselwandter, K., 1989. Metabolic quotient of the soil microflora in relation to plant succession. Oecologia 79, 174–178.

Iqbal, M.T., Joergensen, R.G., Knoblauch, C., Lucassen, R., Singh, Y., Watson, C., Wichern, F., 2016. Rice straw addition does not substantially alter microbial properties under hypersaline soil conditions. Biology and Fertility of Soils 52, 867–877.

Jiang, Z., Lu, Y., Xu, J., Li, M., Shan, G., Li, Q., 2019. Exploring the characteristics of dissolved organic matter and succession of bacterial community during composting. Bioresource technology 292, 121942.

Joergensen, R.G., Mueller, T., 1996. The fumigation-extraction method to estimate soil microbial biomass: Calibration of the kEN value. Soil Biology and Biochemistry 28, 33–37.

Kappenberg, J., Grabemann, I., 2001. Variability of the mixing zones and estuarine turbidity maxima in the Elbe and Weser estuaries. Estuaries 24, 699–706.

Kelleway, J.J., Saintilan, N., Macreadie, P.I., Ralph, P.J., 2016. Sedimentary Factors are Key Predictors of Carbon Storage in SE Australian Saltmarshes. Ecosystems 19, 865–880.

Kerner, M., 2007. Effects of deepening the Elbe Estuary on sediment regime and water quality. Estuarine, coastal and shelf science 75, 492–500.

Knoblauch, C., Beer, C., Sosnin, A., Wagner, D., Pfeiffer, E.-M., 2013. Predicting long-term carbon mineralization and trace gas production from thawing permafrost of Northeast Siberia. Global Change Biology 19, 1160–1172.

Kristensen, E., Ahmed, S.I., Devol, A.H., 1995. Aerobic and anaerobic decomposition of organic matter in marine sediment: Which is fastest? Limnology and Oceanography 40, 1430–1437.

Lozupone, C.A., Knight, R., 2007. Global patterns in bacterial diversity. Proceedings of the National Academy of Sciences of the United States of America 104, 11436–11440.

Luo, M., Huang, J.-F., Zhu, W.-F., Tong, C., 2019. Impacts of increasing salinity and inundation on rates and pathways of organic carbon mineralization in tidal wetlands: a review. Hydrobiologia 827, 31–49.

Lützow, M.v., Kögel-Knabner, I., Ekschmitt, K., Matzner, E., Guggenberger, G., Marschner, B., Flessa, H., 2006. Stabilization of organic matter in temperate soils: mechanisms and their relevance under different soil conditions – a review. European Journal of Soil Science 57, 426–445.

Lützow, M. von, Kögel-Knabner, I., Ekschmitt, K., Flessa, H., Guggenberger, G., Matzner, E., Marschner, B., 2007. SOM fractionation methods: Relevance to functional pools and to stabilization mechanisms. Soil Biology and Biochemistry 39, 2183–2207.

Lützow, M. von, Kögel-Knabner, I., Ludwig, B., Matzner, E., Flessa, H., Ekschmitt, K., Guggenberger, G., Marschner, B., Kalbitz, K., 2008. Stabilization mechanisms of organic matter in four temperate soils: Development and application of a conceptual model. Journal of Plant Nutrition and Soil Science 171, 111–124.

Mazarrasa, I., Neto, J.M., Bouma, T.J., Grandjean, T., Garcia-Orellana, J., Masqué, P., Recio, M., Serrano, Ó., Puente, A., Juanes, J.A., 2023. Drivers of variability in Blue Carbon stocks and burial rates across European estuarine habitats. The Science of the total environment 886, 163957.

Mcleod, E., Chmura, G.L., Bouillon, S., Salm, R., Björk, M., Duarte, C.M., Lovelock, C.E., Schlesinger, W.H., Silliman, B.R., 2011. A blueprint for blue carbon: toward an improved understanding of the role of vegetated coastal habitats in sequestering CO 2. Frontiers in Ecology and the Environment 9, 552–560.

Middelburg, J.J., Klaver, G., Nieuwenhuize, J., Wielemaker, A., Haas, W. de, Vlug, T., van der Nat, J., 1996. Organic matter mineralization in intertidal sediments along an estuarine gradient. Marine Ecology Progress Series 132, 157–168.

Minick, K.J., Mitra, B., Noormets, A., King, J.S., 2019. Saltwater reduces potential CO_2 and CH_4 production in peat soils from a coastal freshwater forested wetland. Biogeosciences 16, 4671–4686.

Mittmann-Goetsch, J., Wilson, M., Jensen, K., Mueller, P., 2024. Root-driven soil reduction in Wadden Sea salt marshes. Wetlands 44. https://doi.org/10.1007/s13157-024-01867-8.

Morrissey, E.M., Gillespie, J.L., Morina, J.C., Franklin, R.B., 2014. Salinity affects microbial activity and soil organic matter content in tidal wetlands. Global Change Biology 20, 1351–1362.

Mueller, P., Granse, D., Nolte, S., Weingartner, M., Hoth, S., Jensen, K., 2020. Unrecognized controls on microbial functioning in Blue Carbon ecosystems: The role

of mineral enzyme stabilization and allochthonous substrate supply. Ecology and evolution 10, 998–1011.

Pabst, H., Gerschlauer, F., Kiese, R., Kuzyakov, Y., 2016. Land Use and Precipitation Affect Organic and Microbial Carbon Stocks and the Specific Metabolic Quotient in Soils of Eleven Ecosystems of Mt. Kilimanjaro, Tanzania. Land Degradation & Development 27, 592–602.

Pabst, H., Kühnel, A., Kuzyakov, Y., 2013. Effect of land-use and elevation on microbial biomass and water extractable carbon in soils of Mt. Kilimanjaro ecosystems. Applied Soil Ecology 67, 10–19.

R Core Team, 2022. R. A language and environment for statistical computing. R Foundation for Statistical Computing, Vienna, Austria.

Rabenhorst, M.C., 2008. Protocol for using and interpreting IRIS tubes. Soil Survey Horizons 49, 74–77.

Rinklebe, J., Langer, U., 2006. Microbial diversity in three floodplain soils at the Elbe River (Germany). Soil Biology and Biochemistry 38, 2144–2151.

Rocci, K.S., Lavallee, J.M., Stewart, C.E., Cotrufo, M.F., 2021. Soil organic carbon response to global environmental change depends on its distribution between mineral-associated and particulate organic matter: A meta-analysis. The Science of the total environment 793, 148569.

Schmidt, M.W.I., Torn, M.S., Abiven, S., Dittmar, T., Guggenberger, G., Janssens, I.A., Kleber, M., Kögel-Knabner, I., Lehmann, J., Manning, D.A.C., Nannipieri, P., Rasse, D.P., Weiner, S., Trumbore, S.E., 2011. Persistence of soil organic matter as an ecosystem property. Nature 478, 49–56.

Schulte Ostermann, T., Heuner, M., Fuchs, E., Temmerman, S., Schoutens, K., Bouma, T.J., Minden, V., 2024. Identifying Key Plant Traits and Ecosystem Properties Affecting Wave Attenuation and the Soil Organic Carbon Content in Tidal Marshes. Estuaries and Coasts 47, 144–161.

Schwendenmann, L., Pendall, E., 2008. Response of soil organic matter dynamics to conversion from tropical forest to grassland as determined by long-term incubation. Biology and Fertility of Soils 44.

Setia, R., Marschner, P., Baldock, J., Chittleborough, D., Smith, P., Smith, J., 2011. Salinity effects on carbon mineralization in soils of varying texture. Soil Biology and Biochemistry 43, 1908–1916.

Smith, J.L., Paul, E.A., 2017. The significance of soil microbial biomass estimations, in: Soil biochemistry. Routledge, pp. 357–398.

Sollins, P., Homann, P., Caldwell, B.A., 1996. Stabilization and destabilization of soil organic matter: mechanisms and controls. Geoderma 74, 65–105.

Spohn, M., Babka, B., Giani, L., 2013. Changes in soil organic matter quality during sea-influenced marsh soil development at the North Sea coast. CATENA 107, 110–117.

Spohn, M., Giani, L., 2012. Carbohydrates, carbon and nitrogen in soils of a marine and a brackish marsh as influenced by inundation frequency. Estuarine, coastal and shelf science 107, 89–96.

Stagg, C.L., Baustian, M.M., Perry, C.L., Carruthers, T.J.B., Hall, C.T., 2018. Direct and indirect controls on organic matter decomposition in four coastal wetland communities along a landscape salinity gradient. Journal of Ecology 106, 655–670.

van de Broek, M., Temmerman, S., Merckx, R., Govers, G., 2016. Controls on soil organic carbon stocks in tidal marshes along an estuarine salinity gradient. Biogeosciences 13, 6611–6624.

van de Broek, M., Vandendriessche, C., Poppelmonde, D., Merckx, R., Temmerman, S., Govers, G., 2018. Long-term organic carbon sequestration in tidal marsh sediments is dominated by old-aged allochthonous inputs in a macrotidal estuary. Global Change Biology 24, 2498–2512.

Vance, E.D., Brookes, P.C., Jenkinson, D.S., 1987. An extraction method for measuring soil microbial biomass C. Soil Biology and Biochemistry 19, 703–707.

Viret, F., Grand, S., 2019. Combined Size and Density Fractionation of Soils for Investigations of Organo-Mineral Interactions. Journal of visualized experiments: JoVE.

Wagai, R., Mayer, L.M., Kitayama, K., 2009. Nature of the "occluded" low-density fraction in soil organic matter studies: A critical review. Soil Science and Plant Nutrition 55, 13–25.

Wang, F., Kroeger, K.D., Gonneea, M.E., Pohlman, J.W., Tang, J., 2019. Water salinity and inundation control soil carbon decomposition during salt marsh restoration: An incubation experiment. Ecology and evolution 9, 1911–1921.

Werth, M., Kuzyakov, Y., 2010. 13C fractionation at the root–microorganisms–soil interface: A review and outlook for partitioning studies. Soil Biology and Biochemistry 42, 1372–1384.

Weston, N.B., Vile, M.A., Neubauer, S.C., Velinsky, D.J., 2011. Accelerated microbial organic matter mineralization following salt-water intrusion into tidal freshwater marsh soils. Biogeochemistry 102, 135–151.

Wickham, H., Chang, W., Wickham, M.H., 2016. Package 'ggplot2'. Create elegant data visualisations using the grammar of graphics. Version 2, 1–189.

Więski, K., Guo, H., Craft, C.B., Pennings, S.C., 2010. Ecosystem Functions of Tidal Fresh, Brackish, and Salt Marshes on the Georgia Coast. Estuaries and Coasts 33, 161–169.

Wiesmeier, M., Urbanski, L., Hobley, E., Lang, B., Lützow, M. von, Marin-Spiotta, E., van Wesemael, B., Rabot, E., Ließ, M., Garcia-Franco, N., Wollschläger, U., Vogel, H.-J., Kögel-Knabner, I., 2019. Soil organic carbon storage as a key function of soils - A review of drivers and indicators at various scales. Geoderma 333, 149–162.

WSV, 2011. MThw-Linie an der Unter- und Außenelbe. www.kuestendaten.de, last accessed 29 Sep 2023.

WSV, 2017. Vegetationskartierung / Biotoptypenkartierung 2017 Unterelbe. www.kuestendaten.de, last accessed 29 Sep 2023.

Yang, W., Qiao, Y., Li, N., Zhao, H., Yang, R., Leng, X., Cheng, X., An, S., 2017. Seawall construction alters soil carbon and nitrogen dynamics and soil microbial biomass in an invasive Spartina alterniflora salt marsh in eastern China. Applied Soil Ecology 110, 1–11.

Yarwood, S.A., 2018. The role of wetland microorganisms in plant-litter decomposition and soil organic matter formation: a critical review. FEMS microbiology ecology 94.

C7 Supplementary Material

Incubation

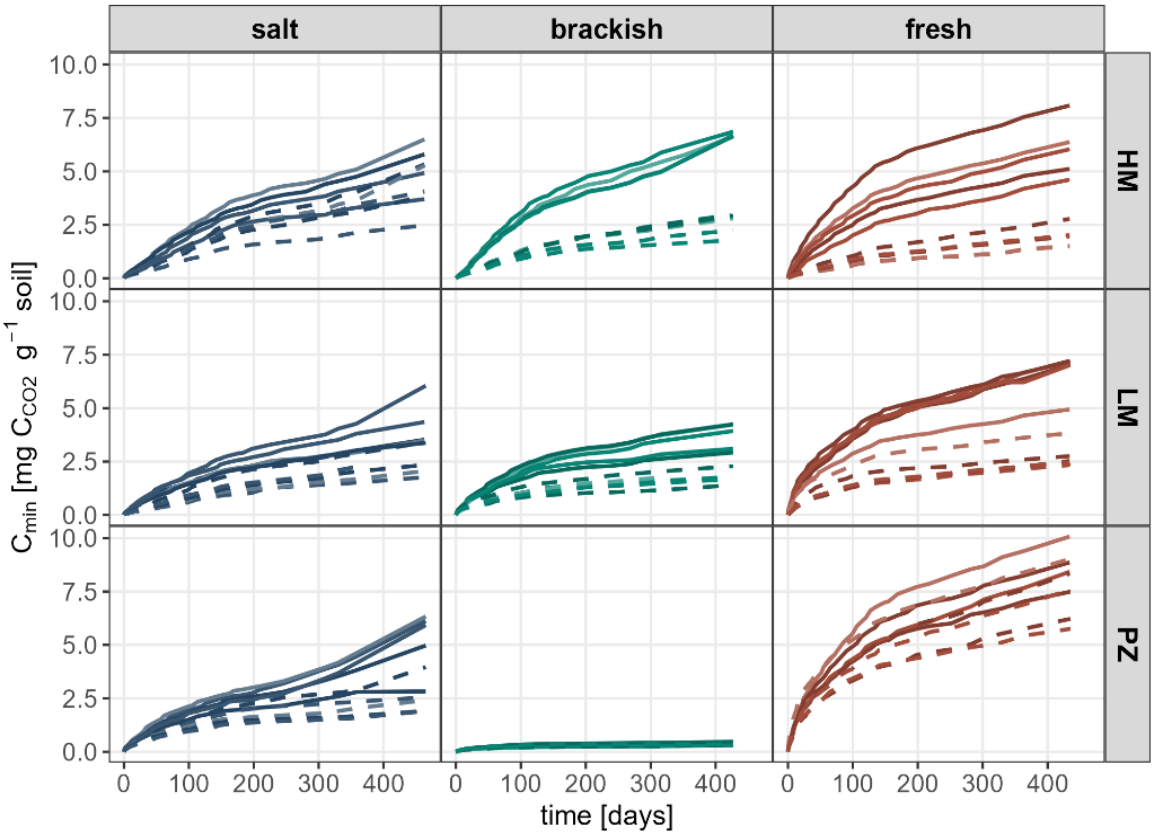

Figure S1: Cumulative mineralized C (C_{min}) [mg C_{CO2} g^{-1} soil] over the incubation period along the salinity (salt marsh, brackish marsh, freshwater marsh) and flooding gradient (HM = high marsh, LM = low marsh, PZ = pioneer zone) of the Elbe Estuary.

Effect of depth

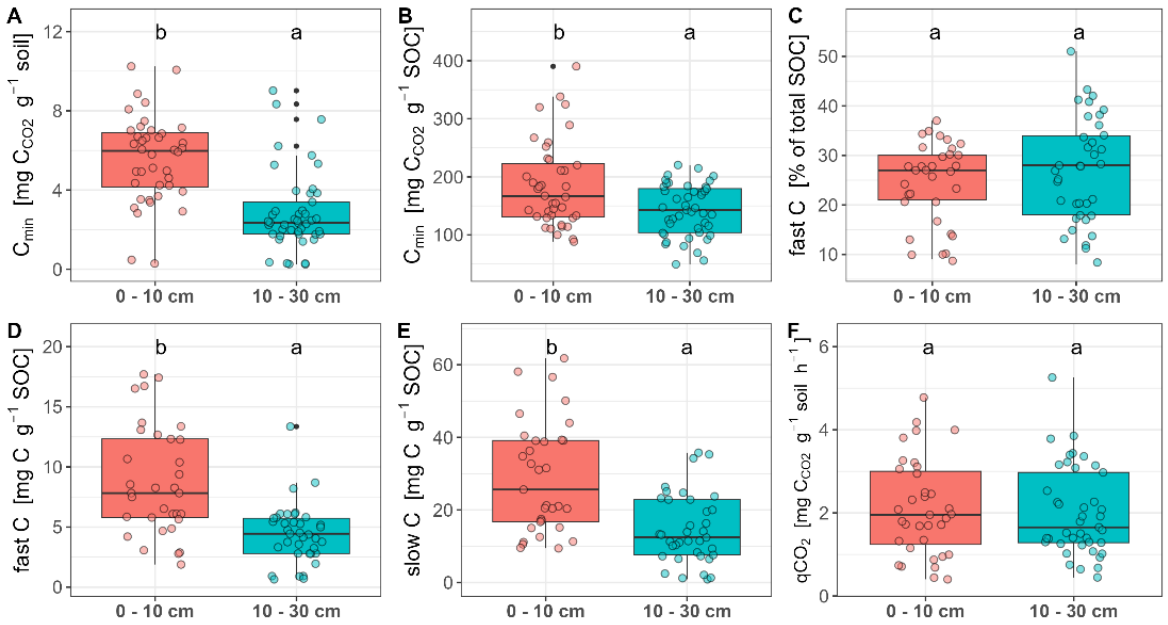

Figure S2: Effect of depth on (A) absolute amount of cumulative mineralized C_{min} [mg C_{CO2} g^{-1} soil] (B) relative proportion of cumulative mineralized C_{min}/SOC [mg C_{CO2} g^{-1} SOC] (C) relative proportion of fast C [%of toal SOC] (D) amount of fast C [mg C g^{-1} soil] (E) amount of slow C [mg C g^{-1} soil] and qCO_2 [mg C_{CO2} g^{-1} MBC h^{-1}]. Lowercase letters indicate significant differences ($p < 0.05$) derived from linear mixed-effects model (LME) for paired comparison, with depth as the main factor and sampling location as a random factor.

SOC pools (proportion)

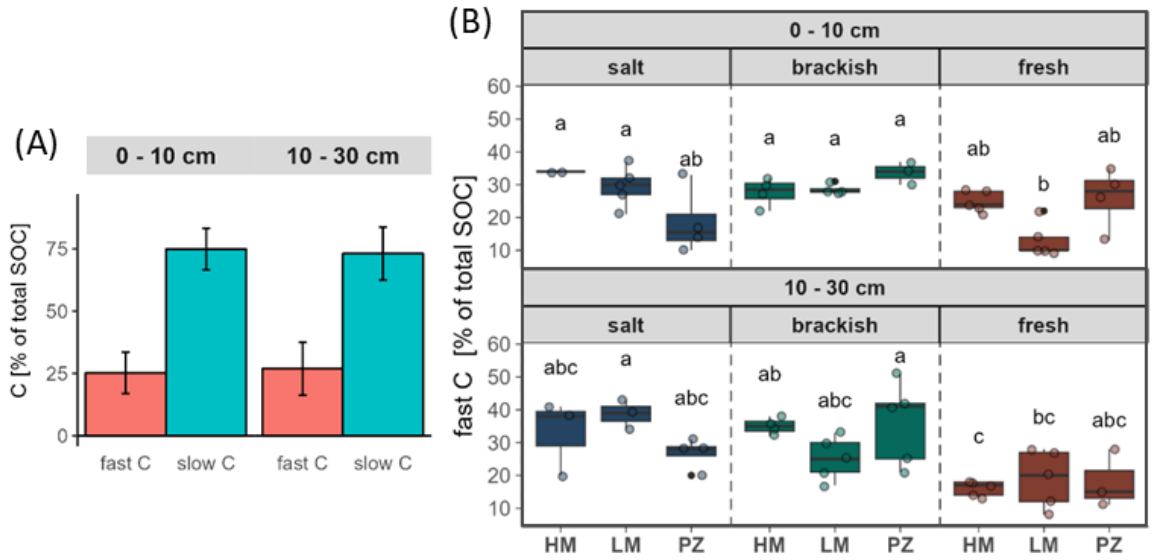

Figure S3: Proportions of fast C and slow C relative to total SOC (A) in topsoil (0 - 10 cm) and subsoil (10 - 30 cm); (B) in topsoil (0 - 10 cm) and subsoil (10 - 30 cm) along the salinity (salt marsh, brackish marsh, freshwater marsh) and flooding gradient (HM = high marsh, LM = low marsh, PZ = pioneer zone) of the Elbe Estuary. Lowercase letters in (B) indicate significant differences ($p < 0.05$) derived from ANOVA with TukeyHSD post-hoc comparison applied on each depth separately.

Dissolved organic carbon

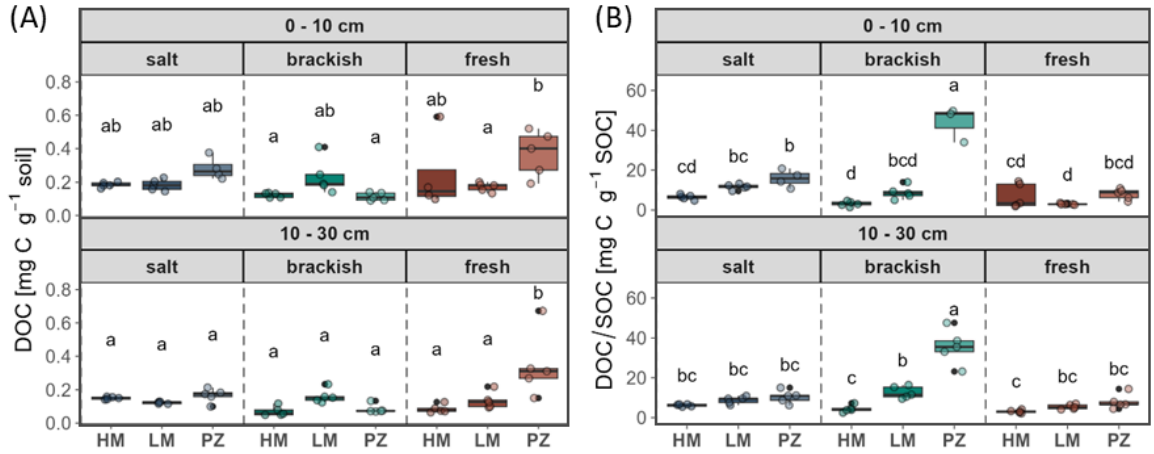

Figure S4: (A) Dissolved organic carbon (DOC) [mg C g^{-1} soil] (B) and DOC in relation to total SOC (DOC/SOC) [mg C g^{--1} SOC] in topsoil (0 - 10 cm) and subsoil (10 - 30 cm) along the salinity (salt marsh, brackish marsh, freshwater marsh) and flooding gradient (HM = high marsh, LM = low marsh, PZ = pioneer zone) of the Elbe Estuary. Lowercase letters indicate significant differences ($p < 0.05$) derived from ANOVA with TukeyHSD post-hoc comparison applied on each depth separately.

Correlation matrices

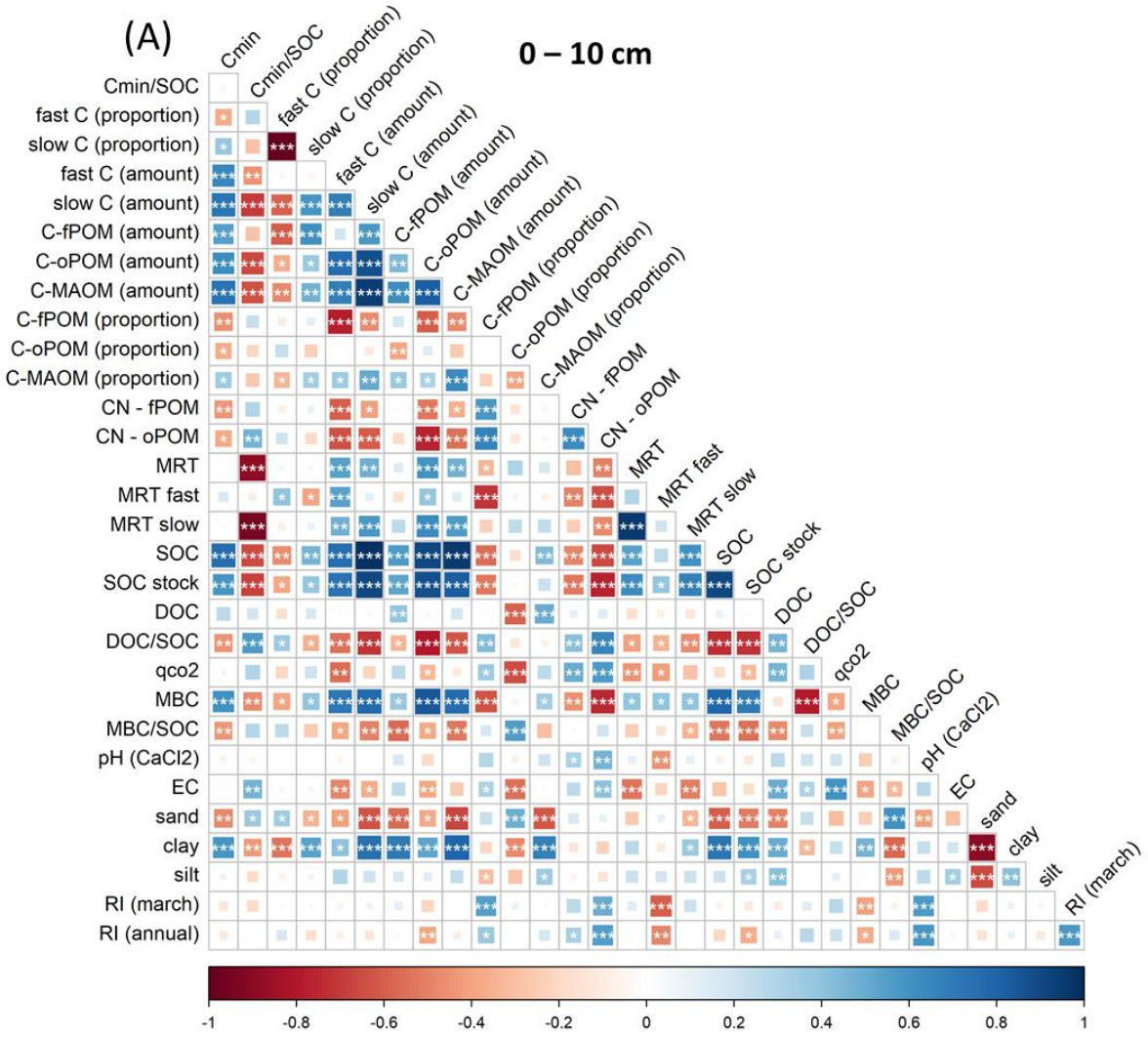

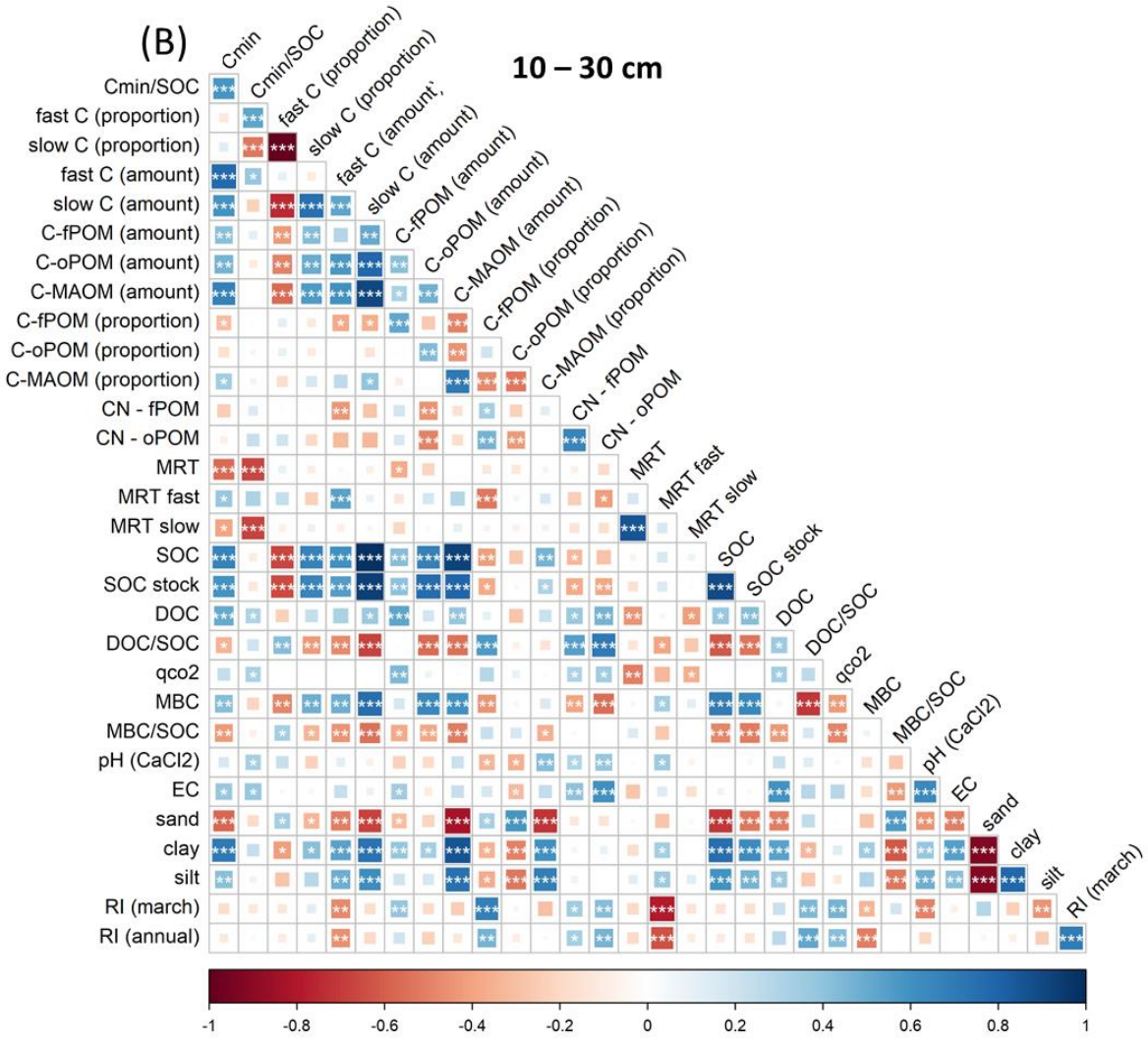

Figure S5: Spearman correlation matrices for (A) topsoil (0 - 10 cm) and (B) subsoil (10 - 30 cm) (n = 45). Asterisk indicate significant correlation at * $p < 0.05$, ** $p < 0.005$, and *** $p < 0.001$.

Plant species

Table S1: Plant species with area coverage [%] and Ellenberg Indicator Values for salinity (EIV-S) along the salinity and flooding gradient of the Elbe Estuary in August 2022.

Salt High Marsh	[%]	**Brackish High Marsh**	[%]	**Fresh High Marsh**	[%]
Agrostis stolonifera	<0.1	*Agrostis stolonifera*	0.1	*Agrostis stolonifera*	0.8
Aster tripolium	13.4	*Berula erecta*	0.3	*Calystegia sepium*	7.2
Atriplex littoralis	0.2	*Calystegia sepium*	28.3	*Equisetum palustre*	0.1
Atriplex prostrata	15.8	*Dactylis glomerata*	<0.1	*Phalaris arundinacea*	7.6
Elymus athericus	62.3	*Epilobium hirsutum*	24.1	*Phragmites australis*	54.0
Salicornia europaea	<0.1	*Galeopsis sp.*	<0.1	*Urtica dioica*	21.1
Suaeda maritima	0.5	*Galium palustre*	0.2	*Valeriana officinalis*	0.6
		Phalaris arundinacea	4.9		
		Phragmites australis	10.9		
		Poa trivalis	0.2		
		Rosa sp.	2.3		
		Urtica dioica	6.7		
		Valeriana officinalis	<0.1		
		Vicia cracca	0.3		
EIV-S: 5.4		EIV-S: 0.3		EIV-S: 0.0	
Salt Low Marsh	[%]	**Brackish Low Marsh**	[%]	**Fresh Low Marsh**	[%]
Agrostis stolonifera	0.2	*Agrostis stolonifera*	0.2	*Bidens sp.*	0.1
Aster tripolium	18.2	*Berula erecta*	6.9	*Caltha palustris*	0.1
Atriplex littoralis	<0.1	*Caltha palustris*	0.3	*Myosotis palustris*	0.1
Atriplex prostrata	5.6	*Calystegia sepium*	9.5	*Nasturtium officinale*	0.1
Elymus athericus	<0.1	*Lycopus europaeus*	0.9	*Phragmites australis*	92.6
Festuca rubra	8.3	*Phragmites australis*	73.0		
Halimione portulacoides	1.4				
Plantago maritima	<0.1				
Puccinellia maritima	40.8				
Salicornia europaea	1.7				
Spartina anglica	2.3				
Spergularia media	0.1				
Suaeda maritima	3.4				
Triglochin maritima	13.2				
EIV-S: 7.0		EIV-S: 0.1		EIV-S: 0.0	
Salt Pioneer Zone	[%]	**Brackish Pioneer Zone**	[%]	**Fresh Pioneer Zone**	[%]
Aster tripolium	3.2	*Bolboschoenus maritimus*	73.5	*Alisma plantago-aquatica*	1.8
Atriplex prostrata	2.0	*Nasturtium officinale*	0.2	*Caltha palustris*	16.0
Halimione portulacoides	0.01			*Mentha aquatica*	0.1
Puccinellia maritima	4.1			*Myosotis palustris*	0.1
Salicornia europaea	<0.1			*Typha angustifolia*	46.0
Spartina anglica	59.1				
Suaeda maritima	2.6				
Triglochin maritima	0.8				
EIV-S: 7.8		EIV-S: 2.0		EIV-S: 0.7	

Appendix

Study:

Characterization of soils and soil redox conditions along environmental gradients in the Elbe Estuary

Extended abstract (manuscript in preparation)

Fay N. Lexmond*[a], **Friederike Neiske***[a], Joscha N. Becker[a], Birgit Grabellus[a], David Holl[a], Kai Jensen[b], Volker Kleinschmidt[a], Lars Kutzbach[a], Julian Mittmann-Götsch[b], Peter Mueller[c], Annette Eschenbach[a]

*equal contribution

[a] Institute of Soil Science, Universität Hamburg, Allende-Platz 2, 20146 Hamburg, Germany

[b] Institute of Plant Science and Microbiology, Universität Hamburg, Ohnhorststrasse 18, 22609 Hamburg, Germany

[c] Institute of Landscape Ecology, Münster University, Heisenbergstraße 2, 48149 Münster, Germany

1 Introduction

Soil redox conditions play a crucial role in controlling a wide range of processes associated with carbon (C) cycling within ecosystems. Specifically, redox conditions influence the transformation of organic matter (OM) by affecting microbial activity (Fiedler et al., 2007; Keiluweit et al., 2017). Microbial activity is thereby driven by oxygen availability. Increasing soil water content reduces the gas diffusion into the soil, which can result in a depletion of oxygen in soil. Under these conditions, some microorganisms are capable of utilizing alternative electron acceptors like nitrate and sulfate, but this reduces the energy yield for the microorganisms (Fiedler et al., 2007). Short-term variations in factors such as precipitation, water table, temperature, and OM availability can strongly influence the redox potential (Thomas et al., 2009). In estuaries, the dynamic interplay between river water and seawater inputs, tidal inundation add additional variations in redox conditions (Patrick and Henderson, 1981; Thomas et al., 2009; Dorau and Mansfeldt, 2016). As a result, redox potential can vary strongly over time (e.g., minutes, hours, or days) and within small spatial scales (Fiedler et al., 2007). These fluctuations create a highly variable environment for microbial communities, impacting their metabolism and, consequently, the overall C cycling within estuaries. Thus, our objective was to assess spatio-temporal variations in redox dynamics in marsh soils of the Elbe Estuary.

2 Material and Methods

We characterized soil redox conditions in the marsh soil of the Elbe Estuary by the Indicator of Reduction in Soils (IRIS) technique, adapted from (Castenson and Rabenhorst, 2006; Rabenhorst, 2008; Mittmann-Goetsch et al., 2024). For this, PVC sticks (5 x 70 cm) were coated with orange $FeCl_3$-paint and installed in soil (0 - 60 cm depth) along the salinity gradient (salt marsh, brackish marsh, and freshwater marsh) and flooding gradient (pioneer zones = daily flooding, low marshes = monthly flooding, and high marsh = yearly flooding) of the estuary. Sticks were retrieved after four weeks and a reduction index (RI) (0 - 1) was calculated based on the area of removed paint. Field incubation of IRIS sticks was conducted over the course of almost one year (11 x 4 weeks from June 2022 until April 2023). Full paint removal (RI = 1) indicates more deducing conditions over the four-week period, while an RI of 0 indicates oxic condition (for detailed description see Study B). The salt marsh was additionally equipped with redox sensors (SWAP instruments B.V., Netherlands), which continuously measured the soil redox potential (Eh, mV). Moreover, reference soil profiles were characterized at each marsh location according to the World

Reference Base for Soil Resources (WRB) (IUSS Working Group WRB, 2022), with a focus on redoximorphic features. Soil samples were taken from each soil profile to characterize physico-chemical soil properties.

3 Initial results

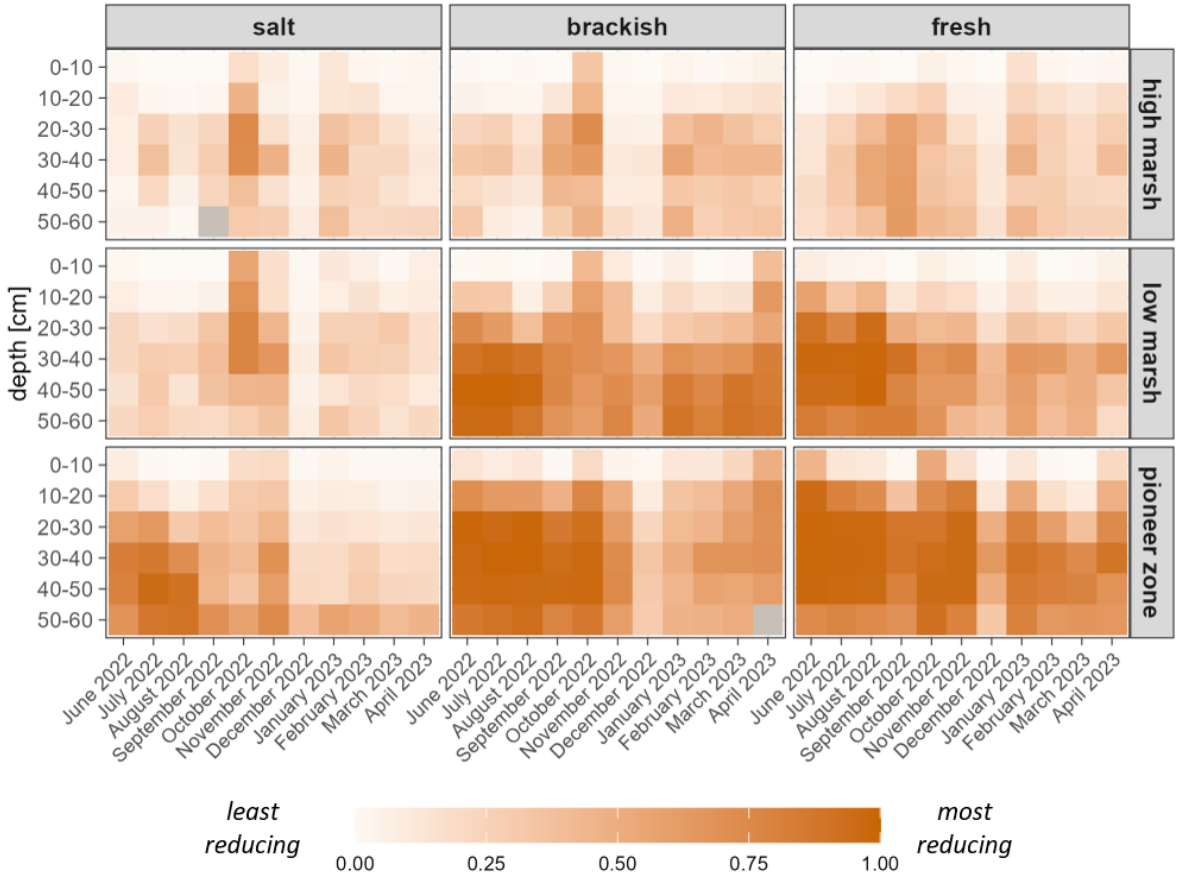

Figure 1: Monthly reduction index (RI) over the measurement period (June 2022 – April 2023) at different depths along the salinity (salt marsh, brackish marsh, freshwater marsh) and flooding gradient (high marsh = yearly flooding, low marsh = monthly, pioneer zone = daily) of the Elbe Estuary. Each RI-value is the mean of five replicate plots per marsh location. Higher RI values reflect stronger reducing soil conditions, indicated by a darker color. Grey color indicates missing values.

Redox Index (RI) values derived from the IRIS method revealed significant trends in reducing soil conditions along the salinity and flooding gradient, as well as with depth and season in the marsh soils of the Elbe Estuary (Figure 1). Soil redox conditions are driven by microbial activity, which is influenced by the interplay of soil temperature and water level (Fiedler et al., 2007). The increase in RI with greater flooding and depth might be related to higher soil water contents (Dorau and Mansfeldt, 2016), while the increasing RI with decreasing salinity could be related to the higher soil organic carbon (SOC) contents associated with lower salinity. Seasonal peaks in RI were particularly notable

during fall (September to November), especially in high marshes and low salt marshes. During the summer months (June to August), higher RI values were observed with increasing flooding; however, the shallow soil layer (0 - 20 cm) often exhibited the lowest RI during this season. Increased microbial activity due to elevated summer temperatures might explain the higher RI values in summer, but this trend depended on sufficient soil moisture. In high marshes and upper soil layers, drier conditions during summer may have led to predominantly oxic conditions (Dorau and Mansfeldt, 2016). The elevated RI values observed in fall might relate to vegetation die-off and the subsequent input of OM into the soil, coupled with higher soil water content during this period. December recorded the lowest RI across all marsh locations, probably reflecting reduced microbial activity due to colder temperatures. Seasonal variation diminished with increasing flooding and depth, as brackish low marshes, pioneer zones, and freshwater pioneer zones maintained consistently higher RI conditions throughout the year. This buffering of seasonal fluctuations might be associated with year-round high soil moisture levels. The highest RI values occurred at depths between 20 and 50 cm, where increased soil moisture might have contributed to stronger reducing conditions. However, a decline in SOM content with depth could potentially counteract this trend, resulting in lower RI values in deeper soil layers.

These results indicate that the soil redox conditions in the Elbe Estuary is driven by the interplay of soil water content, temperature, and OM content. The resulting strong spatio-temporal variations in redox conditions can strongly affect C cycling in this ecosystem. For example, in Study A of this dissertation it was shown that the weight loss of rooibos tea decreased with increasing reducing soil conditions. Moreover, free particulate OM seemed to be preserved under reducing soil conditions (Study B). Overall, this led to an increase in the degradability of SOC with increasing flooding (Study C).

4 References

Castenson, K.L., Rabenhorst, M.C., 2006. Indicator of reduction in soil (IRIS) evaluation of a new approach for assessing reduced conditions in soil. Soil Science Society of America Journal 70, 1222–1226.

Dorau, K., Mansfeldt, T., 2016. Comparison of redox potential dynamics in a diked marsh soil: 1990 to 1993 versus 2011 to 2014. Journal of Plant Nutrition and Soil Science 179, 641–651.

Fiedler, S., Vepraskas, M.J., Richardson, J.L., 2007. Soil Redox Potential: Importance, Field Measurements, and Observations, in: Elsevier, pp. 1–54.

IUSS Working Group WRB, 2022. World reference base for soil resources 2022. International soil classification system for naming soils and creating legends for soil maps, 4th ed. International Union of Soil Sciences (IUSS), Vienna, Austria.

Keiluweit, M., Wanzek, T., Kleber, M., Nico, P., Fendorf, S., 2017. Anaerobic microsites have an unaccounted role in soil carbon stabilization. Nature communications 8, 1771.

Mittmann-Goetsch, J., Wilson, M., Jensen, K., Mueller, P., 2024. Root-driven soil reduction in Wadden Sea salt marshes. Wetlands 44. https://doi.org/10.1007/s13157-024-01867-8.

Patrick Jr, W.H., Henderson, R.E., 1981. Reduction and reoxidation cycles of manganese and iron in flooded soil and in water solution. Soil Science Society of America Journal 45, 855–859.

Rabenhorst, M.C., 2008. Protocol for using and interpreting IRIS tubes. Soil Survey Horizons 49, 74–77.

Thomas, C.R., Miao, S., Sindhoj, E., 2009. Environmental factors affecting temporal and spatial patterns of soil redox potential in Florida Everglades wetlands. Wetlands 29, 1133–1145.

Acknowledgement

Throughout my PhD journey, I have received support from many people, and I would like to take a moment to thank them all, particularly:
My supervisor, **Annette Eschenbach**, for providing me with the opportunity to pursue my PhD and to be part of this exciting research project, as well as for her support throughout the entire PhD.
Kai Jensen, for his support as my second supervisor and for his dedication to the RTG 2530. I appreciate the valuable input provided during my panel meetings and the development of my manuscripts, along with the prompt responses to my emails.
The anonymous **third reviewer**, for reading and evaluating my dissertation.
Jens Hartmann, for agreeing to be my panel chair and for his input during my panel meetings.
The members of the **RTG 2530**, for fostering a supportive atmosphere. I am especially thankful to **Susanne Stirn** for organizing our activities. Being part of the RTG 2530 has been a rewarding experience, and I am grateful for the friendships I've made along the way, particularly **Widhi**, **Fay**, and **Elly**. Special thanks to **Monica** for supporting me as a co-author, for reading my dissertation, and for our unforgettable research stay in Sydney. Navigating together through the challenges of finishing our dissertations has made this process much better. I am thankful for our friendship.
The **German Research Foundation** (*Deutsche Forschungsgemeinschaft*) for funding the RTG 2530 "Biota-mediated Effects on Carbon Cycling in Estuaries".
My **co-authors**, without whom this work would not have been possible; particularly **Maria** and **Daniel** for supporting my research through their master's theses.
My **working group**, for their professional and personal support. I would not have enjoyed my time at the institute as much without you. I value our lunch and coffee breaks, which offered a distraction from work. I thank **Deborah**, **Sumita**, **Annika**, and **Andreas** for their contributions in the lab. I apologize for bringing in many muddy and smelly marsh samples and for occupying the sink to wash my litter bags. I thank all the **student assistants** for their help in the field and lab, particularly **Sophie** for cleaning countless tea bags. A special thanks also goes to **Elisa**, **Maria**, **Johanna**, and **Liz** for their mental support and for creating such a positive atmosphere. I'm additionally grateful to **Maria** and **Elisa** for proofreading this dissertation and for my office mate, **Liz**, for her open ears and heart, and our numerous conversations that helped me throughout this adventure. Additionally, I would like to thank **Volker** for his

technical and personal support. His expertise helped me find answers to many questions, and without his tireless dedication, my work would not have been possible. I also value our personal conversations during many trips to the field sites.

Joscha, for his guidance throughout every phase of this PhD, from idea development, data collection, data analyses, manuscript writing, and the completion of my thesis. I admire his passion for science and his commitment to sharing it with others. Thank you for always believing in my work and in me; this achievement would not have been possible without you.

My family, for their steady support throughout my life. They have provided me with the foundation to achieve this milestone. Thank you for always believing in me and for accompanying me through all the steps in my life.